Quantitative Carbon cycle modelling to inform Climate Mitigation Policy

Submitted by **Christopher David Jones**, to the University of Exeter as a thesis for the degree of Doctor of Philosophy by Publication in Physical Geography, March 2017

I certify that all material in this thesis which is not my own work has been identified and that no material has previously been submitted and approved for the award of a degree by this or any other University.

(Signature) ……

UNIVERSITY OF EXETER

Abstract

The global carbon cycle is a central part of the climate system which forms a direct link between human activity and climate change. This thesis presents my contribution to the field of research into the global carbon cycle with complex numerical models and its use to inform climate mitigation policy.

Firstly, I present work I led to build, configure and apply the Hadley Centre Earth System Model, HadGEM2-ES, that successfully delivered the CMIP5 simulations. Then I present work that led to the design of the next generation of coupled carbon cycle intercomparison experiments. The aim of these experiments is to understand and quantify future century-scale changes in land and ocean carbon storage and fluxes and their impact on climate projections. A set of ESM simulations was devised, with a common protocol, which all participating modelling centres should follow.

A theoretical framework is commonly used to quantify carbon cycle feedbacks. I played an active role in its recommended use and definitions of terms. A feedback analysis I performed of future carbon cycle projections formed a central component of the IPCC's Fifth Assessment Report. This is the first time that that the IPCC carbon cycle chapter had a section devoted to the feedbacks and future projections from coupled carbon cycle ESMs.

Finally, I present three specific applications of my research and their relevance to climate mitigation policy. 1) I was the first to define the concept of committed ecosystem changes and demonstrate that ecosystems may continue to respond for many years or decades after climate is stabilised, leading to the recommendation that such committed change should be included in definitions of dangerous climate change. 2) I performed the first Earth System model analysis of the carbon emissions reductions required to follow the RCP pathways leading to the IPCC AR5 statement that, "For RCP2.6, an average 50% emission reduction is required by 2050 relative to 1990 levels". 3) My research on carbon cycle feedbacks, especially the response of the carbon cycle to low CO_2 pathways, found that models predict significant weakening, or even potential reversal, of natural carbon sinks in response to removal of CO_2, which potentially hinders the effectiveness of the negative emissions.

My research presented in this thesis has been influential in setting international research priorities in this field. It continues to inform global negotiations on climate mitigation policy.

Acknowledgements

I would like to dedicate this thesis to my three fantastic children, Daniel, Kate and Matthew. Ultimately the goal of climate science is to help guide society through the 21st Century without screwing up the planet more than we have done already. History may not smile kindly on my generation in terms of our environmental credentials, but I hope I have played a part in redressing this and providing a way forward which promotes and enables sustainable development for all across the world. It may have become a cliché, but there is much wisdom in the saying that we don't inherit the world from our parents, but we borrow it from our children. So, kids, this is for you.

I would like to particularly thank my two supervisors, Stephen Sitch and Lina Mercado for their support and guidance, and for encouraging me to turn my existing work into a PhD thesis in the first place. Thank you both – it has been enjoyable!

I would also like to thank the two organisations that have made this possible: The University of Exeter, College of Life and Environmental Sciences who very generously waived the normal fees, and the Met Office who have kept me gainfully employed for more than 2 decades and allowed me to waste valuable work time reminiscing over my old papers.

At the risk of simply thanking "everyone who knows me" it's clear from my publication list that my career has benefitted hugely from the input of many (tens if not hundreds) of researchers around the world. Not only has this enriched my science research and professional career, but more importantly I've met some fantastic people and made some firm friends. The greatest privilege of my job has undoubtedly been the chance to travel and meet people. A few individuals though I must mention by name: Peter Cox and Richard Betts, with whom I have worked almost my whole career, have been guiding lights without whom I would not have achieved half of what I have done. Similarly, Olivier Boucher, Stephen Belcher and Pierre Friedlingstein have helped me grow in my leadership and confidence.

My final and biggest thanks must go to Fiona and my parents who have supported me at every step of my career as well as in the writing of this theses. My family and friends remain my inspiration for trying to do a good and worthwhile job. Thank you!

Table of Contents

List of tables and figures

The black-body, or Planck response (black bar), combines with physical climate feedbacks (pale grey) to form the “climate resistance” (dark grey), which is related to the climate feedback parameter but includes the effect of ocean heat uptake. The concentration-carbon and climate-carbon feedbacks (blue bars) refer to the carbon cycle response to CO2 concentration and climate (β and γ) respectively, but also expressed in the same common units of Wm-2K-1.

Figure 6. A synthesis of biogeochemical feedbacks with climate. Based on the quantification techniques derived in **Gregory et al. (2009)** applied to CMIP5 models and also drawing on the review by Arneth et al. (2009). Reproduced from IPCC AR5 figure 6.20.

Figure 7. Summary of carbon cycle feedback metrics from C4MIP (**Friedlingstein et al., 2006**) and CMIP5 models. Reproduced from IPCC AR5 figure 6.21.

Figure 8. Global maps of CMIP5-simulated sensitivity to CO2 (β: top panel) and to climate (γ: bottom panel). Because β and γ can be treated as additive in the linear feedback framework, results can be analysed at the level of individual gridboxes. Reproduced from IPCC AR5 figure 6.22.

Figure 9. CMIP5 multi-model mean projections of cumulative carbon uptake by land (green) and ocean (blue). The top panel shows simulated results since pre-industrial (defined here as 1850). Panels b-e show results up to 2100 from the four RCP scenarios (see Glossary). Standard deviation of model results and full model range are shown in green and blue bars on the right-hand side of each panel. Black bars on panel (a) denote the estimated equivalent real-world uptake up to 2005. Reproduced from IPCC AR5 figure 6.24.

Figure 10. Land carbon sink up to 2100 simulated by CMIP5 models for each of the four RCP scenarios. Blue bars denote the land carbon uptake simulated directly by the models, while the red bars denote the uptake that can occur once the requirement for additional nitrogen has been accounted for. Reproduced from IPCC AR5 figure 6.35.

Figure 11. Schematic representation of (a) emissions-driven and (b) concentration-driven experiments (see Glossary).

Figure 12. CO2 concentration scenarios widely used for carbon cycle simulations – previous analysis has focused on rapid/monotonic increase. For example, **Cox et al. (2000)** used IS92a (blue line), the first C4MIP (**Friedlingstein et al., 2006**) used SRES A2 (green line) and CMIP5 simulations drew on both 1% per annum increase (red line: **Arora et al., 2013; Ciais et al., 2013**) and RCP8.5 (yellow line: **Friedlingstein et al., 2014**; Collins et al., 2013). Note 1% per annum increase nominally begins in 1850 but plotted here relative to 1960 for ease of comparison on this schematic figure. A more relevant scenario which should be used is RCP2.6 (black dashed line).

Figure 13. Schematic representation of the need to consider both "demand" and "supply" of NETs. It illustrates how cross-disciplinary research is required to know if the supply can meet the demand required to achieve climate targets.

Figure 14. TCRE: the transient climate response to cumulative carbon emissions. Black solid arrows show how to read off from a climate target (global mean temperature on the y-axis) to see the compatible carbon budget (on the x-axis). Black dashed arrows show the uncertainty in this quantity, seen here as the width of the orange plume which originates from the spread of results from CMIP5 model simulations.

1. Introduction

1.1. The carbon cycle and why it matters

There is a natural cycling of carbon: known as the global carbon cycle (see, e.g. overview description by Prentice et al., 2001). Carbon exists in the atmosphere mainly in the form of carbon dioxide (CO_2) as well as in smaller quantities as methane, carbon monoxide and other trace gases. This carbon is constantly cycled through nature: it is absorbed by plants on land, via photosynthesis, falls to the ground as plants die or tissues senesce and is returned back to the atmosphere as this organic matter is decomposed by microbes and bacteria. Similarly, in the ocean CO_2 dissolves in sea water, chemically dissociates into carbonate and bicarbonate ions and can be assimilated by marine plankton also through photosynthesis. Some carbon is also transported down rivers into coastal seas and out into the ocean (Battin et al., 2009).

The components of the global carbon cycle including the big stores and flows of carbon are shown in Figure 1 (black arrows and text). Large amounts of carbon are stored on land: approx. 450-650 billion tonnes in living plants and about 2000 billion tonnes as organic matter in soils. Additional organic matter is frozen in permafrost, potentially a similar amount again (approximately 1700 billion tonnes). Published estimates vary on the magnitudes of some of these stores, but the figure shows the latest assessment from the IPCC (**Ciais et al., 2013**).

The ocean is an even bigger store of carbon, containing tens of trillions of tonnes. Much of this is in the deep ocean which circulates slowly and has been isolated from the atmosphere for many decades but even the surface waters which constantly exchange CO_2 with the atmosphere hold up to 1000 billion tonnes of carbon.

The carbon is not static and is constantly being exchanged between these large stores. Approximately 100 billion tonnes every year are exchanged between the land and the atmosphere and a similar amount between the ocean and the atmosphere. These are sizeable fractions of the carbon stores themselves (in the region of 10-20% of the carbon stored in biomass or in the surface oceans). This demonstrates what an active and dynamic system the global carbon cycle is. It is in constant

activity in a way that has profound implications for the Earth, its biogeochemistry and its inhabitants.

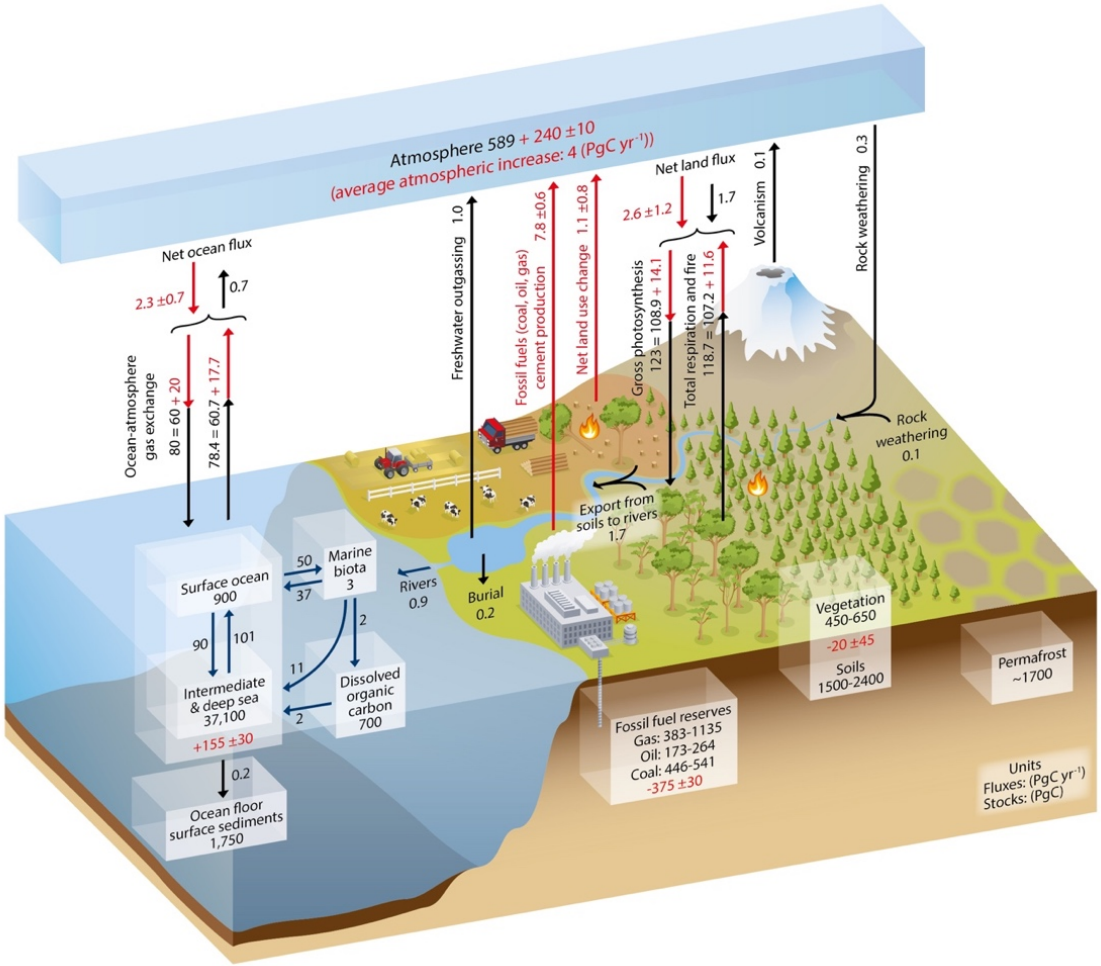

Figure 1. The global carbon cycle, showing stores and fluxes of carbon between the atmosphere and land/ocean reservoirs. Black text and arrows denote the natural baseline from circa 1850, and red arrows and text the present day human perturbation to the carbon cycle. Reproduced from **Ciais et al., 2013**, IPCC AR5 WG1, Ch.6, figure 6.1.

Figure 1 also shows, highlighted in red, the reason why the carbon cycle is of crucial interest and importance for climate science. We know, and have known since the very early work of Tyndall and Arrhenius (Tyndall, 1861; Arrhenius, 1896), that CO_2 is a greenhouse gas. In fact, it represents the strongest climate warming of all human perturbations to our planet (Myhre et al., 2013). While the natural carbon cycle constantly exchanges large amounts of carbon between land, ocean and atmosphere, the effect of human activity has been almost entirely one-way. We have

put CO_2 into the atmosphere (through our actions of deforestation and burning fossil fuel), but this is not fully compensated for by removal processes – thus leading to a long-term build-up of CO_2 above the levels that existed just a couple of hundred years ago.

At an annual scale, fossil fuel emissions are less than 10% of global plant productivity on land. Therefore, it is readily apparent the power of nature – a 10% change in the natural carbon fluxes would be comparable to the effects of human activity. In fact, we know that the natural carbon cycle has changed as a result of this human perturbation: the amount of CO_2 in the atmosphere has increased from about 280ppm (589 PgC in the figure) to now more than 400ppm (850 PgC). Yet this is only about half of the carbon we have emitted. The global carbon cycle therefore has played a crucial role in redistributing some of our emissions into land and ocean carbon stores, i.e. in mitigating climate change (Le Quéré et al., 2016). As a result, we will see about half of the climate change that may have happened had it not been for the natural carbon cycle. These natural sinks are caused by the elevated CO_2 from human activity, but are themselves sensitive to climate change. As CO_2 continues to increase due to our emissions we expect the subsequent climate change to affect nature's ability to continue to absorb it.

Over many years, climate science has been active in communicating robust scientific evidence to governments and decision makers to inform environmental policy. In response to this, the UN implemented a Framework Convention on Climate Change (the UNFCCC, see Glossary) with the express purpose of "preventing dangerous anthropogenic interference with the climate system". The WMO and UNEP (see Glossary) commissioned an Intergovernmental Panel on Climate Change (the IPCC) as an international body which periodically assesses state-of-the-art science in a way designed to be accessible by, and useful to, policy makers and international climate negotiations.

At the Met Office Hadley Centre, I have performed and led research to address key scientific questions to which policy makers require answers, and framed the outcomes of fundamental underpinning research in order to extract maximum use for policy. The nature of the carbon cycle, by forming a direct link from human emissions

of CO_2 to climate change means it can directly and powerfully contribute to climate mitigation policy. If we are to properly plan how society must adapt to cope with and limit climate change it is vital to understand how much carbon is taken up; how, where, when and why this has happened; and how this may (or may not) continue in the future. For this reason, there is a large body of research into the global carbon cycle and its interaction with climate. I have been privileged to be part of this research community for 20 years. In this thesis I present my most important contributions to this field.

1.2. History of coupled climate-carbon cycle modelling

Since the early 1990s an increasing number of studies has suggested the potential for a climate feedback onto the carbon cycle whereby carbon released due to warming would further elevate atmospheric CO_2 and amplify climate change (Jenkinson et al., 1991; Schimel et al., 1994; Kirschbaum, 1995). Such feedbacks became the focus of studies using numerical models of land and ocean carbon cycles.

Dynamic global vegetation models (DGVMs – see Glossary) were used to study the impact of rising CO_2 and climate on the land carbon cycle (Kicklighter et al., 1999; Cramer et al., 2001; McGuire et al., 2001). There is strong empirical evidence for elevated CO_2 leading to higher rates of photosynthesis (Field et al., 1995; Lloyd and Farquhar, 1996). The DGVMs were in consensus that rising CO_2 would thus stimulate additional vegetation growth and storage of carbon in terrestrial ecosystems. Likewise, warming climate would accelerate decomposition of dead organic matter, may also reduce vegetation productivity in some (mainly tropical) ecosystems and may extend the growing season in high-latitude ecosystems.

In the ocean, there was also a model consensus that warming would lead to reduced carbon uptake (Prentice et al., 2001), due to both reduced solubility in warmer waters and reduced rate of transport of carbon to the deep due to more stratified surface waters (Bacastow, 1993; Sarmiento et al., 1998; Joos et al., 1999). The role of ocean biology and the buffering capacity of the ocean were also seen to be

important and not well constrained or represented in models (Sarmiento and Le Quéré, 1996).

Many studies examined spatial variability in carbon sinks using both modelling and empirical techniques. For example, Field et al. (1998) mapped global net primary production (NPP) on land and in the ocean; Takahashi et al. (2002) mapped global ocean pCO_2 and Sabine et al. (2004) mapped anthropogenic carbon stored in the ocean. Uptake of carbon was found to be particularly large in the North Atlantic due to deep mixing of surface waters and strong biological activity (Watson et al., 1991) and also in the Southern Ocean where mixing with deep water and surface wind speeds are both strong (Sabine et al., 2004).

These land and ocean experiments found potentially high sensitivity of the carbon cycle to environmental forcing but were not able to simulate the full effect of this feedback onto climate. Intermediate complexity models were able to simulate this feedback (Joos et al., 1999; Prentice et al., 2001) but lacked spatial detail in their climate response. So by the end of the 1990s some modelling groups were beginning to couple interactive land and ocean carbon cycle modules to their climate models. Early studies (e.g. **Cox et al. 2000**; Friedlingstein et al., 2001; Thompson et al., 2004) were able to recreate an experimental setting more like the real world where a forced climate change affected natural carbon sinks and stores which in turn affected changes in atmospheric CO_2 and hence climate. But they also showed that there were substantial differences in the sensitivities of these new models.

The desire to understand and reduce this uncertainty led to a multi-model intercomparison activity with these fully coupled models (C4MIP: Coupled Climate-carbon cycle model intercomparison – see Glossary), with an agreed simulation and analysis protocol. Results were documented in the first C4MIP intercomparison paper, (**Friedlingstein et al., 2006**; Denman et al., 2007) which quantified the feedback components across 11 models for a common CO_2 emissions scenario. All models agreed qualitatively that the sign of the carbon-climate feedback was positive; a positive feedback is one that acts to amplify the initial signal/perturbation – i.e. climate change acts to reduce net uptake by offsetting land and ocean carbon sinks caused by the increasing CO_2. All models predicted continued carbon uptake

by the oceans, and most by the land also, due to higher atmospheric CO_2, but the strength of the natural land and ocean sinks was reduced due to the effects of climate change. This resulted in an increase in atmospheric CO_2 which amplified the initial climate change (Figure 2).

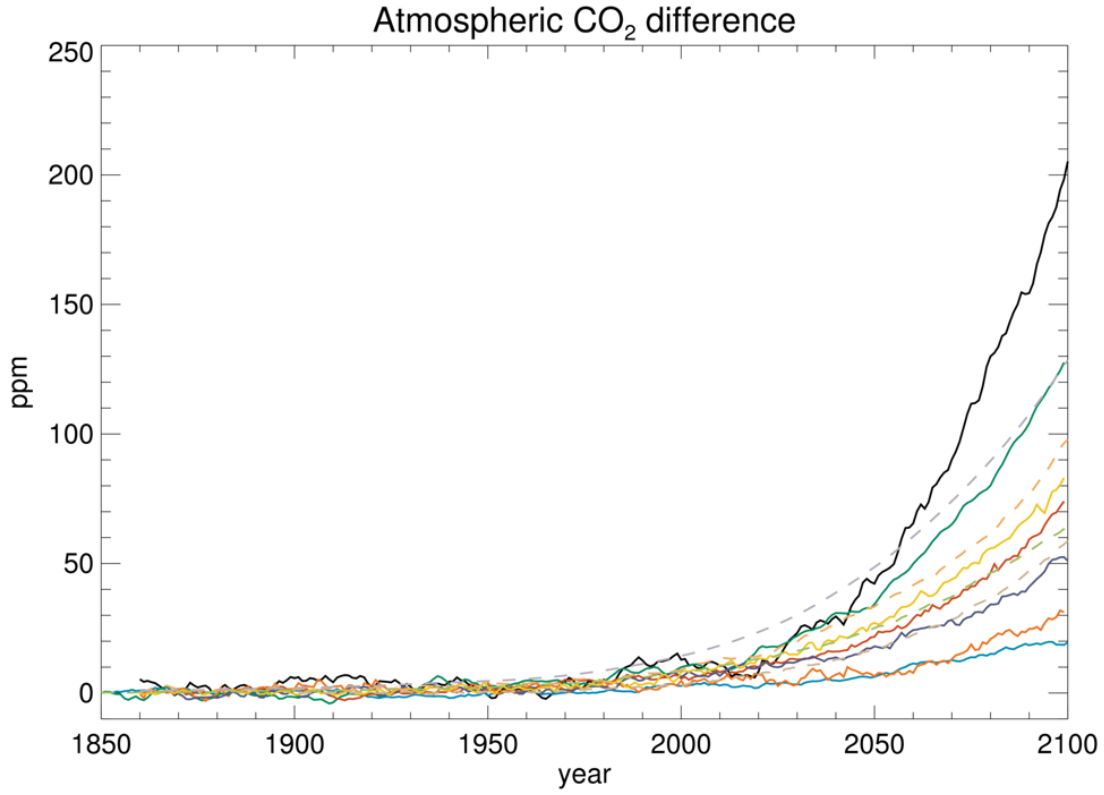

Figure 2. Additional CO_2 that remains in the atmosphere due to the climate feedback simulated by the 11 models taking part in the first C4MIP intercomparison (**Friedlingstein et al., 2006**). The study included seven coupled climate-carbon cycle GCMs (solid lines) and four Earth system models of intermediate complexity (EMICs: dashed lines).

This first intercomparison study of coupled climate-carbon cycle models (C4MIP) heralded the emergence of a new capability in climate modelling. No longer did climate models solely address the response of the climate system to projected CO_2 concentration, but now they could simulate the evolution of CO_2 concentration that results from anthropogenic carbon emissions. The end-to-end chain from emissions to concentration to climate change, and back to concentrations by representing feedbacks of climate impacts on ecosystems led to these models becoming known as “Earth System Models” or ESMs (see Glossary). This new capability opened up

opportunity for much greater policy relevance and advice. However, the large quantitative model spread in the feedback and its sensitivity components hinders the usefulness of these models to policy makers. Aside from my role in pioneering these early developments, my work over the last decade has therefore been to try to understand and reduce the sources of this uncertainty, and to try to extract maximal utility from existing models through careful experimental design and framing of results.

1.3. Structure of thesis

My thesis is divided into 5 chapters. The chapters describe a logical progression from (1) the background and history of carbon cycle modelling, (2) the building of models and design of coordinated experiments, (3) feedback analysis of models to understand their behaviour and how analysis of model results contributed to the IPCC's Fifth Assessment Report, (4) Some specific model applications to inform mitigation policy and (5) main conclusions and discussion of next steps for carbon cycle research. Chapters 2-4 are built around key published studies that I have contributed to the field since 2009. In each chapter I first briefly outline how the science has evolved over the last decade, and describe my specific contribution to this field, before focusing on my recent paper(s). My full publication record from 20 years of research in this field is attached as an Appendix. Throughout this thesis, references of which I was an author or co-author are highlighted in bold.

Chapter 2 focusses on the process of building a coupled climate-carbon cycle model and planning its use in international, coordinated, multi-model experiments. So-called "MIP"s are Model Intercomparison Projects, which involve modelling centres around the world performing the same specified experiment with their model in order to facilitate comparison of results across many models. See the Glossary for a list and description of MIPs and CMIP generations. In this chapter I present work that I led: i) to configure and apply the HadGEM2-ES model to the CMIP5 experimental design (**Jones et al., 2011**), and ii) to design the multi-model carbon cycle experiments for the next round of intercomparison: CMIP6 (**Jones et al., 2016a**).

In chapter 3 I present my role in developing feedback frameworks and their application to understand how the models behave and how we can understand the causes of differences between them in order to try to reduce the uncertainty. Here I also present my contribution as a lead-author to the IPCC's Fifth Assessment Report. Working Group 1's carbon cycle chapter (Chapter 6, **Ciais et al., 2013**) included a section on "Projections of Future Carbon and Other Biogeochemical Cycles" which I led. My analysis of coupled climate modelling was central to the key results from that IPCC section and in turn informed priorities for further model developments.

In chapter 4 I present applications of coupled climate-carbon cycle modelling which I have led. Specifically: i) the development of the new concept of "committed ecosystem changes" with an example of the Amazon forest (**Jones et al., 2009**); ii) the presentation of future carbon cycle changes in terms of "compatible emissions" required to achieve certain climate targets (**Jones et al., 2013**); and iii) an analysis of how the carbon cycle may behave dynamically under low CO_2 concentration pathways which are now a central part of global climate policy since the Paris Agreement was adopted in 2015 (**Jones et al., 2016b**).

Finally, Chapter 5 includes a summary of my contribution to this field of research and briefly discusses future research priorities, including how the uncertainty that arises from model spread hinders the full potential of these models to inform climate mitigation policy and therefore the growing need for evaluation and constraint of the models.

2. Building and applying coupled climate-carbon cycle models

Numerical modelling is the central scientific technique used to address questions on climate change and the carbon cycle. The models used have evolved over decades into extremely complex tools. Therefore, they cannot be treated as a “black box” that can be simply applied: it is essential that scientific expertise in the use of these models ensures they are applied and interpreted appropriately. In this chapter I describe the role I have played in developing such models and applying them. This chapter is based around my first author papers describing HadGEM2-ES implementation for CMIP5, and preparation of experimental design for CMIP6.

2.1. Anatomy of climate models

Climate modelling relies on numerical models of the atmospheres and oceans in order to simulate the behaviour of the climate system, gain understanding of dynamical and physical processes and make projections of future changes. The most complex models, which embody the most complete representation of the climate system are known as General Circulation Models (GCMs; see Glossary). This term explicitly describes that they have spatially resolved representation of the fluid dynamics of the atmosphere and/or ocean. They represent a description of the state of the atmosphere or ocean around the world, split into a number of points on a three-dimensional grid (see Figure 3). The models use numerical discretisation of fluid dynamics equations to simulate how the atmosphere or ocean evolves in time. The models also represent physical (or chemical or biological) processes that operate at grid scale (“resolved”) or at scales smaller than the model grid (“sub-grid” or “parametrised”).

The level of detail that can be represented is limited by the available computational resource. These models are extremely intensive in terms of computational demand and so in order to perform a simulation for many decades or centuries they typically use a grid spacing of the order of 1 degree (approximately 100km grid spacing in mid-latitudes). Even so a climate simulation from pre-industrial (1850) to 2100 can take many weeks on a state-of-the-art super computer. As high performance computing has evolved, this resolution has increased so that finer level detail can be included, and so also has the degree of complexity in the processes to be

represented (see e.g. **Pope et al., 2007**). Computational expense remains a limiting factor on our ability to model the Earth System.

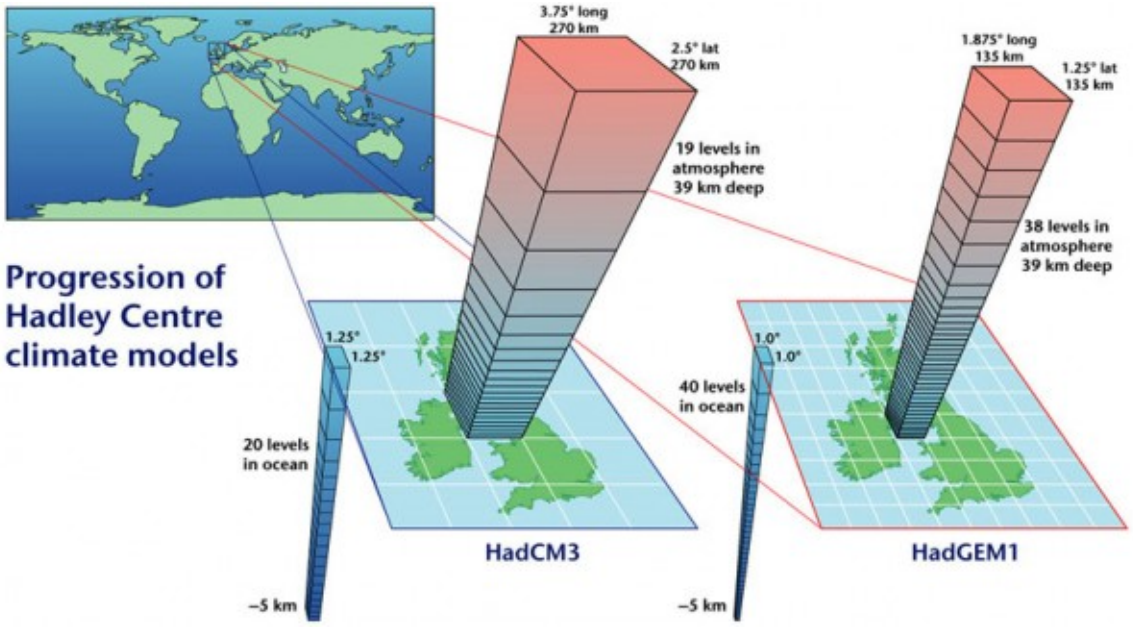

Figure 3. Schematic representation of the 3D grid structure of GCMs. Using Met Office Hadley Centre models as an example the figure shows the horizontal spacing of (usually) rectangular grids, and vertical stacking of gridboxes. The horizontal grid is commonly regular in latitude and longitude, although irregular grids are increasingly common, especially in ocean models. Vertical grids are often irregular and can be framed in terms of height or pressure coordinates in the atmosphere, and depth or density coordinates in the ocean.

Figure 4 shows how the complexity of GCMs has evolved over the last 40 years. In the late 1990s we began to develop coupled GCMs with interactive carbon cycle components. I played a large role in developing the first such model, HadCM3LC, which was used for the simulations presented in **Cox et al. (2000)**. This study first proposed the positive climate carbon cycle feedback, the vulnerability of large-stocks of soil carbon to warming, and the vulnerability of the Amazon rainforest to future dieback. My role included setting up the fully coupled model, and testing and tuning it so that the individual components and the coupled system performed well. I used its internal variability and response to volcanic eruptions to understand the processes of carbon cycle sensitivity, on land and in the ocean, to climate perturbations (**Jones et al., 2001; Jones and Cox, 2001a**) and to constrain model parameters of soil respiration sensitivity to temperature (**Jones and Cox, 2001b**). The IPCC Third

assessment report (labelled TAR in Figure 4) was published in 2001 and its carbon cycle chapter (Prentice et al., 2001) included only brief discussion of early coupled carbon cycle GCM results.

By the Fifth Assessment Report (AR5), it was common among GCMs to have interactive climate-carbon cycle components and the carbon cycle chapter of IPCC Working Group 1 (Chapter 6; **Ciais et al., 2013**) had a whole section, which I led, devoted to future projections with these models.

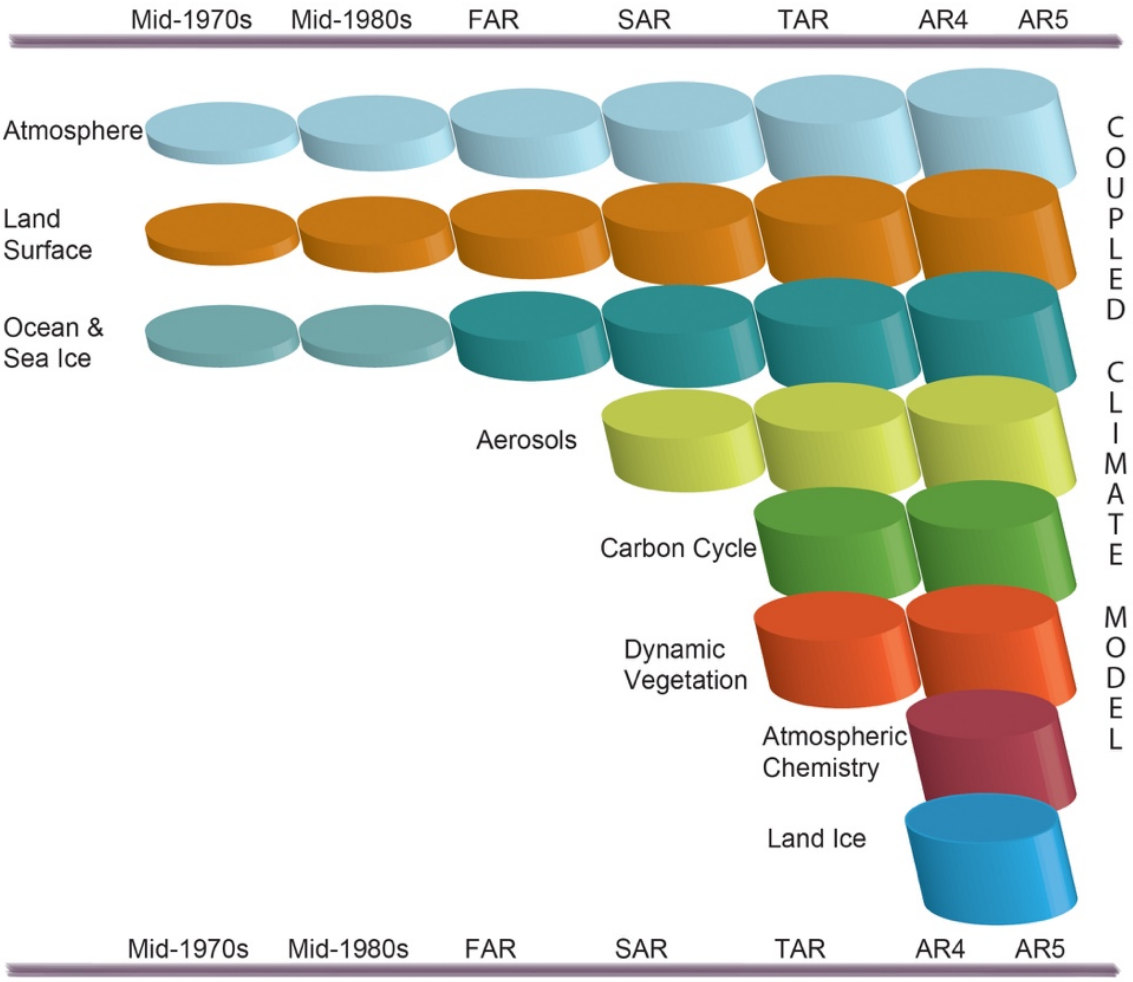

Figure 4. Chronology of GCM complexity showing how different sub-components have been added over time since the mid-1970s. The size of the symbol for each process denotes how increased complexity of process representation has also increased within each component. Reproduced from IPCC AR5 Ch.1 (Cubasch et al., 2013), figure 1.13.

Over time these models have become known as Earth System Models (ESMs). In this context, an ESM can be understood to mean a coupled GCM with an interactive carbon cycle and throughout this thesis, the phrase “ESM” should be understood in that context. Here I describe my role in ESM developments from TAR to AR5.

2.2. Building HadGEM2-ES for CMIP5

In 2009 I was active in planning modelling activity for the IPCC’s Fifth Assessment report. It was clear that many modelling centres would have coupled ESMs and would use them for the standard CMIP5 simulations (Taylor et al., 2012; see Glossary), and so I ensured that the CMIP5 experimental design included carbon cycle simulations and analysis. At the Met Office Hadley Centre, I was manager of the carbon cycle group where we developed a new model, called HadGEM2, in order to perform the CMIP5 simulations. The development of the physical aspects of the model, from HadGEM1, are described in **Martin et al., (2011)**, and the development of the coupled carbon cycle components (that therefore define HadGEM2-ES, “earth system”, from HadGEM2-AO, “atmosphere-ocean”) is presented in **Collins et al. (2011)**. HadGEM2-ES also included representation of atmospheric composition in the form of aerosols and tropospheric chemistry (see **Martin et al., 2011**, figure 1 and table 1).

Here I present how I led work that produced a fully tested set-up of HadGEM2-ES and successful delivery of CMIP5 simulations. Even though HadGEM2-ES had been built, the work to test and configure it to perform the CMIP5 simulations, to run the model, and to process and publish the output data involved 37 authors from 16 different institutes across 4 continents. This process of configuring the model is documented in my paper, **Jones et al. (2011)**, which forms the body of this section. The simulations took over 1 year to run on the Met Office super computer, and in total, more than 50 TB of data was published (http://www.metoffice.gov.uk/research/news/cmip5).

CMIP5 represented a coordinated attempt to define a common modelling protocol in order to facilitate comparison of complex ESM experiments and thus avoid the impacts of arbitrary decisions. However, by necessity there may still be a number of

subjective decisions required when elements of the experimental protocol are not applicable to a certain model or model configuration.

Detailed scientific understanding is therefore required of the intended use of the model in order to ensure it is fit for purpose. Some of the components of HadGEM2-ES are simulated interactively rather than being prescribed as external boundary conditions. For example, it includes interactive tropospheric chemistry and hence can simulate the evolution of atmospheric methane and ozone concentration in response to meteorological conditions and emissions of reactive gases. Therefore, atmospheric composition may not exactly follow the CMIP5-prescribed values. In our experiments we forced the surface methane concentrations to follow the CMIP5 values in order to reduce any model drift away from the scenarios, while still allowing for differences in CH_4 concentrations in the free atmosphere away from the surface. We also investigated the sensitivity of the model to forcing from different greenhouse gases and were able to simplify the treatment of 27 halocarbon species into two aggregate species: “equivalent CFC-12” and “equivalent HFC-134a”, representing all gases controlled under the Montreal and Kyoto protocols, respectively (**Jones et al., 2011**, section 3.3).

Additionally, by prescribing anthropogenic disturbance in addition to simulated, dynamic vegetation we risked diverging from the intended impact of the prescribed land-use change. For example, if the model initially simulates too much or too little forest in a region to be deforested then the impact of this deforestation on both carbon storage and physical surface properties will be too great or too little. We mitigated this risk in the emission-driven experiments by overwriting the land-use flux seen by the atmosphere by the CMIP5-prescribed land-use emissions dataset.

This enhanced, process-based functionality of the model is a benefit – the rationale behind developing such a complex earth system model is precisely to study these interactions and allow them to change consistently with future climate in a way not possible with prescribed concentrations. But it highlights the care and caution required to configure and perform such complex scientific experiments.

Geosci. Model Dev., 4, 543–570, 2011
www.geosci-model-dev.net/4/543/2011/
doi:10.5194/gmd-4-543-2011

Geoscientific Model Development

The HadGEM2-ES implementation of CMIP5 centennial simulations

C. D. Jones[1], J. K. Hughes[1], N. Bellouin[1], S. C. Hardiman[1], G. S. Jones[1], J. Knight[1], S. Liddicoat[1], F. M. O'Connor[1], R. J. Andres[2], C. Bell[3,†], K.-O. Boo[4], A. Bozzo[5], N. Butchart[1], P. Cadule[6], K. D. Corbin[7,*], M. Doutriaux-Boucher[1], P. Friedlingstein[8], J. Gornall[1], L. Gray[9], P. R. Halloran[1], G. Hurtt[10,16], W. J. Ingram[1,11], J.-F. Lamarque[12], R. M. Law[7], M. Meinshausen[13], S. Osprey[9], E. J. Palin[1], L. Parsons Chini[10], T. Raddatz[14], M. G. Sanderson[1], A. A. Sellar[1], A. Schurer[5], P. Valdes[15], N. Wood[1], S. Woodward[1], M. Yoshioka[15], and M. Zerroukat[1]

[1]Met Office Hadley Centre, Exeter, EX1 3PB, UK
[2]Environmental Sciences Division, Oak Ridge National Laboratory, Oak Ridge, TN 37831-6335, USA
[3]Meteorology Dept, University of Reading, Reading, RG6 6BB, UK
[4]National Institute of Meteorological Research, Korea Meteorological Administration, Korea
[5]School of GeoSciences, University of Edinburgh, The King's Buildings, Edinburgh EH9 3JW, UK
[6]Institut Pierre-Simon Laplace, Université Pierre et Marie Curie Paris VI, 4 Place de Jussieu, case 101, 75252 cedex 05 Paris, France
[7]Centre for Australian Weather and Climate Research, CSIRO Marine and Atmospheric Research, Aspendale, Victoria, Australia
[8]College of Engineering, Mathematics and Physical Sciences, University of Exeter, Exeter, EX4 4QF, UK
[9]National Centre for Atmospheric Science, Department of Physics, University of Oxford, Oxford, OX1 3PU, UK
[10]Department of Geography, University of Maryland, College Park, MD 21403, USA
[11]Department of Physics, University of Oxford, Oxford, OX1 3PU, UK
[12]Atmospheric Chemistry Division, UCAR, Boulder, USA
[13]Earth System Analysis, Potsdam Institute for Climate Impact Research, Germany
[14]Max Planck Institute for Meteorology, Hamburg, Germany
[15]School of Geographical Sciences, University of Bristol, Bristol BS81SS, UK
[16]Pacific Northwest National Laboratory, Joint Global Change Research Institute, University of Maryland, College Park, MD 20740, USA
[*]now at: Colorado State University, Fort Collins, USA
[†]deceased, 20 June 2010

Received: 7 March 2011 – Published in Geosci. Model Dev. Discuss.: 31 March 2011
Revised: 14 June 2011 – Accepted: 19 June 2011 – Published: 1 July 2011

Abstract. The scientific understanding of the Earth's climate system, including the central question of how the climate system is likely to respond to human-induced perturbations, is comprehensively captured in GCMs and Earth System Models (ESM). Diagnosing the simulated climate response, and comparing responses across different models, is crucially dependent on transparent assumptions of how the GCM/ESM has been driven – especially because the implementation can involve subjective decisions and may differ between modelling groups performing the same experiment. This paper outlines the climate forcings and setup of the Met Office Hadley Centre ESM, HadGEM2-ES for the CMIP5 set of centennial experiments. We document the prescribed greenhouse gas concentrations, aerosol precursors, stratospheric and tropospheric ozone assumptions, as well as implementation of land-use change and natural forcings for the HadGEM2-ES historical and future experiments following the Representative Concentration Pathways. In addition, we provide details of how HadGEM2-ES ensemble members were initialised from the control run and how the palaeoclimate and AMIP experiments, as well as the "emission-driven" RCP experiments were performed.

Correspondence to: C. D. Jones
(chris.d.jones@metoffice.gov.uk)

Published by Copernicus Publications on behalf of the European Geosciences Union.

1 Introduction

Phase 5 of the Coupled Model Intercomparison Project (CMIP5) is a standard experimental protocol for studying the output of coupled ocean-atmosphere general circulation models (GCMs). It provides a community-based infrastructure in support of climate model diagnosis, validation, intercomparison, documentation and data access. The purpose of these experiments is to address outstanding scientific questions that arose as part of the IPCC Fourth Assessment report (AR4) process, improve understanding of climate, and to provide estimates of future climate change that will be useful to those considering its possible consequences and the effect of mitigation strategies.

CMIP5 began in 2009 and is meant to provide a framework for coordinated climate change experiments over a five year period and includes simulations for assessment in the IPCC Fifth Assessment Report (AR5) as well as others that extend beyond the AR5. The IPCC's AR5 is scheduled to be published in September 2013. CMIP5 promotes a standard set of model simulations in order to:

- evaluate how realistic the models are in simulating the recent past,
- provide projections of future climate change on two time scales, near term (out to about 2035) and long term (out to 2100 and beyond), and
- understand some of the factors responsible for differences in model projections, including quantifying some key feedbacks such as those involving clouds and the carbon cycle.

A much more detailed description can be found on the CMIP5 project webpages (see URL 1 in Appendix A) and in Taylor et al. (2009).

There are a number of new types of experiments proposed for CMIP5 in comparison with previous incarnations. As in previous intercomparison exercises, the main focus and effort rests on the longer time-scale ("centennial") experiments, including now emission-driven runs of models that include a coupled carbon-cycle (ESMs). These centennial experiments are being performed at the Met Office Hadley Centre with the HadGEM2-ES Earth System model (Collins et al., 2011; Martin et al., 2011); a configuration of the Met Office's Unified Model. Figure 1 outlines the main experiments and groups them into categories. The inner circle denotes "core" priority experiments with tier 1 (middle circle) and tier 2 (outer circle) having successively lower priority. Experiments are split between climate projections (blue), idealised experiments aimed at elucidating process understanding in the models (yellow), model evaluation, including pre-industrial control runs and historical experiments (red), and additional experiments for models with a coupled carbon cycle (green).

In the following, we briefly describe HadGEM2-ES ESM, which is documented in detail in Collins et al. (2011). HadGEM2-ES is a coupled AOGCM with atmospheric resolution of N96 ($1.875° \times 1.25°$) with 38 vertical levels and an ocean resolution of 1° (increasing to 1/3° at the equator) and 40 vertical levels. HadGEM2-ES also represents interactive land and ocean carbon cycles and dynamic vegetation with an option to prescribe either atmospheric CO_2 concentrations or to prescribe anthropogenic CO_2 emissions and simulate CO_2 concentrations as described in Sect. 2. An interactive tropospheric chemistry scheme is also included, which simulates the evolution of atmospheric composition and interactions with atmospheric aerosols. The model timestep is 30 min (atmosphere and land) and 1 h (ocean). Extensive diagnostic output is being made available to the CMIP5 multi-model archive. Output is available either at certain prescribed frequencies or as time-average values over certain periods as detailed in the CMIP5 output guidelines (see URL 2 in Appendix A).

The CMIP5 simulations include 4 future scenarios referred to as "Representative Concentration Pathways" or RCPs (Moss et al., 2010). These future scenarios have been generated by four integrated assessment models (IAMs) and selected from over 300 published scenarios of future greenhouse gas emissions resulting from socio-economic and energy-system modelling. These RCPs are labelled according to the approximate global radiative forcing level in 2100 for RCP8.5 (Riahi et al., 2007), during stabilisation after 2150 for RCP4.5 (Clarke et al., 2007; Smith and Wigley, 2006) and RCP6 (Fujino et al., 2006) or the point of maximal forcing levels in the case RCP3-PD (van Vuuren et al., 2006, 2007), with PD standing for "Peak and Decline". The latter scenario has previously been known as RCP2.6, as radiative forcing levels decline towards $2.6\,\mathrm{Wm}^{-2}$ by 2100. Note that these radiative forcing levels are illustrative only, because greenhouse gas concentrations, aerosol and tropospheric ozone precursors are prescribed, resulting in a wide spread in radiative forcings across different models.

The experimental protocol involves performing a historical simulation (defined for HadGEM2-ES as 1860 to 2005) using the historical record of climate forcing factors such as greenhouse gases, aerosols and natural forcings such as solar and volcanic changes. The model state at 2005 is then used as the initial condition for the 4 future RCP simulations. Further extension of the RCP simulations to 2300 is also implemented as detailed in the RCP White Paper (see URL 3 in Appendix A) and Meinshausen et al. (2011).

Many of these experiments require technical implementation by means of either or both of the following:

- time-varying boundary conditions such as concentrations of greenhouse gases or emissions of reactive chemical species or aerosol pre-cursors. These may be given as single, global-mean numbers, or supplied as 2-D or 3-D fields of data,

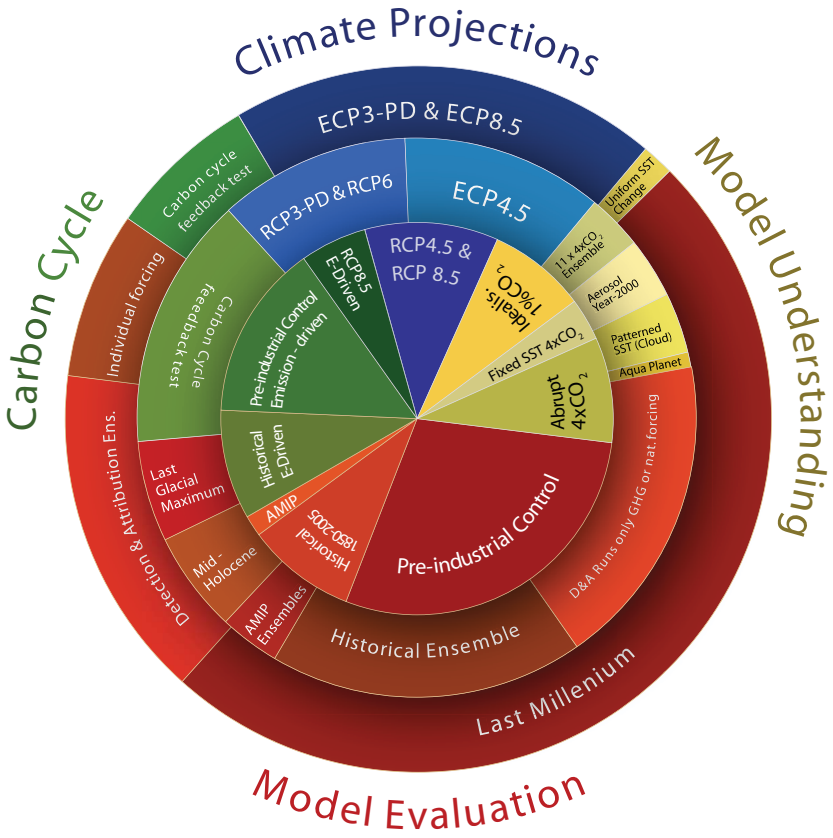

Fig. 1. Schematic of CMIP5 centennial simulations, adapted from Taylor et al. (2009) with each experiment being represented by an area that is proportional to the experiment's length in model years. The inner circle denotes "core" priority experiments with tier 1 (middle circle) and tier 2 (outer circle) having successively lower priority. Experiments are split between climate projections (blue), idealised experiments aimed at elucidating process understanding in the models (yellow), model evaluation, including pre-industrial control runs and historical experiments (red), and additional experiments for models with a coupled carbon cycle (green). See CMIP5 project webpage (Appendix A) for more detailed information. (D&A: detection and attribution, ECP: extended RCP simulations to 2300).

– code changes to alter the scientific behaviour of the model, such as to decouple various feedbacks and interactions (e.g. the "uncoupled" carbon cycle experiments).

This paper presents in detail the technical aspects of how these model forcings are implemented in HadGEM2-ES. It is not our intention here to present scientific results from the experiments. This analysis will be left for subsequent work.

The CMIP5 experiments performed with HadGEM2-ES are listed in Table 1 along with the relevant forcings for each experiment. How these forcings are then implemented is detailed in the following sections with Sect. 2 describing the atmospheric CO_2 concentrations for the concentration-driven runs as well as the CO_2 emission assumptions for the emission-driven experiments. Section 3 details the boundary conditions of atmospheric concentrations of the other well-mixed greenhouse gases. Tropospheric and stratospheric ozone assumptions are detailed in Sect. 4. Section 5 details the treatment of aerosols, while Sect. 6 documents that applied to land use pattern changes. Natural forcings, both solar and volcanic, are described in Sect. 7. Apart from these recent history, centennial 21st century and longer-term experiments, we describe as well the setup for the palaeoclimatic runs in Sect. 8. The more general issue of how the ensemble members are branched off the control run is described in Sect. 9, and Sect. 10 concludes. A list of URL locators for websites holding relevant data is included as an Appendix.

2 Carbon dioxide

2.1 CO_2 concentration

For simulations requiring prescribed atmospheric CO_2 concentrations, a single global 3-D constant provided as an annual mean mass mixing ratio was used – linearly interpolated in the model at each timestep. This prescribed CO_2 concentration is then passed to the model's radiation scheme, and constitutes a boundary condition for the terrestrial and ocean

Table 1. Overview of CMIP5 experiments and their prescribed boundary conditions, i.e., atmospheric concentrations or emissions. This Table lists the climate forcings required to be changed from the control run (Experiment 3.1) in order to set-up and perform each CMIP5 experiment. The presence of a cross denotes that that forcing is changed, and is documented in the section listed in the column title. An absence of a cross does not mean that forcing is missing, but that it is kept the same as in the control run.

Experiment number[a]	Experiment name	2.1. CO_2 concentration	2.2. CO_2 emissions	3. well-mixed GHG[b]	4. Ozone	5. Aerosols	6. Land Use	7. Natural[c]	8. geophysical[d]
3.1	Pre-industrial control [e]	X		X	X	X	X	X	
3.2(E)[f]	historical	X		X	X	X	X	X	
3.3(E)	AMIP	X		X	X	X	X[g]	X	
3.4	Mid-Holocene	X		X			X	X [h]	
3.5	LGM	X		X			X	X	X
3.6	Last Millennium	X		X			X [g]	X	
4.1, 4.2, 4.3, 4.4	RCP projections to 2100	X		X	X	X	X	X	
4.1L, 4.2L, 4.3L	RCP extensions to 2300	X		X	X	X	X	X	
5.1	ESM control	X [i]							
5.2, 5.3	ESM historical/RCP		X	X	X	X	X	X	
6.1	Idealised 1 %	X							
6.3, 6.3 E	Idealised 4 × CO_2	X							
5.4(1), 5.5(1)	Carbon-cycle decoupled 1 %	X							
5.4(2), 5.5(2)	Carbon-cycle decoupled Historical/RCP4.5	X		X	X	X	X	X	
7.1 (E)	D&A[j] Natural							X	
7.2 (E)	D&A GHG	X		X					
7.3	D&A "individual" LU – only						X		

[a] experiments are numbered as per Centennial experiments (Table B in Taylor et al., 2009). We explicitly don't consider the idealised SST experiments 6.2, 6.4, 6.5, 6.6, 6.7, 6.8 which will be documented elsewhere. [b] "well mixed GHG" here covers CH_4, N_2O, and halocarbons, but not CO_2 which is treated in Sect. 2. "Ozone" covers tropospheric and stratospheric and includes emissions of pre-cursor gases which affect tropospheric ozone (see Sect. 4) [c] "natural" forcing covers both solar and volcanic changes (Sect. 7) [d] "geophysical" here is taken to include changes in: prescribed ice sheet extent (incl. height), land-sea mask, ocean bathymetry. [e] the control run does have "forcing" in that we prescribe several things to be constant. The relevant sections describe how each climate forcing is set up for the control run. The Table then lists aspects which differ from the control (either by being time varying in scenarios, or by being held constant at different values such as in the 4 × CO_2 simulation). [f] "(E)" denotes that an initial-condition ensemble is required for these experiments. Section 9 describes how the initial conditions are derived. [g] land-use in the AMIP and last millennium experiments is described in their respective Sects. (9.2, 8.3) rather than the land-use Sect. 6. [h] palaeoclimate orbital forcing is described in Sect. 8 rather than under solar forcing in Sect. 7.1. [i] The "ESM control" simulation actually has an absence of forcing as CO_2 is simulated in this experiment, not prescribed. [j] "D&A" stands for detection and attribution.

carbon cycle. The oceanic partial pressure of CO_2, pCO_2, is always simulated prognostically from this, i.e. it is not itself prescribed.

The CO_2 concentrations used were taken from the CMIP5 dataset (see URL 4 in Appendix A). The historical part of the concentrations (1860–2005) is derived from a combination of the Law Dome ice core (Etheridge et al., 1996), NOAA global mean data (see URL 5 in Appendix A) and measurements from Mauna Loa (Keeling et al., 2009). After 2005, CO_2 concentrations recommended for CMIP5 were calculated for the 21st century from harmonized CO_2 emissions of the four IAMs that underlie the four RCPs. Beyond 2100, these concentrations were extended, so that the CO_2 concentrations under the highest RCP, RCP8.5, stabilize just below 2000 ppm by 2250. Both the medium RCPs smoothly stabilize around 2150, with RCP4.5 stabilizing close to the 2100 value of the former SRES B1 scenario (∼540 ppm). The lower RCP, RCP3-PD, illustrates a world with net negative emissions after 2070 and sees declining CO_2 concentrations after 2050, with a decline of 0.5 ppm yr^{-1} around 2100 (see Fig. 2). These CO_2 concentrations are prescribed in HadGEM2-ES's historical, AMIP, RCP simulations and the carbon-cycle uncoupled experiments. The detection and attribution experiments with time varying CO_2 also use these values, but the detection and attribution experiments with fixed CO_2 levels use a constant, pre-industrial value of 286.3 ppm. This CMIP5 dataset also provides the CO_2 concentration used for the pre-industrial control simulation (taken here to be 1860 AD), which is 286.3 ppm. CO_2 for the palaeoclimate simulations is described in Sect. 8. More details on the CMIP5 CO_2 concentrations and how they were derived are provided in Meinshausen et al. (2011).

Aside from these centennial simulations, idealized experiments are performed with HadGEM2-ES for CMIP5 in order to estimate, inter alia, transient and equilibrium climate

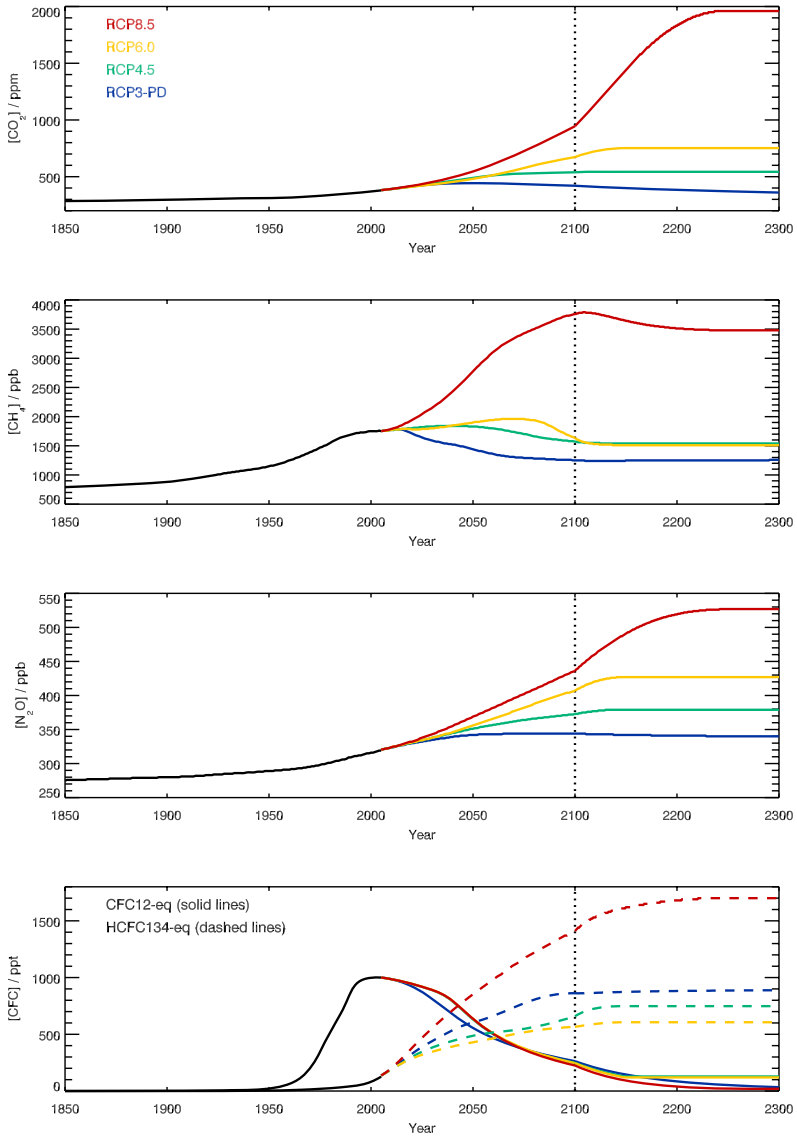

Fig. 2. Well mixed GHG concentrations used for concentration driven simulations: **(a)** CO_2, **(b)** CH_4, **(c)** N_2O, **(d)** halocarbons. Plotted are historical observed concentrations (black lines), and the four RCPs as well as their extensions beyond 2100 (RCP8.5: red; RCP6: yellow; RCP4.5: green; RCP3-PD: blue). See Meinshausen et al. (2011) for further details. Note that the x-axis beyond 2100 is compressed.

sensitivity and the climate-carbon cycle feedback. For the idealised annual 1 % increase in CO_2 concentration, we start from the control-run level of 286.3 ppm in 1859 up to $4 \times CO_2$ (1144 ppm) after 140 yr (Experiment 6.1). Equivalently, our instantaneous quadrupling to $4 \times CO_2$ uses a concentration of 1144 ppm in order to allow diagnosis of short-term forcing adjustments and equilibrium climate sensitivities (Experiment 6.3).

2.1.1 Decoupled carbon cycle experiments

Using additional code modifications to the appropriate modules of the HadGEM2-ES model, it is possible to decouple different carbon-cycle feedbacks. For the decoupled carbon cycle experiments (5.4, 5.5) we decoupled the climate and carbon cycle in 2 different ways. The C4MIP intercomparison exercise (Friedlingstein et al., 2006) defined an "UNCOUPLED" methodology in which only the carbon cycle component responded to changes in atmospheric CO_2 levels. Gregory et al. (2009) additionally describe the counterpart experiment where only the model's radiation scheme responds to changes in CO_2. Gregory et al. (2009) recommend performing both experiments (as the results may not combine linearly to give the fully coupled behaviour) and labelling such experiments in terms of what *is* rather than *is not* coupled.

Hence we performed the biogeochemically coupled ("BGC") experiments (5.4) in which the models biogeochemistry is coupled (i.e., the biogeochemistry modules respond to the changing atmospheric CO_2 concentration) and the radiation scheme is uncoupled (and uses the preindustrial level of CO_2 which is held constant) and also radiatively coupled ("RAD") experiments (5.5) in which the model's radiation scheme is allowed to respond to changes in atmospheric CO_2 levels, but the biogeochemistry components (land vegetation and ocean chemistry and ecosystem) use a constant CO_2 level, again set to the preindustrial value. Both decoupled experiments can be achieved with single simulations in which time-varying or time-fixed values of CO_2 are used as input data to the respective sections of model code. We performed both BGC and RAD experiments for the idealised (1 %) and transient, multi-forcing (historical/RCP4.5) scenarios.

2.2 CO_2 emissions

2.2.1 Emissions data

In addition to running with prescribed atmospheric CO_2 concentrations, HadGEM2-ES can be configured to run with a fully interactive carbon cycle. Here, atmospheric CO_2 is treated as a 3-D prognostic tracer, transported by atmospheric circulation, and free to evolve in response to prescribed surface emissions and simulated natural fluxes to and from the oceans and land. This approach is required for the "Emission-driven" simulations (5.1–5.3) shown in green in Fig. 1, and it also allows additional model evaluation by comparison with flask and station measuring sites such as at Mauna Loa (e.g. Law et al., 2006; Cadule et al., 2010).

A 2-D timeseries of total anthropogenic emissions was constructed by summing contributions from fossil fuel use and land-use change. For the historical simulation, annual mean emissions from fossil fuel burning, cement manufacture, and gas-flaring were provided on a $1^\circ \times 1^\circ$ grid from 1850 to 1949 (Boden et al., 2010), with monthly means from 1950 to 2005 (Andres et al., 2011). For the RCP8.5 simulation, the harmonized fossil fuel emissions for 2005 to 2100 were used (as available in the RCP database, see URL 6 in Appendix A). The land use change (LUC) emissions are based on the regional totals of Houghton (2008), which were provided as annual means of the period 1850–2005. Within each of the ten regions the emissions were linearly weighted by population density on a $1^\circ \times 1^\circ$ grid (for more information, see URL 7 in Appendix A). These population data were also used by Klein Goldewijk (2001) and are linearly interpolated between the years 1850, 1900, 1910, 1920, 1930, 1940, 1950, 1960, 1970, 1980, and 1990. After the year 1990 population density is assumed to stay constant. Additionally, high population density was set to a limit of 20 persons per km^2 to avoid large emissions in urban centres. The weighting with population data inhibits land use change emissions in deserts and high northern latitudes, which improves the latitudinal distribution of the emissions. However, the method is insufficient to provide realistic local land use change emissions (e.g. in tropical forests).

The gridded ($1^\circ \times 1^\circ$) fossil fuel and land-use emissions data, originally provided as a flux per gridbox, were converted to flux per unit area, then regridded as annual means onto the HadGEM2-ES model grid. A small scaling adjustment was made after regridding to ensure the global totals matched those of the $1^\circ \times 1^\circ$ data exactly. Future emissions were not provided with spatial information so we scaled the 2005 geographical pattern for fossil-fuel and land-use emissions to give the correct global total into the future. The CO_2 emissions are updated daily in the model by linearly interpolation between the annual values (or monthly, from 1950–2005). HadGEM2-ES has the functionality to interactively simulate land-use emissions of CO_2 directly from a prescribed scenario of land-use change and simulated vegetation cover and biomass (see Sect. 6). However, the model has not been fully evaluated in this respect, so for CMIP5 experiments we disable this feature and choose rather to prescribe reconstructed land-use emissions from Houghton (2008). By simulating changes in carbon storage due to imposed land use change, but imposing land-use CO_2 emissions to the atmosphere from an external dataset we introduce some degree of inconsistency in this simulation. Work is required to evaluate and improve the simulation of land-use emissions so that they can be used interactively in such simulations in the future.

The uncertainty in annual land-use emissions of ± 0.5 GtC (cf. Le Quéré et al., 2009) is relatively large compared to the total land use emissions (an estimated 1.467 GtC in 2005, Houghton, 2008). The RCP scenarios have been harmonised towards the average LUC emission value of all four original IAM emission estimates, i.e., 1.196 GtC in 2005. This is substantially lower than the value calculated by Houghton (2008) of 1.467 GtC in the same year, although still within the uncertainty. The climate-carbon cycle modelling community preferred to use the original Houghton (2008) estimates for historical emissions. A smooth transition between the historical and the RCP simulations was ensured by scaling the last five years of the historical LUC emissions to factor in a linearly-increasing contribution from the harmonised RCP values. In 2001 the two values were combined in the ratio 80 %:20 % (Houghton: RCP), followed by 60 %:40 % in 2002, and so on until 0 %:100 % (i.e. the RCP value) in 2005, as shown in Fig. 3.

By rescaling the Houghton (2008) data between 2000 and 2005 to merge smoothly with the RCP value in 2005, we lower total emissions in this period by 0.94 GtC compared to the original Houghton estimates (Table 2). In the presence of fossil emissions of more than 40 GtC in this period this difference is small. Total emissions and the relative contribution of fossil fuel and LUC are shown in Fig. 4.

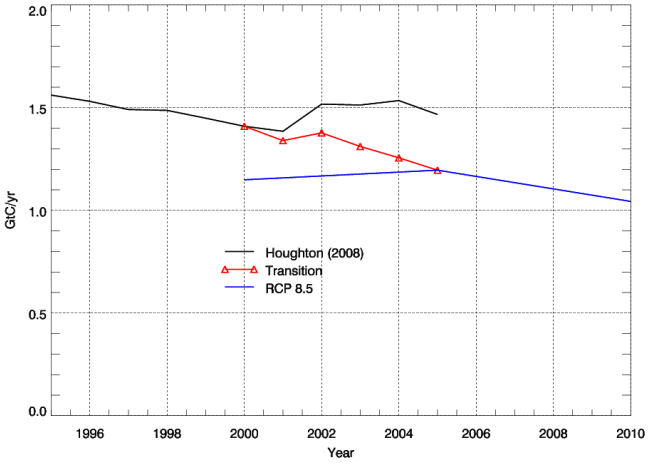

Fig. 3. Global land use emissions data during the transition from the historical simulation to the RCP 8.5 simulation. The Houghton (2008) land use emissions data (black line) were scaled to meet the RCP data (blue line), resulting in the red line with triangles, which replaced the black line during 2000–2005.

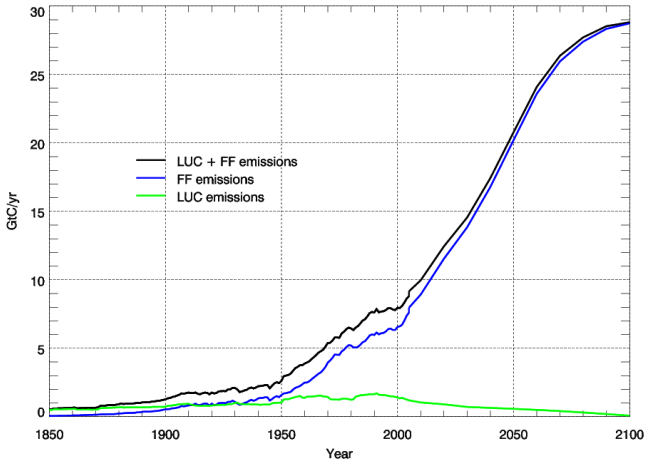

Fig. 4. Total CO_2 emissions used to force HadGEM2-ES for the emissions-driven historical and future RCP8.5 simulation. Total CO_2 emissions (black) and the individual components of fossil fuel emissions (blue) and LUC emissions (green).

2.2.2 Carbon conservation

In the emissions-driven experiments, conservation of carbon in the earth system is required. The concentration of atmospheric CO_2 influences the carbon exchange with the oceans and terrestrial biosphere. Any drift in atmospheric CO_2 will modify these fluxes accordingly, and thereby impact the land and ocean carbon stores as well as the climate itself. While the transport of atmospheric tracers in HadGEM2-ES is designed to be conservative, the conservation is not perfect and in centennial scale simulations this non-conservation becomes significant. This has been addressed by employing an explicit "mass fixer" which calculates a global scaling of CO_2 to ensure that the change in the global mean mass mixing ratio of CO_2 in the atmosphere matches the total flux of CO_2 into or out of it each timestep (Corbin and Law, 2011).

Figure 5 demonstrates HadGEM2-ES's ability to conserve atmospheric CO_2, following implementation of the mass fixer scheme described here. The evolution of the atmospheric CO_2 burden calculated by the model matches almost exactly the accumulation over time of the CO_2 flux to the atmosphere. The lower panel of Fig. 5 shows the difference between the two. This residual difference is most likely explained by changes in the total mass of the atmosphere in HadGEM2-ES over time, since CO_2 mass mixing ratio is conserved rather than CO_2 mass. CO_2 is chemically inert in HadGEM2-ES so all of the changes in its concentration are driven by surface emissions or sinks.

3 Non-CO_2 well mixed greenhouse gases

Specification of the following non-CO_2 well-mixed greenhouse gases is required in HadGEM2-ES: CH_4, N_2O and halocarbons. For the control run, historical and RCP simulations they are implemented as described below and shown in Fig. 2. The CO_2 emissions-driven experiment and the historical/RCP decoupled carbon cycle experiments also use these time varying values, as do the AMIP runs and the detection and attribution experiments which require time variation of GHGs. GHG concentrations during the palaeo-climate simulations are described in Sect. 8.

3.1 CH_4 concentration

Atmospheric methane concentrations were prescribed as global mean mass mixing ratios. For experiments with time-variable CH_4 concentrations (historical RCP experiments), these were linearly interpolated from the annual concentrations for every time step of the model. These interpolated CH_4 concentrations were then passed to the tropospheric chemistry scheme in HadGEM2-ES (United Kingdom Chemistry and Aerosols: UKCA, O'Connor et al., 2011). Within UKCA, the surface CH_4 concentration was forced to follow the prescribed scenario and surface CH_4 emissions were decoupled. CH_4 concentrations above the surface were calculated interactively, and the full 3-D CH_4 field was then passed from UKCA to the HadGEM2-ES radiation scheme.

As CH_4 concentrations were only prescribed at the surface, CH_4 in HadGEM2-ES above the surface is free to evolve in a non-uniform structure and may differ from prescribed, well-mixed historical or RCP CH_4 concentrations. The impact of passing a full 3-D CH_4 field from UKCA to the

Table 2. Definition of the manner in which the Houghton (2008) land use emissions data (H08) and RCP data were combined in years 2000 to 2005. The last two columns show how the cumulative emissions from the original H08 data compare with those of the rescaled data, the latter being 0.94 GtC lower over the period considered.

Year	H08 contribution (fraction)	RCP contribution (fraction)	H08 value, TgC yr^{-1}	RCP value, TgC yr^{-1}	Rescaled value, TgC yr^{-1}	Cumulative emissions from 2000 onwards, TgC	
						H08	Rescaled
2000	1	0	1409.9	1149	1409.9	1409.9	1409.9
2001	0.8	0.2	1385.4	1158.4	1340	2795.3	2749.9
2002	0.6	0.4	1517.7	1167.8	1377.74	4313	4127.64
2003	0.4	0.6	1513.2	1177.2	1311.6	5826.2	5439.24
2004	0.2	0.8	1534.9	1186.6	1256.26	7361.1	6695.5
2005	0	1	1467.3	1196	1196	8828.4	7891.5

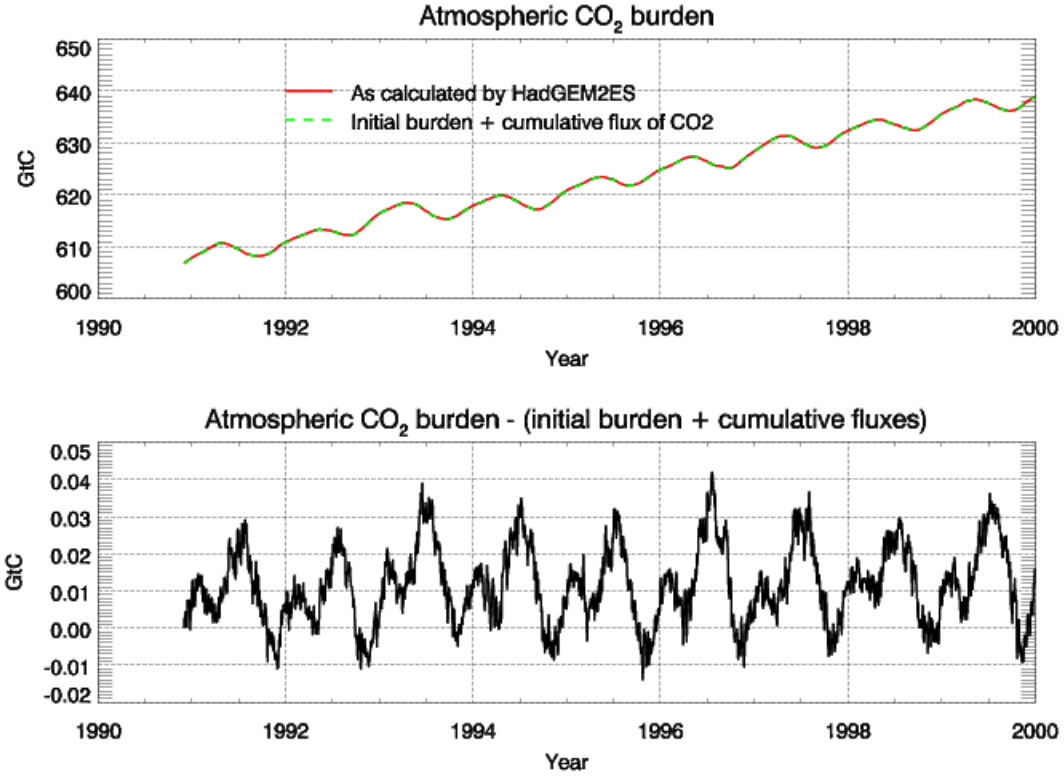

Fig. 5. The evolution of atmospheric CO_2 in HadGEM2-ES. Daily atmospheric CO_2 amount (top panel) simulated by HadGEM2-ES (red line), overlaid with the initial atmospheric burden plus the cumulative sum of CO_2 into the atmosphere (dashed green line). The lower panel shows the difference between the two.

radiation scheme rather than passing a uniform concentration everywhere was evaluated in a present-day atmosphere-only configuration of the HadGEM1 model (Johns et al., 2006; Martin et al., 2006). The full 3-D CH_4 field lead to the extra-tropical stratosphere being cooler by 0.5–1.0 K, thereby reducing the warm temperature biases in the model (O'Connor et al., 2009).

The CH_4 concentrations used were taken from the recommended CMIP5 dataset. For the historical period (1860 to 2005), these were assembled from Law Dome ice core measurements reported by Etheridge et al. (1998) and prepared for the NASA GISS model (see URL 8 in Appendix A). Beyond 1984, concentrations were provided by E. Dlugokencky and from the global NOAA/ESRL global monitoring network (see URL 9 in Appendix A). For more details, see Meinshausen et al. (2011). Figure 2b shows CH_4 concentrations over the historical period (1860 to 2005) and for the RCP scenarios up to 2300. This dataset also provided the

CH_4 concentration used in the pre-industrial control simulation (taken here to be 1860 AD) which was 805.25 ppb.

3.2 N_2O concentration

Atmospheric N_2O concentrations were prescribed as a time series of annual global mean mass mixing ratios in the centennial CMIP5 simulations, as described in Meinshausen et al. (2011). The annual concentrations were linearly interpolated onto the time steps of HadGEM2-ES and passed to the model's radiation scheme. Figure 2c shows the N_2O concentrations for the 4 RCPs over the historical period and from the RCPs from 2005–2300. This dataset also provided the N_2O concentration used in the pre-industrial control simulation (taken here to be 1860 AD) which was 276.4 ppb.

3.3 Atmospheric halocarbon concentration

Atmospheric concentrations of halocarbons were prescribed as a time series of annual global mean concentrations in the centennial multi-forcing CMIP5 simulations and interpolated linearly to the model's time steps. The future concentrations of halocarbons controlled under the Montreal Protocol are primarily based on the emissions underlying the WMO A1 scenario (Daniel et al., 2007) – calculated with a simplified climate model MAGICC, taking into account changes in atmospheric lifetimes due to changes in tropospheric OH-related sinks and stratospheric sinks due to an enhancement of the Brewer-Dobson circulation (Meinshausen et al., 2011).

The CMIP5 dataset provided concentrations of 27 halocarbon species, more than GCMs generally represent separately (for example, HadGEM2-ES explicitly represents the radiative forcing of 6 of these species). The data is therefore also supplied aggregated into concentrations of "equivalent CFC-12" and "equivalent HFC-134a", representing all gases controlled under the Montreal and Kyoto protocols, respectively. These equivalent concentrations were used in HadGEM2-ES (Fig. 2d). Halocarbon concentrations were set to zero for the pre-industrial control run.

The CMIP5 "equivalent" concentrations of CFC12 and HFC134a were derived by simply summing the radiative forcing of individual species and assuming linearity of the relationship between the concentration and radiative forcing for a single species and additivity of multiple species. To quantify the difference between using equivalent CFC-12 and HFC-134a and the full set of possible species a set of five test simulations was completed:

1. Control: halocarbons assumed zero, CO_2 at $1 \times CO_2$ (286.3 ppm).
2. Halocarbons assumed zero, CO_2 at 2100 RCP8.5 concentrations (936 ppm).
3. Halocarbons assumed constant at 2100 RCP8.5 concentrations (aggregated as CFC-12eq and HFC-134Aeq), CO_2 at $1 \times CO_2$.
4. Halocarbons assumed constant at 2100 RCP 8.5 concentrations with Montreal species split (i.e., CFC-11, CFC-12, CFC-113 and HCFC-22, remaining gases aggregated as CFC-12eq and HFC-134Aeq), CO_2 at $1 \times CO_2$.
5. Halocarbons assumed constant at RCP 8.5 2100 concentrations with Kyoto species split (i.e., HFC-134a and HFC125 and remaining gases aggregated as CFC-12eq and HFC-134Aeq), CO_2 at $1 \times CO_2$.

Upward and downward fluxes of longwave radiation were saved on all vertical levels in the atmosphere after the first model timestep (so that the meteorology is identical). It should be noted that species not available in HadGEM2-ES are combined into either HFC-134a or CFC-12 according to their classification. Species are combined into equivalent HFC-134a and CFC-12 by summing their radiative forcing consistently with the CMIP5 methodology. Figure 6 shows excellent agreement between the "equivalent" gases and the more detailed representation from experiments 3, 4, 5 above. Zonal mean differences are within $1\,\mathrm{m\,Wm^{-2}}$ everywhere showing that the use of 2 CFC equivalent species in CMIP5 is justified.

4 Ozone

4.1 Tropospheric ozone pre-cursor emissions and concentrations

Tropospheric ozone (O_3) is a significant greenhouse gas due to its absorption in the infrared, visible, and ultraviolet spectral regions (Lacis et al., 1990). It has increased substantially since pre-industrial times, particularly in the northern mid-latitudes (e.g. Staehelin et al., 2001), which has been linked by various studies to increasing emissions of tropospheric O_3 pre-cursors: nitrogen oxides ($NO_x = NO + NO_2$), carbon monoxide (CO), methane (CH_4), and non-methane volatile organic compounds (NMVOCs; e.g. Wang and Jacob, 1998). As a result, the tropospheric chemistry configuration of the UKCA model (O'Connor et al., 2011) was implemented in HadGEM2-ES and used in all CMIP5 simulations to simulate the time evolution of tropospheric O_3 interactively rather than having it prescribed. The UKCA chemistry scheme includes a description of inorganic odd oxygen (O_x), nitrogen (NO_y), hydrogen (HO_x), and CO chemistry with near-explicit treatment of CH_4, ethane (C_2H_6), propane (C_3H_8), and acetone (Me_2CO) degradation (including formaldehyde (HCHO), acetaldehyde (MeCHO), peroxy acetyl nitrate (PAN), and peroxy propionyl nitrate (PPAN). It makes use of 25 tracers and represents 41 species, which participate in 25 photolytic reactions, 83 bimolecular reactions, and 13 uni- and termolecular reactions. Wet and dry deposition is also taken into account. Emissions from surface sources and aircraft were prescribed as monthly mean

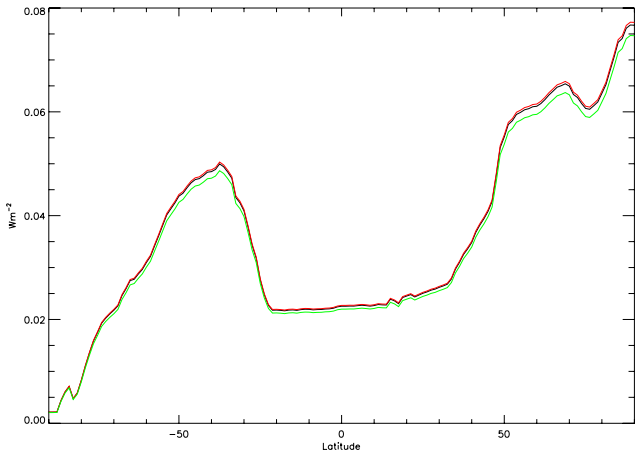

Fig. 6. Zonal-mean net tropopause forcing in which halocarbons controlled under the Montreal and Kyoto Protocol are represented as one equivalent species each, CFC-12 and HFC-134a, respectively (black line). The sensitivity tests with Montreal gases split into individual species (red line) and Kyoto gases split into individual species (green line) show a close agreement.

fields and lightning emissions were computed interactively. A full description and evaluation of the chemistry scheme in HadGEM2-ES can be found in O'Connor et al. (2011). Although transport and chemistry were calculated up to the model lid, boundary conditions were applied within UKCA. In the case of O_3, it was overwritten in those model levels which were 3 levels (approximately 3–4 km) above the diagnosed tropopause (Hoerling et al., 1993) using the stratospheric O_3 concentration dataset described in Sect. 4.2. It is this combined O_3 field which is then passed to the model's radiation scheme. Furthermore, oxidation of sulphur dioxide and dimethyl sulphide (DMS) into sulphate aerosol (described in Sect. 5) involves hydroxyl (OH), hydroperoxyl (HO_2), hydrogen peroxide (H_2O_2), and O_3, whose concentrations are provided to the model's sulphur cycle from UKCA.

No prescribed tropospheric ozone abundance data were used within HadGEM2-ES. Instead, the tropospheric evolution of ozone was simulated using surface and aircraft emissions of tropospheric ozone precursors and reactive gases. It is these emissions, rather than tropospheric ozone concentrations which are held constant in the pre-industrial control simulation. For the palaeoclimate simulations, the same pre-industrial emissions are also used as described in Sect. 8. For the historical and future simulations (including the emissions driven and decoupled carbon cycle experiments, and AMIP runs) a time-varying data set of emissions is used. As the time evolution of tropospheric ozone is simulated rather than prescribed, it may diverge from historical or RCP supplied tropospheric ozone (Lamarque et al., 2011). The emissions data used by HadGEM2-ES has been supplied for CMIP5 by Lamarque et al. (2010) and by the IAMs for the 4 RCPs. Speciated surface emissions were provided for the following sectors: land-based anthropogenic sources (agriculture, agricultural waste burning, energy production and distribution, industry, residential and commercial combustion, solvent production and use, land-based transportation, and waste treatment and disposal), biomass burning (forest fires and grass fires), and shipping. They were valid for the specific year provided with a time resolution of 10 years in the case of anthropogenic and shipping emissions but as decadal means for biomass burning. This was considered appropriate for biomass burning emissions due to their substantial inter-annual variability both globally and regionally (Lamarque et al., 2010). All surface emissions were provided as monthly means on a $0.5° \times 0.5°$ grid. In the case of aircraft emissions, they were provided as monthly means on a $0.5° \times 0.5°$ horizontal grid and on 25 levels in the vertical, extending from the surface up to 15 km.

For the UKCA tropospheric chemistry scheme used in HadGEM2-ES, surface emissions for the following species were considered: C_2H_6, C_3H_8, CH_4, CO, HCHO, Me_2CO, MeCHO, and NO_x. For the CMIP5 simulations, the spatially uniform surface CH_4 concentration is prescribed (as described in Sect. 3.1), and hence the surface CH_4 emissions are essentially redundant in this case. For each species the provided emissions were re-gridded onto the model's N96 grid ($1.75° \times 1.25°$). A small adjustment was made after re-gridding to ensure the global totals matched those of the original data.

For emissions of C_2H_6, it was decided to combine all C2 species (C_2H_6, ethene (C_2H_4), and ethyne (C_2H_2)) and treat as emissions of C_2H_6. These were each converted to $kg(C_2H_6)\,m^{-2}\,s^{-1}$, added together, and then regridded. For C_3H_8, the C3 species (propane and propene (C_3H_6)) were similarly combined and treated as emissions of C_3H_8.

For CO, emissions from land-based anthropogenic sources, biomass burning, and shipping were taken for the historical period from Lamarque et al. (2010). These were added together and re-gridded on to an intermediate $1° \times 1°$ grid in terms of $kg(CO)\,m^{-2}\,s^{-1}$. Oceanic CO emissions were also added ($45\,Tg(CO)\,yr^{-1}$), and their spatial and temporal distribution were provided by the Global Emissions Inventory Activity (see URL 10 in Appendix A), based on distributions of oceanic VOC emissions from Guenther et al. (1995). In the absence of an isoprene (C_5H_8) oxidation mechanism in the UKCA tropospheric chemistry scheme used in HadGEM2-ES, an additional $354\,Tg(CO)\,yr^{-1}$ was added based on a global mean CO yield of 30 % from C_5H_8 from a study by Pfister et al. (2008) and a global C_5H_8 emission source of 506 TgC yr (Guenther et al., 1995). It is distributed spatially and temporally using C_5H_8 emissions from Guenther et al. (1995) and added to the other monthly mean emissions on the $1° \times 1°$ grid before regridding.

For HCHO emissions, the monthly mean land-based anthropogenic sources were combined with monthly mean biomass burning emissions from Lamarque et al. (2010) for

the historical period and re-gridded. Similar processing was applied to the future emissions supplied by the IAMs for the 4 RCPs.

For MeCHO, the monthly mean NMVOC biomass burning emissions from Lamarque et al. (2010) for the historical period were used. Using different emission factors from Andreae and Merlet (2001) for grass fires, tropical forest fires, and extra-tropical forest fires, emissions of NMVOCs were converted into emissions of MeCHO (i.e. kg(MeCHO) m^{-2} s^{-1}). Surface emissions of Me_2CO were taken from land-based anthropogenic sources and biomass burning from Lamarque et al. (2010, 2011). These were added together and re-gridded on to an intermediate $1^\circ \times 1^\circ$ grid in terms of kg(Me_2CO) m^{-2} s^{-1}. Then, the dominant source of Me_2CO from vegetation was added, based on a global distribution from Guenther et al. (1995) and scaled to give a global annual total of 40.0 Tg(Me_2CO) yr^{-1}. The total monthly mean emissions were then re-gridded on to the model's N96 grid. For future emissions, the processing was identical.

Finally for NO_x surface emissions, contributions from land-based anthropogenic sources, biomass burning, and shipping from Lamarque et al. (2010) were added together and re-gridded on to an intermediate $1^\circ \times 1^\circ$ grid in terms of kg(NO) m^{-2} s^{-1}. Added to these were a contribution from natural soil emissions, based on a global and monthly distribution provided by GEIA on a $1^\circ \times 1^\circ$ grid (see URL 10 in Appendix A), and based on the global empirical model of soil-biogenic emissions from Yienger and Levy II (1995). These were scaled to contribute an additional 12 Tg(NO) yr^{-1}. A similar approach was adopted when processing the future emissions. All emissions provided were processed as above for the years supplied and a linear interpolation applied between years to produce emissions for every year. Figure 7 shows the time evolution of tropospheric O_3 pre-cursor surface emissions over the 1850–2100 time period. After 2100, tropospheric ozone precursor emissions were kept constant.

In the case of NO_x emissions, 3-D emissions from aircraft were also considered. These were supplied as monthly mean fields of either NO or NO_2 on a 25 level (L25) 0.5×0.5 grid by Lamarque et al. (2010) for the historical period. For HadGEM2-ES we used the NO emissions. They were first re-gridded on to an N96 $\times$ L25 grid and then projected on to the model's N96 $\times$ L38 grid, ensuring that the global annual total emissions were conserved. A similar approach was adopted when processing the future emissions.

No additional coding in the HadGEM2-ES or UKCA models was necessary for the treatment of tropospheric ozone pre-cursor emissions. The only code change was required for the Detection and Attribution "greenhouse gases only" simulation (7.2). In this case, the UKCA model was modified to maintain the global mean surface CH_4 concentration at pre-industrial levels i.e. 805.25 ppb. This was to ensure that the increase in CH_4 concentration as seen by the radiation scheme did not affect concentrations of tropospheric oxidants, thereby influencing the rate of sulphate aerosol formation.

4.2 Stratospheric ozone concentration

HadGEM2-ES requires stratospheric ozone to be input as monthly zonal/height ancillary files. CMIP5 recommends the use of the AC&C/SPARC ozone database (Cionni et al., 2011) which covers the period 1850 to 2100 and can be used in climate models that do not include interactive chemistry. The pre-industrial dataset consists of a repeating seasonal cycle of ozone values, and this is also used for the palaeoclimate simulations described in Sect. 8. For the historical and future simulations (including the emissions driven and decoupled carbon cycle experiments, and AMIP runs) a time-varying data set of stratospheric ozone is used.

The historical part of the AC&C/SPARC ozone database spans the period 1850 to 2009 and consists of separate stratospheric and tropospheric data sources. The future part of the AC&C/SPARC ozone database covers the period 2010 to 2100 and seamlessly extends the historical database also including separate stratospheric and tropospheric data sources based on 13 CCMs that performed a future simulation until 2100 under the SRES A1B GHG scenario.

The AC&C/SPARC ozone is provided on pressure levels between 1000-1 hPa. The UK National Centre for Atmospheric Science (NCAS) has produced an updated version of the SPARC ozone dataset as follows.

A multiple-linear regression was performed on the historical raw pressure-level data between 1000-1 hPa consistent with the Randel and Wu (1999) method used to construct the timeseries. The ozone was then represented as: $O_3(t) = a*\mathrm{SOL} + b*\mathrm{EESC} + \mathrm{seasonal\_cycle} + \mathrm{residuals}$. For consistency, the indices of 11-yr solar cycle (SOL) and total equivalent chlorine (EESC) are identical to those used to prepare the original dataset. The SOL index is a 180.5 nm timeseries provided by Fei Wu at NCAR. The standard SPARC ozone dataset which extends into the future does not include solar cycle variability post-2009. For production of a dataset extending into the future including an 11-yr ozone solar cycle, the solar regression index is used to build a future time series consistent with a repeating solar irradiance compiled by the Met Office Hadley Centre (see Sect. 7.1) and is modelled as a sinusoid with a period of 11 yr, with mean and max-min values corresponding to solar cycle 23 normalised against the 180.5 nm timeseries used in the historical ozone. There is no solar ozone signal in the high latitudes.

The data were then horizontally interpolated onto a N96 grid. Vertical interpolation was achieved by hydrostatically mapping the SPARC ozone data from pressure surfaces onto pressure surface equivalent levels corresponding to the height-based grid used by HadGEM2-ES using a scale height of 7 km.

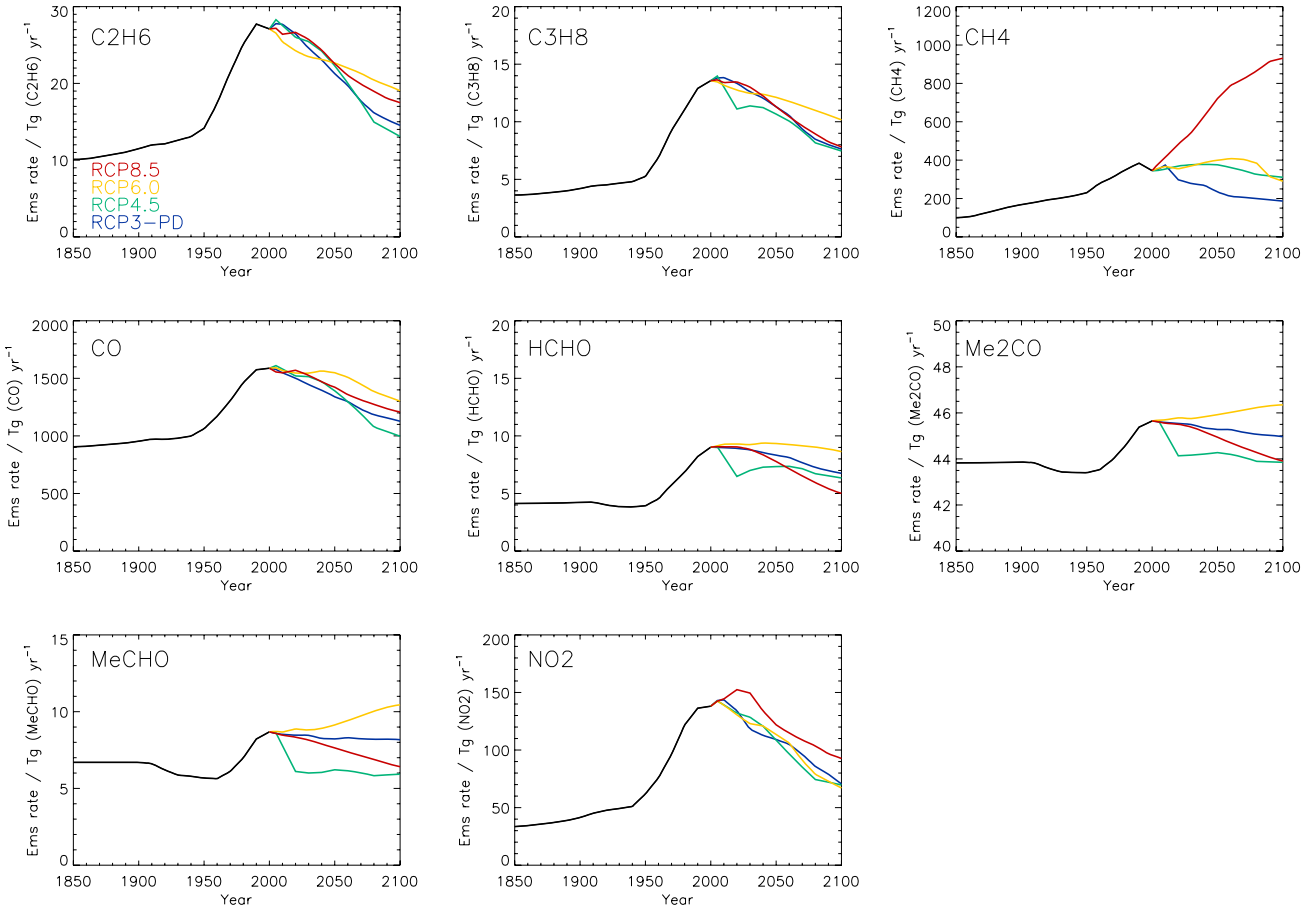

Fig. 7. Tropospheric ozone pre-cursor surface emissions over the historical period (1850–2005) and over the future period (2005–2100) from the 4 RCPs: RCP3-PD (blue), RCP4.5 (green), RCP6 (yellow), and RCP8.5 (red). The methane (CH_4) emissions shown do not include a contribution from wetlands.

5 Tropospheric aerosol forcing

HadGEM2-ES simulates concentrations of six tropospheric aerosol species: ammonium sulphate, fossil-fuel black carbon, fossil-fuel organic carbon, biomass-burning, sea-salt, and mineral dust aerosols (Bellouin et al., 2007; Collins et al., 2011). Although an ammonium nitrate aerosol scheme is available to HadGEM2-ES, it was still in its developmental version when CMIP5 simulations started, hence nitrate aerosols are not included in the CMIP5 simulations. In addition, secondary organic aerosols from biogenic emissions are represented by a fixed climatology. All aerosol species can exert a direct effect by scattering and absorbing shortwave and longwave radiation, and a semi-direct effect whereby this direct effect modifies atmospheric vertical profiles of temperature and clouds. In HadGEM2-ES all aerosol species, except fossil-fuel black carbon and mineral dust, also contribute to both the first and second indirect effects on clouds, modifying cloud albedo and precipitation efficiency, respectively. Changes in direct and indirect effects since 1860 are termed aerosol radiative forcing. The magnitude of this forcing depends on changes in aerosols, which are due in part to changes in emissions of primary aerosols and aerosol precursors. Changes in emission rates are either derived from external datasets or due to changes in the simulated climate. Here we document how any changes in emission rates are implemented in the HadGEM2-ES CMIP5 centennial experiments. In the control run we specify a repeating seasonal cycle of 1860 emissions, and this is also used in the palaeoclimate simulations (Sect. 8). Historical and future simulations (including the emissions-driven and decoupled carbon cycle experiments and AMIP runs) use time-varying emissions as described in this section.

In HadGEM2-ES sea-salt and mineral dust aerosol emissions are computed interactively, whereas emission datasets drive schemes for sulphate, fossil-fuel black and organic carbon, and biomass aerosols. Unless otherwise stated, datasets are derived from the historical and RCP time series prepared for CMIP5. All non-interactive emission fields are interpolated by the model every five simulated days from prescribed monthly-mean fields. Timeseries of non-interactive emissions are shown in Fig. 10. Aircraft emissions of aerosol

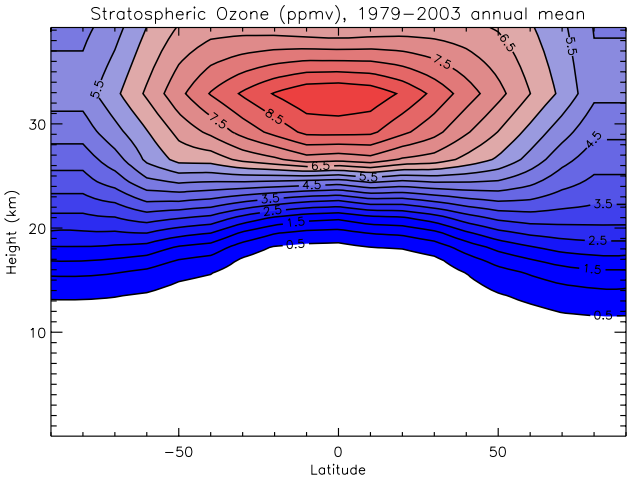

Fig. 8. Annual mean climatology of ozone volume mixing ration (ppmv) for 1979–2003.

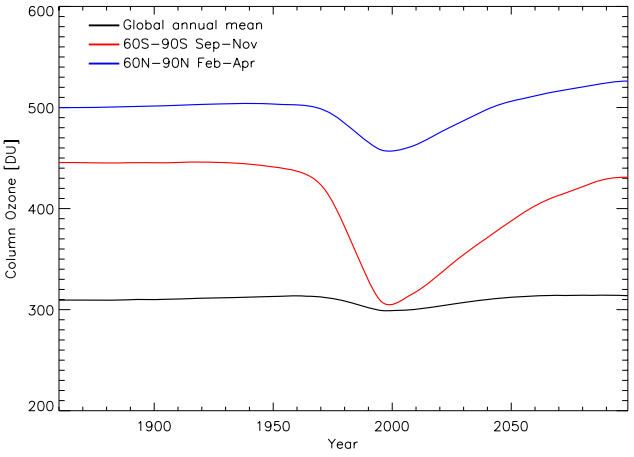

Fig. 9. Timeseries of column ozone (in Dobson Units, DU) for global annual mean (black line), 60° S–90° S September–November mean (red line) and 60° N–90° N February–April mean (blue line).

precursors and primary aerosols are not included in the model.

The sulphur cycle, which provides concentrations of ammonium sulphate aerosols, requires emissions of sulphur dioxide (SO_2) and dimethyl-sulphide (DMS). Sulphur dioxide emissions are derived from sector-based emissions. Emissions for all sectors are injected at the surface, except for energy emissions and half of industrial emissions which are injected at 0.5 km to represent chimney-level emissions. Sulphur dioxide emissions from biomass burning are not included. The model accounts for three-dimensional background emissions of sulphur dioxide from degassing volcanoes, taken from Andres and Kasgnoc (1998). This represents a constant rate of 0.62 Tg[S] yr^{-1} on a global average, independent of the year simulated and is not part of the implementation of volcanic climate forcing which we discuss in Sect. 7.2. Similarly, land-based DMS emissions do not vary in time and give 0.86 Tg yr^{-1} (Spiro et al., 1992). Oceanic DMS emissions are provided interactively by the biogeochemical scheme of the ocean model as a function of local chlorophyll concentrations and mixed layer depth (based on Simo and Dachs, 2002). In an objective assessment against ship-board and time-series DMS observations, the HadGEM2-ES interactive ocean DMS scheme performs with similar skill to that found in the widely used Kettle et al. (1999) climatology (Halloran et al., 2010). The primary differences between the model-simulated and the climatology-interpolated surface ocean DMS fields are; lower model Southern Hemisphere summer Southern Ocean DMS concentrations, higher model annual equatorial DMS concentrations, and a reduced model seasonal cycle amplitude. Oxidation of sulphur-dioxide and DMS into sulphate aerosol involves hydroxyl (OH), hydroperoxyl (HO_2), hydrogen peroxide (H_2O_2), and ozone (O_3): concentrations for those oxidants are provided by the tropospheric chemistry scheme.

Emissions of primary black and organic carbon from fossil fuel and biofuel are injected at 80 m. Emissions of biomass-burning aerosols are the sum of the biomass-burning emissions of black and organic carbon. Grassfire emissions are assumed to be located at the surface, while forest fire emissions are injected homogeneously across the boundary layer (0.8 to 2.9 km).

Sea-salt emissions are computed interactively over open oceans at each model time step from near-surface (10 m) wind speeds (Jones et al., 2001). Mineral dust emissions are also interactive, and depend on near-surface wind speed, land cover and soil properties. The scheme is described in Woodward (2011). It is based on that designed for HadAM3 (Woodward, 2001) with major developments including the modelling of particles up to 2 mm in the horizontal flux, threshold friction velocities based on Bagnold (1941), a modified version of the Fécan et al. (1999) soil moisture treatment and the utilisation of a preferential source multiplier similar to that described in Ginoux et al. (2001).

Finally, secondary organic aerosols from biogenic emissions are represented by monthly distributions of three-dimensional mass-mixing ratios obtained from a chemistry transport model (Derwent et al., 2003). These distributions are constant for all simulated years.

6 Land-use and land-use change

The HadGEM2-ES land-surface scheme incorporates the TRIFFID DGVM (Cox, 2001), and as such simulates internally the land cover (and its evolution) in response to climate (and climate change). Hence we do not directly impose prescribed land-cover or vegetation types, but rather provide a fractional mask of anthropogenic disturbance as a boundary

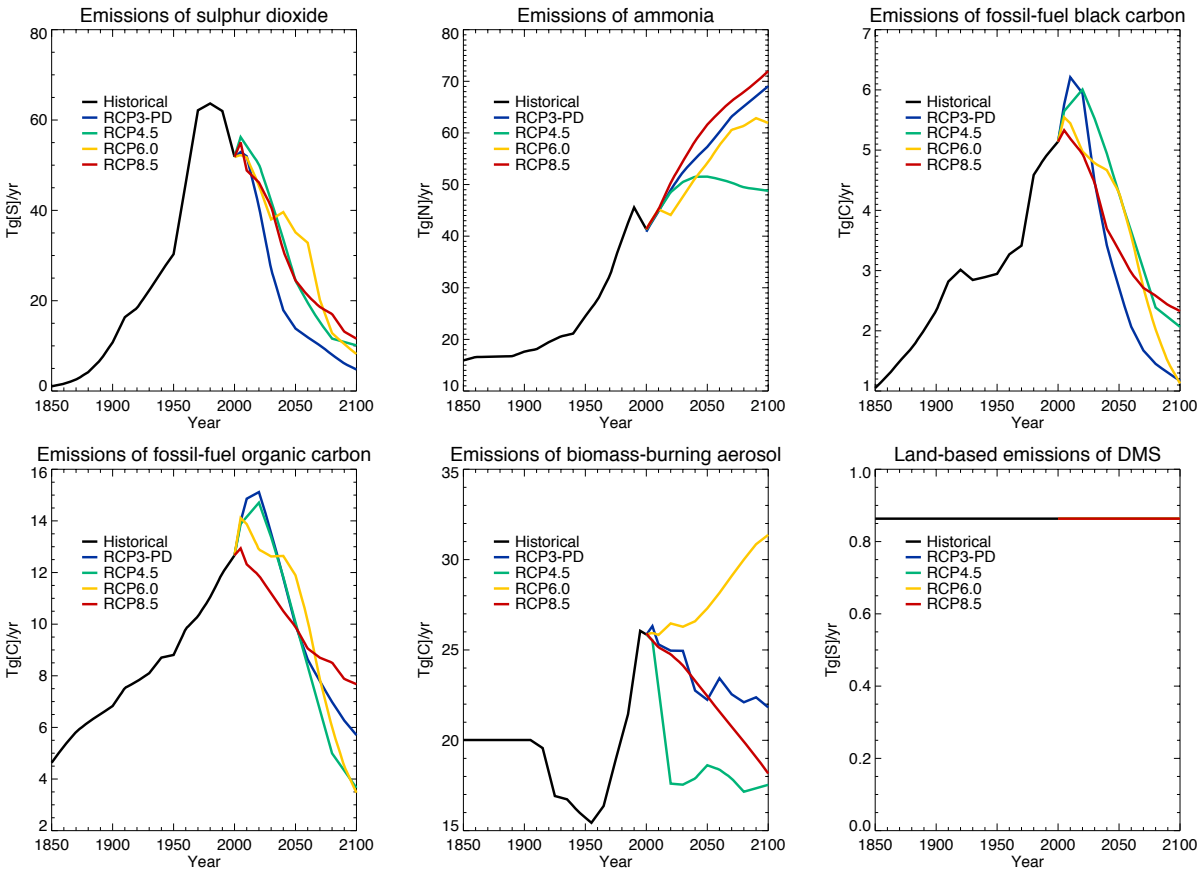

Fig. 10. Tropospheric aerosol precursors and aerosol primary emissions over the historical period (1860–2005), and future period (2005–2100) for 4 RCPs: RCP3-PD (blue), RCP4.5 (green), RCP6.0 (yellow), RCP8.5 (red).

condition to the dynamic vegetation scheme. Previous Met Office Hadley Centre coupled climate-carbon cycle simulations (e.g. Cox et al., 2000; Freidlingstein et al., 2006) used a static (present day) agricultural mask. However the dynamic vegetation scheme, TRIFFID has now been updated to allow time-varying land-use distributions in the CMIP5 simulations.

TRIFFID represents the fractional coverage in each grid cell of 5 plant functional types (PFTs: broadleaf tree, needleleaf tree, C3 grass, C4 grass, shrub) and also bare soil. Prescribed fractions of urban areas, lakes and ice are also included from the IGBP land cover map (Loveland et al., 2000) and do not vary in time. The summed fractional coverage of crop and pasture is provided as a time-varying input. Within a grid box tree and shrub PFTs are excluded from this fraction allowing natural grasses to grow and represent "crops". Abandonment of crop land removes this constraint on trees and shrubs but we do not specify instant replacement by these woody PFTs, but rather their regrowth is simulated by the model's vegetation dynamics. If woody vegetation cover reduces because of a land use change, vegetation carbon from the removed woody PFTs goes partially to the soil carbon pool and partially to a series of wood products pools. These wood products pools have turnover rates of 1, 10 and 100 yr and are not sensitive to environmental conditions. The fraction of vegetation carbon directed into the wood products pool is proportional to the ratio of above ground and below ground carbon pools ((leaf carbon + stem carbon)/root carbon). Distribution of disturbed biomass into the different carbon pools depends on the vegetation type consistent with McGuire et al. (2001) and is shown in Table 3.

Table 3. Allocation of aboveground displaced carbon to the different wood products pools, based on the values given in McGuire et al. (2001, Table 3) but recalculated to be applied to just the aboveground carbon flux.

	1 yr	10 yr	100 yr
Broadleaf tree	60 %	30 %	10 %
Needleleaf tree	60 %	40 %	0 %
Shrub	80 %	20 %	0 %

HadGEM2-ES is therefore able to simulate both biophysical and biogeochemical effects of land-use change as well as natural changes in vegetation cover in response to changing climate and CO_2. In this version of the model only anthropogenic disturbance in the form of crop and pasture is represented. Data on within-grid-cell transitions due to shifting cultivation or the impact of wood harvest are not yet used. As described in Sect. 2.2, CO_2 emissions from land-use change can be simulated by HadGEM2-ES but are not used interactively in the emissions driven experiment.

The biophysical impacts of land use change include the direct effect of changes to surface albedo and roughness due to land-cover change and also changes to the hydrological cycle due to changes in evapotranspiration and runoff. There is also an indirect physical effect due to changes in surface emissions of mineral dust caused by changes in bare soil fraction, windspeed and soil moisture, which has a radiative effect in the atmosphere.

Historic and future simulations (including the emissions-driven and decoupled carbon cycle simulations and AMIP runs) use time varying disturbance from the Hurtt et al. (2011) dataset described below. The pre-industrial control simulation uses an agricultural disturbance mask, fixed in time at 1860 values in this same dataset. The natural and GHG detection and attribution simulations (7.1, 7.2) also use a fixed, pre-industrial land-use disturbance mask, but the land-use only simulations (7.3) use the time varying historical data as in the full historical simulation. For the mid-Holocene and LGM experiments, there is no agricultural disturbance (which therefore differs from the control run where a pre-industrial disturbance mask is used). The Last Millennium and AMIP simulations do not use the dynamic vegetation scheme of HadGEM2-ES and instead directly prescribe land-cover as described in Sects. 8 and 9, respectively.

The historical land use data is based on the HYDE database v3.1 (Klein Goldewijk et al., 2010, 2011), whilst the future RCP land use scenarios were produced by the respective IAMs and are thus internally consistent with the socio-economic storylines and carbon emissions of the scenarios. A harmonization manipulation was performed, as described in Hurtt et al. (2009, 2011), that attempts to preserve gridded and regional IAM crop and pasture changes as much as possible while minimizing the differences in 2005 between the historical estimates and future projections (Fig. 11). The harmonization procedure employs the Global Land-use Model (GLM) that ensures a smooth and consistent transition in the harmonization year, grids (or re-grids) the data when necessary, spatially allocates national/regional wood harvest statistics, and computes all the resulting land-use states and transitions between land-use states annually from 1500–2100 at half-degree (fractional) spatial resolution, including the effects of wood harvesting and shifting cultivation. Both historical and future scenarios were made available at $0.5° \times 0.5°$ resolution with annual increments and were downloaded (see URL 11 in Appendix A).

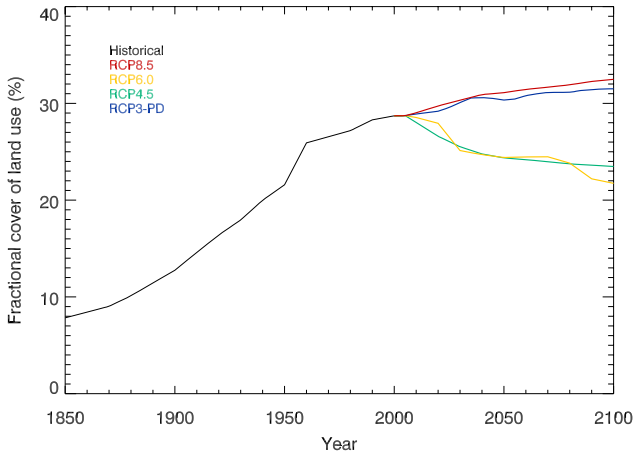

Fig. 11. Fractional coverage of anthropogenic disturbance, defined as the sum of crop and pasture, for the historical period 1860–2005, and up to 2100 following the 4 RCP scenarios, RCP3-PD (blue), RCP4.5 (green), RCP6 (yellow) and RCP8.5 (red).

The crop and pasture fraction is re-gridded onto the HadGEM2-ES grid using area average re-gridding. Crop and pasture are then combined to produce a combined "agriculture" mask (Fig. 12). It is assumed crop and pasture both mean "only grass, no tree or shrub". This assumption is simplistic as in some regions of the world "pasture" refers to rangeland where animals are allowed to graze on whatever natural vegetation exists there (which may include trees and shrub). Similarly, woody biofuel crops are treated (erroneously in this case) as non-woody crops. As noted by Hurtt et al. (2011), the definition and reporting of biofuel differs even within the IAMs producing the 4 RCP scenarios. However, the necessary data to avoid these problems are not available and we expect the impact of any inconsistency to be minor. It remains an outstanding research activity to improve past and present reconstructions of land-cover which can account for temporally and regionally varying changes in definitions and terminology.

Our approach of allocating displaced woody biomass into product pools which subsequently release CO_2 to the atmosphere means that our definition of "land use CO_2 flux" that will be reported in this diagnostic is rather limited – it will not contain any subsequent changes in soil carbon for example, nor will it capture any effects of agricultural abandonment and regrowth. This diagnostic, therefore, should be seen as a part of the complex system of land-use carbon fluxes. A more complete picture of the impact of land-use change on carbon storage in HadGEM2-ES would require further simulations as discussed in Arora and Boer (2010). For example calculations could be made with offline simulations of the land-surface model, or two different GCM simulations (with and without land-use changes) and diagnosing the differences between them. It is vital when reporting or

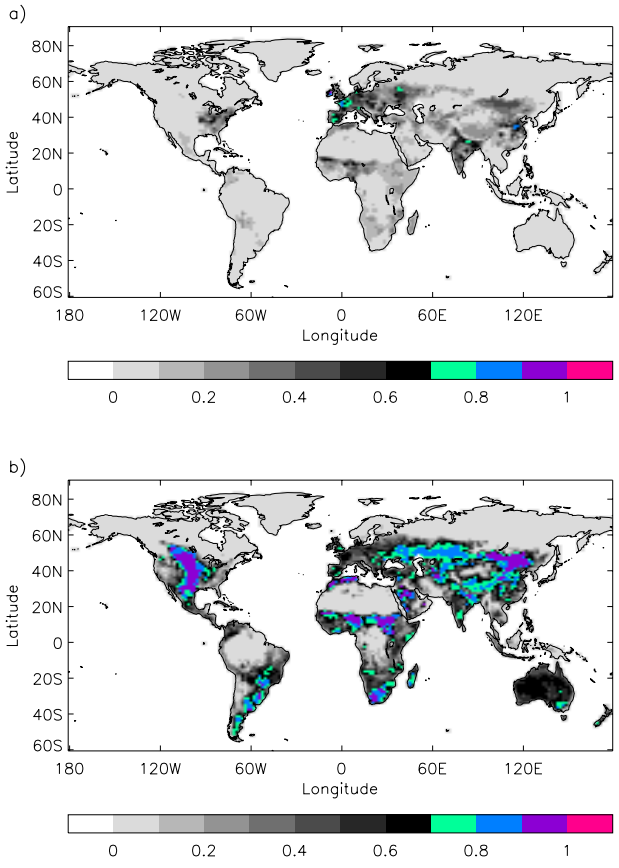

Fig. 12. Historical land use presented as fractional anthropogenic disturbance at **(a)** 1860 and **(b)** 2005.

analysing land-use emissions from such models, or comparing between different models or techniques that the precise methodology is described to avoid misunderstanding. It remains a research priority to formally define methodologies for reporting simulated land-use fluxes.

An additional uncertainty in reporting the land use carbon fluxes is that the wood products pools are assumed to be zero everywhere at 1860 whilst the terrestrial carbon cycle (carbon content and vegetation fractions) have been run to equilibrium with 1860 climate and anthropogenic disturbance. Changes in land use cover prior to 1860 involve land use expansion and hence both direct emissions prior to 1860 and some legacy emissions post-1860 due to inputs of disturbed biomass to the soil carbon. No attempt has been made to include these effects in our output but future work will assess and quantify this effect.

7 Natural climate forcing

HadGEM2-ES can simulate the climate response to two aspects of natural climate forcing: changes in solar irradiance and stratospheric volcanic aerosol. In the control experiment these forcings are kept constant in time. For the historical experiments (including the emissions-driven and decoupled carbon cycle simulations and AMIP runs) they are varied due to observed reconstructions. For simulations of future periods, where natural forcings are not known, they are varied as described here to minimise the impact of possibly incorrect assumptions about the natural forcings. See Sect. 8 for details on the solar and volcanic forcings applied to the palaeoclimate simulations.

7.1 Total solar irradiance

The way the model deals with variations in total solar irradiance (TSI) is the same as in earlier generations of Hadley Centre models, HadCM3 (Stott et al., 2000; Tett et al., 2002) and HadGEM1 (Stott et al., 2006). Annual mean variations in TSI are partitioned across the six shortwave spectral bands (0.2–10 μm) to estimate the associated spectral changes with TSI variations (Lean et al., 1995a). With the changes across the spectral bands the Rayleigh scattering and ozone absorption properties are also varied. See Stott et al. (2006) for further details.

The TSI data used for the historic period were recommended by CMIP5 (Lean et al., 2009 -L09) and are created from reconstructions of solar cycle and background variations in TSI. The solar cycle component is produced from a multiple regression of proxy measures of bright and dark regions of the Sun with satellite reconstructions of TSI (Fröhlich and Lean, 2004). Background variations in TSI are produced from a model of solar magnetic flux incorporating historic sunspot numbers (Wang et al., 2005). The annual mean TSI was processed to force the mean of the 1700–2004 period to be the same as the model control solar constant value (1365 Wm^{-2}).

The annual mean TSI and variations across the UV, visible and IR bands are shown in Fig. 13. For comparison the TSI used in previous model simulations are also shown. The TSI now recommended for use in CMIP5 studies is consistent with the latest assessment of TSI variations by the IPCC's Fourth Assessment report – AR4 – (Forster et al., 2007) which estimated the solar radiative forcing to be 50 % of that given in the previous report. The increase in TSI for L09 between the Maunder minimum in the 17th century and the average over the last 2 solar cycles of the 20th century is 1.11 Wm^{-2}. This compares to 2.73 Wm^{-2} for the TSI used in the HadGEM1 simulations (Stott et al., 2006) and 2.95 Wm^{-2} in the HadCM3 simulations (Stott et al., 2000).

7.2 Stratospheric volcanic aerosol

How HadGEM2-ES incorporates changes in stratospheric volcanic aerosol is the

same as in the HadGEM1 model (Stott et al., 2006). Aerosols in the troposphere are linked to emission sources and sulphur and chemistry feedbacks. Aerosols in the

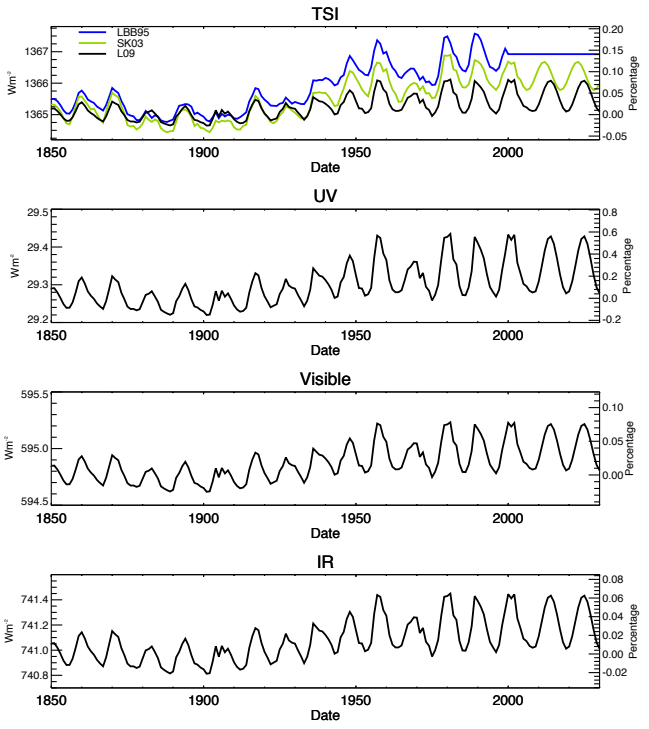

Fig. 13. Annual mean solar irradiance variations used in the historic model simulation (L09 - Lean et al., 2009). **(a)** Total solar irradiance. Also shown are the TSI used in previous model simulations, LBB95 (Lean et al., 1995b) used in HadCM3 (Stott et al., 2000) and SK03 (Solanki and Krivova, 2003) used in HadGEM1 (Stott et al., 2006). Solar irradiance averaged over **(b)** the ultraviolet band (200–320 nm), **(c)** the two visible bands (320–690 nm), and **(d)** infrared bands (690–1190, 1190–2380, and 2380–10 000 nm). Percentages are given with respect to the solar constant (1365 Wm^{-2}), and associated distribution across the shortwave spectral bands.

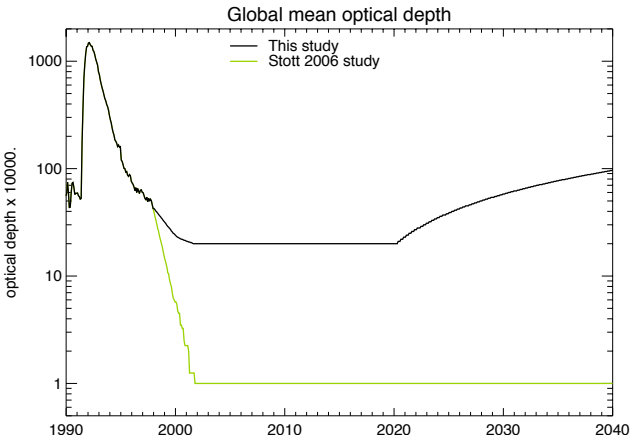

Fig. 14. Monthly global mean stratospheric optical depth as used in this study and what was included in the HadGEM1 simulations (Stott, 2006), for the period 1990–2040.

stratosphere are separated from these processes and are prescribed. Stratospheric aerosol concentrations are varied across four equal area latitudinal zones on a monthly timescale. The aerosol is distributed vertically above the tropopause such that the mass mixing ratio is constant across the levels. In this version of the model, volcanic aerosol is not related to, and does not interact with, other simulated aerosol behaviour.

The dataset used for the historic period was monthly stratospheric optical depths, at 550 nm, from 1850 to 2000 (Sato et al., 1993, see URL 12 in Appendix A) which was averaged over the four equal area latitudinal zones and converted into aerosol concentrations (Stott et al., 2006 and figures therein).

In a previous study (Stott et al., 2006) the data was extended past 2000 by continuing an assumed 1 yr timescale decay, from 1997, to a minimum and then keeping concentrations constant. There is some evidence that background aerosol concentrations are not as low as this assumes (Thomason et al., 2008). Also future volcanic activity is likely to introduce further aerosol into the stratosphere. There was no specific CMIP5 recommendations, apart from suggesting that the same concentration of stratospheric aerosol is present in the future simulations as in the control (Taylor et al., 2009), being aware of any step-change in aerosol.

The future dataset of optical depth is constructed as follows. The 1 yr decay timescale constructed for the post 1997 period appears to give a break point in the data. We reconstruct the data, to remove the break point, from 1997 to 2002 by continuing the decay timescale of 3.3 yr seen in the 1995–1997 period of the data. A value of stable observed optical depth at 1020 nm since 2000 was found to be 0.001 (Thomason et al., 2008). As optical depth is estimated to vary inversely with wavelength, this suggests a minimum of global stratospheric aerosol optical depth of 0.002 at 550 nm, approximately 20 times more than used in the HadGEM1 study. During the period 2020–2040 concentrations were increased to match those in the control simulation (optical depth 0.0097). This compromise was an attempt to balance the lack of knowledge of when large eruptions would occur in the future with the unlikely possibility of no major volcanic eruptions significantly influencing aerosol amounts in the stratosphere for 100 yr. The global mean of the stratospheric optical depth is shown in Fig. 14, compared with what was used in the HadGEM1 simulation.

8 Palaeoclimate boundary conditions, including geophysical changes

In order to complete the palaeo-climate simulations (3.4–3.6) a number of modifications need to be made to the model. The mid-Holocene simulation (3.4) required GHG concentrations of CH_4 (650 ppb) and N_2O (270 ppb), and halocarbon concentrations of zero (as in the pre-industrial control

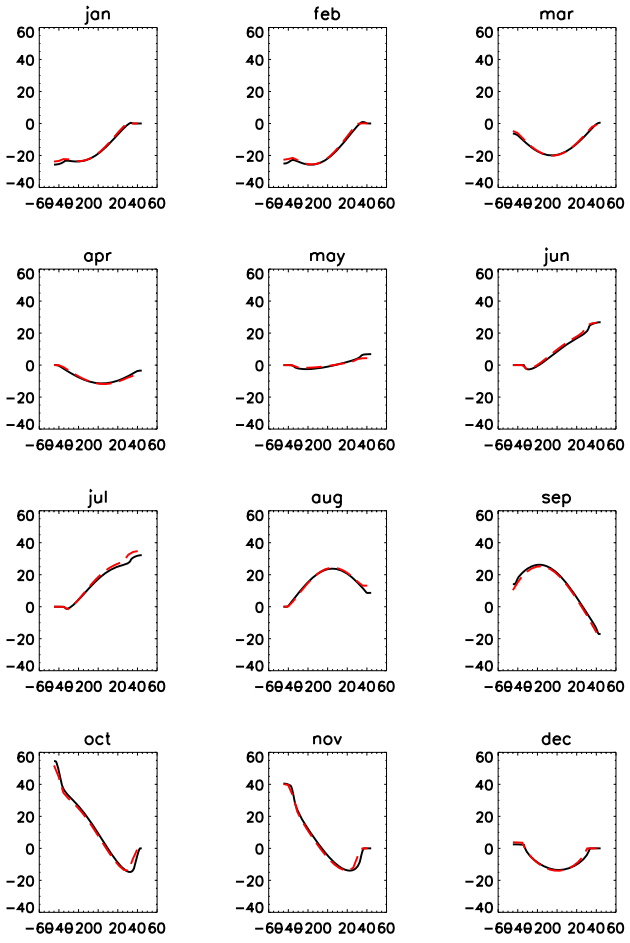

Fig. 15. Mid-Holocene changes in monthly TOA solar insolation relative to the present day, as a function of latitude as supplied by PMIP3 and calculated within HadGEM2-ES.

simulation). Stratospheric Ozone and pre-cursor emissions of tropospheric ozone remain the same as the pre-industrial control run, as do concentrations of CO_2 and the land sea mask. Because tropospheric Ozone is calculated interactively in HadGEM2-ES, Ozone concentrations in the palaeo simulations may not be identical to those in the pre-industrial control simulation: it is the pre-cursor emissions which we keep the same as the control run. This is also the case for dust and ocean DMS emissions which are simulated interactively and may differ due to changes in the simulated climate or vegetation cover.

8.1 Mid-Holocene (6 kya)

In the mid-Holocene, Earth's orbit differed from present day affecting the timing and magnitude of solar energy reaching the surface. Orbital parameters were modified to correspond to those required by the PMIP3 protocol (see URL 13 in Appendix A). Figure 15 shows the monthly anomalies of

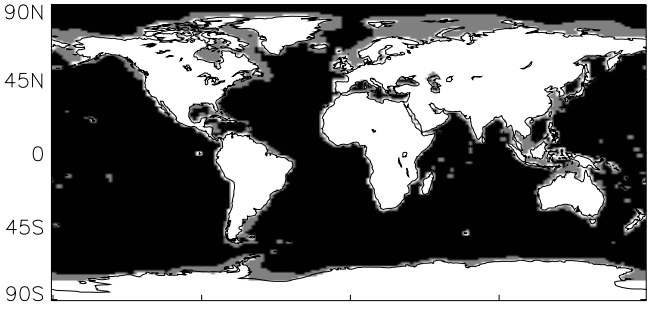

Fig. 16. Land sea masks used by HadGEM2-ES. Modern and mid-Holocene land points are denoted by white and additional LGM land points by grey. Black points denote points that are ocean in all simulations.

TOA SW radiation relative to the present day for the official PMIP3 requirements (black) and as calculated within HadGEM2-ES (red). The land use disturbance mask is set to zero everywhere for the mid-Holocene thus assuming that there is no human activity which would displace forests in any location.

8.2 Last glacial maximum (LGM, 21 kya)

The LGM simulation (3.5) setup requires major changes to the geophysical state of the land and ocean bed. This simulation has not yet been performed and some of these modifications are ongoing. The land sea mask and orography are changed to increase ice sheet volumes and to represent the associated decreased sea level. The bathymetry of the ocean model is also changed to reflect the decreased sea-level. Figure 16 shows how the land-sea mask changes. GHG concentrations are prescribed as, CO_2 of 185 ppm, CH_4 of 350 ppb, N_2O of 200 ppb. Halocarbons are zero (as in the pre-industrial control setup) and O_3 is treated the same as in the pre-industrial control run by using the same stratospheric ozone concentrations and tropospheric ozone precursor emissions. Boundary condition files were downloaded from the PMIP3 website (see URL 13 in Appendix A). Orbital parameters will be changed to the required configuration and the river routing ancillary will also be manually updated to take into account changes in the land sea mask and ensure that all rivers flow into the ocean rather than terminating at a land-point.

8.3 Last Millennium (800 AD–present)

Different from the centennial simulation, in the Last Millennium simulation no anthropogenic disturbance is used to update the land cover boundary conditions. Instead the land cover is updated from historical land cover reconstruction data from Pongratz et al. (2008, hereafter P08). The original data are on a grid of $0.5° \times 0.5°$ and provide the spatial distribution of 14 vegetation types from the present day back

Table 4. Mapping of the P08 land classes into HadGEM2-ES vegetation types.

Classification in P08	Classification in MOSES2
Tropical evergreen forest	Broadleaf trees
Tropical deciduous forest	Broadleaf trees
Temperate evergreen broadleaf forest	Broadleaf trees
Temperate/boreal deciduous broadleaf forest	Broadleaf trees
Temperate/boreal evergreen conifers	Needle leaf trees
Temperate/boreal deciduous conifers	Needle leaf trees
Raingreen shrub	Shrubs
Summergreen shrub	Shrubs
C3 natural grasses	C3 grasses
C4 natural grasses	C4 grasses
Tundra	multiple mapping
Crop	multiple mapping
C3 pasture	C3 grasses
C4 pasture	C4 grasses

to year 800 AD. The vegetation types in the P08 database are mapped into the 5 TRIFFID vegetation classes. The details of the reclassification are shown in Table 4. In case of no one-to-one mapping, the following rules are applied:

- C3/C4 pasture is treated as natural C3/C4 grass.
- Tundra is treated as mixture of shrubs, grass and bare soil. The mixture is chosen to match as close as possible the distribution obtained in Essery et al. (2003) in tundra regions for the present time.
- Crops are treated as in Essery et al. (2003), as a mixture of C3/C4 grass and soil. The ratio between C3 and C4 grass is used as threshold to discriminate between C3 and C4 grass to be used in crop.

After the application of inland water mask and ice mask, the unclassified fraction of each grid cell is filled with the soil land class. For the urban land class we used the data from HYDE3.1 (Klein Goldewijk et al., 2010, 2011). The data provide the urban/built-up area on a grid cell of $0.083° \times 0.083°$. We used local area-averaging interpolation to regrid HYDE 3.1 data into the P08 grid. In the coastal areas only the grid cells where at least 30 % of the original data showed urban coverage were considered as urban. The half-degree historical land cover data is then re-gridded onto the HadGEM2-ES grid using area average re-gridding. Figure 17 shows the total woodland (needle leaf+broad leaf trees) reduction with respect to year 800 respectively in year 1000, 1500 and 1990 on the HadGEM2 grid.

For the volcanic forcing we use the reconstruction of aerosol optical depth (AOD) provided by Crowley et al. (2008) and we maintain the same latitudinal distribution as described in Sect. 7.2. The reconstruction is based on ice-core records from Antarctic and Greenland calibrated based

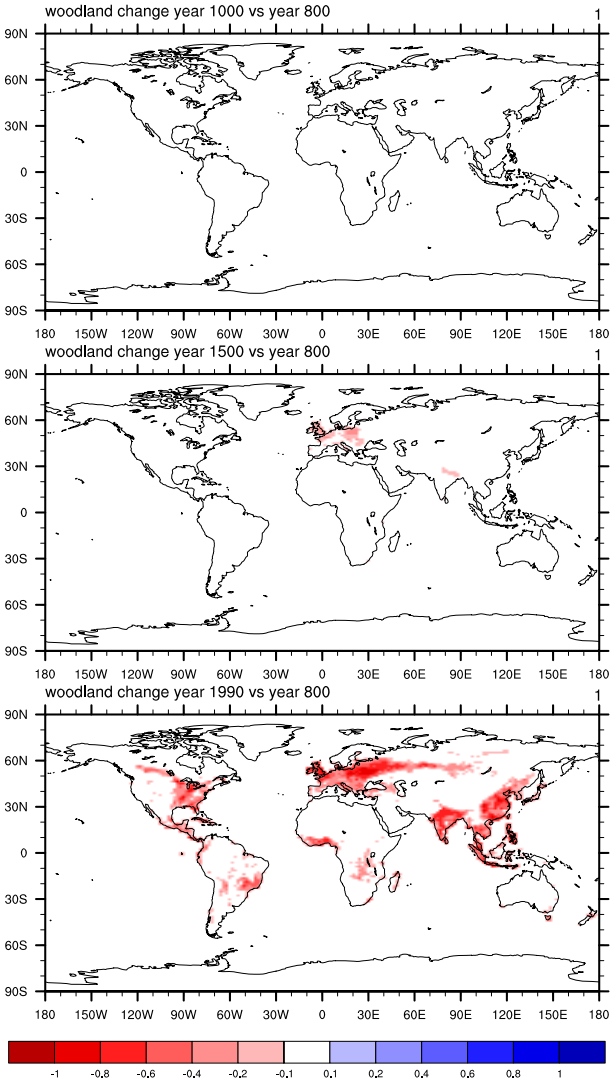

Fig. 17. Changes in fractional area coverage of woodland (broad leaf+needle leaf tree) in year 1000 AD, 1500 AD and 1990 AD with respect to the year 800 AD. Data from Pongratz et al. (2008) regridded on HadGEM2-ES grid.

on the Pinatubo eruption and is validated by comparison to the 20th century instrumental records. The data closely match the Sato et al. (1993) reconstruction for the 20th century. Figure 18 shows the volcanic aerosol optical depth at 0.55 μm integrated across the lower stratosphere between 15 and 25 km for the 4 latitudinal bands from the year 800 to 2000.

For the solar forcing up to 1810 we implemented the data of Steinhilber et al. (2009), a Total Solar Irradiance (TSI) reconstruction based on the cosmogenic radionuclide ^{10}Be measured in ice cores. The TSI was calculated using the observed correlation between open solar flux and TSI derived by Fröhlich (2009). Because cosmogenic nuclide based reconstructions do not perfectly match the instrumentally

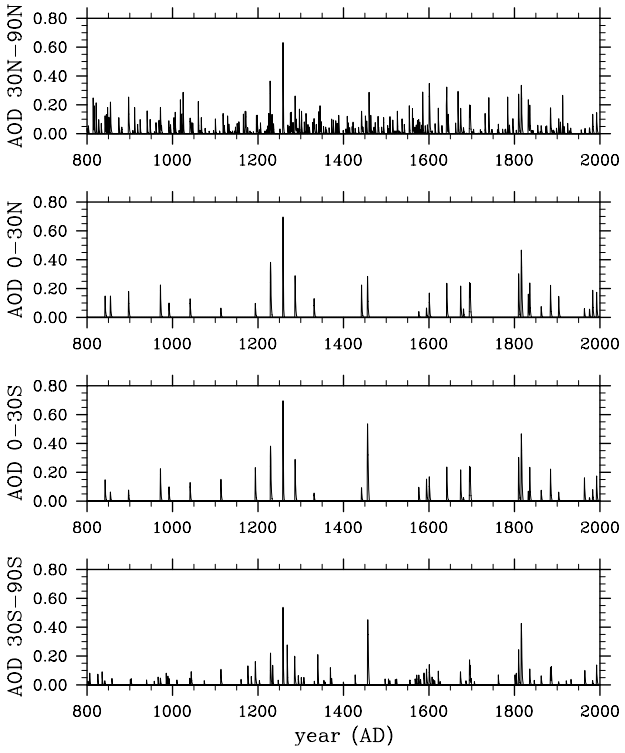

Fig. 18. Reconstructed stratospheric volcanic aerosol optical depth at 550 nm since year 800. From Crowley et al. (2008), for four different latitudinal bands.

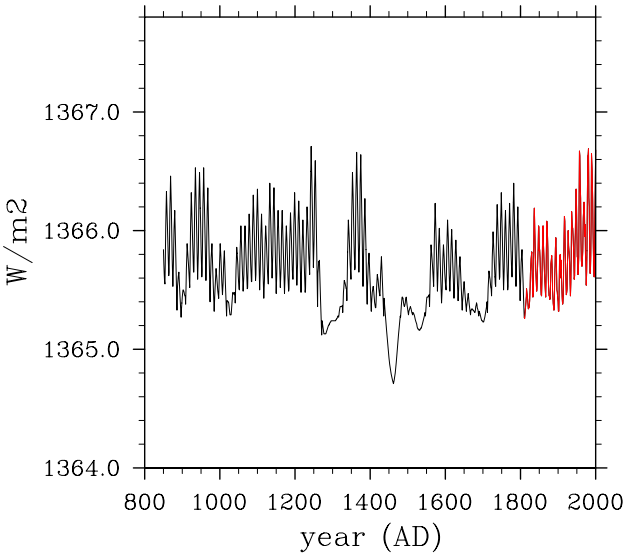

Fig. 19. Reconstruction of total solar irradiance since year 850AD. The black line indicates data from Steinhilber et al. (2009), the red line data from Wang et al. (2005).

observed TSI changes from 1976 onwards, for the period 1810–2000 we used the solar reconstruction of Wang et al. (2005), which is based on a flux transport model of the open and closed flux which used the observed sunspot record as the main input. For consistency between the two forcings, the Steinhilber et al., reconstruction was normalised to the Wang et al., values from 1976–2006 and also had a synthetic 11 yr cycle overlaid, according to the PMIP3 guidelines (Schmidt et al., 2011). To get the two different reconstructions to match up, a linear combination of the Wang et al., reconstruction with background and without background was used so that the mean values of the two reconstructions were identical between 1810 and 1820. Eventually the whole TSI has been normalized to a mean value over the whole period of 1365 Wm^{-2}. The forcing over the total duration of the simulation runs is shown in Fig. 19, with different colours to highlight the two reconstructions used.

UKCA is included in these simulations allowing the simulation of a 3-D methane field and interaction with O_3 and aerosols, but with the concentrations of well-mixed GHGs CO_2, CH_4 and N_2O prescribed. The set up follows the PMIP3 standard (Schmidt et al., 2011): data over the post-1860 industrial period (Hansen and Sato, 2004) are linked with splines through the ice core results of the last 2 millennia.

For the pre-1860 period, black carbon aerosols are set to zero, while the biomass burning is kept constant at the pre-industrial, 1860 value.

9 Ensemble initialisation

9.1 HadGEM2-ES coupled model historical simulations (3.2E)

CMIP5 requests initial-condition ensembles of simulations of some experiments in order to be able to estimate any component of apparent changes in climate which may be due to internal variability in the model. In order to produce an ensemble of initial condition members for the historical simulations it is necessary to somehow perturb the initial conditions. A standard technique for this is simply to choose different points on the control run from which to take the initial conditions for a simulation. GCMs possess sufficient sensitivity to initial conditions that for even a small perturbation, their day-to-day weather will soon diverge. But they may also possess some long-term "memory" which may mean ensemble members taken too close together in the control simulation, or from widespread but similar initial states, are not fully independent.

Extensive evidence exists from previous long control simulations showing simulated climate possesses large-scale variations on decadal to centennial timescales (Delworth et al., 1993; Delworth and Mann, 2000; Latif et al., 2004; Knight et al., 2005). Typically, these variations are associated with the principal modes of decadal variability of

the climate system – the Atlantic Multidecadal Oscillation (AMO) (Enfield et al., 2001) and the Pacific Decadal Oscillation (PDO), sometimes referred to as the Interdecadal Pacific Oscillation (IPO) (Power et al., 1999). The AMO is a North Atlantic-centred mode in which sea surface temperatures (SSTs) vary coherently within the basin on multidecadal to centennial timescales, and which can have far reaching climate impacts (Knight et al., 2006). The PDO/IPO has a characteristic pattern of anomalously warm and cool SSTs in the Pacific Ocean that resembles a modified El Niño pattern, and typically has a shorter timescale of about two decades (Kwon and Deser, 2007). So-called "perfect model" experiments (Collins and Sinha, 2003), in which sections of model control simulations are repeated after small initial perturbations, demonstrate the potential for multidecadal oceanic processes to provide a long-term memory of the initial state. This is undesirable as we would like the ensemble mean to provide an unbiased estimate of the model's response to imposed forcings. In terms of the initialisation of the transient simulations from the model control described here, this implies that care needs to be taken in choosing a sufficient range of initial states with respect to decadal modes.

North Atlantic and Pacific patterns of the decadal-centennial variability in the HadGEM2-ES control simulation were derived from a principal component analysis of low-pass filtered simulated annual mean SST data in each basin. The filter half-power timescales were chosen to preserve only the decadal and longer components of the variability. The patterns derived bear a strong resemblance to those seen in observations (Parker et al., 2007). Projecting these patterns from 500 yr of the control run against the low-pass filtered SST fields, indices of Atlantic and Pacific decadal variability were derived (Fig. 20). The Atlantic index (labelled "AMO") has considerable variability on decadal to centennial timescales, whereas the Pacific mode (labelled "IPO") tends towards variations on shorter timescales. Despite long-term variability, neither index exhibits a long-term drift.

Figure 21 shows the trajectory of the control model in the space defined by these two indices, as well as the points at which the ensemble members of the transient simulation were initialised. We wanted to retain an objective method for selecting initial conditions rather than using this metric to subjectively choose years from the control run. As such we select initial conditions at 50 yr intervals from the control run (as indicated by red dashed lines in Fig. 20), and use these indices of long-term variability to monitor whether these initial states are independent as desired. The range of initial states selected possesses an average that is close to zero compared to the variability in both indices. This indicates that there is no mean signal of the AMO or IPO in the initial conditions, giving confidence that the net long-term signal from the initial state has been minimised in the transient ensemble. We note that the 4 ensemble members chosen span a reasonable range of the IPO variability but a relatively narrow range of AMO variability, clustered close to zero. Future work may explore the response of extra ensemble members which start from deliberately chosen high or low AMO states.

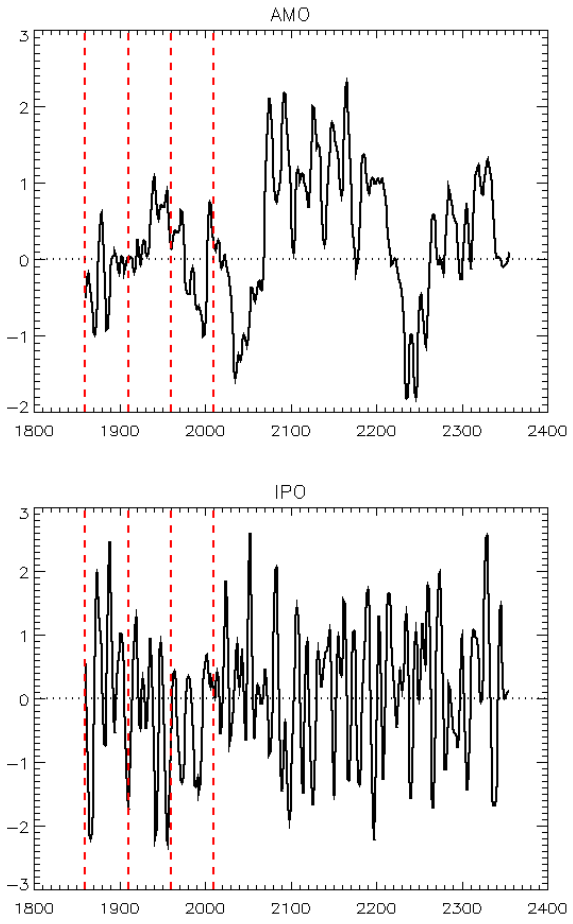

Fig. 20. Evolution of the AMO and IPO indices in the HadGEM2-ES pre-industrial control simulation. Vertical red lines show 50-yr intervals chosen as interval between ensemble member initial conditions. 4 ensemble members have been performed to date.

9.2 Atmosphere only model (AMIP) simulations (3.3E)

Traditionally, AMIP experiments (Gates, 1992) comprise the atmosphere-only version of a GCM forced only by time-varying fields of prescribed sea-surface temperatures (SSTs) and sea-ice. The atmospheric component of GCMs generally includes the land-surface model which means that surface properties such as soil temperature and moisture are simulated in AMIP experiments, but the land-cover would be prescribed from a climatology and held constant in time.

For CMIP5 the AMIP experiments, 3.3(E), use time-varying datasets of SST and sea-ice at monthly resolution as recommended by CMIP5 (Hurrell et al., 2008). The experiment design also recommends time varying forcing of the other climate drivers such as GHGs, aerosols and natural

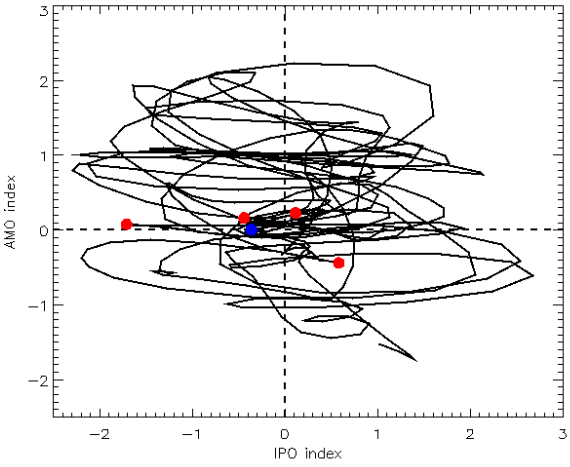

Fig. 21. HadGEM2-ES control run evolution in AMO/IPO phase space. Red dots show 50-yr intervals used for four existing HadGEM2-ES historical ensemble members. The blue dot shows the mean position of these four initial conditions.

forcing as imposed in the coupled historical simulation, 3.2. For ESMs such as HadGEM2-ES which include dynamic vegetation there is a decision to make regarding whether to prescribe or simulate the land cover, and if the latter how to initialise it for the start of the AMIP period (1979–2010). For the HadGEM2 AMIP simulations we chose to prescribe the land cover, but from a time-varying dataset to represent the impact of historical changes in anthropogenic land use. The land-cover dataset was derived from the IGBP present-day climatology (Loveland et al., 2000) and reconstructions of anthropogenic land-use from the HYDE3 dataset (Klein Goldewijk et al., 2010) as processed for CMIP5 by Hurtt et al. (2011). It is thus consistent with the land-use changes imposed in the fully coupled HadGEM2-ES simulations with dynamic vegetation (see Sect. 6). Historical land-use and future projections (see URL 11 in Appendix A) and the dataset of crop, pasture and urban area in version 1 used to construct time varying land cover. Land cover in HadGEM2 consists of nine surface types; broadleaf trees, needleleaf trees, C3 grass, C4 grass, shrubs, urban, water, soil and ice (Essery et al., 2003). Consistent with our use of this data in the HadGEM2-ES simulations, here crop and pasture are assumed to be a combination of C3 and C4 grass. Using the fractions of C3 and C4 grasses derived from the IGBP climatology, crop and pasture are converted into C3 and C4 grass. Changes due to time-variant C3, C4 grass and urban area are matched by removing equally distributed fractions of broadleaf, needleleaf tress and shrubs in order to conserve the total vegetated fraction of each grid cell. Water, soil, and ice are represented by the IGBP climatology. As a result of the atmosphere-only version of HadGEM2 having a different land-cover and different surface climatology it was decided to retune the mineral dust emissions scheme to enable better simulation of present day dust emissions. No other parameter changes were made from the fully coupled HadGEM2-ES simulations.

Table 5. Initial perturbation date and technique for the HadGEM2-ES AMIP ensemble members.

AMIP ensemble member	Initial condition	Initial perturbation
1	From previous atmosphere-only run	Atmos
2	2001 from #1	Atmos + surface
3	2001 from #1	Atmos
4	2008 from #3	Atmos + surface
5	2008 from #4	Atmos + surface

As long-term memory in coupled GCMs is mainly due to ocean processes it was not necessary to separate AMIP ensemble member initial conditions by 50 years in the control run. Rather, in order to initialise the 5 HadGEM2 AMIP ensemble members we chose to perturb the initial conditions in 2 different ways (Table 5). Firstly we could take the atmospheric (including land surface) state from part-way through a previous AMIP simulation (perturbation method listed as "atmos and surface" in Table 5), or secondly we could reset the land-surface state back to climatological values (listed as "atmos"). As recommended in the CMIP5 experimental design, we used a mix of the two approaches. For all experiments, there was a 3-month spin-up period from September to December 1978. In such atmosphere-only experiments we expect the atmospheric state to adjust rapidly ($<$ 1 month) to the prescribed SST and sea-ice boundary conditions. However, the land surface could exhibit memory on seasonal or longer timescales (Koster and Suarez, 2001). Hence these two approaches to initialising AMIP ensemble members can be later analysed as two sub-ensembles to assess the importance of land-surface state for predictability on seasonal to decadal timescales.

10 Discussion and concluding comments

Arbitrary or subjective decisions in experimental design can cause differences in results which hamper attempts to quantify and understand model spread and uncertainty in future climate projections. CMIP5 represents a coordinated attempt to define a common modelling protocol by which modelling centres worldwide can abide, in order to facilitate comparison of complex GCM experiments and thus avoid the impacts of subjective decisions. However, by necessity there may still be a number of subjective decisions required when elements of the experimental protocol are not applicable to a certain model or model configuration. It is our hope that any such

occurrences with HadGEM2-ES will not have a large impact on the interpretation of the results, but we discuss here for completeness some possible impacts.

In the HadGEM2-ES earth system model (Collins et al., 2011), some of the components of the earth system are now simulated interactively by the model rather than being prescribed as external boundary conditions. For example, HadGEM2-ES includes interactive tropospheric chemistry and hence can simulate the evolution of atmospheric methane and ozone concentration in response to meteorological conditions and emissions of reactive gases. Therefore atmospheric composition may not follow exactly the CMIP5-prescribed values. In our experiments we have forced the surface methane concentrations to follow the CMIP5 values in order to reduce any model drift away from the scenarios, but there may still be differences in CH_4 concentrations in the free atmosphere away from the surface.

Similarly, simulated tropospheric ozone may not follow the exact CMIP5-prescribed concentrations. In general, we see this enhanced, process-based functionality of the model as a benefit – the rationale behind developing such a complex earth system model is precisely to study these interactions and allow them to change consistently with future climate in a way not possible with prescribed concentrations. But we do acknowledge that these differences also represent a divergence from the precise CMIP5 protocol which should be borne in mind during subsequent multi-model analysis.

Other areas where a divergence may occur due to the structure of the ESM include land-use forcing and set-up of detection and attribution experiments.

By prescribing anthropogenic disturbance in addition to simulated, dynamic vegetation we risk diverging from the intended impact of the prescribed land-use change. For example, if the model initially simulates too much or too little forest in a region to be deforested then the impact of this deforestation on both carbon storage and physical surface properties will be too great or too little. We mitigate the risk of this impact in the emission-driven experiments by overwriting the land-use flux seen by the atmosphere by the CMIP5-prescribed land-use emissions dataset. However, the issue remains for any biophysical effect of land-use change. Future work is required to quantify the impact of this effect.

Detection and attribution studies aim to attribute changes in observed climate to driving processes. Model experiments are designed to do this by varying or holding constant separate forcings such as natural, greenhouse gases or aerosols. In this way the characteristic spatial or temporal patterns of response to each forcing can be derived and an optimal scaling found to best match observations. The scaling is then used to deduce if the signal for the forcing is detected and if the scaled response is consistent with the original signal, thus providing confidence for an attribution statement. In GCMs to date the distinction between, say, natural and greenhouse gas forcing is clear, and it is easy in the model to hold one fixed whilst varying the other. However, in an ESM where simulated GHG concentrations (such as methane or ozone) or aerosols may respond to climate, this distinction becomes slightly blurred. If natural forcings affect atmospheric processes which alter GHG or aerosol amounts then should these be allowed to vary or not in the "natural" detection and attribution experiment? Or should the HadGEM2-ES "natural" simulations be forced to solely consider the direct radiative effects of the natural forcings?

In the HadGEM2-ES natural experiment we varied the TSI and stratospheric volcanic aerosol concentrations as per the historical simulation, kept all other emissions/concentrations the same as in the control simulation and allowed the earth system processes to vary as normal. We decided on a more complicated set up for the GHG only forced run. Concentrations of the greenhouse gases (CO_2, CH_4, N_2O and the halocarbon species) were prescribed throughout the atmosphere for the radiation scheme. However, prescribing the methane seen by the chemistry scheme would influence the chemistry and thus species like ozone, which we did not want to be varied in this experiment. So in the interactive chemistry part of the model, the set up was as in the control, i.e. methane emissions at surface and concentrations in the atmosphere as in the control simulation. This "chemistry methane" does not interact with the radiation scheme. Our choice to do this was therefore a pragmatic compromise between the ESM part of the model and the needs of a detection and attribution study.

In this paper we have documented how we have implemented the CMIP5 experimental protocol for the centennial simulations in the Met Office HadGEM2-ES earth system model. We have successfully set-up and performed the experiments as described here and will make the results available via the PCMDI multi-model database. We hope these will form a valuable contribution to the CMIP5 modelling activity.

Appendix A

List of URLs / websites

1. The main CMIP5 web page
   http://cmip-pcmdi.llnl.gov/cmip5/index.html
2. CMIP5 output guidelines
   http://cmip-pcmdi.llnl.gov/cmip5/output_req.html
3. The RCP White Paper: document 8 at:
   http://cmip-pcmdi.llnl.gov/cmip5/modeling_documents.html
4. The CO_2 concentrations used were taken from the CMIP5 dataset
   http://cmip-pcmdi.llnl.gov/cmip5/forcing.html
5. NOAA global mean CO_2 data
   ftp://ftp.cmdl.noaa.gov/ccg/co2/trends/co2_annmean_gl.txt

6. RCP database
http://www.iiasa.ac.at/web-apps/tnt/RcpDb
7. Information on gridding of land use CO_2 emissions data
http://www.mpimet.mpg.de/en/wissenschaft/land-im-erdsystem/wechselwirkung-klima-biogeosphaere/landcover-change-emission-data.html
8. Global mean CH4 data
http://data.giss.nasa.gov/modelforce/ghgases/Fig1B.ext.txt
9. The global NOAA/ESRL global monitoring network
ftp://ftp.cmdl.noaa.gov/ccg/ch4/flask/month/
10. Global Emissions Inventory Activity (GEIA)
http://www.geiacenter.org/inventories/present.html
11. UNH land use data
http://luh.unh.edu
12. Monthly stratospheric optical depths, at 550 nm, from 1850 to 2000 (Sato et al., 1993)
http://data.giss.nasa.gov/modelforce/strataer/
13. PMIP3 protocol and data
https://pmip3.lsce.ipsl.fr/wiki/doku.php/pmip3:index

Acknowledgements. This work was supported by the Joint DECC/Defra Met Office Hadley Centre Climate Programme (GA01101) and also by the European Commission's 7th Framework Programme, under Grant Agreement number 226520, COMBINE project. R. Andres was sponsored by US Department of Energy, Office of Science, Biological and Environmental Research (BER) programs and performed at Oak Ridge National Laboratory (ORNL) under US Department of Energy contract DE-AC05-00OR22725. The contribution of K. Corbin and R. Law has been undertaken as part of the Australian Climate Change Science Program, funded jointly by the Department of Climate Change, the Australian Bureau of Meteorology and CSIRO, and was undertaken on the NCI National Facility in Canberra, Australia, which is supported by the Australian Commonwealth Government. A. Bozzo and A. Schurer were supported by NCAS. W. J. Ingram received additional support from the EU WATCH project and NERC contract NE/D012287/1. We are especially grateful to Karl Taylor for continued help and advice throughout the process of experiment design and set-up. We are also grateful to Victor Brovkin for help and advice regarding land-use CO_2 emissions.

Edited by: M. Kawamiya

References

Andreae, M. O. and Merlet, P.: Emission of Trace Gases and Aerosols From Biomass Burning, Global Biogeochem. Cy., 15(4), 955–966, 2001.

Andres, R. J. and Kasgnoc, A. D.: A time-averaged inventory of subaerial volcanic sulfur emissions, J. Geophys. Res., 103, 25251–25261, 1998.

Andres, R. J., Gregg, J. S., Losey, L., Marland, G., and Boden, T.A.: Monthly, global emissions of carbon dioxide from fossil fuel consumption, Tellus B, 63, 309–327, doi:10.1111/j.1600-0889.2011.00530.x, 2011.

Arora, V. K. and Boer, G. J.: Uncertainties in the 20th century carbon budget associated with land use change, Glob. Change Biol., 16, 3327–3348, doi:10.1111/j.1365-2486.2010.02202.x, 2010.

Bagnold, R. A.: The Physics of Blown Sand and Desert Dunes, 265 pp., Methuen, New York, 1941.

Bellouin, N., Boucher, O., Haywood, J., Johnson, C., Jones, A., Rae, J., and S. Woodward: Improved representation of aerosols for HadGEM2, Met Office Hadley Centre, Technical Note 73, 2007.

Boden, T. A., Marland, G., and Andres, R. J.: Global, Regional, and National Fossil-Fuel CO2 Emissions, Carbon Dioxide Information Analysis Center, Oak Ridge National Laboratory, US Department of Energy, Oak Ridge, Tenn., USA, doi:10.3334/CDIAC/00001V2010, 2010.

Cadule, P., Friedlingstein, P., Bopp, L., Sitch, S., Jones, C. D., Ciais, P., Piao, S. L., and Peylin, P.: Benchmarking coupled climate-carbon models against long-term atmospheric CO_2 measurements, Glob Biogeochem. Cy., 24, GB2016, doi:10.1029/2009GB003556, 2010.

Clarke, L., Edmonds, J., Jacoby, H., Pitcher, H., Reilly, J., and Richels, R.: Scenarios of Greenhouse Gas Emissions and Atmospheric Concentrations. Sub-report 2.1A of Synthesis and Assessment Product 2.1 by the US Climate Change Science Program and the Subcommittee on Global Change Research, Department of Energy, Office of Biological & Environmental Research, Washington, 7 DC, USA, 154 pp., 2007.

Cionni, I., Eyring, V., Lamarque, J. F., Randel, W. J., Stevenson, D. S., Wu, F., Bodeker, G. E., Shepherd, T. G., Shindell, D. T., and Waugh, D. W.: Ozone database in support of CMIP5 simulations: results and corresponding radiative forcing, Atmos. Chem. Phys. Discuss., 11, 10875–10933, doi:10.5194/acpd-11-10875-2011, 2011.

Collins, M. and Sinha, B.: Predictability of decadal variations in the thermohaline circulation and climate, Geophys. Res. Lett., 30(6), 1306, doi:10.1029/2002GL016504, 2003.

Collins, W. J., Bellouin, N., Doutriaux-Boucher, M., Gedney, N., Halloran, P., Hinton, T., Hughes, J., Jones, C. D., Joshi, M., Liddicoat, S., Martin, G., O'Connor, F., Rae, J., Senior, C., Sitch, S., Totterdell, I., Wiltshire, A., and Woodward, S.: Development and evaluation of an Earth-system model HadGEM2, Geosci. Model Dev. Discuss., 4, 997–1062, doi:10.5194/gmdd-4-997-2011, 2011.

Corbin, K. D. and Law, R. M.: Extending Atmospheric CO_2 and Tracer Capabilities in ACCESS. CAWCR Technical Report No. 035, Centre for Australian Weather and Climate Research, Australia, available at:http://www.cawcr.gov.au/publications/technicalreports/CTR_035.pdf (last access: 10 June 2011), 2011.

Cox, P. M.: Description of the TRIFFID dynamic global vegetation model. Hadley Centre Technical Note 24, Met Office, UK, 2001.

Cox, P. M., Betts, R. A., Jones, C. D., Spall, S. A., and Totterdell, I. J.: Acceleration of global warming due to carbon-cycle feedbacks in a coupled climate model, Nature, 408, 184–187, 2000.

Crowley, T. J., Zielinski, G., Vinther, B., Udisti, R., Kreutz, K., Cole-Dai, J., and Castellano, E.: Volcanism and the Little Ice Age, PAGES Newsletter, 16, 22–23, 2008.

Daniel, J. S., Velders, G. J. M., Douglass, A. R., Forster, P. M. D., Hauglustaine, D. A., Isaksen, I. S. A., Kuijpers, L. J. M., McCulloch, A., and Wallington, T. J.: Halocarbon scenarios, ozone depletion potentials, and global warming potentials, Chapter 8, Scientific Assessment of Ozone Depletion: 2006, Global Ozone Research and Monitoring Project – Report No. 50, World Meteorological Organization, Geneva, 2007.

Delworth, T. L. and Mann, M. E.: Observed and simulated multidecadal variability in the Northern Hemisphere, Clim. Dynam., 16(9), 661–676, 2000.

Delworth, T. L., Manabe, S., and Stouffer, R. J.: Interdecadal variations of the thermohaline circulation in a coupled ocean-atmosphere model, J. Clim., 6(11), 1993–2011, 1993.

Derwent, R. G., Collins, W. J., Jenkin, M. E., and Johnson, C. E.: The global distribution of secondary particulate matter in a 3-D Lagrangian chemistry transport model, J. Atmos. Chem., 44, 57–95, 2003.

Enfield, D. B., Mestas-Nunez, A. M., and Trimble, P.J.: The Atlantic multidecadal oscillation and its relation to rainfall and river flows in the continental US, Geophys. Res. Lett., 28(10), 2077–2080, 2001.

Essery, R. L. H., Best, M. J., Betts, R. A., and Cox, P. M.: Explicit Representation of Subgrid Heterogeneity in a GCM Land Surface Scheme, J. Hydrometeorol., 4, 530–543, 2003.

Etheridge, D. M., Steele, L. P., Langenfelds, R. L., Francey, R. J., Barnola, J. M., and Morgan, V. I.: Natural and anthropogenic changes in atmospheric CO_2 over the last 1000 years from air in Antarctic ice and firn, J. Geophys. Res.-Atmos., 101(D2), 4115–4128, 1996.

Etheridge, D. M., Steele, L. P., Francey, R. J., and Langenfelds, R. L.: Atmospheric methane between 1000 A.D. and present: Evidence of anthropogenic emissions and climatic variability, J. Geophys. Res., 103(D13), 15979–15993, 1998.

Fécan, F., Marticorena, B., and Bergametti, G.: Parametrisation of the increase of the aeolian erosion threshold wind friction velocity due to soil moisture for arid and semi-arid areas, Ann. Geophys. 17, 149–157, 1999.

Forster, P., Ramaswamy, V., Artaxo, P., Berntsen, T., Betts, R., Fahey, D. W., Haywood, J., Lean, J., Lowe, D.C., Myhre, G., Nganga, J., Prinn, R., Raga, G., Schulz, M., and Van Dorland, R.: Changes in Atmospheric Constituents and in Radiative Forcing, in: Climate Change 2007: The Physical Science Basis. Contribution of Working Group I to the Fourth Assessment Report of the Intergovernmental Panel on Climate Change, edited by: Solomon, S., Qin, D., Manning, M., Chen, Z., Marquis, M., Averyt, K. B., Tignor, M., and Miller, H. L., Cambridge University Press, Cambridge, United Kingdom and New York, NY, USA, 2007.

Friedlingstein, P., Cox, P. M., Betts, R. A., Bopp, L., von Bloh, W., Brovkin, V., Cadule, P., Doney, S., Eby, M., Fung, I., Bala, G., John, J., Jones, C. D., Joos, F., Kato, T., Kawamiya, M., Knorr, W., Lindsay, K., Matthews, H. D., Raddatz, T., Rayner, P., Reick, C., Roeckner, E., Schnitzler, K. G., Schnur, R., Strassmann, K., Weaver, A. J., Yoshikawa, C., and Zeng, N.: Climate-carbon cycle feedback analysis, results from the C4MIP model intercomparison, J. Climate, 19, 3337–3353, doi:10.1175/JCLI3800.1, 2006.

Fröhlich, C. and Lean, J.: Solar radiative output and its variability: Evidence and Mechanisms, Astron. Astrophys. Rev., 12(4), 273–320, 2004.

Fujino, J., Nair, R., Kainuma, M., Masui, T., and Matsuoka, Y.: Multi-gas mitigation analysis on stabilization scenarios using AIM global model. Multigas Mitigation and Climate Policy, Energ. J. Special Issue, 343–354, 2006.

Gates, L. W.: AMIP: The atmospheric model intercomparison project, Bull. Am. Meteorol. Soc., 73, 1962–1970, 1992.

Ginoux, P., Chin, M., Tegen, I., Prospero, J. M., Holben, B., Dubovik, O., and Lin, S.-J.: Sources and distributions of dust aerosols simulated with the GOCART model, J. Geophys.-Res., 106(D17), 20255–20273, 2001.

Gregory, J. M., Jones, C. D., Cadule, P., and Friedlingstein, P.: Quantifying carbon-cycle feedbacks, J. Climate, 22, 5232–5250, doi:10.1175/2009JCLI2949.1, 2009.

Guenther, A., Hewitt, C. N., Erickson, D., Fall, R., Geron, C., Graedel, T., Harley, P., Klinger, L., Lerdau, M., McKay, W. A., Pierce, T., Scholes, B., Steinbrecher, R., Tallamraju, R., Taylor, J., and Zimmerman, P.: A global model of natural volatile organic compound emissions, J. Geophys. Res., 100(D5), 8873–8892, 1995.

Halloran, P. R., Bell, T. G., and Totterdell, I. J.: Can we trust empirical marine DMS parameterisations within projections of future climate?, Biogeosciences, 7, 1645–1656, doi:10.5194/bg-7-1645-2010, 2010.

Hoerling, M. P., Schaack, T. K., and Lenzen, A. J.: A global analysis of stratosphere-tropospheric exchange during northern winter, Mon. Weather Rev., 121(1), 162–172, 1993.

Houghton, R. A.: Carbon Flux to the Atmosphere from Land-Use Changes: 1850–2005, in: TRENDS: A Compendium of Data on Global Change. Carbon Dioxide Information Analysis Center, Oak Ridge National Laboratory, US Department of Energy, Oak Ridge, Tenn., USA, 2008.

Hurrell, J. W., Hack, J. J., Shea, D., Caron, J. M., and Rosinski, J.: A New Sea Surface Temperature and Sea Ice Boundary Dataset for the Community Atmosphere Model, J. Climate, 21, 5145–5153, 2008.

Hurtt, G. C., Chini, L. P., Frolking, S., Betts, R., Feddema, J., Fischer, G., Klein Goldewijk, K., Hibbard, K., Janetos, A., Jones, C., Kindermann, G., Kinoshita, T., Riahi, K., Shevliakova, E., Smith, S., Stehfest, E., Thomson, A., Thornton, P., van Vuuren, D., and Wang, Y. P.: Harmonisation of global land-use scenarios for the period 1500–2100 for IPCC-AR5, iLEAPS Newsletter, 7, 3 pp., 2009.

Hurtt, G. C., Chini, L. P., Frolking, S., Betts, R., Feddema, J., Fischer, G., Fisk, J. P., Hibbard, K., Houghton, R. A., Janetos, A., Jones, C., Kindermann, G., Kinoshita, T., Klein Goldewijk, K., Riahi, K., Shevliakova, E., Smith, S., Stehfest, E., Thomson, A., Thornton, P., van Vuuren, D. P., and Wang, Y.: Harmonization of Land-Use Scenarios for the Period 1500–2100: 600 Years of Global Gridded Annual Land-Use Transitions, Wood Harvest, and Resulting Secondary Lands, Clim. Change, accepted, 2011.

Johns, T. C., Durman, C. F., Banks, H. T., Roberts, M. J., McLaren, A. J., Ridley, J. K., Senior, C. A., Williams, K. D., Jones, A., Rickard, G. J., Cusack, S., Ingram, W. J., Crucifix, M., Sexton, D. M. H., Joshi, M. M., Dong, B. W., Spencer, H., Hill, R. S. R., Gregory, J. M., Keen, A. B., Pardaens, A. K., Lowe, J. A., Bodas-Salcedo, A., Stark, S., and Searl, Y.: The new Hadley Centre climate model HadGEM1: Evaluation of coupled simulations, J. Climate, 19, 1302–1328, 2006.

Jones, A., Roberts, D. L., Woodage, M. J., and Johnson, C. E.: Indirect sulphate aerosol forcing in a climate model with an interactive sulphur cycle, J. Geophys Res., 106, 20293–20310, 2001.

Keeling, R. F., Piper, S. C., Bollenbacher, A.F., and Walker, J.S.: Atmospheric CO_2 records from sites in the SIO air sampling network. In Trends: A Compendium of Data on Global Change, Carbon Dioxide Information Analysis Center, Oak Ridge National Laboratory, US Department of Energy, Oak Ridge, Tenn., USA, doi:10.3334/CDIAC/atg.035, 2009.

Kettle, A., Andreae, M., Amouroux, D., Andreae, T., Bates, T., Berresheim, H., Bingemer, H., Boniforti, R., Curran, M., DiTullio, G., Helas, G., Jones, G., Keller, M., Kiene, R., Leck, C., Levasseur, M., Malin, G., Maspero, M., Matrai, P., McTaggart, A., Mihalopoulos, N., Nguyen, B., Novo, A., Putaud, J., Rapsomanikis, S., Roberts, G., Schebeske, G., Sharma, S., Simo, R., Staubes, R., Turner, S., and Uher, G.: A global database of sea surface dimethylsulfide (DMS) measurements and a procedure to predict sea surface DMS as a function of latitude, longitude, and month, Global Biogeochem. Cy., 13, 399–444, 1999.

Klein Goldewijk, K.: Estimating Global Land Use Change Over the Past 300 Years: the HYDE Database, Global Biogeochem. Cy., 15, 417–433, 2001.

Klein Goldewijk, K., Beusen, A., and Janssen, P.: Long term dynamic modeling of global population and built-up area in a spatially explicit way: HYDE 3.1., Holocene, 20, 565–573, 2010.

Klein Goldewijk, K., Beusen, A., van Drecht, G., and de Vos, M.: The HYDE 3.1 spatially explicit database of human induced land use change over the past 12 000 years, Global Ecol. Biogeogr., 20, 73–86, 2011.

Knight, J. R., Allan, R. J., Folland, C. K., Vellinga, M., and Mann, M. E.: A signature of persistent natural thermohaline circulation cycles in observed climate, Geophys. Res. Lett., 32, L20708, doi:10.1029/2005GL024233, 2005.

Knight, J. R., Folland, C. K., and Scaife, A. A.: Climate impacts of the Atlantic Multidecadal Oscillation, Geophys. Res. Lett., 33, L17706, doi:10.1029/2006GL026242, 2006.

Koster, R. D. and Suarez, M. J.: Soil moisture memory in climate models, J. Hydromet., 2(6), 558–570, 2001.

Kwon, Y.-O. and Deser, C.: North Pacific decadal variability in the Community Climate System Model Version 2, J. Climate, 20, 2416–2433, 2007.

Lacis, A. A., Wuebbles, D. J., and Logan, J. A.: Radiative Forcing of Climate by Changes in the Vertical Distribution of Ozone, J. Geophys. Res., 95(D7), 9971–9981, 1990.

Lamarque, J.-F., Bond, T. C., Eyring, V., Granier, C., Heil, A., Klimont, Z., Lee, D., Liousse, C., Mieville, A., Owen, B., Schultz, M. G., Shindell, D., Smith, S. J., Stehfest, E., Van Aardenne, J., Cooper, O. R., Kainuma, M., Mahowald, N., McConnell, J. R., Naik, V., Riahi, K., and van Vuuren, D. P.: Historical (1850-2000) gridded anthropogenic and biomass burning emissions of reactive gases and aerosols: methodology and application, Atmos. Chem. Phys., 10, 7017–7039, doi:10.5194/acp-10-7017-2010, 2010.

Lamarque, J.-F., Riahi, K., Smith, S., van Vuuren, D. P., Vitt, F., and Meinshausen, M.: Simulated evolution of the distribution of short-lived greenhouse gases and aerosols using the emissions from the Representative Concentration Pathways, Clim. Change, accepted, 2011.

Latif, M., Roeckner, E., Botzet, M., Esch, M., Haak, H., Hagemann, S., Jungclaus, J., Legutke, S., Marsland, S., Mikolajewicz, U., and Mitchell, J.: Reconstructing, Monitoring, and Predicting Multidecadal-Scale Changes in the North Atlantic Thermohaline Circulation with Sea Surface Temperature, J. Climate, 17(7), 1605–1614, 2004.

Law, R. M., Kowalczyk, E. A., and Wang, Y.-P.: Using atmospheric CO_2 data to assess a simplified carbon-climate simulation for the 20th century, Tellus, 58B, 427–437, doi:10.1111/j.1600-0889.2006.00198.x, 2006.

Lean, J. L.: available at: http://www.geo.fu-berlin.de/en/met/ag/strat/forschung/SOLARIS/Input_data/Calculations_of_Solar_Irradiance.pdf last access: 2 June 2009, 2009.

Lean, J. L., White, O. R., and Skumanich, A.: On the solar ultraviolet spectral irradiance during the Maunder Minimum, Global Biogeochem. Cy., 9(2), 171–182, 1995a.

Lean, J. L., Beer, J., and Bradley, R.: Reconstruction of solar irradiance since 1610: implications for climate change, Geophys. Res. Lett., 22, 3195–3198, 1995b.

Le Quéré, C., Raupach, M. R., Canadell, J. G., Marland, G., Bopp, L., Ciais, P., Conway, T. J., Doney, S. C., Feely, R. A., Foster, P., Friedlingstein, P., Gurney, K., Houghton, R. A., House, J. I., Huntingford, C., Levy, P. E., Lomas, M. R., Majkut, J., Metzl, N., Ometto, J. P., Peters, G. P., Prentice, I. C., Randerson, J. T., Running, S. W., Sarmiento, J. L., Schuster, U., Sitch, S., Takahashi, T., Viovy, N., van der Werf, G. R. and Woodward, F. I.: Trends in the sources and sinks of carbon dioxide, Nat. Geosci., 2, 831–836, doi:10.1038/ngeo689, 2009.

Loveland, T. R., Reed, B. C., Brown, J. F., Ohlen, D. O., Zhu, Z., Yang, L., and Merchant, J. W.: Development of a global land cover characteristics database and IGBP DISCover from 1 km AVHRR data, Int. J. Remote Sens., 21, 1303–1330, 2000.

McGuire, A. D., Sith, S., Clein, J. S., Dargaville, R., Esser, G., Foley, J., Heimann, M., Joos, F., Kaplan, J., Kicklighter, D. W., Meier, R. A., Melillo, J. M., Moore III, B., Prentice, I. C., Ramankutty, N., Reichenau, T., Schloss, A., Tian, H., Williams, L. J., and Wittenberg, U.: Carbon balance of the terrestrial biosphere in the twentieth century: Analysis of CO_2, climate and land-use effects with four process-based ecosystem models, Global Biogeochem. Cy., 15, 183–206, 2001.

Martin, G. M., Ringer, M. A., Pope, V. D., Jones, A., Dearden, C., and Hinton, T. J.: The physical properties of the atmosphere in the new Hadley Centre global environmental model (HADGEM1), Part I: Model description and global climatology, J. Climate, 19, 1274–1301, 2006.

The HadGEM2 Development Team: Martin, G. M., Bellouin, N., Collins, W. J., Culverwell, I. D., Halloran, P. R., Hardiman, S. C., Hinton, T. J., Jones, C. D., McDonald, R. E., McLaren, A. J., O'Connor, F. M., Roberts, M. J., Rodriguez, J. M., Woodward, S., Best, M. J., Brooks, M. E., Brown, A. R., Butchart, N., Dearden, C., Derbyshire, S. H., Dharssi, I., Doutriaux-Boucher,

M., Edwards, J. M., Falloon, P. D., Gedney, N., Gray, L. J., Hewitt, H. T., Hobson, M., Huddleston, M. R., Hughes, J., Ineson, S., Ingram, W. J., James, P. M., Johns, T. C., Johnson, C. E., Jones, A., Jones, C. P., Joshi, M. M., Keen, A. B., Liddicoat, S., Lock, A. P., Maidens, A. V., Manners, J. C., Milton, S. F., Rae, J. G. L., Ridley, J. K., Sellar, A., Senior, C. A., Totterdell, I. J., Verhoef, A., Vidale, P. L., and Wiltshire, A.: The HadGEM2 family of Met Office Unified Model Climate configurations, Geosci. Model Dev. Discuss., 4, 765–841, doi:10.5194/gmdd-4-765-2011, 2011..

Meinshausen, M., Smith, S. J., Calvin, K. V., Daniel, J. S., Kainuma, M. L. T., Lamarque, J.-F., Matsumoto, K., Montzka, S. A., Raper, S. C. B., Riahi, K., Thomson, A. M., Velders, G. J. M., and van Vuuren, D.: The RCP Greenhouse Gas Concentrations and their Extension from 1765 to 2300, Clim. Change, Special RCP Issue, accepted, 2011.

Moss, R. H., Edmonds, J. A., Hibbard, K. A., Manning, M. R., Rose, S. K., van Vuuren, D. P., Carter, T. R., Emori, S., Kainuma, M., Kram, T., Meehl, G. A., Mitchell, J. F. B., Nakicenovic, N., Riahi, K., Smith, S. J., Stouffer, R. J., Thomson, A. M., Weyant, J. P., and Wilbanks, T. J.: The next generation of scenarios for climate change research and assessment, Nature, 463, 747–756, doi:10.1038/nature08823, 2010.

O'Connor, F. M., Johnson, C. E., Morgenstern, O., and Collins, W. J.: Interactions between tropospheric chemistry and climate model temperature and humidity biases, Geophys. Res. Lett., 36, L16801, doi:10.1029/2009GL039152, 2009.

O'Connor, F. M., Johnson, C. E., Morgenstern, O., Sanderson, M. G., Young, P.J., Zeng, G., Collins, W. J., and Pyle, J. A.: Evaluation of the new UKCA climate-composition model, Part II, The Troposphere, Geosci. Model Dev. Discuss., in preparation, 2011.

Parker, D., Folland, C., Scaife, A., Knight, J., Colman, A., Baines, P., and Dong, B.: Decadal to multidecadal variability and the climate change background, J. Geophys. Res., 112, D18115, doi:10.1029/2007JD008411, 2007.

Pfister, G. G., Emmons, L. K., Hess, P. G., Lamarque, J.-F., Orlando, J. J., Walters, S., Guenther, A., Palmer, P. I., and Lawrence, P. J.: Contribution of isoprene to chemical budgets: A model tracer study with the NCAR CTM MOZART-4, J. Geophys. Res., 113, D05308, doi:10.1029/2007JD008948, 2008.

Pongratz, J., Reick, C., Raddatz, T., and Claussen, M.: A reconstruction of global agricultural areas and land cover for the last millennium, Global Biogeochem. Cy., 22, B3018, doi:10.1029/2007GB003153, 2008.

Power, S. B., Casey, T., Folland, C., Colman, A., and Mehta, V.: Inter-decadal modulation of the impact of ENSO on Australia, Clim. Dynam., 15, 319–324, 1999.

Randel, W. J. and Wu, F.: A stratospheric ozone trends data set for global modelling studies, Geophys. Res. Lett., 26, 3089–3092, 1999.

Riahi, K. Gruebler, A., and Nakicenovic, N.: Scenarios of long-term socio-economic and environmental development under climate stabilization, Technol. Forecast. Soc., 74(7), 887–935, 2007.

Sato, M., Hansen, J. E., McCormick, M. P., and Pollack, J. B.: Stratospheric aerosol optical depths (1850–1990), J. Geophys. Res., 98, 22987–22994, 1993.

Schmidt, G. A., Jungclaus, J. H., Ammann, C. M., Bard, E., Braconnot, P., Crowley, T. J., Delaygue, G., Joos, F., Krivova, N. A., Muscheler, R., Otto-Bliesner, B. L., Pongratz, J., Shindell, D. T., Solanki, S. K., Steinhilber, F., and Vieira, L. E. A.: Climate forcing reconstructions for use in PMIP simulations of the last millennium (v1.0), Geosci. Model Dev., 4, 33–45, doi:10.5194/gmd-4-33-2011, 2011.

Simo, R. and Dachs, J.: Global ocean emission of dimethylsulfide predicted from biogeophysical data, Global Biogeochem. Cy., 16, 1078, doi:10.1029/2001GB001829, 2002.

Smith, S. J. and Wigley, T. M. L.: Multi-Gas Forcing Stabilization with the MiniCAM, Energ. J. Special Issue, 3, 373–391, 2006.

Solanki, S. and Krivova, N.: Can solar variability explain global warming since 1970?, J. Geophys.-Res., 108, 1200, doi:10.1029/2002JA009753, 2003.

Spiro, P. A., Jacob, D. J., and Logan, J. A.: Global inventory of sulfur emissions with 1×1 resolution, J. Geophys. Res., 97, 6023–6036, 1992.

Staehelin, J., Harris, N. R. P., Appenzeller, C., and Eberhard, J.: Ozone trends: A review, Rev. Geophys., 39(2), 231–290, doi:10.1029/1999RG000059, 2001.

Steinhilber, F., Beer, J., and Fröhlich, C.: Total solar irradiance during the Holocene, Geophys. Res. Lett., 36, L19704, doi:10.1029/2009GL040142, 2009.

Stott, P. A., Tett, S. F. B., Jones, G. S., Allen, M. R., Mitchell, J. F. B., and Jenkins, G. J.: External Control of 20th Century Temperature by Natural and Anthropogenic Forcing, Science, 290(5499), 2133–2137, 2000.

Stott, P. A., Jones, G. S., Lowe, J. A., Thorne, P., Durman, C., Johns, T. C., and Thelen, J.-C.: Transient climate simulations with the HadGEM1 climate model: causes of past warming and future climate change, J. Climate, 19, 2763–2782, 2006.

Taylor, K. E., Stouffer, R. J., and Meehl, G. A.: L A Summary of the CMIP5 Experiment Design, available at: http://www-pcmdi.llnl.gov/ (last access: 18 December 2009), 2009.

Tett, S. F. B., Jones, G. S., Stott, P. A., Hill, D. C., Mitchell, J. F. B., Allen, M. R., Ingram, W. J., Johns, T. C., Johnson, C. E., Jones, A., Roberts, D. L., Sexton, D. M. H., and Woodage, M. J.: Estimation of natural and anthropogenic contributions to 20th Century temperature change, J. Geophys. Res., 107, D16, doi:10.1029/2000JD000028, 2002.

Thomason, L. W., Burton, S. P., Luo, B.-P., and Peter, T.: SAGE II measurements of stratospheric aerosol properties at non-volcanic levels, Atmos. Chem. Phys., 8, 983–995, doi:10.5194/acp-8-983-2008, 2008.

van Vuuren, D. P., Eickhout, B., Lucas, P. L., and den Elzen, M. G. J.: Long-term multi-gas scenarios to stabilise radiative forcing – Exploring costs and benefits within an integrated assessment framework, Multigas Mitigation and Climate Policy, Energ. J. Special Issue, 201–234, 2006.

van Vuuren, D. P., den Elzen, M., Lucas, P., Eickhout, B., Strengers, B., van Ruijven, B., Wonink, S., and van Houdt, R.: Stabilizing greenhouse gas concentrations at low levels: an assessment of reduction strategies and costs, Clim. Change, 119–159, doi:10.1007/s10584-006-9172-9, 2007.

Wang, Y. and Jacob, D. J.: Anthropogenic forcing on tropospheric ozone and OH since preindustrial times, J. Geophys. Res., 103(D23), 31123–31135, 1998.

Wang, Y.-M., Lean, J. L., and Sheeley Jr., N. R.: Modelling the Sun's magnetic field and irradiance since 1713, Astrophys. J., 625, 522–538, 2005.

Woodward, S.: Modelling the atmospheric life cycle and radiative impact of mineral dust in the Hadley Centre climate model. J. Geophys. Res., 106, D16, 18155–18166, 2001.

Woodward S.: Mineral Dust in HadGEM2, Met Office Hadley Centre, Technical Note 87, 2011.

Yienger, J. and Levy II, H.: Empirical model of global soil-biogenic NO_x emissions, J. Geophys. Res., 100(D6), 11447–11464, 1995.

2.3. C4MIP experimental design for CMIP6

I am a co-chair of the Coupled Climate Carbon Cycle MIP (C4MIP; www.c4mip.net) and over the last three years I have led scientific planning of the next generation of coupled climate-carbon cycle experiments.

Processes in the natural carbon cycle currently remove approximately half of anthropogenic emissions of CO_2, helping to reduce the magnitude and rate of climate change. The primary scientific focus of C4MIP is therefore to understand and quantify future century-scale changes in land and ocean carbon storage and fluxes and their impact on climate projections. In order to achieve this, we have devised a set of ESM simulations, with a common protocol, which modelling centres should follow. To enhance clarity and to reduce computational demand, I ensured that we chose a minimum set of targeted simulations to achieve our three goals of evaluation, understanding and prediction. They comprise:

- Evaluation through historical experiments. The only way to evaluate models is to try to make them behave realistically over a period with available observations. Simulations from pre-industrial (circa 1850) to present day allow models to be tested for their simulation of properties such as vegetation cover and land and ocean carbon fluxes. Evaluation will draw on a range of observations including in-situ and remote sensed and focus on both long-term trends and variability and document the progress of models since CMIP5.
- Feedback quantification and process understanding through idealized experiments. The carbon cycle response during the historical period is a complex interaction of responses to multiple forcings including rising CO_2 levels, changing climate and changes in land-use, diffuse light and nutrient deposition. It is impossible to easily separate the role of these different factors, so factorial experiments will be carried out to separate the sensitivity to individual forcings. See chapter 3.1 for more details on the feedback framework we will apply.
- Prediction and projection using future scenarios. Projections of future climate and carbon cycle will be used to quantify changes in carbon storage and hence quantify the atmospheric CO_2 concentration and related climate change for a given set of CO_2 emissions, or, conversely, to diagnose the

emissions compatible with a prescribed atmospheric CO_2 concentration pathway. Section 4.3 describes the importance of better understanding carbon cycle behaviour under future pathways of low CO_2 levels. Quantification and understanding of uncertainty, informed by the spread of results across multiple models, is an essential aspect of C4MIP.

C4MIP is an endorsed CMIP6 activity, meaning that at least eight climate modelling centres around the world have committed to perform its experiments. It will focus on the coupled Earth system, comprising land–atmosphere–ocean physical realms and both the terrestrial and marine carbon cycle components. Offline studies of land only or ocean only will complement our analyses but are outside the specific remit of C4MIP. I have also been influential in the design and planning of land-use simulations that will contribute to the Land Use Model Intercomparison Project (LUMIP; **Lawrence et al., 2016**).

The construction of CMIP6 is presented in Eyring et al., (2016), and there is a special issue of the journal Geoscientific Model Development to document the associated MIPs (http://www.geosci-model-dev.net/special_issue590.html). My contribution, through leading C4MIP, is central to the plans for CMIP6 to address questions of how the Earth system responds to forcing and what this means for future climate change. The careful description of the planned experimental design and specification of the desired model outputs is laid out in the C4MIP documentation paper which I led (**Jones et al., 2016a**) and which forms the rest of this section.

Geosci. Model Dev., 9, 2853–2880, 2016
www.geosci-model-dev.net/9/2853/2016/
doi:10.5194/gmd-9-2853-2016

Geoscientific Model Development
Open Access
EGU

C4MIP – The Coupled Climate–Carbon Cycle Model Intercomparison Project: experimental protocol for CMIP6

Chris D. Jones[1], Vivek Arora[2], Pierre Friedlingstein[3], Laurent Bopp[4], Victor Brovkin[5], John Dunne[6], Heather Graven[7], Forrest Hoffman[8], Tatiana Ilyina[5], Jasmin G. John[6], Martin Jung[9], Michio Kawamiya[10], Charlie Koven[11], Julia Pongratz[5], Thomas Raddatz[5], James T. Randerson[12], and Sönke Zaehle[9]

[1]Met Office Hadley Centre, Exeter, EX1 3PB, UK
[2]Canadian Centre for Climate Modelling and Analysis, Climate Research Division, Environment and Climate Change, Victoria, Canada
[3]College of Engineering, Mathematics and Physical Sciences, University of Exeter, Exeter, EX4 4QE, UK
[4]Laboratoire des Sciences du Climat et de l'Environnement, LSCE/IPSL, CEA-CNRS-UVSQ, Université Paris-Saclay, 91191 Gif-sur-Yvette, France
[5]Max Planck Institute for Meteorology, Hamburg, Germany
[6]NOAA/GFDL, Princeton, NJ, USA
[7]Department of Physics and Grantham Institute, Imperial College London, London, UK
[8]Oak Ridge National Lab., Oak Ridge, TN, USA
[9]Biogeochemical Integration Department, Max Planck Institute for Biogeochemistry, 07745 Jena, Germany
[10]Japan Agency for Marine-Earth Science and Technology, Kanagawa, Japan
[11]Earth Sciences Division, Lawrence Berkeley National Laboratory, Berkeley, CA, USA
[12]Department of Earth System Science, University of California, Irvine, CA USA

Correspondence to: Chris D. Jones (chris.d.jones@metoffice.gov.uk)

Received: 12 February 2016 – Published in Geosci. Model Dev. Discuss.: 16 March 2016
Revised: 1 July 2016 – Accepted: 5 July 2016 – Published: 25 August 2016

Abstract. Coordinated experimental design and implementation has become a cornerstone of global climate modelling. Model Intercomparison Projects (MIPs) enable systematic and robust analysis of results across many models, by reducing the influence of ad hoc differences in model set-up or experimental boundary conditions. As it enters its 6th phase, the Coupled Model Intercomparison Project (CMIP6) has grown significantly in scope with the design and documentation of individual simulations delegated to individual climate science communities.

The Coupled Climate–Carbon Cycle Model Intercomparison Project (C4MIP) takes responsibility for design, documentation, and analysis of carbon cycle feedbacks and interactions in climate simulations. These feedbacks are potentially large and play a leading-order contribution in determining the atmospheric composition in response to human emissions of CO_2 and in the setting of emissions targets to stabilize climate or avoid dangerous climate change. For over a decade, C4MIP has coordinated coupled climate–carbon cycle simulations, and in this paper we describe the C4MIP simulations that will be formally part of CMIP6. While the climate–carbon cycle community has created this experimental design, the simulations also fit within the wider CMIP activity, conform to some common standards including documentation and diagnostic requests, and are designed to complement the CMIP core experiments known as the Diagnostic, Evaluation and Characterization of Klima (DECK).

C4MIP has three key strands of scientific motivation and the requested simulations are designed to satisfy their needs: (1) pre-industrial and historical simulations (formally part of the common set of CMIP6 experiments) to enable model evaluation, (2) idealized coupled and partially coupled simulations with 1 % per year increases in CO_2 to enable diagnosis of feedback strength and its components, (3) future scenario simulations to project how the Earth system will re-

spond to anthropogenic activity over the 21st century and beyond.

This paper documents in detail these simulations, explains their rationale and planned analysis, and describes how to set up and run the simulations. Particular attention is paid to boundary conditions, input data, and requested output diagnostics. It is important that modelling groups participating in C4MIP adhere as closely as possible to this experimental design.

1 Introduction

Over the industrial era since about 1750, it is estimated that cumulative anthropogenic carbon emissions from fossil fuels and cement (405 ± 20 PgC) and land-use change (190 ± 65 PgC) have been partitioned between the atmosphere (255 ± 5 PgC), the ocean (170 ± 20 PgC), and the terrestrial biosphere (165 ± 70 PgC) (values to the nearest 5 PgC, from Le Quéré et al., 2015). The carbon uptake by land and ocean, since the start of the industrial era, has thus slowed the rate of increase of atmospheric CO_2 concentration in response to anthropogenic carbon emissions. Had the land and ocean not provided this "ecosystem service", the atmospheric CO_2 concentration at present would be much higher. The manner in which the land and ocean will continue to absorb anthropogenic carbon emissions has both scientific and policy relevance. Understanding the future partitioning of anthropogenic CO_2 emissions into the atmosphere, land and ocean components, and the resulting climate change, accounting for biogeochemical feedbacks requires a full Earth system approach to modelling the climate and carbon cycle.

The primary focus of the Coupled Climate–Carbon Cycle Model Intercomparison Project (C4MIP; http://www.c4mip.net) is to understand and quantify future century-scale changes in land and ocean carbon storage and fluxes and their impact on climate projections. In order to achieve this, a set of Earth system model (ESM) simulations has been devised. As a consequence of the very high computational demand on modelling centres to perform a multitude of simulations for many different intercomparison studies as part of CMIP6, we have carefully chosen a minimum set of targeted simulations to achieve C4MIP goals. They comprise

- idealized experiments, which will be used to separate and quantify the sensitivity of land and ocean carbon cycle to changes in climate and atmospheric CO_2 concentration;
- historical experiments, which will be used to evaluate model performance and investigate the potential for using contemporary observations as a constraint on future projections;
- future scenario experiments, which will be used to quantify future changes in carbon storage and hence quantify the atmospheric CO_2 concentration and related climate change for a given set of CO_2 emissions, or, conversely, to diagnose the emissions compatible with a prescribed atmospheric CO_2 concentration pathway.

The simulations are designed to complement those requested in the CMIP6 Diagnostic, Evaluation and Characterization of Klima (DECK) and the CMIP6 historical simulation (Eyring et al., 2016a). They also align closely with simulations performed as part of ScenarioMIP (O'Neill et al., 2016) by quantifying the role of carbon cycle feedbacks in the evolution of atmospheric CO_2 due to anthropogenic carbon emissions. Synergies with other MIPs are discussed in Sect. 2. C4MIP simulations and analyses will play a major role contributing to the WCRP Carbon Feedbacks in the Climate System – Grand Challenge (http://www.wcrp-climate.org/gc-carbon-feedbacks). This is the third generation of C4MIP following the first coordinated experiments described in Friedlingstein et al. (2006) and the carbon cycle simulations that formed part of CMIP5 (Taylor et al., 2012).

In this paper we first briefly describe the scientific rationale and motivation for the C4MIP simulations and then carefully document the experimental protocol in Sect. 3. Modelling groups intending to participate in C4MIP should follow the design described here as closely as possible. Particular attention should be given to the set-up of boundary conditions in terms of atmospheric CO_2 concentration or emissions and which aspects of the model experience changes in the fully coupled or partially coupled simulations. Output requirements (diagnostics) are also carefully documented in Sect. 4.

Along with our science motivation (Sect. 2), we highlight initial plans for the analyses of the carbon cycle and its interactions with the physical climate system. Modelling groups will be invited to contribute to the primary C4MIP analysis papers. We anticipate, and hope, that many further studies and analyses will also be conducted throughout the climate–carbon cycle research community and that these simulations provide a valuable resource to further carbon cycle research.

2 Background and science motivation

2.1 C4MIP history

The potential for a climate feedback on the carbon cycle whereby carbon released due to warming would further elevate atmospheric CO_2 and amplify climate change was first discussed in the late 1980s–early 1990s (e.g. Lashof et al., 1989; Jenkinson et al., 1991; Schimel et al., 1994; Kirschbaum, 1995; Sarmiento and Le Quéré, 1996). On the land side, dynamic global vegetation models were used to study the impact of rising CO_2 and climate change on the carbon cycle (Cramer et al., 2001). There was a strong model consensus that rising CO_2 would stimulate additional vegetation growth and storage of carbon in terrestrial ecosystems,

likewise warming climate would accelerate decomposition of dead organic matter and may also reduce vegetation productivity in some (mainly tropical) ecosystems (Prentice et al., 2001). Similarly for the ocean, there was also a model consensus that warming would lead to reduced carbon uptake (Prentice et al., 2001). This was due to both reduced solubility in warmer waters and reduced rate of transport of anthropogenic carbon to the deep ocean as a consequence of increasing stratification and shutdown of meridional overturning circulation. The processes behind the former (carbonate chemistry and solubility) were reasonably well understood (Bacastow, 1993), but the latter was much more uncertain being sensitive to the underlying ocean model circulation (Maier-Reimer et al., 1996; Sarmiento et al., 1998; Joos et al., 1999). The role of ocean biology and the buffering capacity of the ocean were also seen to be important and not well constrained or represented in models (Sarmiento and Le Quéré, 1996).

These "offline" land and ocean experiments found potentially high sensitivity of the carbon cycle to environmental forcing but were not able to simulate the full effect of this feedback onto climate. By the end of the 1990s some modelling groups were beginning to implement interactive carbon cycle modules in their physical climate models. These early studies (e.g. Cox et al., 2000; Friedlingstein et al., 2001; Dufresne et al., 2002; Thompson et al., 2004) were able to recreate an experimental setting more like the real world where a climate change forced by anthropogenic CO_2 emissions would affect natural carbon sinks and stores, which in turn would affect changes in atmospheric CO_2 and hence climate.

It soon became apparent from the first publications that there were substantial differences in the sensitivities of these new models. The desire to understand and reduce this uncertainty led to the development of a linearized feedback framework to diagnose the sensitivity of different parts of the system and their contribution to the overall feedback (Friedlingstein et al., 2003), and also of a multi-model intercomparison activity (C4MIP: Coupled Climate–Carbon Cycle Model Intercomparison; Fung et al., 2000). The result was the first C4MIP intercomparison paper, (Friedlingstein et al., 2006), which quantified the feedback components across 11 models for a common CO_2 emissions scenario. All models agreed qualitatively that the sign of the carbon–climate feedback was positive – i.e. the interaction of the carbon cycle with climate led to reduced carbon uptake and hence an increase in atmospheric CO_2, which amplified the initial climate change. However, there was large quantitative model spread in the total feedback and its sensitivity components. Initial analysis of the causes of this uncertainty concluded that the land played a greater role than the ocean, in particular its sensitivity to climate. Regionally, the tropics were seen to be particularly different between models (Raddatz et al., 2007), bearing in mind that none of these models included representation of permafrost carbon. The CMIP5 experimental design for carbon cycle feedback diagnosis (Taylor et al., 2012) closely followed the C4MIP protocol. Modelling centres around the world contributed results to CMIP5 and their analysis led to many key papers including a special collection of 15 papers published in the *Journal of Climate* (http://journals.ametsoc.org/topic/c4mip).

The C4MIP activity under CMIP5 was central to Working Group 1 of the IPCC 5th Assessment. Several of the main findings from C4MIP studies were included in the Summary for Policymakers of WG1, such as the positive feedback between climate and carbon cycle – "climate change will affect carbon cycle processes in a way that will exacerbate the increase of CO_2 in the atmosphere"; the impact of elevated CO_2 on ocean acidification – "further uptake of carbon by the ocean will increase ocean acidification"; the emissions compatible with given CO_2 concentrations – "by the end of the 21st century, [for RCP2.6] about half of the models infer emissions slightly above zero, while the other half infer a net removal of CO_2 from the atmosphere"; and the very policy relevant relationship between cumulative CO_2 emissions and global warming – "cumulative emissions of CO_2 largely determine global mean surface warming by the late 21st century and beyond".

2.2 Key science motivation and analysis plans for C4MIP

The key science motivations behind C4MIP are (1) to quantify and understand the carbon-concentration and carbon–climate feedback parameters which respectively, capture the modelled response of land and ocean carbon cycle components to changes in atmospheric CO_2 and the associated climate change; (2) to evaluate models by comparing historical simulations with observation-based estimates of climatological states of carbon cycle variables, their variability, and long-term trends; (3) to assess the future projections of the components of the global carbon budget for different scenarios, including atmospheric CO_2 concentration, atmosphere–land and atmosphere–ocean fluxes of CO_2, diagnosed CO_2 emissions compatible with future scenarios of CO_2 pathway and crucially to provide new estimates of the cumulative CO_2 emissions compatible with specific climate targets. In light of the COP21 Paris agreement (https://unfccc.int/resource/docs/2015/cop21/eng/l09r01.pdf), these experiments will quantify carbon cycle feedbacks in low emissions scenarios and inform cumulative budgets consistent with a 1.5 or 2 °C stabilization objective.

Relative to CMIP5 there are three key areas where we expect CMIP6 models to have made substantial progress and hence may cause significant differences in the simulated response of the carbon cycle to anthropogenic forcing.

i. In CMIP5, only two participating ESMs included a land surface component (CLM4) that explicitly considered constraints of terrestrial N availability on primary production and net land carbon storage (Lindsay et al.,

2014; Tjiputra et al., 2013). An increasing number of land models now include a prognostic representation of the terrestrial N cycle and its coupling to the land C cycle (Zaehle and Dalmonech, 2011). Some of these prognostic N cycle representations are expected to be used in land components of ESMs participating in CMIP6. Coupling of carbon and nitrogen dynamics changes the response of the terrestrial biosphere to global change in four ways: (1) it generally reduces the response of net primary production and carbon storage to elevated levels of atmospheric CO_2 because of an increasing limit of nitrogen availability for carboxylation enzymes and new tissue construction; (2) it allows for changes in plant allocation in response to changing nutrient availability; (3) it generally decreases net ecosystem C losses associated with soil warming, because increased decomposition leads to increased plant N availability, which can potentially increase plant productivity and C storage in N-limited ecosystems; and (4) it alters primary production due to anthropogenic N deposition and fertilizer application, which may regionally enhance net C uptake. The magnitude of each of these processes is uncertain given strong natural gradients in the natural N availability in ecosystems and sparse ecosystem data to constrain these models (Thornton et al., 2009; Zaehle et al., 2014; Meyerholt and Zaehle, 2015) but offline analysis of CMIP5 simulations suggests significant overestimation of terrestrial carbon uptake in models that neglect the role of nitrogen (Wieder et al., 2015; Zaehle et al., 2015). The new generation of models will provide a more comprehensive assessment of the attenuating effect of nitrogen on carbon cycle dynamics compared to CMIP5 and in particular provide a better constrained estimate of the carbon storage capacity of land ecosystems.

ii. In CMIP5, all land models used a single-layer, vertically integrated representation of soil biogeochemistry (Luo et al., 2016). Such an approach necessarily ignores vertical variation in soil carbon turnover times, which can be very important in governing ecosystem carbon storage. This omission is most notable in the extreme case of permafrost soils, where there exists a depth at which soils remain frozen year-round and, because of the abrupt change in decomposition rates in frozen vs. unfrozen soils, otherwise highly decomposable carbon can be preserved indefinitely until it is thawed. The majority of global soil carbon is in permafrost-affected ecosystems, which creates the possibility for permafrost climate feedbacks (Burke et al., 2013). Some of the models in CMIP6 are expected to include representation of permafrost soil carbon dynamics, either explicitly by representing soil biogeochemistry along the full soil depth axis (Koven et al., 2013), or by means of reduced-complexity methods to incorporate permafrost dynamics. IPCC Fifth Assessment Report (AR5) concluded that permafrost carbon release was likely, and therefore would increase the climate–carbon cycle feedback, but with low confidence in the magnitude (Ciais et al., 2013). Assessing the role of this process in governing fully coupled climate feedbacks will be an important contribution to CMIP6.

iii. Representation of ocean dynamics in the ESMs is another important constraint affecting the oceanic carbon uptake and storage. There is evidence that by shifting to an eddy-permitting grid configuration of the ocean general circulation model, the representation of some key features of oceanic circulation, such as the interior water-mass properties and surface ocean current systems, are improved (Jungclaus et al., 2013). The increased horizontal resolution of the underlying ocean model has a positive impact on the performance of the marine biogeochemistry model in the deeper layers (Ilyina et al., 2013). Spatial resolution of some ESMs is expected to increase as they move into CMIP6. The increased resolution of the oceanic components of the ESMs is expected to have some explicit advantages for projections of the oceanic carbon uptake. First, it allows us to estimate the role of previously unresolved small-scale ocean hydrodynamical process on projections of marine biogeochemistry. Second, by improving the representation of coastal processes and ocean–shelf exchange, their contribution to the global carbon cycle can be assessed.

2.2.1 Carbon cycle feedback parameters

The first key motivation for C4MIP is to document the changes in magnitude of the feedback parameters that characterize the response of the carbon cycle and their spread across models through time. In this respect, C4MIP aims to calculate the magnitude of the carbon-concentration and carbon–climate feedbacks in a manner similar to Friedlingstein et al. (2006) or Arora et al. (2013) and as discussed in Sect. 3.1 using results from the idealized 1 % per year increasing CO_2 experiments.

The 1pctCO2 experiment has gained recognition as a standard CMIP simulation and it is one of the DECK simulations for CMIP6 (Eyring et al., 2016a). The 1pctCO2 experiment is now routinely used to characterize the transient climate response (TCR) defined as the change in globally averaged near-surface air temperature at the time of CO_2 doubling as well as the transient climate response to cumulative emissions (TCRE) defined as change in globally averaged near-surface air temperature per unit cumulative CO_2 emissions at the time of CO_2 doubling (Gillett et al., 2013). In addition, since the 1pctCO2 simulation does not include the confounding effects of changes in land use, non-CO_2 greenhouse gases, and aerosols it provides a clean controlled experiment

with which to compare carbon–climate interactions across models. Its backwards compatibility enables direct comparison of models with previous generations, which has been hindered previously as the scenario-dependence of the feedback metrics has prevented a like-for-like comparison (Gregory et al., 2009).

C4MIP will use partially coupled simulations to isolate and quantify the sensitivity of carbon cycle components to climate and CO_2 separately and also the potentially large non-linear combination of these two components (Gregory et al., 2009; Schwinger et al., 2014). Simulations with only the carbon cycle model components experiencing rising CO_2 (biogeochemically (BGC) coupled) and the radiation model components experiencing rising CO_2 (radiatively (RAD) coupled) are used to quantify the carbon-concentration and carbon–climate feedbacks. Spatial patterns of these metrics can also be calculated (e.g. Roy et al., 2011; or Fig. 6.22 of the last IPCC WG1 assessment report Ciais et al., 2013) to establish areas of model agreement or disagreement.

2.2.2 Evaluation of global carbon cycle models

The historical simulations will be used for evaluation of the components of the carbon cycle (ocean and terrestrial carbon fluxes, anthropogenic carbon storage in the ocean, atmospheric CO_2 growth rate and variability). ESMs have increased rapidly in complexity but evaluation has not kept pace. Some evaluation of the carbon cycle was already performed in CMIP5 (e.g. Anav et al., 2013; Bopp et al., 2013; Hoffman et al., 2014), highlighting significant biases in key quantities in many ESMs. There is increasing need to develop evaluation techniques and activities, applied consistently and routinely across models, at both fine scales (process-level, "bottom-up" evaluation) and large scales (system-level, "top-down" evaluation"), as well as using complementary data streams relating to (bio)physical and biogeochemical processes to evaluate the ensemble of simulated processes (e.g. Luo et al., 2012; Foley et al., 2013).

Evaluation of ocean carbon cycle components of ESMs has been classically based on the use of the monthly surface pCO_2 climatology of Takahashi et al. (2009), derived from more than 3 million in situ ocean pCO_2 measurements, as in Pilcher et al. (2015) for an evaluation of pCO_2 seasonality of the CMIP5 ESMs. This evaluation is complemented by the use of additional climatological gridded products, as in Anav et al. (2013), with model–data comparison for related physical variables (e.g. mixed layer depth) or biological variables (e.g. net primary production). In the past few years, ESM evaluation has extended in many directions, making use of advanced observation-based gridded products (e.g. the three-dimensional distribution of anthropogenic carbon in the ocean from Khatiwala et al., 2013) and ocean databases with millions of in situ point measurements (e.g. with the Surface Ocean CO_2 Atlas (SOCAT) as in Tjiputra et al. (2014) for CMIP5 ESMs), or developing new techniques for model–data comparisons (e.g. water-mass framework; Iudicone et al., 2011).

In the coming years, the increasing complexity of marine biogeochemical schemes used in ESMs will call for more advanced model–data comparison strategies. These will include the use of new data sets, such as biomass data for plankton functional types (MAREDAT; Buitenhuis et al., 2013) or ocean distribution of the micro-nutrient iron (Tagliabue et al., 2012).

Evaluations of land surface components of ESMs have often used gridded flux products (e.g. Bonan et al., 2011; Anav et al., 2013; Piao et al., 2013) obtained by extrapolating the FLUXNET measurement network of biosphere–atmosphere exchanges (e.g. Jung et al., 2011), for instance to constrain modelled spatial and seasonal distribution of gross primary production (GPP). Such products are convenient for such model evaluations because those are available at a resolution comparable to that of the models and because they retain the pertinent patterns of the observed fluxes while abstracting from measurement noise, local site representativeness and other possible site-specific features. Yet it is important to bear in mind the limitations of the "upscaled" flux and stock products and to tailor the model evaluation to robust patterns that the individual products are ideally suited for. Insights may also be gained from evaluation of functional patterns and sensitivities to certain climate forcing variables. For example the spatial sensitivity of GPP with mean annual precipitation in the water-limited domain, and the temperature sensitivity of ecosystem respiration (Mahecha et al., 2010).

While data-model comparisons of fluxes are important, they alone cannot constrain longer-term dynamics and associated climate–carbon cycle feedbacks. In addition, consideration of residence times is crucial, which together with carbon fluxes jointly determine the stores. Analysis of CMIP5 ESMs revealed unacceptably large errors in land carbon stores (both in living biomass and soil organic matter) (Anav et al., 2013). Future simulation results were found to depend on the initial conditions as well as the model sensitivity to changes (Todd-Brown et al., 2014) and therefore better evaluation and constraint of carbon stores is seen as vital. Xia et al. (2013) showed the importance of residence time in determining carbon stores and Carvalhais et al. (2014) showed the mismatch between CMIP5 ESMs and an observationally derived data set of land-carbon residence times. As more observations become available (Saatchi et al., 2011; Baccini et al., 2012; Avitabile et al., 2015; FAO, 2012; Batjes et al., 2012; Hengl et al., 2014) as well as data constrained products such as residence time (Bloom et al., 2016), we stress the importance of rapid development and application of evaluation techniques to ESMs.

Carbon isotopes (carbon-13 and carbon-14) provide unique insights into the mechanisms and timescales of carbon cycling. Differences between the isotopic fractionation of carbon from dissolution in the ocean and from photosynthetic assimilation on land have enabled atmospheric ob-

servations of the ^{13}C / ^{12}C ratio ($\delta^{13}C$) in atmospheric CO_2 to be used in differentiating land and ocean carbon fluxes (Ciais et al., 1995; Joos et al., 1998; Rubino et al., 2013). The perturbation of the ^{14}C / C ratio ($\Delta^{14}C$) in atmospheric CO_2 from nuclear weapons testing in the 1950s and 60s has provided a valuable tracer of carbon turnover rates in terrestrial carbon pools (Trumbore, 2000; Naegler and Levin, 2009), and the rates of air–sea exchange and ocean mixing, including constraints on ocean CO_2 uptake (Matsumoto et al., 2004; Sweeney et al., 2007; Graven et al., 2012). Integration of carbon isotopes into ESMs is an emerging activity and we request the reporting of carbon isotopic variables for the first time in C4MIP. Carbon isotopes are also included in OMIP (Orr et al., 2016). ESMs that simulate carbon isotopes are requested to report fluxes and stocks of carbon isotopes in their land and ocean components. This will enable comparison between models currently simulating carbon isotopes and their evaluation by observations, as well as encourage future development of carbon isotopes in ESMs. Simulation of carbon isotopes in C4MIP is expected to provide novel insights on ocean mixing and air–sea exchange, marine ecosystem change, plant water use efficiency and stomatal closure especially during drought periods, and terrestrial carbon residence times.

Historical simulations will be needed to explore potential emergent constraints from observations on the future response of the carbon cycle, with a particular focus on carbon cycle feedbacks. Recent studies showed the potential of observed interannual CO_2 variability to constrain the future tropical land carbon cycle sensitivity to climate change (Cox et al., 2013; Wenzel et al., 2014).

In the same way that Earth system modelling has become an internationally collaborative activity involving shared expertise and development of tools, we also expect that evaluation techniques will evolve in this way. Community evaluation activities such as ILAMB (http://www.ilamb.org/) and ESMValTool (Eyring et al., 2016b) look likely to become increasingly useful for addressing the complexities of multi-model ESM evaluation.

2.2.3 Future projections of the components of the global carbon budget

While idealized experiments are useful for intercomparison of climate–carbon interactions across multiple models, they do not take into account the effect of non-CO_2 GHGs, aerosols, and land-use change, all of which affect the behaviour of the carbon cycle in the real world. In contrast, the scenarios considered by the ScenarioMIP are internally coherent in all aspects of anthropogenic forcings. Within each socio-economic storyline, changes in fossil fuel CO_2 emissions are consistent with those in aerosols emissions, N deposition, and changes in land-use areas, all of which are based on plausible assumptions of demographic and economic development in the future. This plausibility is of special interest to policymakers. Scenarios also indicate the range of possible future developments and opportunities for mitigation and adaptation; this information is used widely in climate impact analyses.

The scenario simulations, therefore, provide more realistic conditions compared to the idealized 1 % experiments due to their plausibility of anthropogenic forcings as well as the longer timescale over which the CO_2 increase occurs. Since shared socio-economic pathway (SSP) scenarios include all forcings, their climate and biogeochemical effects are able to influence the atmosphere–surface carbon exchange for both land and ocean components. Emission-driven historical and the future SSP5-8.5 simulations replicate a more realistic model setting where ESMs are directly forced by anthropogenic CO_2 emissions, allowing for the carbon cycle feedbacks to impact on atmospheric CO_2 and simulated climate change. These will be compared with the concentration-driven equivalents in ScenarioMIP and additionally will form a baseline control experiment for analysis of alternative future land-use scenarios in LUMIP (Lawrence et al., 2016).

The proposed biogeochemically coupled versions of the historical and future SSP5-8.5 in Sect. 3.1, in which CO_2 induced warming is not accounted for, when compared to their fully coupled versions will allow us to investigate the effect of CO_2 induced warming on atmosphere–land and atmosphere–ocean CO_2 fluxes over the 20th and 21st century and beyond (Randerson et al., 2015). An important objective with these simulations will be to identify how land and ocean contributions to feedbacks and compatible emissions evolve century by century from sustained increases in ocean heat content and thawing of permafrost soils.

ScenarioMIP (O'Neill et al., 2016) acknowledges scientific and policy interest in a scenario with a substantial overshoot in radiative forcing during the 21st century. As such they include a tier-2 concentration-driven scenario called SSP5-3.4-OS: an overshoot pathway, which follows SSP5-8.5 up to 2040, followed by aggressive mitigation to reduce emissions to zero by about 2070, and by substantial negative global emissions thereafter. The carbon cycle response to peak-and-decline CO_2 levels is likely to differ from the response to continued strong increases in CO_2. The 21st century airborne fraction from CMIP5 models varied substantially between RCPs, with RCP2.6 in particular having a much lower airborne fraction than the 20th century or other RCPs (Jones et al., 2013). However, to date there have been no coordinated experiments to quantify the carbon-cycle feedback components in such a scenario. Hence, for C4MIP we include a BGC simulation of the SSP5-3.4-OS scenario.

2.3 Links to and requirements from other MIPs

The Ocean Model Intercomparison Project (OMIP; Griffies et al., 2016; Orr et al., 2016) will provide a baseline for assessment of ocean component model biogeochemical and

historical carbon uptake fidelity. Ocean carbon cycle analysis has previously been conducted under the OCMIP (Ocean carbon-cycle model intercomparison project) intercomparison (Orr et al., 2001). In response to the WGCM (Working Group on Coupled Modelling) request, the OMIP and OCMIP have been merged under the OMIP umbrella. One main objective of OMIP is to coordinate CMIP6 ocean diagnostics including ocean physics, inert chemical tracers, and biogeochemistry for all CMIP6 simulations that include an ocean component. The second objective is to perform a global ocean–sea-ice simulation forced with common atmospheric data sets. In this way, ocean models including online biogeochemistry components will be part of "Path-II" simulation, (whereas "Path-I" is designated to models without the biogeochemistry). Within OMIP, ocean-only simulations will be performed as described in Griffies et al. (2016).

Analysis of changes in terrestrial carbon stocks for historical and future scenarios as result of changes in atmospheric CO_2, climate, and land-use and land-use-induced land cover change (LULCC) will be done in coordination with LUMIP (Lawrence et al., 2016). The emission-driven future scenario performed within C4MIP serves as control simulation for LUMIP. By replacing the LULCC forcing of SSP5-8.5 by the one from SSP1-2.6 under otherwise identical forcings the effect of LULCC can thus be isolated. This also implies that output provided for the emission-driven simulation should account for the additional requirements of LUMIP such as tile-level reporting of variables. Offline land-surface process studies form part of LS3MIP (van den Hurk et al., 2016) and offline simulations to quantify the contemporary land carbon budget are performed under the TRENDY intercomparison (Sitch et al., 2015).

The scientific scope of the Detection and Attribution intercomparison (DAMIP) includes attempting some observational constraint on the transient climate response to cumulative emissions (TCRE) (Gillett et al., 2016), whose assessment is also an important target of C4MIP. Collaborative opportunities exist between C4MIP and DAMIP for analyses of TCRE with C4MIP covering carbon cycle aspects of the historical runs. Furthermore, results from DAMIP analysis runs will provide insights on the mechanism of fluctuations of past CO_2 growth rate. Synergies also exist between DAMIP and LUMIP, and also RFMIP (Radiative Forcing Model Intercomparison Project), regarding the biophysical effects of land-use change.

3 C4MIP Experiments

3.1 Overview of simulations and their purpose

The C4MIP protocol for CMIP6 builds on DECK and historical CMIP6 simulations, which are documented in detail in Eyring et al. (2016a). The following experiments are not formally C4MIP simulations but are considered prerequisite simulations for C4MIP analyses:

- CMIP DECK pre-industrial control simulation (piControl), with specified CO_2 concentration ("concentration driven").
- CMIP DECK pre-industrial control simulation (esm-piControl), with interactively simulated atmospheric CO_2 ("emissions driven", but with zero emissions).
- CMIP DECK 1 % per year increasing CO_2 simulation (1pctCO_2) initialized from pre-industrial CO_2 concentration until quadrupling. In C4MIP terminology this is "fully coupled" meaning that both the model's radiation and carbon cycle components see the increasing CO_2 concentration.
- CMIP6 concentration-driven historical simulation for 1850–2014 (historical).
- CMIP6 emissions-driven historical simulation with interactively simulated atmospheric CO_2 (esm-hist) forced by anthropogenic emissions of CO_2. Other forcings such as non-CO_2 GHGs, aerosols, and land-cover change are being prescribed as in the CMIP6 concentration-driven historical simulation.

These simulations are documented in detail in Eyring et al. (2016a), but here we emphasise some carbon-cycle-specific aspects and requirements.

The simulations specifically identified as C4MIP simulations are separated into two tiers. We require only a minimalistic two experiments for C4MIP tier-1 analysis. These are

- biogeochemically coupled version of the 1 % per year increasing CO_2 simulation (1pctCO2-bgc);
- emissions-driven future scenario based on the SSP5-8.5 scenario (esm-ssp585).

The rationale for these two required simulations is that they form a minimum set of outputs required to quantify the climate–carbon cycle feedback in a model and to simulate the full effects of this feedback on future climate under a high-end emissions scenario. The emissions scenario also provides a control for the LUMIP esm-ssp585-ssp126Lu simulation.

Further simulations are then requested under C4MIP tier-2, which allow a more complete investigation of the feedback components, their non-linearities, their sensitivity to nitrogen limitations (if included in the model) and the role of their effects on future scenarios including sustained CO_2 increases and a peak-and-decline in forcing. It is highly desirable that as many of these as possible are performed to accompany the tier-1 simulations. They are divided into two categories:

i. Idealized simulations
   - RAD version of the 1 % per year increasing CO_2 simulation (1pctCO2-rad);

- COU (fully coupled) 1 % per year increasing CO_2 simulation with nitrogen deposition (1pctCO2Ndep);
- BGC version of the 1 % per year increasing CO_2 simulation with nitrogen deposition (1pctCO2Ndep-bgc).

ii. Scenario simulations

- biogeochemically coupled version of the concentration-driven historical CMIP6 simulation (hist-bgc);
- biogeochemically coupled version of the concentration-driven future SSP5-8.5 scenario (ssp585-bgc);
- biogeochemically coupled version of the concentration-driven future extension of the SSP5-8.5 scenario (ssp585-bgcExt);
- biogeochemically coupled version of the concentration-driven future SSP5-3.4-over scenario (ssp534-over-bgc);
- biogeochemically coupled version of the concentration-driven future extension of the SSP5-3.4-over scenario (ssp534-over-bgcExt),

Note that 1pcCO2Ndep and 1pcCO2Ndep-bgc are only applicable to models whose simulation will be affected by the deposition of reactive nitrogen either due to terrestrial or marine nitrogen cycle effects on carbon fluxes and stores. Similarly, the biogeochemically forced scenario simulations (ssp585-bgc and ssp534-over-bgc) are only required if the coupled ScenarioMIP counterpart has been performed (ssp585 and ssp534-over). If computing resource limits the number of simulations performed we recommend prioritising ssp585-bgc over ssp534-over-bgc.

The simulations required for C4MIP are summarized in Table 1 and the CO_2 concentration is shown schematically in Fig. 1 in the context of the CMIP6 DECK, historical simulations, and the ssp585 future scenario, which is a tier 1 experiment of the ScenarioMIP (O'Neill et al., 2016). Table 2 shows the main simulations from other MIPs, which form crucial counterparts to C4MIP simulations. The rest of this section documents detailed instructions on how to set up and perform the C4MIP simulations. Detailed definitions of the output requirements are listed in Sect. 4.

3.2 Experimental details

3.2.1 Model requirements and spin-up

To participate in C4MIP a climate model must have the capability to run with an interactive carbon cycle. This means it must simulate both terrestrial and marine carbon cycle processes, and it must simulate the exchange of CO_2 between the land/ocean and the atmosphere in order to prognostically

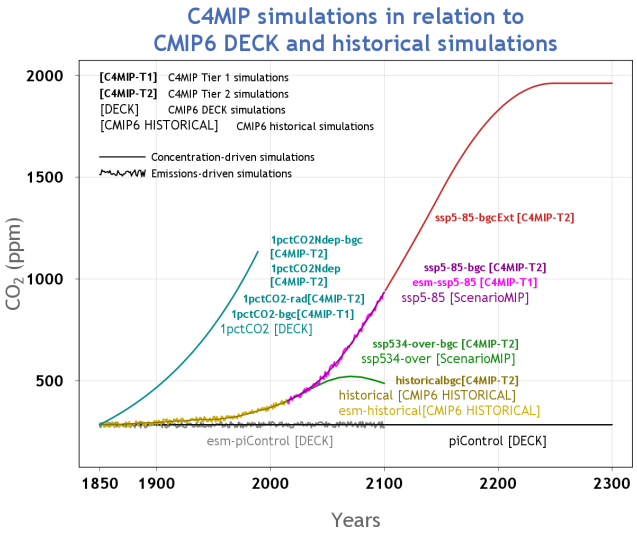

Figure 1. Relation of C4MIP simulations to CMIP6 DECK and historical simulations and the ssp585 and ssp5-34-over future scenario simulation proposed for the ScenarioMIP. Note that at the time of preparing this manuscript the details of the SSP5-3.4-OS-Ext extension to 2300 are not available; hence, it could not be included in the figure, but it is still requested as a C4MIP tier-2 simulation.

simulate the evolution of atmospheric CO_2. Some C4MIP simulations prescribe a concentration of CO_2 in the atmosphere as a boundary condition and simulate the changes in carbon fluxes and stores in response. Other simulations prescribe emissions of CO_2 to the atmosphere (from human activity) as an external forcing and require the model to also simulate the evolution of atmospheric CO_2. A model must be able to run in both these configurations in order to perform the C4MIP simulations. The evolution of atmospheric CO_2 concentration can be simulated by assuming that CO_2 is completely well mixed with the same globally averaged concentration everywhere in space or by transporting CO_2 as a three-dimensional tracer. This choice is up to the modelling groups. Throughout this document we refer to the former – prescribing atmospheric CO_2 concentration as a boundary condition – as a "concentration-driven" simulation, and the latter – prescribing emissions and in turn simulating the CO_2 concentration – as an "emissions driven" simulation. IPCC AR5 WG1 Ch.6 Box 6.4 described the use of these configurations in some detail (Ciais et al., 2013). Figure 6.4 from that Box is reproduced here for reference (Fig. 2). Although the same terminology (concentration-driven or emissions-driven) can be applied to aerosols or non-CO_2 GHGs this paper focuses only on CO_2.

Before beginning the simulations described below, a model must be spun-up to eliminate any long-term drift in carbon stores or fluxes. Indeed, it has been shown recently that the large diversity in spin-up protocols used for marine biogeochemistry in CMIP5 ESMs contribute to large model-to-model differences in simulated fields, and that drifts have

Table 1. Summary of the C4MIP tier-1 and tier-2 simulations. Simulations can be "concentration driven" or "emissions driven" as described in the text. Coupling mode refers to which model components see changes in atmospheric CO_2.

Category	Type of scenario	Emission or concentration driven	Coupling mode	Simulation years	Short name
Tier 1					
1 %BGC	Idealized 1 % per year CO_2 only, BGC mode	C driven	CO_2 affects BGC	140	1pctCO2-bgc
SSP5-8.5	SSP5-8.5 up to 2100	E driven	Fully coupled	85	esm-ssp585
Tier 2					
1 %RAD	Idealized 1 % per year CO_2 only, RAD mode	C driven	CO_2 affects RAD	140	1pctCO2-rad
1 %COU-Ndep	Idealized 1 % per year CO_2 only, fully coupled, increasing N-deposition	C driven	Fully coupled	140	1pctCO2Ndep
1 %BGC-Ndep	Idealized 1 % per year CO_2 only, BGC mode, increasing N-deposition	C driven	CO_2 affects BGC	140	1pctCO2Ndep-bgc
Hist/SSP5-8.5-BGC	Historical+SSP5-8.5 up to 2300, BGC mode	C driven	CO_2 affects BGC	165 85 200	hist-bgc, ssp585-bgc and ssp585-bgcExt
SSP5-3.4-Overshoot-BGC	SSP5-3.4-OS up to 2300 in BGC mode	C driven	CO_2 affects BGC	60 (from 2040–2100) 200	ssp534-over-bgc, ssp534-over-bgcExt

potential implications on model performance assessments in addition to possibly aliasing estimates of climate change impacts (Séférian et al., 2016). Separate spin-up simulations should be performed for both concentration-driven and emission-driven configurations. There are many possible techniques to ensure that a model's carbon fluxes and pools exhibit minimal drift. These include simply performing very long simulations, running components offline from the coupled system, numerical acceleration techniques or semi-analytical schemes such as described by Xia et al. (2012). The choice of technique is up to the modelling groups and there is no requirement to submit data from the spin-up period, but a proper documentation of the spin-up technique and duration is required. The test of whether a model is spun-up properly and exhibits minimal drift will be based on the performance of the piControl simulation. It is suggested that the model first be spun-up in concentration-driven mode and this state can be used as an initial basis for the emission-driven spin-up.

Our definition of an acceptably small drift in a properly spun-up model is that land, ocean, and atmosphere carbon stores each vary by less than 10 PgC/century (i.e., a long-term average $\leq 0.1\,\mathrm{PgC\,yr^{-1}}$). This is broadly equivalent to an atmospheric CO_2 drift of less than about 5 ppm/century. We suggest that a drift smaller than this value is highly desirable but this value is a guideline. Exceeding this drift in the control run may preclude a model from being included in a C4MIP analysis, but we would expect that decision to be made on a case-by-case basis. For example, a large ocean drift in a concentration-driven experiment may not preclude analysis of land carbon fluxes and vice-versa. We also stress that being within these drifts is a minimum but not necessarily sufficient quality condition. Regional patterns and drifts of stores and fluxes will also be assessed and depending on the analysis may preclude inclusion of a given model's results.

For simulations of carbon isotopes, spin-up times of many thousands of years or the use of an equivalent fast spin-up technique may be required to eliminate drift, particularly for carbon-14 in ocean carbon and soil carbon. The spin-up technique is left to the modellers' discretion.

3.2.2 DECK piControl and historical

The pre-industrial control run (piControl) is a required simulation of the CMIP DECK, and a prerequisite simulation for participating in C4MIP. The run begins from a spun-up state as described above and all forcings should continue to be applied as per the spin-up. The global land and ocean carbon stores should not drift by more than 10 PgC/century each. The length of the pre-industrial control run should be at least

Table 2. Summary of key simulations from CMIP6 DECK, historical or other MIPs on which C4MIP analysis will rely. The emissions-driven control and historical runs in particular are entry card requirements for C4MIP.

Type of simulation	Simulation name	Owning MIP	Notes
Control			
	piControl	DECK	Prescribed pre-industrial CO_2 concentration
	esm-piControl	DECK	Prognostically simulated atmospheric CO_2 concentration; required if performing any emissions-driven simulations for C4MIP
Idealized			
	1pctCO2	DECK	Forms essential counterpart for C4MIP BGC and RAD 1 % simulations
Historical			
	historical	CMIP6 historical	
	esm-hist	CMIP6 historical	Prognostically simulated atmospheric CO_2 concentration; required if performing any emissions-driven simulations for C4MIP; provides starting point for C4MIP emissions-driven SSP5-8.5
Future scenarios			
	ssp585, ssp585ext	ScenarioMIP	Essential counterpart for SSP5-8.5-BGC decoupled simulation and its extension to 2300
	ssp534-over, ssp534-over -ext	ScenarioMIP	Essential counterpart for SSP5-3.4-over-bgc decoupled simulation and its extension to 2300; branches from SSP5-8.5 at 2040
	esm-ssp585-ssp126Lu	LUMIP	Same as esm-ssp585 except uses SSP1-2.6 land use (afforestation scenario)

equal to any simulation for which it will serve as the control simulation thereby allowing correction for model drift. The piControl run must be run for both concentration-driven and emission-driven configurations of the model. In both cases all forcings should be held constant at pre-industrial levels as described in the CMIP DECK documentation. The only difference between concentration-driven and emission-driven control runs is that the emission-driven simulation simulates atmospheric CO_2 internally in response to natural fluxes of carbon from land and ocean, whereas in the concentration-driven case atmospheric CO_2 concentration is specified. No anthropogenic fossil fuel emissions of CO_2 should be applied to the model during this control run, and fixed pre-industrial land-use should be imposed. The simulated atmospheric CO_2 in esm-piControl should therefore remain stable, with drifts below 5 ppm/century.

The CMIP6 historical run, a CMIP6 required simulation, must be performed in both concentration-driven and emission-driven configurations for participation in C4MIP. It is expected that the historical simulation would begin from the same starting point as the pre-industrial control run (Fig. 3). This nominally is set as 1 January 1850. We note though that this neglects the small but non-zero effect of pre-1850 land-use changes (see e.g., Pongratz et al., 2009; Sentman et al., 2011). Some modelling groups might therefore opt for an earlier starting date or perform additional offline land-surface simulations in order to account for pre-1850 land cover change. This would mean though that the control and historical simulations begin from different states and with different trends and this should therefore be very clearly documented. The protocol for the historical simulation is documented in detail in the CMIP6 paper (Eyring et al., 2016a). Here we stress the need for the emission-driven historical run (esm-hist) to also be performed as an "entry card" for C4MIP. The only difference between concentration-driven and emission-driven simulations is the treatment of atmospheric CO_2. All other forcings must be identical in both simulations. The concentration-driven simulation will use historical atmospheric CO_2 concentration provided by CMIP6.

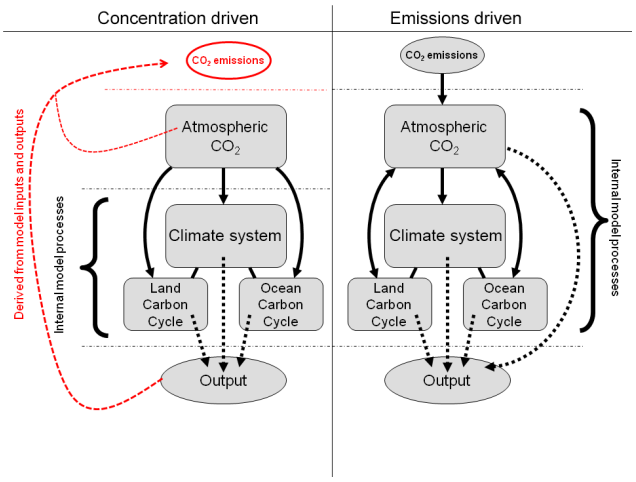

Figure 2. Schematic representation of carbon cycle numerical experimental design. Concentration-driven (left) and emissions-driven (right) simulation experiments make use of the same Earth system models (ESMs), but configured differently. Concentration-driven simulations prescribe atmospheric CO_2 as a pre-defined input to the climate and carbon cycle model components. Compatible emissions can be calculated from the output of the concentration-driven simulations. Emissions-driven simulations prescribe CO_2 emissions as the input, and atmospheric CO_2 is an internally calculated state variable within the ESM. Adapted from Ciais et al. (2013). Solid arrows depict internal data flow within the model, dashed arrows depict data output from the model.

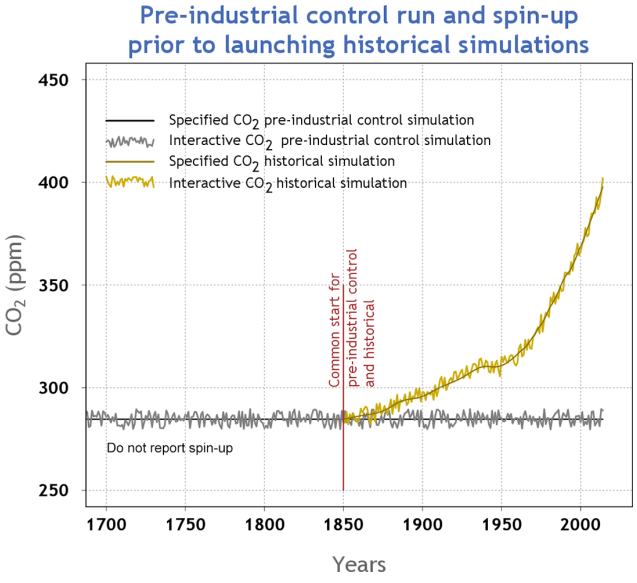

Figure 3. Schematic representation of model spin-up followed by control and historical simulations through 2014. The interactive CO_2 pre-industrial control should ideally have a drift of less than 5 ppm/century.

The emission-driven simulation will use anthropogenic CO_2 emissions documented here. Model groups have a choice over the treatment of land-use forcing as described below.

- Fossil fuel emissions: CMIP6 will provide gridded, annual CO_2 emissions from burning of fossil fuels, from the beginning of 1850 to the end of 2014 for the historical simulation and through to the end of 2100 for ssp5-8.5. See Sect. 3.3.1.
- Land-use carbon emissions: there are two allowable options:
  - If possible, drive the model with the CMIP6 land-use forcing (Hurtt et al., 2016; http://luh.umd.edu/_LUH2/LUH2_1.0h/) and the model simulates its own CO_2 emissions (including both from deforestation and uptake from regrowth) to/from the atmosphere as an internal process. In this case the only external input of carbon to the system is fossil fuel emissions.
  - If that is not possible for the model, then C4MIP will provide land-use carbon emissions; see Sect. 3.3.1.

3.2.3 Idealized 1 % simulations

A concentration-driven simulation with a 1 % per year increase in atmospheric CO_2 concentration beginning from pre-industrial is a required simulation of the DECK. In C4MIP there are further variants of this 1 % simulation designed to quantify the concentration-carbon and climate–carbon feedback parameters (Friedlingstein et al., 2006; Arora et al., 2013).

The tier-1 C4MIP simulation 1pctCO2-bgc requires the simulation to be repeated but with a change to the model set-up such that only the model's carbon cycle components (both land and ocean) respond to the increase in CO_2, whereas the model's radiation code uses a constant, pre-industrial concentration of CO_2. This simulation was previously known as "Uncoupled" in Friedlingstein et al. (2006), and was re-named "Biogeochemically coupled" by Gregory et al. (2009). All other forcings must be identical to the DECK 1pctCO2 simulation.

A tier-2 C4MIP simulation 1pctCO2-rad is the counterpart of 1pctCO2-bgc. It requires the simulation to be repeated but with a change to the model set-up such that only the model's radiation code sees the increase in CO_2 and the model's carbon cycle components (both land and ocean) see a constant, pre-industrial concentration of CO_2. This simulation was not performed in Friedlingstein et al. (2006), and was termed "Radiatively coupled" by Gregory et al. (2009). All other forcings must be identical to the DECK 1pctCO2 simulation. Although this simulation is in tier-2 we strongly encourage all modelling groups to perform it as the non-linearities

of biogeochemical and radiative response can be large (e.g. Schwinger et al., 2014).

For models with a nitrogen cycle, there are two further 1 % simulation variants requested as C4MIP tier-2: 1pctCO2Ndep and 1pctCO2Ndep-bgc. These can be run if the model includes either land- or marine nitrogen cycle in a way that changes carbon uptake and storage. If the input of reactive nitrogen to the model will not affect the carbon cycle, then there is no need to perform these simulations. If changes in nitrogen deposition will affect either land or ocean carbon uptake then these simulations are requested. 1pctCO2Ndep and 1pctCO2Ndep-bgc are parallel to the 1pctCO2 and 1pctCO2-bgc simulations but with the addition of a time-varying deposition of reactive nitrogen (see Sect. 3.3.3).

3.2.4 Scenario simulations

Concentration-driven scenario simulations, which follow on from the end of the concentration-driven historical simulation, are performed under ScenarioMIP. In C4MIP we request simulations that complement some of these.

Under C4MIP tier-1, we request an emission-driven esm-ssp585 simulation, which parallels the ScenarioMIP concentration-driven SSP-5-8.5 simulation. This simulation should begin from the end point of the emissions-driven historical simulation (1 January 2015). As with the historical simulation the only difference from the concentration-driven counterpart should be the treatment of atmospheric CO_2, which is simulated within the model driven by prescribed emissions. SSP8.5 gridded fossil fuel emissions will be provided as will SSP8.5 land-use forcing and land-use CO_2 emissions. Models should implement these in the scenario run in exactly the same manner as they did in the emission-driven historical simulation.

Under C4MIP tier-2, we also request a biogeochemically coupled (BGC) version of the concentration-driven SSP5-8.5, ssp585-bgc and ssp585-bgcExt. As with the 1pctCO2-bgc simulation, this run should be performed with only the carbon cycle components (land and ocean) seeing the prescribed increase in atmospheric CO_2. The model's radiation scheme should see fixed pre-industrial CO_2. All other non-CO_2 forcings should be applied in an identical way to the ScenarioMIP SSP5-8.5 and SSP5-8.5ext simulations. If possible this simulation should be extended to 2300, as should its counterpart from ScenarioMIP, as one of the priority focus areas for analysis is on long-term processes such as ocean carbon and heat uptake and permafrost loss (e.g., Randerson et al., 2015).

3.3 Forcings and inputs

3.3.1 CO_2 concentrations and anthropogenic CO_2 emissions

For concentration-driven simulations, atmospheric CO_2 should be prescribed as a globally well-mixed value provided by CMIP6. The CMIP6 paper (Eyring et al., 2016a) and a range of papers in the *GMD* CMIP6 Special Issue will document the forcings in more detail. The data will be made available from the CMIP6 and PCMDI webpages (http://www.wcrp-climate.org/wgcm-cmip/wgcm-cmip6, https://pcmdi.llnl.gov/search/input4mips). For emissions-driven simulations, atmospheric CO_2 should be simulated prognostically by the model. External boundary conditions of anthropogenic CO_2 emissions will be provided and should be used as follows:

- In esmPIcontrol, the emissions-driven control run, atmospheric CO_2 should be simulated by the model but no external emissions should be added during this simulation.

- Fossil fuel emissions should be used for the emissions-driven historical and future scenario simulations. C4MIP will provide gridded, annual CO_2 emissions from burning of fossil fuels, from the beginning of 1850 to the end of 2014 for the historical simulation and through to the end of 2100 for ssp5-8.5. They will be provided on land points on a $1^\circ \times 1^\circ$ grid. It is up to model groups to re-grid or interpolate these emissions to suit their own model. Global annual totals must be conserved and must match the global annual totals of the gridded data provided. Conserving the global annual total is more important than the spatial patterns of emissions.

- C4MIP strongly recommends that land-use carbon emissions are simulated internally by applying the land-use forcing by Hurtt et al. (2016). In the event that this is not possible in a model, C4MIP will provide annual land-use carbon emissions mainly based on the results of two bookkeeping models: BLUE (Hansis et al., 2015) and Houghton (Houghton et al., 2012). For the years 1850 to 2010 the average result of these two bookkeeping models defines the global emission rate, whereas the spatial distribution of the emissions is taken solely from BLUE at a 0.5° resolution. This approach provides input emissions more spatially consistent with the land-use forcing applied to models than population-weighted spatial patterns used in CMIP5. For the years 2010 to 2014 the global land-use emission rate is specified by the Global Carbon Project (Le Quéré et al., 2015) and the spatial pattern is that of BLUE at the year 2010. At the time of writing this C4MIP protocol, future land-use scenarios have not yet been processed within LUH2.

Our intention is that for the future scenarios we will provide gridded land-use emissions using global totals from the scenario and the spatial pattern either provided from the scenario or from the BLUE spatial pattern for 2010. As with fossil fuel emissions, it is up to model groups to re-grid or interpolate these emissions to suit their own model. Global annual totals must be conserved and must match the global annual totals of the gridded data provided.

3.3.2 Land-use and land-use-induced land cover change

LULCC affects climate via two aspects in CMIP6 simulations. In both concentration-driven and emission-driven simulations LULCC alters the distribution of vegetation covering the land surface, with consequences for the exchange of heat, water, and momentum with the atmosphere. Its effects on terrestrial carbon stocks allow us to infer LULCC emissions, more accurately labelled the "et LULCC flux" (Brovkin et al., 2013). In emission-driven simulations the net LULCC flux influences the atmospheric CO_2 concentration, contributing to subsequent carbon cycle feedbacks (e.g., Strassmann et al., 2008; Arora and Boer, 2010; Pongratz et al., 2014).

The LULCC forcing for the historical simulations will be based on the protocol and forcing data provided by CMIP6 for the DECK and the historical CMIP6 simulations. LULCC is kept fixed at its pre-industrial state for all 1pctCO2 simulations (fully coupled, biogeochemically and radiatively coupled versions). It is essential that the biogeochemically coupled simulations required for C4MIP of the historical and future SSP simulations and their extensions to 2300 use identically the same LULCC forcing as for the parallel ScenarioMIP simulations.

3.3.3 N deposition

Models including a nitrogen cycle are encouraged to use a consistent set of forcings of anthropogenic nitrogen deposition as drivers for the respective ocean and land biogeochemical components. Rates of speciated nitrogen deposition at the land and ocean surface are not available from observations and so need to be determined by models. C4MIP will coordinate with CCMI to provide gridded, time-varying fields of nitrogen deposition from chemistry transport models (CTMs) for use as driving inputs in C4MIP simulations (http://www.met.reading.ac.uk/ccmi/?page_id=375). This will be provided partitioned into four categories of wet or dry and oxidized or reduced N deposition velocities at the bottom of the atmosphere. If a model requires more or fewer categories or species of nitrogen deposition then it is up to the model group to produce these. When aggregating or disaggregating components of deposition the total amount of reactive nitrogen should be conserved. Inputs into the land biosphere depend on vegetation characteristics, and these aspects should be dealt with by the individual model groups.

C4MIP simulations should use N deposition fields as follows:

- Pre-industrial control (piControl and esm-piControl) should use time-invariant, but spatially explicit, N deposition appropriate to 1850. This is so that there are no discontinuities in carbon pools or fluxes at the beginning of the historical simulation.

- Historical (historical, esm-hist, hist-bgc) and future scenarios (esm-ssp585, ssp585-bgc, ssp585-bgcExt, ssp534-over-bgc, ssp534-over-bgcExt) should use the provided time-varying N-deposition data derived from CTM simulations. It is essential that all C4MIP simulations use identically the same N-deposition fields for the C4MIP simulations as the parallel DECK, historical and ScenarioMIP simulations.

- The idealized simulations (1pctCO2, 1pctCO2-bgc, 1pctCO2-rad) should also use the time-invariant pre-industrial N deposition as used in the control runs, as CO_2 is the only time-varying forcing in these experiments.

- For the first time, C4MIP requests additional idealized simulations (1pctCO2Ndep, 1pctCO2Ndep-bgc) designed to quantify the effect of N deposition on the carbon–climate and carbon-concentration interactions. These simulations should use an idealized scenario of time-varying N deposition as follows. A scenario will be generated by adding to the pre-industrial base-line the geographically explicit difference between the year 2100 SSP5-8.5 N deposition scenario and pre-industrial values, such that the relative growth rates of N deposition and CO_2 match and the global total N deposition at the time when atmospheric CO_2 concentrations reach the SSP5-8.5 value for the year 2100 correspond to the year 2100 N deposition total. C4MIP will generate these fields of N deposition and make them available as annual fields to be applied in these idealized simulations.

If the ESM simulates atmospheric chemistry and composition and therefore provides N deposition internally, then this can be used in place of a prescribed field of N deposition for the control, historical, and scenario simulations. However, irrespective of whether an ESM generates N deposition or not, for the 1 % idealized simulations, it is preferable to use the provided fields as anomalies, which should be added to the ESM's pre-industrial N-deposition fields.

The provided N-deposition data will cover both land and ocean, but we acknowledge that some models have their own established sources of reactive nitrogen to the oceans and to change this would require costly repeat-spinup simulations. So it is left to the model groups' discretion how to apply N deposition to the ocean. If a source other than that provided

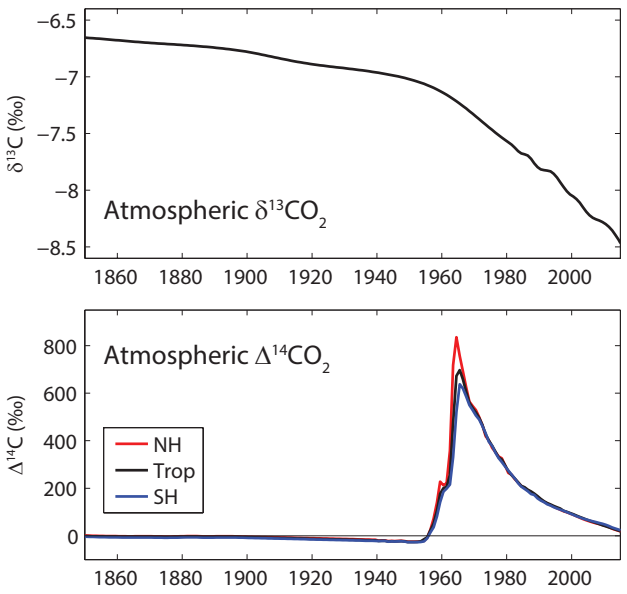

Figure 4. Carbon isotopes in atmospheric CO_2 for the historical period 1850–2014. Data for $\delta^{13}C$ is from Law Dome, South Pole (Rubino et al., 2013), and Mauna Loa (Keeling et al., 2001) and includes smoothing of the observations. Data for $\Delta^{14}C$ are compiled from Levin et al. (2010) and other sources (I. Levin, personal communication, 2016), following a similar data set used by Orr et al. (2000).

by C4MIP is used this should be documented and made available to aid analyses.

3.3.4 Carbon isotopes

Models including carbon isotopes ($\delta^{13}C$ and $\Delta^{14}C$) in land or ocean realms are encouraged to simulate and report variables relating to carbon isotopes for control, historical, and future scenario simulations.

For historical concentration-driven runs (piControl, historical and hist-bgc), atmospheric $\delta^{13}CO_2$ and $\Delta^{14}CO_2$ forcing based on observations will be provided (Fig. 4). The atmospheric forcing data sets will be available at the C4MIP website. We also plan to make available atmospheric forcing data for carbon isotopes for the ssp585 scenario and for other scenarios and extensions using a simple carbon cycle model, following Graven (2015).

Carbon isotopes are only requested to be simulated in land and ocean model components using the provided historical or future atmospheric forcing data sets for $\delta^{13}CO_2$ and $\Delta^{14}CO_2$. It is not requested that atmospheric $\delta^{13}CO_2$ and $\Delta^{14}CO_2$ be simulated by ESMs, even for emission-driven simulations of atmospheric CO_2.

3.3.5 Other forcings

If the model requires any other external forcing not documented here, for example deposition of phosphorous, then it is at the model groups' discretion how to provide it. In the case of a model with an interactive phosphorous cycle, we recommend the forcing data are prepared in a way analogous to the nitrogen deposition described above. We recommend modelling groups to contact C4MIP for more details if this is applicable. Any additional forcings must be documented through the CMIP meta-data process or in the appropriate model description paper.

4 Output requirements

It is vital for accurate analysis and model intercomparison that every model adheres to the definitions of each output variable in order for a like-for-like comparison to be made. In this section we describe in detail each requested output variable. The data request will be documented separately (by the WGCM Infrastructure Panel; https://www.earthsystemcog.org/projects/wip/) and will list the required variables output for each CMIP6 simulation along with their precise variable names, description, and required units. Here we aim to describe each variable so that its implementation and use are made consistent across all models and analyses.

4.1 Land

4.1.1 Land carbon cycle variables

The primary aim of C4MIP is to compare the aspects of the global carbon cycle and its response to environmental changes across the participating ESMs. To achieve this objective, it is essential that all carbon stocks and fluxes are reported so that total amount of carbon in the system can be tracked and their conservation checked. To achieve this, compulsory tier-1 diagnostics have been defined that close the carbon cycle as simply as possible. Desirable tier-2 diagnostics should also be reported where possible, which allow for more detailed analysis by breaking down tier-1 output into sub-components.

Land carbon pools: tier-1

Figure 5 shows the requested carbon cycle stores over land. Tier-1 variables are intended to be simple but still capture the total land carbon store. Tier-2 variables provide the same information as the tier-1 variables but in more detail. As shown in Fig. 5 the total carbon can be calculated from tier-1 variables and is not the combined sum of tier-1 and tier-2 variables.

The carbon stored in the vegetation–litter–soil system is simply represented by tier-1 variables, cVeg, cLitter, and cSoil respectively. For models that do not repre-

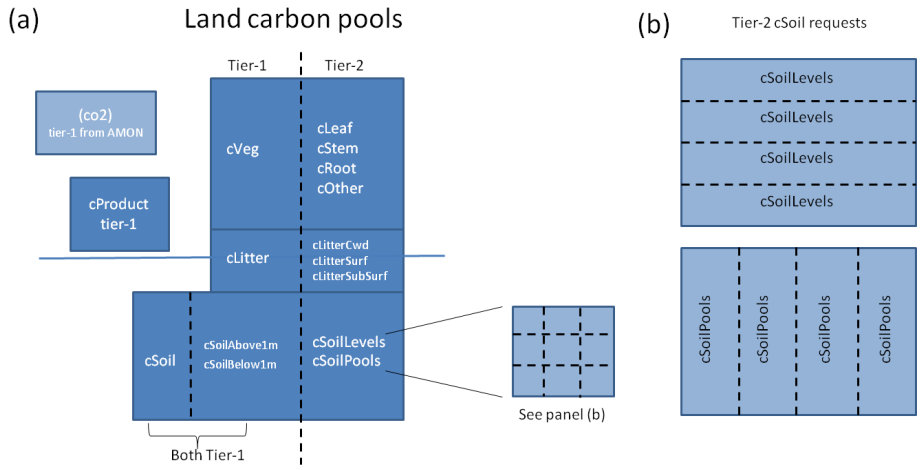

Figure 5. **(a)** Requested tier-1 and tier-2 variables representing land carbon pools. Although not a land carbon quantity, atmospheric CO_2 is shown here for completeness. **(b)** Detailed view of the tier-2 breakdown for soil carbon by vertical level (cSoilLevels) and by soil carbon pool (cSoilPools).

sent a vertical discretization of soil carbon, all soil carbon should be reported simply as cSoil. Additionally in tier-1 for models with vertically discretized soil carbon, we request output on the vertical distribution above and below 1 m depth (cSoilAbove1m, cSoilBelow1m). These should be reported in addition to cSoil, such that cSoil=cSoilAbove1m+cSoilBelow1m. The rationale for requesting this is the availability of several observation-based data sets that report soil organic matter content to 1 m depth. It is important that any evaluation of cSoil outputs against observed data sets makes use of the appropriate depth of soil in both the observations and model outputs.

A fourth pool, cProduct, represents the carbon stored in product pools (harvested wood, paper products, furniture, etc.) as a result of anthropogenic land-use change. The total carbon stored per unit area on land is then simply:

$$\mathrm{cLand} = \mathrm{cVeg} + \mathrm{cLitter} + \mathrm{cSoil} + \mathrm{cProduct} \quad (1)$$

Some models may not explicitly simulate a litter pool distinct from their soil carbon pool. In this case cLitter should be reported as zero. We would normally expect cProduct to be non-zero in simulations that include anthropogenic land-use or land-use change. Hence, for the idealized 1 % per year increasing CO_2 simulations (biogeochemically, radiatively or fully coupled) we would expect models to report cProduct = 0. For models whose land-use fluxes contribute straight to the atmosphere and/or to their litter or soil carbon pools, but not to the product pools, cProduct = 0 should also be reported for historical and scenario simulations. Obviously, for models that do not simulate the effect of LULCC on the carbon cycle, cProduct will also be expected to be zero.

Land carbon pools: tier-2 vegetation and litter carbon

Tier-2 output variables allow for more detailed breakdown and analysis of their parent carbon stores. They are subcomponents of their parent tier-1 variables, and not additional stores. For example, the vegetation carbon pool can be represented by carbon in the leaf, stem, and root as well as possibly other (e.g. fruit) components. For models that report these tier-2 variables, the total amount of carbon per unit area should be identical to the tier-1 variable, i.e.

$$\mathrm{cVeg} = \mathrm{cLeaf} + \mathrm{cStem} + \mathrm{cRoot} + \mathrm{cOther}. \quad (2)$$

The same applies for the litter carbon pool, which is requested to be broken down into coarse woody debris (cLitterCWD) and above- and below-surface litter (cLitterSurf, cLitterSubSurf) pools. When a model has a continuous profile of litter with depth, take above and below 10 cm as the definition of above and below the surface. CWD here is assumed to be on the surface.

Land carbon pools: tier-2 soil carbon

For CMIP5 the soil carbon pool was requested to be divided into components with fast, medium, and slow turnover timescales. However, this distinction was not found useful by the community and as a result was not used in many analyses. For CMIP6, we request a breakdown in two different ways (Fig. 5b). First, models with a vertical structure to their soil carbon are requested to report total soil carbon for each soil layer. In the same way as soil moisture or temperature, this should be reported as a multi-level output, cSoilLevels. As the structure for this may vary between models, it is essential that the model is thoroughly documented. The sum of soil carbon over all cSoilLevels should be identical to the total cSoil tier-1 variable.

Table 3. Summary of tier-2 data request of carbon pools and fluxes by sub-grid land cover fraction.

Portion of gridbox	Pools	Fluxes
treeFrac	cVegTree, cLitterTree, cSoilTree	gppTree, nppTree, raTree, rhTree
shrubFrac	cVegShrub, cLitterShrub, cSoilShrub	gppShrub, nppShrub, raShrub, rhShrub
grassFrac	cVegGrass, cLitterGrass, cSoilGrass	gppGrass, nppGrass, raGrass, rhGrass
cropFrac	cVegCrop, cLitterCrop, cSoilCrop	gppCrop, nppCrop, raCrop, rhCrop
pastureFrac	cVegPast, cLitterPast, cSoilPast	gppPast, nppPast, raPast, rhPast

Most soil carbon models represent multiple soil carbon pools (such as fast or slow turnover, or decomposable and resistant organic material). In order to be able to diagnose and evaluate the turnover rates of carbon within the terrestrial system, we make a second tier 2 request to report individual soil carbon pools (Fig. 5b, lower panel). It is also required to report the turnover rate (tSoilPools: defined as 1/residence time) for each pool. The pool-flux structure of each model should be fully documented in its model description paper. This output will enable reduced complexity approaches (e.g. Xia et al., 2013) to recreate and analyse the soil carbon dynamics within each model. The sum of soil carbon over all cSoilPools should be identical to the total cSoil tier-1 variable.

Land carbon pools: tier-2 carbon on sub-grid tiles

A final tier-2 breakdown is required to report the main stores and fluxes separately for different land cover types. The LUMIP data request (Lawrence et al., 2016) requests carbon pools and fluxes for four land cover types: crop, pasture, primary and secondary land (combined as one tile), and urban. For C4MIP we additionally request a breakdown of carbon pools and fluxes within "primary and secondary" land onto tree, shrub, and grass separately. Section 4.1.4 describes the C4MIP requested output of land cover fractions. Carbon pools (cVeg, cLitter and cSoil) and fluxes (gpp, npp, ra, rh) are therefore requested on the treeFrac, shrubFrac, grassFrac, cropFrac, and pastureFrac fractions shown in Fig. 11. Table 3 lists all of these requests.

Land carbon fluxes

Equally important to the land carbon pools are the fluxes going into and out of them, which will allow us to gain insight into how the pools have changed and why. For ease of understanding, we have adopted a convention for newly defined variables that a carbon pool is prefixed by a "c" (as in cVeg or cSoil) and a flux by an "f" (as in fLandToOcean). Some existing variables (e.g. gpp and npp) do not conform to this but are considered to be well known and do not need to be changed.

Figure 6 shows the variables requested for terrestrial carbon fluxes. Similar to land carbon pools, the objective of tier-1 fluxes is to capture the primary system behaviour, and tier-2 fluxes provide breakdown within the tier-1 fluxes allowing for a more detailed analysis. The directions of the arrows indicate the sign convention of the flux, which is considered positive in the direction in which the arrows are pointing. For example, gross primary productivity (gpp) is positive downwards indicating flux of carbon *from* the atmosphere *to* the vegetation, whereas autotrophic respiration (ra) is positive upwards indicating flux of carbon *from* the vegetation *to* the atmosphere.

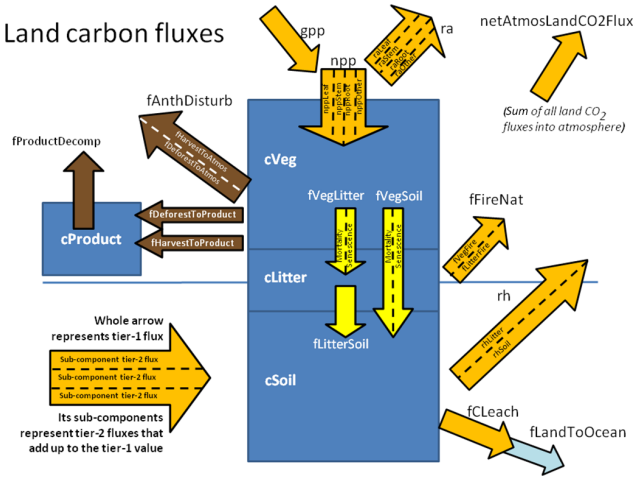

Figure 6. Requested tier-1 and tier-2 variables representing land carbon fluxes. The colours of the arrows correspond to the type of flux. The orange arrows represent "natural" fluxes that represent pathways of carbon exchange between the land and atmosphere. These natural fluxes would generally be expected to be non-zero in all simulations. The brown arrows represent fluxes associated with anthropogenic disturbance between land pools or between the land and the atmosphere. These fluxes would be expected to be non-zero in simulations that implement anthropogenic land-use change based on land-use change scenarios. The yellow arrows represent internal fluxes within the veg–litter–soil system. Finally, the blue arrow represents carbon loss from land to the ocean, which may be a subset of leached carbon, although not all models may simulate this flux.

Gross primary productivity is the flux of carbon from the atmosphere to the vegetation that is associated with photosynthesis. Net primary productivity (npp) represents the carbon uptake by vegetation after the autotrophic respiration (ra) costs have been taken into account (npp = gpp − ra). Both ra and npp are sub-divided into tier-2 outputs representing flux

from the leaf, stem, and root, components respectively, plus also a category "other", which should include all the components (if any) reported under cOther tier-2 carbon pool. Also, similar to land surface pools, the sum of the tier-2 fluxes must be identical to their parent tier-1 flux.

$$\text{npp} = \text{nppLeaf} + \text{nppStem} + \text{nppRoot} + \text{nppOther} \quad (3)$$

Heterotrophic respiratory flux (rh) and CO_2 emissions associated with natural wildfires (fFireNat) represent carbon loss from the land carbon stores to the atmosphere. rh is requested to be sub-divided into its tier-2 components from the litter and soil pools. Similarly, fFireNat is sub-divided into fire CO_2 emissions from vegetation and litter carbon pools. Note, that fFireNat should not include CO_2 emissions from fires associated with anthropogenic land-use change.

Anthropogenic land-use change or land management can result in transfer of carbon out of the vegetation, litter and soil carbon pools either directly to the atmosphere (fAnthDisturb) or to the product pool. fAnthDisturb is proposed to be split into fluxes due to land-cover change (fDeforestToAtmos) or management (fHarvestToAtmos), if this distinction is made in the model. Anthropogenic fires, associated with LUC, should be included in fAnthDisturb. Fluxes into the product pool should similarly be reported as either fDeforestToProduct or fHarvestToProduct. Decomposition of carbon in the product pool represents a carbon flux back to the atmosphere (fProductDecomp).

Due to the complexity of the processes involved, especially in the treatment of land use and management, and the growing complexity in the manner in which LUC is represented in the models, it is possible that this simple framework may not be completely compatible with all models. It is simply not possible to define in advance of CMIP6 a framework that may cover every possible flux in every model. Our request is, therefore, that all fluxes of carbon are reported somewhere, in the best possible way that they may fit within the framework shown in Fig. 6, and not missed. This will ensure conservation of carbon within the reported variables.

An example of differences in model structure and processes is the manner in which litter from the vegetation pool is transferred to the soil carbon pool. Some models simulate litter fall from vegetation into the litter pool and then subsequent assimilation into the soil carbon pool. Some models may also simulate this flux directly from vegetation to soil carbon. In either case tier-2 breakdown of the litterfall flux due to senescence (normal turnover) and mortality is requested; this breakdown is expected to help to diagnose changes in turnover time of the litter and soil carbon pools.

Figure 6 also forms the basis of carbon conservation properties that must be obeyed by the reported outputs. These include the manner in which fluxes should add up and that the rate of change of carbon in carbon pools must be equal to the sum of fluxes going in and out of the pools, or equivalently changes in pools must be equal to the sum of time integral of the fluxes into and out of the pools.

$$\text{gpp} = \text{npp} + \text{ra} \quad (4)$$

$$\frac{\text{d cVeg}}{\text{d}t} = \text{npp} - \text{fVegLitter} - \text{fVegSoil} - \text{fAnthDisturb} - \text{fDeforestToProduct} - \text{fHarvestToProduct} - \text{fVegFire} \quad (5)$$

$$\frac{\text{d cLitter}}{\text{d}t} = \text{fVegLitter} - \text{fLitterSoil} - \text{fLitterFire} - \text{rhLitter} \quad (6)$$

$$\frac{\text{d cSoil}}{\text{d}t} = \text{fLitterSoil} + \text{fVegSoil} - \text{rhSoilfLandToOcean} \quad (7)$$

$$\frac{\text{d cProduct}}{\text{d}t} = \text{fDeforestToProduct} + \text{fHarvestToProductfProductDecomp} \quad (8)$$

We define a new variable, *netAtmosLandCO2Flux*, which is the total flux of CO_2 from the land to the atmosphere. It should encompass every flux from land to atmosphere so that the total from each model can be compared without having to know model details of which component fluxes to sum. Due to differences in naming convention, we have chosen not to call this NBP (net biome productivity). This is an essential tier-1 variable requested from all C4MIP simulations.

4.1.2 Land nitrogen cycle variables

Figures 7 and 8 summarize the requested terrestrial nitrogen pools and flux variables from models that include a representation of terrestrial nitrogen cycle and its coupling to the terrestrial carbon cycle. The nitrogen pools are designed to parallel their corresponding carbon stores as closely as possible, giving primarily the storage of nitrogen in the vegetation (nVeg), litter (nLitter), and soil organic matter (nSoil) pools. Additionally, we are requesting mineral nitrogen in soil (nMineral), which is sub-divided into tier-2 variables representing ammonium (nMineralNH4) and nitrate (nMineralNO3) mineral nitrogen. We do not envisage much interest in the nProduct variable (nitrogen stored in anthropogenic product pools), but it is required as a tier-1 output in order to close the nitrogen budget and ensure mass conservation of analyses. There will also be likely little interest in separating nLitter into its tier-2 components nLitterCwd, nLitterSurf and nLitterSubSurf but these variables are being requested for consistency with their carbon counterparts.

Requested fluxes associated with the flow of nitrogen over land are summarized in Fig. 8 and differ more from their carbon counterparts than do the carbon and nitrogen pools. As with the pools, all fluxes should be reported somewhere in order to be able to close nitrogen cycle budget over land and ensure mass conservation of analyses. As with carbon fluxes, the sign convention of the flux is considered positive in the direction in which the arrows are pointing

Nitrogen enters the terrestrial ecosystems either through anthropogenic inputs (which can be either atmospheric deposition, fNdep, or fertilizer input fNfert) or through biological fixation (fBNF). Flows between vegetation, litter, and

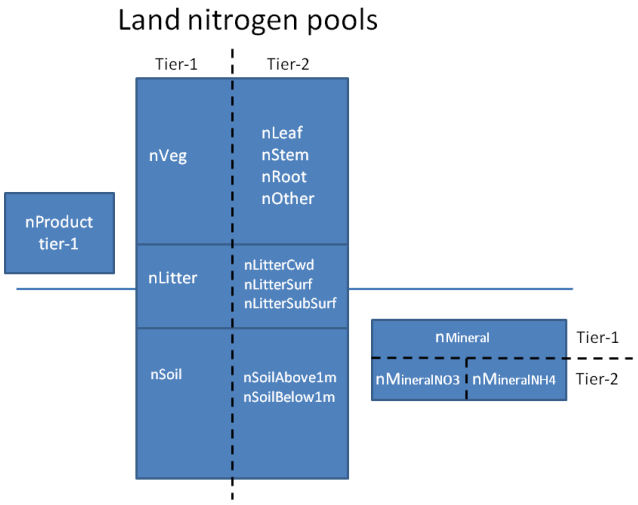

Figure 7. Requested tier-1 and tier-2 variables representing land nitrogen pools.

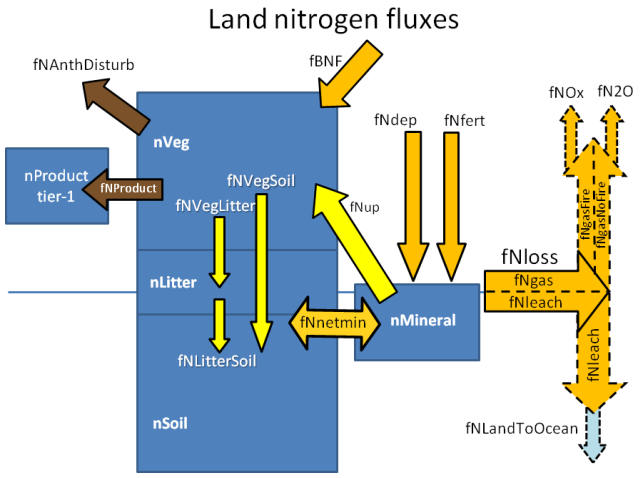

Figure 8. Requested tier-1 and tier-2 variables representing land nitrogen fluxes.

soil organic N pools mirror the carbon fluxes, but with additional terms that represent inorganic mineral nitrogen uptake by vegetation (fNup) and the net mineralization flux, i.e. the difference between gross mineralization and immobilization, from the dead litter and soil organic matter pools to the mineral nitrogen pool (fNnetmin). fNnetmin should be reported as positive *into* the nMineral pool. Negative values of fNnetmin then imply net immobilization.

The tier-1 variables that represent the loss of nitrogen from the primary terrestrial pools of vegetation, litter and soil organic matter include fluxes due to anthropogenic disturbance: either into the LUC product pool (fNproduct) or loss direct to the atmosphere fNAnthDisturb and loss from the mineral nitrogen pool (fNloss). In order to conserve nitrogen, all losses of N must be reported into one of these variables. fNloss may be further sub-divided (if represented in the model) into tier-2 outputs of gaseous loss to the atmosphere (fNgas) and loss of dissolved organic and inorganic nitrogen through leaching (fNleach), i.e. fNloss = fNgas + fNleach. If represented in the model, fNgas can be split into that due to fire and non-fire. A further breakdown of tier-2 fluxes is also requested, if available, but these do not necessarily have to add up to the tier-1 flux value: fNOx and fN2O are components (but do not necessarily have to add up to fNgas) and may be of interest for evaluation activities or coupling to atmospheric chemistry models. fNLandToOcean may be a subset of fNleach and is of interest for studying the impact of terrestrial nitrogen cycle on coastal ocean ecosystems.

4.1.3 Land physical variables

While most variables representing the land surface physical state and water fluxes will likely be requested by the land surface, snow, and soil moisture model intercomparison project (LS3MIP, van den Hurk et al., 2016) and land-use model intercomparison project (LUMIP, Lawrence et al., 2016), C4MIP requests some basic land surface physical variables as well. These include soil moisture and temperature, vegetation leaf area index (LAI) and height, and basic water fluxes.

Physical state variables

Figure 9 shows the state variables requested that characterize the physical vegetation structure (through leaf area index and vegetation height) and the physical state of the soil (through the soil moisture and temperature of a model's soil layers).

The only tier-1 state variable requested for vegetation structure is LAI, which represents the area of leaves per unit area of ground. Vegetation height may also be considered an important evaluation metric but this is requested as tier-2 variable. It is likely more useful to distinguish vegetation height by vegetation type, i.e. by tree, shrub, grass, and crop. If this distinction is not made or unavailable in a model then only the grid-averaged vegetation height may be reported.

Soil moisture and temperature are requested as tier-1 variables to be able to analyse carbon and moisture fluxes together and to identify the role of the physical state of the soil conditions on carbon stores and fluxes. The total, liquid, and frozen soil moisture contents are aggregated and disaggregated in various ways as shown in Fig. 9 and described below:

- soil temperature (tsl) is requested for each model level
- soil moisture is requested as
  - total soil moisture content (sum of frozen and liquid) in the top 10 cm, mrsos;
  - total (mrsol), liquid (mrsll) and frozen (mrsfl) soil moisture content at each model level;

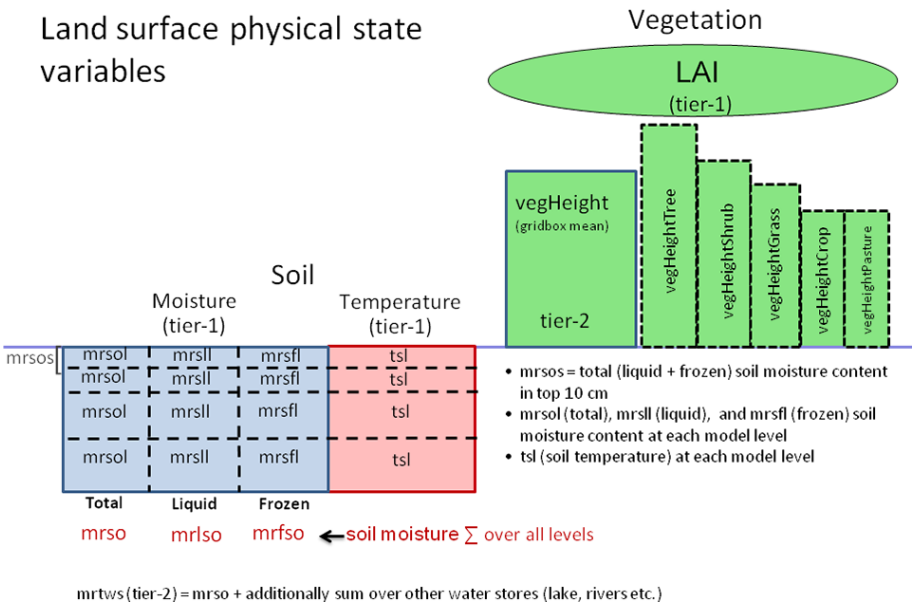

Figure 9. Requested state variables that characterize the physical vegetation structure and the physical state of the soil.

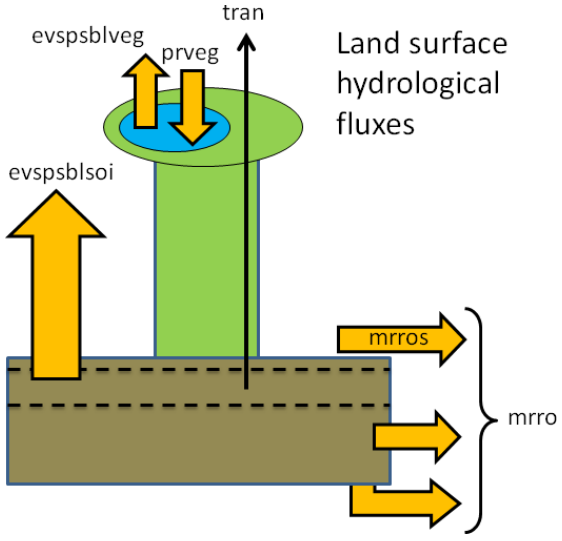

Figure 10. Requested land surface hydrological flux variables.

– column integrated total (mrso), liquid (mrlso) and frozen (mrfso) soil moisture contents.

Additionally, a total water diagnostic, mrtws, is requested as tier-2 variable. This includes all soil moisture as reported above (mrso) but additionally includes water from other stores such as sub-grid lakes, aquifers, or rivers if they are represented in the model.

Physical water fluxes

Figure 10 summarizes the small number of land surface hydrological fluxes being requested. As with the carbon and nitrogen fluxes the sign convention is shown by the direction of the arrows.

– prveg represents precipitation intercepted by the canopy, and evspsblveg represents evaporation from the canopy leaves (including sublimation).

– evspsblsoi represent evaporation from bare soil, and includes sublimation.

– tran represents transpiration flux of moisture through the vegetation and out of the leaf stomata.

Models may represent runoff in multiple ways. The runoff variables requested here are distinct from river/stream flow variables, which other MIPs may request. Runoff is represented in depth units ($kg\,m^{-2}\,s^{-1}$), while river/stream flow represents volume of water per unit time generated by integrating runoff from upstream grid cells ($m^3\,s^{-1}$). mrros represents the surface runoff from each grid cell, and mrro represents the total runoff (including from the surface, the subsurface and any drainage through the base of the soil model).

4.1.4 Land cover state variables

Figure 11 summarizes the land cover variables requested from all models. As with other requested variables, these are categorized as simpler tier-1 variables, which represent the primary land cover types, while the tier-2 variables further break down the tier-1 variables into more detail. Tier-1 land cover variables are required from all models so that the land cover is completely described. Where possible modelling groups are requested to provide the additional details through tier-2 variables. It is important that the combined totals of tier-2 variables agree with their tier-1 counterparts.

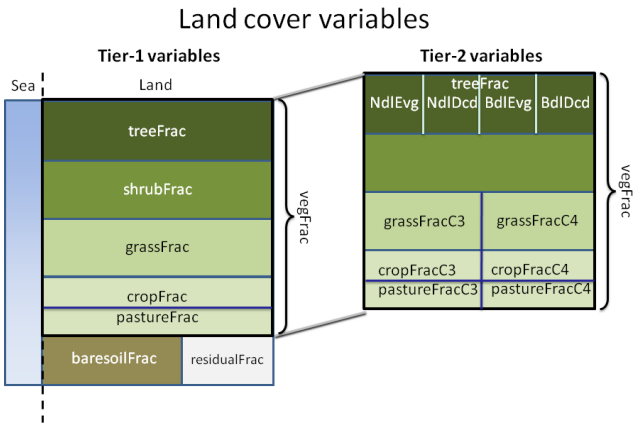

Figure 11. Requested land cover variables. Sea fraction is assume to be fixed, so must be reported under "climatology". Fractions must sum to 1 for every grid cell (including the sea fraction). Fractions are per grid cell, not per land area.

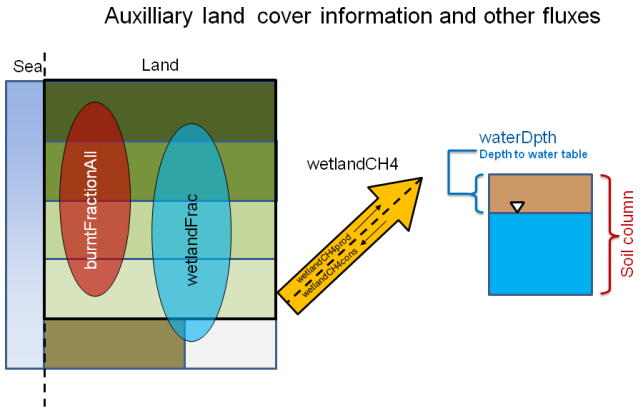

Figure 12. Fire and wetland variables. Other than burntFractionAll, all other variables are requested as tier 2 variables.

A grid cell is described in terms of vegetation fractional coverage (vegFrac), fractional coverage of bare soil (baresoilFrac), and a residual term (residualFrac) that may include fractional coverage of urban areas, sub-grid-scale lakes, and stony outcrops. For grid cells at the continental edges, a fraction of the grid cell may also be covered by open ocean/sea. The vegFrac is further subdivided into fractional coverage by trees (treeFrac), shrubs (shrubFrac), grasses (grassFrac), crops (cropFrac), and pasture (pastureFrac). Crop and pasture fractions are the same as those requested by LUMIP (Lawrence et al., 2016). Tree, shrub, and grass fractions represent additional detail within the LUMIP tile called "primary and secondary land". All land cover must be reported, such that

$$\text{VegFrac} + \text{baresoilFrac} + \text{residualFrac} + \text{SeaFrac} = 1, \quad (9)$$

$$\text{treeFrac} + \text{shrubFrac} + \text{grassFrac} + \text{cropFrac} + \text{pastureFrac} = \text{VegFrac}. \quad (10)$$

The tier-2 land cover variables follow the separation of trees based on their leaf structure (broadleaf and needleleaf) and leaf phenology (evergreen and deciduous) as treeFracNdlEvg, treeFracNdlDcd, treeFracBdlEvg, treeFracBdlDcd. The fractional coverage of grasses, crops, and pasture is separated into C_3 and C_4 variants based on their photosynthetic pathway. Tier-2 totals should sum to be identical to their tier-1 counterparts. For example

$$\text{treeFracNdlEvg} + \text{treeFracNdlDcd} + \text{treeFracBdlEvg} + \text{treeFracBdlDcd} = \text{treeFrac}, \quad (11)$$

$$\text{grassFracC3} + \text{grassFracC4} = \text{grassFrac}. \quad (12)$$

4.1.5 Auxiliary land cover fractions and fluxes

Figure 12 shows auxiliary land cover diagnostics and fluxes that may be reported. The additional land cover types are fractions of a grid cell related to a biogeochemical process that models may specifically simulate. These include burned area (burntFractionAll) and wetland fraction (wetlandFrac). burntFractionAll is expected to include burned area from all natural and anthropogenic processes (anthropogenic fires, and land-use change and management-related fires). wetlandFrac is expected to include natural wetlands (dynamically calculated in the model or specified) including any area of rice paddies if it is explicitly represented. Both the burnt and wetland fractions must be reported as the fraction of the grid cell and not as fraction of the land or vegetation area. Where models also estimate natural methane wetland emissions from the wetland fraction these can also be reported (wetlandCH4prod) and must include emissions from rice paddies (if represented) to make methane emissions consistent with the reported wetland fraction. If models simulate methane uptake by soils then this may be reported as wetlandCH4cons. The net land-to-atmosphere methane flux is to be reported as wetlandCH4. Models that simulate methane emissions from wetlands and/or rice paddies may explicitly simulate the depth to the water table and this may also be reported as waterDpth. Positive values of waterDpth indicate that the water table is below the ground surface and negative values indicate that the water table is above the ground surface.

4.2 Ocean diagnostics

Ocean biogeochemical stores and fluxes are described below. As with the land, it is important that all carbon stocks are reported so that total carbon can be tracked and conservation checked. Figures 13–16 show the requested diagnostics. Tier-1 diagnostics are intended to be simple and capture the whole ocean carbon cycle, while tier-2 diagnostics repeat tier-1 but

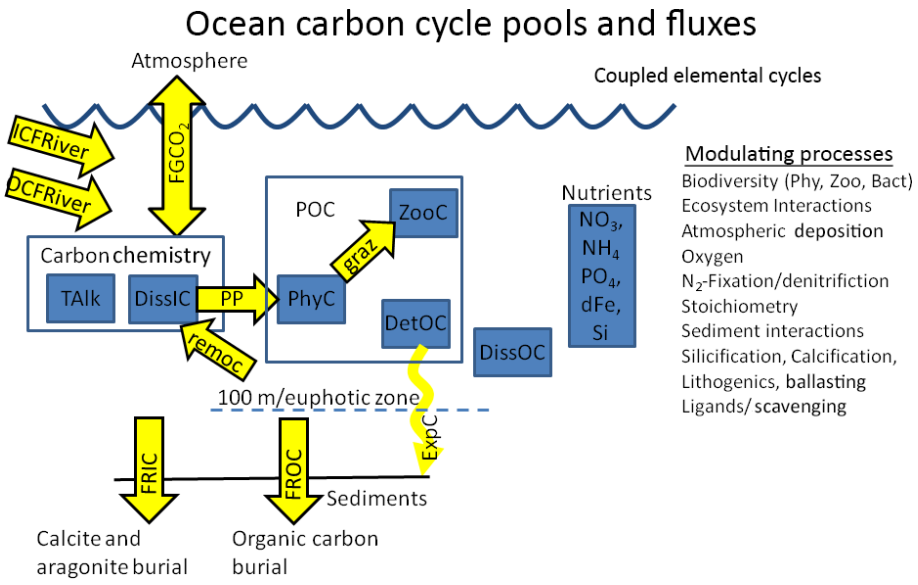

Figure 13. Ocean carbon cycle pools (blue boxes) and fluxes (yellow arrows) with associated processes. Where appropriate, pools are grouped into components like particulate organic carbon (POC).

in more detail. As such the total carbon is the sum of tier-1 and not the combined sum of tier-1 plus tier-2. The main (tier-1) processes considered are (1) gas exchange with the atmosphere that requires modelling the coupled cycle of alkalinity, and (2) biological processes coupling the carbon cycle with nitrogen, phosphorus, iron, silicon nutrients. These biological processes are centred around phytoplankton-based primary production of organic carbon, ecosystem modulation through zooplankton grazing and higher trophic interactions, sinking of organic material out of the 100 m reference level (nominal euphotic zone depth), and recycling of nutrients. Additional mechanisms working at the process level may include: biodiversity among phytoplankton, zooplankton and bacteria, dissolved organic carbon cycling, oxygen cycling and its modulation of remineralization and denitrification, N_2 fixation/denitrification, flexibility in the stoichiometry among elements, sediment interactions, silicification, calcification, lithogenics, mineral ballasting of sinking material, aspects of iron cycle modulation through scavenging and the role of ligands, phytoplankton mortality by aggregation, and viruses. The integral of a particular tracer XXX over model vertical levels is IntXXX, and the total time rate of change of tracer XXX is diagnosed as FddtXXX. Similarly, the time rate of change due to the sum of all biological terms acting on tracer XXX is diagnosed as FbddtXXX. XXXs is the surface value of XXX.

The ocean ecosystem in ESMs typically comprises up to five phytoplankton functional groups: diazotrophs, which can fix N_2 but may take up nitrate or ammonia as well depending on the model formulation, diatoms, which take up silicate to form opal tests, calcareous phytoplankton, which take up dissolved carbonate and alkalinity to form calcite, or aragonite tests, picophytoplankton, and miscellaneous phytoplankton in which any other phytoplankton groups are combined. Zooplankton groups may be separated by size into microzooplankton, mesozooplankton, and macrozooplankton. Combined with bacteria and detritus, these pools form the particulate organic carbon pool. Carbon stores in each of these sub-components are requested as tier-2 (Fig. 14) and should sum to be identical to their tier-1 counterparts.

As shown in Fig. 15, phytoplankton growth consumes dissolved organic carbon and nutrients in the presence of light to form particulate organic carbon and oxygen through primary production (i.e. intPb), some of which is exported (i.e. expC). For each phytoplankton group, the degree of limitation by light (i.e. limIrrdiat), nitrogen (i.e. limNdiat), and iron (i.e. limFediat) availability can be diagnosed. For each elemental cycle the external sources (i.e. FSC) and removal (i.e. FRC) can be diagnosed. As model implementation of multiple factor limitation is very model dependent, limitation terms for light and nutrients should be diagnosed in a manner consistent with model implementation. For each model participant, it will be important to document how combinations of limitation terms should be combined, multiplicatively, as the minimum, or otherwise

Chemistry associated with the carbon system and gas exchange is kept track of through the variables provided in Fig. 16. Cycles include the full carbon system associated with dissolved inorganic carbon and alkalinity as well as additional components relevant to specific tracer analysis such as the natural carbon system that is unaffected by anthropogenic CO_2, and simplified abiotic dissolved inorganic carbon and abiotic alkalinity used for simulation of radiocarbon (dissic14C, dissic14Cabio).

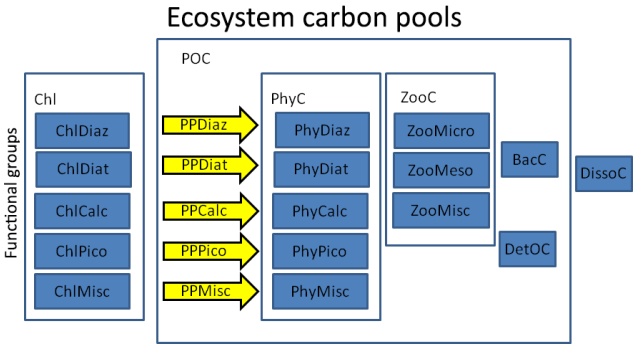

Figure 14. Ocean ecosystem carbon pools in terms of chlorophyll-based and carbon-based phytoplankton functional groups, zooplankton size groups, bacteria, detritus, and dissolved organic carbon. As with land carbon diagnostics, the tier-2 requests are subcomponents of the tier-1 aggregate quantities. For example, ZooC should report the total carbon pool in zooplankton. The sum of the tier-2 components ZooMicro, ZooMeso and ZooMisc should be identical to the tier-1 total. They are not additional pools to it.

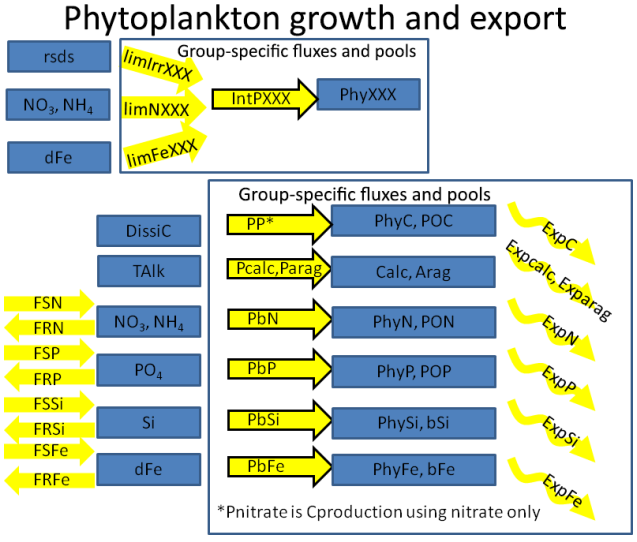

Figure 15. Phytoplankton growth and export variables by phytoplankton group and by associated elemental cycle including external sources and removal. Export refers to the export flux due to sinking.

4.3 Carbon isotopes

Carbon isotopes are not simulated in all models and have not been requested or used before in C4MIP analyses. For CMIP6 we request that any model that simulates isotopes of carbon (13 or 14) either on land or in the ocean report them in the same way as the tier-1 carbon outputs.

Figure 17 shows carbon isotope diagnostics, which are requested. These represent stocks of carbon-13 and carbon-14 in both land and ocean reservoirs and their exchange fluxes with the atmosphere. Net air–sea fluxes of carbon-13 and

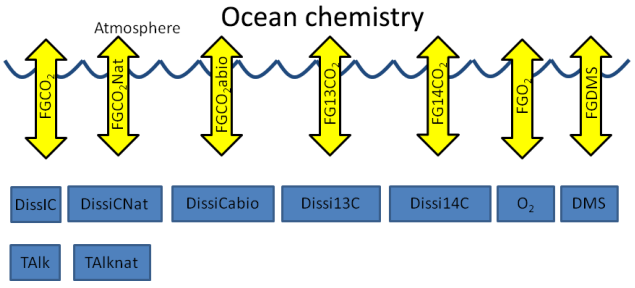

Figure 16. Ocean chemistry including the suite of carbon system tracers and those undergoing gas exchange.

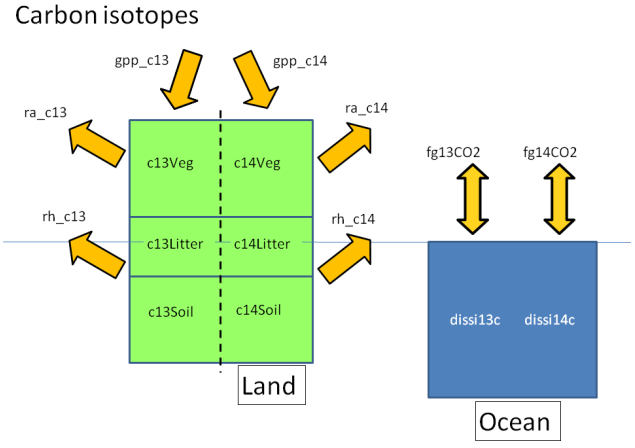

Figure 17. Carbon isotope diagnostics. Only report for models simulating isotopes. We define c13Land=c13Veg+c13Litter+c13Soil and likewise for c14Land. As for cSoil, models with vertical discretization should also report above and below 1 m separately as c13SoilAbove1m and c13SoilBelow1m and likewise for c14.

carbon-14 and dissolved inorganic of carbon-13 and carbon-14 concentrations in the ocean are requested. On land, fluxes of carbon-13 and carbon-14 associated with gross primary productivity, autotrophic respiration, and heterotrophic respiration, and stocks of carbon-13 and carbon-14 in vegetation, litter, and soil are requested. The same units used for carbon should be used for carbon-13 and carbon-14. Stocks and fluxes of carbon-14 should be normalized with the standard ^{14}C / C ratio, Rs, of 1.176×10^{-12} (Karlen et al., 1968). This means that reported stocks and fluxes of carbon-14 should be divided by Rs.

Decay of carbon-14 should use the currently accepted half-life of 5700 ± 30 years. In ocean models, carbon-14 can be run as an abiotic variable (Orr et al., 2000) or integrated into marine ecosystem carbon cycling. If carbon-14 is run as an abiotic variable, abiotic dissolved inorganic carbon concentrations and abiotic carbon air–sea fluxes must also be reported. For carbon-13 in the ocean, we request only net air–sea fluxes of carbon-13 and carbon-13 in DIC. We do not request variables related to carbon-13 in phytoplankton or carbon-13 fluxes between DIC and phytoplankton, even

though ocean models including carbon-13 are likely to include marine ecosystem cycling of carbon-13. More detail on implementing carbon isotopes in ocean models for CMIP6 can be found in Orr et al. (2016).

5 Conclusions

Processes in the natural carbon cycle currently remove approximately half of anthropogenic emissions of CO_2, helping to reduce the magnitude and rate of climate change. How these processes may change in the future in response to environmental changes and direct human forcing is uncertain.

As an endorsed activity of CMIP6, C4MIP will contribute coordinated simulations and analyses targeted at 3 key carbon cycle areas.

- Feedback quantification through idealized simulations. Here we hope to better understand and quantify the sensitivity of land and ocean carbon uptake to key environmental changes, and in particular the impact of climate change on carbon uptake.
- Model evaluation through analysis of historical simulations. Here we hope to build trust in projections through process-based and top-down evaluation, advancing our understanding of the strengths and weakness of ESMs and documenting progress since CMIP5.
- Future projections of climate and CO_2 under scenarios of CO_2 emissions. Here we hope to better project the future response to anthropogenic activity through CO_2 emissions-driven simulations that allow for the full range of feedbacks to operate from CO_2 emissions to the evolution of atmospheric CO_2 and the associated climate response.

C4MIP will focus on the coupled Earth system, comprising land–atmosphere–ocean physical realms and both the terrestrial and marine carbon cycle components. Offline studies of land only or ocean only will complement our analyses but are outside the specific remit of C4MIP.

Over the last 2 years the C4MIP community has devised a compact and efficient set of numerical experiments to be performed with ESMs to address the above questions. In this paper we have documented the rationale and set-up of these simulations and the required outputs. This therefore constitutes the C4MIP contribution to CMIP6.

6 Data availability

As with all CMIP6-endorsed MIPs, the model output from the C4MIP simulations described in this paper will be distributed through the Earth System Grid Federation (ESGF). The natural and anthropogenic forcing data sets required for the simulations will be described in separate invited contributions to this special issue and made available through the ESGF with version control and digital object identifiers (DOIs) assigned. Links to all forcings data sets will be made available via the CMIP Panel website.

Acknowledgements. CRESCENDO project members (CDJ, PF, LB, VB, TI, SZ) acknowledge funding received from the Horizon 2020 European Union's Framework Programme for Research and Innovation under grant agreement no. 641816. CDJ was supported by the Joint UK BEIS/Defra Met Office Hadley Centre Climate Programme (GA01101). HDG was supported by a Marie Curie Career Integration Grant from the European Commission. JP is supported by the German Research Foundation's Emmy Noether Program (PO 1751/1-1).

Edited by: C. Sierra
Reviewed by: C. Huntingford and two anonymous referees

References

Anav, A., Friedlingstein, P., Kidston, M., Bopp, L., Cox, P., Jones, C., Jung, M., Myneni, R., and Zhu, Z.: Evaluating the land and ocean components of the global carbon cycle in the CMIP5 earth system models, J. Climate, 26, 6801–6843, doi:10.1175/jcli-d-12-00417.1, 2013.

Arora, V. K. and G. J. Boer: Uncertainties in the 20th century carbon budget associated with land use change, Glob. Change Biol., 16, 3327–3348, 2010.

Arora, V. K., Boer, G. J., Friedlingstein, P., Eby, M., Jones, C. D., Christian, J. R., Bonan, G., Bopp, L., Brovkin, V., Cadule, P., Hajima, T., Ilyina, T., Lindsay, K., Tjiputra, J. F., and Wu, T.: Carbon–Concentration and Carbon–Climate Feedbacks in CMIP5 Earth System Models, J. Climate, 26, 5289–5314, 2013.

Avitabile, V., Herold, M., Heuvelink, G. B. M., Lewis, S. L., Phillips, O. L., Asner, G. P., Armston, J., Asthon, P., Banin, L. F., Bayol, N., Berry, N., Boeckx, P., de Jong, B., DeVries, B., Girardin, C., Kearsley, E., Lindsell, J. A., Lopez-Gonzalez, G., Lucas, R., Malhi, Y., Morel, A., Mitchard, E., Nagy, L., Qie, L., Quinones, M., Ryan, C. M., Slik, F., Sunderland, T., Vaglio Laurin, G., Valentini, R., Verbeeck, H., Wijaya, A., and Willcock, S: An integrated pan-tropical biomass map using multiple reference datasets, Glob Change Biol., 22, 1406–1420, 2015.

Bacastow, R. B.: The effect of temperature change of the warm surface waters of the oceans on atmospheric CO_2, Global Biogeochem. Cy., 10, 319–333, 1993.

Baccini, A., Goetz, S. J., Walker, W. S., Laporte, N. T., Sun, M., Sulla-Menashe, D., Hackler, J., Beck, P. S. A., Dubayah, R., Friedl, M. A., Samanta, S., and Houghton, R. A.: Estimated carbon dioxide emissions from tropical deforestation improved by carbon-density maps, Nature Climate Change, 2, 182–185, 2012.

Batjes, N. H: ISRIC-WISE derived soil properties on a 5 by 5 arc-minutes global grid (ver. 1.2). Report 2012/01, Wageningen: ISRIC – World Soil Information, 57 pp., 2012.

Bloom, A. A., Exbrayat, J.-F., van der Velde, I.R., Feng, L., and Williams, M.: The decadal state of the terrestrial carbon cycle: global retrievals of terrestrial carbon allocation, pools and residence times, P. Natl. Acad. Sci., 113, 1285–1290, 2016.

Bonan, G. B., Lawrence, P. J., Oleson, K. W., Levis, S., Jung, M., Reichstein, M., Lawrence, D. M., and Swenson, S. C.: Improving canopy processes in the Community Land Model version 4 (CLM4) using global flux fields empirically inferred from FLUXNET data, J. Geophys. Res.-Biogeosci., 116, G02014, doi:10.1029/2010JG001593, 2011.

Bopp, L., Resplandy, L., Orr, J. C., Doney, S. C., Dunne, J. P., Gehlen, M., Halloran, P., Heinze, C., Ilyina, T., Séférian, R., Tjiputra, J., and Vichi, M.: Multiple stressors of ocean ecosystems in the 21st century: projections with CMIP5 models, Biogeosciences, 10, 6225–6245, doi:10.5194/bg-10-6225-2013, 2013.

Brovkin, V., Boysen, L., Arora, V. K., Boisier, J. P., Cadule, P., Chini, L., Claussen, M., Friedlingstein, P., Gayler, V., van den Hurk, B. J. J. M., Hurtt, G. C., Jones, C. D., Kato, E., de Noblet-Ducoudré, N., Pacifico, F., Pongratz, J., and Weiss, M.: Effect of Anthropogenic Land-Use and Land-Cover Changes on Climate and Land Carbon Storage in CMIP5 Projections for the Twenty-First Century, J. Climate, 26, 6859–6881, 2013.

Buitenhuis, E. T., Vogt, M., Moriarty, R., Bednaršek, N., Doney, S. C., Leblanc, K., Le Quéré, C., Luo, Y.-W., O'Brien, C., O'Brien, T., Peloquin, J., Schiebel, R., and Swan, C.: MAREDAT: towards a world atlas of MARine Ecosystem DATa, Earth Syst. Sci. Data, 5, 227–239, doi:10.5194/essd-5-227-2013, 2013.

Burke, E. J., Jones, C. D., and Koven, C. D.: Estimating the Permafrost-Carbon Climate Response in the CMIP5 Climate Models Using a Simplified Approach, J. Climate, 26, 4897–4909, 2013.

Carvalhais, N., Forkel, M., Khomik, M., Bellarby, J., Jung, M., Migliavacca, M., Mu, M., Saatchi, S., Santoro, M., Thurner, M., Weber, U., Ahrens, B., Beer, C., Cescatti, A., Randerson, J. T., and Reichstein, M.: Global covariation of carbon turnover times with climate in terrestrial ecosystems, Nature, 514, 213–217, doi:10.1038/nature13731, 2014.

Ciais, P., Tans, P. P., Trolier, M., White, J. W. C., and Francey, R. J.: A large northern hemisphere terrestrial CO_2 sink indicated by the 13C/12C ratio of atmospheric CO_2, Science, 269, 1017–1188, 1995.

Ciais, P., Sabine, C., Bala, G., Bopp, L., Brovkin, V., Canadell, J., Chhabra, A., DeFries, R., Galloway, J., Heimann, M., Jones, C., Le Quéré, C., Myneni, R. B., Piao, S., and Thornton, P.: Carbon and Other Biogeochemical Cycles. In: Climate Change 2013: The Physical Science Basis, Contribution of Working Group I to the Fifth Assessment Report of the Intergovernmental Panel on Climate Change, edited by: Stocker, T. F., Qin, D., Plattner, G.-K., Tignor, M., Allen, S. K., Boschung, J., Nauels, A., Xia, Y., Bex, V., and Midgley, P. M., Cambridge University Press, Cambridge, United Kingdom and New York, NY, USA, 2013.

Cox, P. M., Betts, R. A., Jones, C. D., Spall, S. A., and Totterdell, I. J.: Acceleration of global warming due to carbon-cycle feedbacks in a coupled climate model, Nature, 408, 184–187, 2000.

Cox, P. M., Pearson, D., Booth, B. B., Friedlingstein, P., Huntingford, C., Jones, C. D., and Luke, C.: Sensitivity of tropical carbon to climate change constrained by carbon dioxide variability, Nature, 494, 341–345, doi:10.1038/nature11882, 2013.

Cramer, W., Bondeau, A., Woodward, F. I., Prentice, I. C., Betts, R. A., Brovkin, V., Cox, P. M., Fisher, V., Foley, J. A., Friend, A. D., Kucharik, C., Lomas, M. R., Ramankutty, N., Sitch, S., Smith, B., White, A., and Young-Molling, C.: Global response of terrestrial ecosystem structure and function to CO_2 and climate change: results from six dynamic global vegetation models, Glob. Change Biol., 7, 357–373, 2001.

Dufresne, J.-L., Friedlingstein, P., Berthelot, M., Bopp, L., Ciais, P., Fairhead, L., Le Treut, H., and Monfray, P.: On the magnitude of positive feedback between future climate change and the carbon cycle, Geophys. Res. Lett., 29, 43-1–43-4, doi:10.1029/2001GL013777, 2002.

Eyring, V., Bony, S., Meehl, G. A., Senior, C. A., Stevens, B., Stouffer, R. J., and Taylor, K. E.: Overview of the Coupled Model Intercomparison Project Phase 6 (CMIP6) experimental design and organization, Geosci. Model Dev., 9, 1937–1958, doi:10.5194/gmd-9-1937-2016, 2016a.

Eyring, V., Righi, M., Lauer, A., Evaldsson, M., Wenzel, S., Jones, C., Anav, A., Andrews, O., Cionni, I., Davin, E. L., Deser, C., Ehbrecht, C., Friedlingstein, P., Gleckler, P., Gottschaldt, K.-D., Hagemann, S., Juckes, M., Kindermann, S., Krasting, J., Kunert, D., Levine, R., Loew, A., Mäkelä, J., Martin, G., Mason, E., Phillips, A. S., Read, S., Rio, C., Roehrig, R., Senftleben, D., Sterl, A., van Ulft, L. H., Walton, J., Wang, S., and Williams, K. D.: ESMValTool (v1.0) – a community diagnostic and performance metrics tool for routine evaluation of Earth system models in CMIP, Geosci. Model Dev., 9, 1747–1802, doi:10.5194/gmd-9-1747-2016, 2016b.

FAO/IIASA/ISRIC/ISS-CAS/JRC: Harmonized World Soil Database (version 1.2), Rome: FAO, 2012.

Foley, A. M., Dalmonech, D., Friend, A. D., Aires, F., Archibald, A. T., Bartlein, P., Bopp, L., Chappellaz, J., Cox, P., Edwards, N. R., Feulner, G., Friedlingstein, P., Harrison, S. P., Hopcroft, P. O., Jones, C. D., Kolassa, J., Levine, J. G., Prentice, I. C., Pyle, J., Vázquez Riveiros, N., Wolff, E. W., and Zaehle, S.: Evaluation of biospheric components in Earth system models using modern and palaeo-observations: the state-of-the-art, Biogeosciences, 10, 8305–8328, doi:10.5194/bg-10-8305-2013, 2013.

Friedlingstein, P., Bopp, L., Ciais, P., Dufresne, J.-L., Fairhead, L., LeTreut, H., Monfray, P., and Orr, J.: Positive feedback between future climate change and the carbon cycle, Geophys. Res. Lett., 28, 1543–1546, 2001.

Friedlingstein, P., Dufresne, J.-L., Cox, P. M., and Rayner, P.: How positive is the feedback between climate change and the carbon cycle?, Tellus, 55B, 692–700, 2003.

Friedlingstein, P., Cox, P., Betts, R., Bopp, L., von Bloh, W., Brovkin, V., Cadule, P., Doney, S., Eby, M., Fung, I., Bala, G., John, J., Jones, C., Joos, F., Kato, T., Kawamiya, M., Knorr, W., Lindsay, K., Matthews, H. D., Raddatz, T., Rayner, P., Reick, C., Roeckner, E., Schnitzle, K.-G., Schnur, R., Strassmann, K., Weaver, A. J., Yoshikawa, C., and Zeng, N.: Climate–carbon cycle feedback analysis: Results from the C4MIP model intercomparison, J. Climate, 19, 3337–3353, 2006.

Fung, I., Rayner, P., and Friedlingstein, P.: Full-form earth system models: Coupled carbon-climate interaction experiment (the flying leap), IGBP Global Change Newslet., 41, 7–8, 2000.

Gillett, N. P., Arora, V. K., Matthews, H. D., and Allen, M. R.: Constraining the Ratio of Global Warming to Cumulative CO_2 Emissions Using CMIP5 Simulations, J. Climate, 26, 6844–6858, 2013.

Gillett, N. P., Shiogama, H., Funke, B., Hegerl, G., Knutti, R., Matthes, K., Santer, B. D., Stone, D., and Tebaldi, C.: Detection and Attribution Model Intercomparison Project (DAMIP),

Geosci. Model Dev. Discuss., doi:10.5194/gmd-2016-74, in review, 2016.

Graven, H. D.: Impact of fossil fuel emissions on atmospheric radiocarbon and various applications of radiocarbon over this century, P. Natl. Acad. Sci. USA, 112, 9542–9545, doi:10.1073/pnas.1504467112, 2015.

Graven, H. D., Gruber, N., Key, R., Khatiwala, S., and Giraud, X.: Changing controls on oceanic radiocarbon: New insights on shallow-to-deep ocean exchange and anthropogenic CO_2 uptake, J. Geophys. Res., 117, C10005, doi:10.1029/2012JC008074, 2012.

Gregory, J. M., Jones, C. D., Cadule, P., and Friedlingstein, P.: Quantifying carbon cycle feedbacks, J. Climate, 22, 5232–5250, 2009.

Griffies, S. M., Danabasoglu, G., Durack, P. J., Adcroft, A. J., Balaji, V., Böning, C. W., Chassignet, E. P., Curchitser, E., Deshayes, J., Drange, H., Fox-Kemper, B., Gleckler, P. J., Gregory, J. M., Haak, H., Hallberg, R. W., Hewitt, H. T., Holland, D. M., Ilyina, T., Jungclaus, J. H., Komuro, Y., Krasting, J. P., Large, W. G., Marsland, S. J., Masina, S., McDougall, T. J., Nurser, A. J. G., Orr, J. C., Pirani, A., Qiao, F., Stouffer, R. J., Taylor, K. E., Treguier, A. M., Tsujino, H., Uotila, P., Valdivieso, M., Winton, M., and Yeager, S. G.: Experimental and diagnostic protocol for the physical component of the CMIP6 Ocean Model Intercomparison Project (OMIP), Geosci. Model Dev. Discuss., doi:10.5194/gmd-2016-77, in review, 2016.

Hansis, E., Davis, S. J., and Pongratz, J.: Relevance of methodological choices for accounting of land use change carbon fluxes, Global Biogeochem. Cy., 29, 1230–1246, doi:10.1002/2014GB004997, 2015.

Hengl, T., Mendes de Jesus, J., MacMillan, R. A., Batjes, N. H., Heuvelink, G. B. M., Ribeiro, E. C., Samuel-Rosa, A., Kempen, B., Leenaars, J. G. B., Walsh, M. G., and Gonzalez, M. R.: SoilGrids1km – global soil information based on automated mapping, PLoS ONE, 9, e105992, doi:10.1371/journal.pone.0105992, 2014.

Hoffman, F. M., Randerson, J. T., Arora, V. K., Bao, Q., Cadule, P., Ji, D., Jones, C. D., Kawamiya, M., Khatiwala, S., Lindsay, K., Obata, A., Shevliakova, E., Six, K. D., Tjiputra, J. F., Volodin, E. M., and Wu, T.: Causes and implications of persistent atmospheric carbon dioxide biases in Earth System Models, J. Geophys. Res.-Biogeosci., 119, 141–162, doi:10.1002/2013JG002381, 2014.

Houghton, R. A., House, J. I., Pongratz, J., van der Werf, G. R., DeFries, R. S., Hansen, M. C., Le Quéré, C., and Ramankutty, N.: Carbon emissions from land use and land-cover change, Biogeosciences, 9, 5125–5142, doi:10.5194/bg-9-5125-2012, 2012.

Hurtt, G., Chini, L., Sahajpal, R., Frolking, S., Calvin, K., Fujimori, S., Klein Goldewijk, K., Hasegawa, T., Havlik, P., Heinemann, A., Kaplan, J., Lawrence, D., Lawrence, P., Mertz, O., Popp, A., Stehfest, E., van Vuuren, D., and Zhang, X.: Harmonization of global land-use change and management for the period 850–2100, in preparation, 2016.

Ilyina, T., Six, K. D., Segschneider, J., Maier-Reimer, E., Li, H., and Nunez-Riboni, I.: Global ocean biogeochemistry model HAMOCC: Model architecture and performance as component of the MPI-Earth System Model in different CMIP5 experimental realizations, J. Adv. Model. Earth Systems, 5, 287–315, 2013.

Iudicone, D., Rodgers, K. B., Stendardo, I., Aumont, O., Madec, G., Bopp, L., Mangoni, O., and Ribera d'Alcala', M.: Water masses as a unifying framework for understanding the Southern Ocean Carbon Cycle, Biogeosciences, 8, 1031–1052, doi:10.5194/bg-8-1031-2011, 2011.

Jenkinson, D. S., Adams, D. E., and Wild, A.: Model estimates of CO2 emissions from soil in response to global warming, Nature, 351, 304–306, 1991.

Jones, C. D., Robertson, E., Arora, V., Friedlingstein, P., Shevliakova, E., Bopp, L., Brovkin, V., Hajima, T., Kato, E., Kawamiya, M., Liddicoat, S., Lindsay, K., Reick, C. H., Roelandt, C., Segschneider, J., and Tjiputra, J.: 21st century compatible CO2 emissions and airborne fraction simulated by CMIP5 Earth System Models under four representative concentration pathways, J. Climate, 13, 4398–4413, doi:10.1175/JCLI-D-12-00554.1, 2013.

Joos, F. and Bruno, M.: Long-term variability of the terrestrial and oceanic carbon sinks and the budgets of the carbon isotopes ^{13}C and ^{14}C, Global Biogeochem. Cy., 12, 277–295, 1998.

Joos, F., Plattner, G.-K., Stocker, T. F., Marchal, O., and Schmittner, A.: Global warming and marine carbon cycle feedbacks on future atmospheric CO_2, Science, 284, 464–467, 1999.

Jung, M., Reichstein, M., Margolis, H. A., Cescatti, A., Richardson, A. D., Arain, M. A., Arneth, A., Bernhofer, C., Bonal, D., Chen, J., Gianelle, D., Gobron, N., Kiely, G., Kutsch, W., Lasslop, G., Law, B. E., Lindroth, A., Merbold, L., Montagnani, L., Moors, E. J., Papale, D., Sottocornola, M., Vaccari, F., and Williams, C.: Global patterns of land-atmosphere fluxes of carbon dioxide, latent heat, and sensible heat derived from eddy covariance, satellite, and meteorological observations, J. Geophys. Res.-Biogeosci., 116, G00J07, doi:10.1029/2010JG001566, 2011.

Jungclaus, J. H., Fischer, N., Haak, H., Lohmann, K., Marotzke, J., Matei, D., Mikolajewicz, U., Notz, D., and von Storch, J.-S.: Characteristics of the ocean simulations in MPIOM, the ocean component of the MPI Earth System Model, J. Adv. Model. Earth Syst., 5, 422–446, 2013.

Karlen, I., Olsson, I. U., Kallburg, P., and Kilici, S.: Absolute determination of the activity of two ^{14}C dating standards, Arkiv Geofysik, 4, 465–471, 1968.

Keeling, C. D., Piper, S. C., Bacastow, R. B., Wahlen, M., Whorf, T. P., Heimann, M., and Meijer, H. A.: Exchanges of atmospheric CO_2 and $13CO_2$ with the terrestrial biosphere and oceans from 1978 to 2000. I. Global aspects, SIO Reference Series, No. 01-06, Scripps Institution of Oceanography, San Diego, 88 pp., 2001.

Khatiwala, S., Tanhua, T., Mikaloff Fletcher, S., Gerber, M., Doney, S. C., Graven, H. D., Gruber, N., McKinley, G. A., Murata, A., Ríos, A. F., and Sabine, C. L.: Global ocean storage of anthropogenic carbon, Biogeosciences, 10, 2169–2191, doi:10.5194/bg-10-2169-2013, 2013.

Kirschbaum, M. U. F.: The temperature dependence of soil organic matter decomposition and the effect of global warming on soil organic carbon storage, Soil Biol. Biochem., 27, 753–760, 1995.

Koven, C. D., Riley, W. J., Subin, Z. M., Tang, J. Y., Torn, M. S., Collins, W. D., Bonan, G. B., Lawrence, D. M., and Swenson, S. C.: The effect of vertically resolved soil biogeochemistry and alternate soil C and N models on C dynamics of CLM4, Biogeosciences, 10, 7109–7131, doi:10.5194/bg-10-7109-2013, 2013.

Lashof, D. A.: The dynamic greenhouse – Feedback processes that may influence future concentrations of atmospheric trace gases and climatic change, Clim. Change., 14, 213–242, 1989.

Lawrence, D. M., Hurtt, George C., Arneth, A., Brovkin, V., Calvin, K. V., Jones, Andrew D., Jones, C. D., Lawrence, P. J., de Noblet-Ducoudré, N., Pongratz, J., Seneviratne, S. I., and Shevliakova, E.: The Land Use Model Intercomparison Project (LUMIP): Rationale and experimental design, Geosci. Model Dev. Discuss., doi:10.5194/gmd-2016-76, in review, 2016.

Le Quéré, C., Moriarty, R., Andrew, R. M., Canadell, J. G., Sitch, S., Korsbakken, J. I., Friedlingstein, P., Peters, G. P., Andres, R. J., Boden, T. A., Houghton, R. A., House, J. I., Keeling, R. F., Tans, P., Arneth, A., Bakker, D. C. E., Barbero, L., Bopp, L., Chang, J., Chevallier, F., Chini, L. P., Ciais, P., Fader, M., Feely, R. A., Gkritzalis, T., Harris, I., Hauck, J., Ilyina, T., Jain, A. K., Kato, E., Kitidis, V., Klein Goldewijk, K., Koven, C., Landschützer, P., Lauvset, S. K., Lefèvre, N., Lenton, A., Lima, I. D., Metzl, N., Millero, F., Munro, D. R., Murata, A., Nabel, J. E. M. S., Nakaoka, S., Nojiri, Y., O'Brien, K., Olsen, A., Ono, T., Pérez, F. F., Pfeil, B., Pierrot, D., Poulter, B., Rehder, G., Rödenbeck, C., Saito, S., Schuster, U., Schwinger, J., Séférian, R., Steinhoff, T., Stocker, B. D., Sutton, A. J., Takahashi, T., Tilbrook, B., van der Laan-Luijkx, I. T., van der Werf, G. R., van Heuven, S., Vandemark, D., Viovy, N., Wiltshire, A., Zaehle, S., and Zeng, N.: Global Carbon Budget 2015, Earth Syst. Sci. Data, 7, 349–396, doi:10.5194/essd-7-349-2015, 2015.

Levin, I., Naegler, T., Kromer, B., Diehl, M., Francey, R. J., Gomez-Pelaez, A. J., Steele, L. P., Wagenbach, D., Weller, R., and Worthy, D. E.: Observations and modelling of the global distribution and long-term trend of atmospheric $^{14}CO_2$, Tellus B, 62, 26–46, 2010.

Lindsay, K., Bonan, G. B., Doney, S. C., Hoffman, F. M., Lawrence, D. M., Long, M. C., Mahowald, N. M., Moore, J. K., Randerson, J. T., and Thornton, P. E.: Preindustrial control and 20th century carbon cycle experiments with the Earth system model CESM1(BGC), J. Climate, 27, 8981–9005, doi:10.1175/JCLI-D-12-00565.1, 2014.

Luo, Y. Q., Randerson, J. T., Abramowitz, G., Bacour, C., Blyth, E., Carvalhais, N., Ciais, P., Dalmonech, D., Fisher, J. B., Fisher, R., Friedlingstein, P., Hibbard, K., Hoffman, F., Huntzinger, D., Jones, C. D., Koven, C., Lawrence, D., Li, D. J., Mahecha, M., Niu, S. L., Norby, R., Piao, S. L., Qi, X., Peylin, P., Prentice, I. C., Riley, W., Reichstein, M., Schwalm, C., Wang, Y. P., Xia, J. Y., Zaehle, S., and Zhou, X. H.: A framework for benchmarking land models, Biogeosciences, 9, 3857–3874, doi:10.5194/bg-9-3857-2012, 2012.

Luo, Y., Ahlström, A., Allison, S. D., Batjes, N. H., Brovkin, V., Carvalhais, N., Chappell, A., Ciais, P., Davidson, E. A., Finzi, A., Georgiou, K., Guenet, B., Hararuk, O., Harden, J. W., He, Y., Hopkins, F., Jiang, L., Koven, C., Jackson, R. B., Jones, C. D., Lara, M. J., Liang, J., McGuire, A. D., Parton, W., Peng, C., Randerson, J. T., Salazar, A., Sierra, C. A., Smith, M. J., Tian, H., Todd-Brown, K. E. O., Torn, M., van Groenigen, K. J., Wang, Y. P., West, T. O., Wei, Y., Wieder, W. R., Xia, J., Xu, X., Xu, X., and Zhou, T.: Towards more realistic projections of soil carbon dynamics by Earth System Models, Global Biogeochem. Cy., 30, 40–56, doi:10.1002/2015GB005239, 2016.

Maier-Reimer, E., Mikolajewicz, U., and Winguth, A.: Future ocean uptake of CO_2: interaction between ocean circulation and biology, Clim. Dynam., 12, 711–722, 1996.

Mahecha, M. D., Reichstein, M., Carvalhais, N., Lasslop, G., Lange, H., Seneviratne, S. I., Vargas, R., Ammann, C., Arain, M. A., Cescatti, A., Janssens, I. A., Migliavacca, M., Montagnani, L., and Richardson, A. D.: Global convergence in the temperature sensitivity of respiration at ecosystem level, Science, 329, 838–840, 2010.

Matsumoto, K., Sarmiento, J. L., Key, R. M., Aumont, O., Bullister, J. L., Caldeira, K., Campin, J.-M., Doney, S. C., Drange, H., Dutay, J.-C., Follows, M., Gao, Y., Gnanadesikan, A., Gruber, N., Ishida, A., Joos, F., Lindsay, K., Maier-Reimer, E., Marshall, J. C., Matear, R. J., Monfray, P., Mouchet, A., Najjar, R., Plattner, G.-K., Schlitzer, R., Slater, R., Swathi, P. S., Totterdell, I. J., Weirig, M.-F., Yamanaka, Y., Yool, A., and Orr, J. C.: Evaluation of ocean carbon cycle models with data-based metrics, Geophys. Res. Lett., 31, L07303, doi:10.1029/2003gl018970, 2004.

Meyerholt, J. and Zaehle, S.: The role of stoichiometric flexibility in modelling forest ecosystem responses to nitrogen fertilization, New Phytol., 208, 1042–1055, doi:10.1111/nph.13547, 2015.

Naegler, T. and Levin, I.: Biosphere-atmosphere gross carbon exchange flux and the $\delta^{13}CO_2$ and $\Delta^{14}CO_2$ disequilibria constrained by the biospheric excess radiocarbon inventory, J. Geophys. Res., 114, D17303, doi:10.1029/2008JD011116, 2009.

O'Neill, B. C., Tebaldi, C., van Vuuren, D., Eyring, V., Friedlingstein, P., Hurtt, G., Knutti, R., Kriegler, E., Lamarque, J.-F., Lowe, J., Meehl, J., Moss, R., Riahi, K., and Sanderson, B. M.: The Scenario Model Intercomparison Project (ScenarioMIP) for CMIP6, Geosci. Model Dev. Discuss., doi:10.5194/gmd-2016-84, in review, 2016.

Orr, J., Najjar, R., Sabine, C., and Joos, F.: Abiotic-HOWTO, Technical report, available at: http://ocmip5.ipsl.jussieu.fr/OCMIP/phase2/simulations/Abiotic/HOWTO-Abiotic.html (last access: February 2016), 2000.

Orr, J., Maier-Reimer, E., Mikolajewicz, U., Monfray, P., Sarmiento, J. L., Toggweiler, J. R., Taylor, N. K., Palmer, J., Gruber, N., Sabine, C. L., Le Queìreì, C., Key, R. M., and Boutin, J.: Estimates of anthropogenic carbon uptake from four 3-D global ocean models, Global Biogeochem. Cy., 15, 43–60, 2001.

Orr, J. C., Najjar, R. G., Aumount, O., Bopp, L., Bullister, J. L., Danabasoglu, G., Doney, S. C., Dunne, J. P., Dutay, J.-C., Graven, H., Griffies, S. M., John, J. G., Joos, F., Levin, I., Lindsay, K., Matear, R. J., McKinley, G. A., Mouchet, A., Oschlies, A., Romanou, A., Schlitzer, R., Tagliabue, A., Tanhua, T., and Yool, A.: Biogeochemical protocols and diagnostics for the CMIP6 Ocean Model Intercomparison Project (OMIP), Geosci. Model Dev. Discuss., doi:10.5194/gmd-2016-155, in review, 2016.

Piao, S., Sitch, S., Ciais, P., Friedlingstein, P., Peylin, P., Wang, X., Ahlström, A., Anav, A., Canadell, J. G., Cong, N., Huntingford, C., Jung, M., Levis, S., Levy, P. E., Li, J., Lin, X., Lomas, M. R., Lu, M., Luo, Y., Ma, Y., Myneni, R. B., Poulter, B., Sun, Z., Wang, T., Viovy, N., Zaehle, S. and Zeng, N.: Evaluation of terrestrial carbon cycle models for their response to climate variability and to CO_2 trends, Glob. Change Biol., 19, 2117–2132, doi:10.1111/gcb.12187, 2013.

Pilcher, D. J., Brody, S. R., Johnson, L., and Bronselaer, B.: Assessing the abilities of CMIP5 models to represent the seasonal cycle

of surface ocean pCO2, J. Geophys. Res.-Oceans, 120, 4625–4637, 2015.

Pongratz, J., Reick, C. H., Raddatz, T., and Claussen, M.: Effects of anthropogenic land cover change on the carbon cycle of the last millennium, Global Biogeochem. Cy., 23, GB4001, doi:10.1029/2009GB003488, 2009.

Pongratz, J., Reick, C. H., Houghton, R. A., and House, J. I.: Terminology as a key uncertainty in net land use and land cover change carbon flux estimates, Earth Syst. Dynam., 5, 177–195, doi:10.5194/esd-5-177-2014, 2014.

Prentice, I. C., Farquhar, G. D., Fasham, M. J. R., Goulden, M. L., Heimann, M., Jaramillo, V. J., Kheshgi, H. S., Le Quéré, C., Scholes, R. J., and Wallace, D. W. R.: The carbon cycle and atmospheric carbon dioxide. In: Climate Change 2001: The Scientific Basis, Contribution of Working Group I to the Third Assessment Report of the Intergovernmental Panel on Climate Change, edited by: Houghton, J. T., Ding, Y., Griggs, D. J., Noquer, M., van der Linden, P. J., Dai, X., Maskell, K., and Johnson, C. A., Cambridge University Press, Cambridge, United Kingdom and New York, NY, USA, 183–237, 2001.

Raddatz, T. J., Reick, C. H., Knorr, W., Kattge, J., Roeckner, E., Schnur, R., Schnitzler, K.-G., Wetzel, P., and Jungclaus, J.: Will the tropical land biosphere dominate the climate-carbon cycle feedback during the twenty first century?, Clim. Dyn., 29, 565–574, doi:10.1007/s00382-007-0247-8, 2007.

Randerson, J. T., Lindsay, K., Munoz, E., Fu, W., Moore, J. K., Hoffman, F. M., Mahowald, N. M., and Doney, S. C.: Multicentury changes in ocean and land contributions to the climate-carbon feedback, Global Biogeochem. Cy., 29, 744–759, doi:10.1002/2014GB005079, 2015.

Roy, T., Bopp, L., Gehlen, M., Schneider, B., Cadule, P., Frolicher, T. L., Segschneider, J., Tjiputra, J., Heinze, C., and Joos, F.: Regional impacts of climate change and atmospheric CO2 on future ocean carbon uptake: A multimodel linear feedback analysis, J. Clim., 24, 2300–2318, 2011.

Rubino, M., Etheridge, D. M., Trudinger, C. M., Allison, C. E., Battle, M. O., Langenfelds, R. L., Steele, L. P., Curran, M., Bender, M., White, J. W. C., Jenk, T. M., Blunier, T., and Francey, R. J.: A revised 1000 year atmospheric δ^{13}C-CO_2 record from Law Dome and South Pole, Antarctica, J. Geophys. Res.-Atmos., 118, 8482–8499, doi:10.1002/jgrd.50668, 2013.

Saatchi, S. S., Harris, N. L., Brown, S., Lefsky, M., Mitchard, E. T. A., Salas, W. Zutta, B. R., Buermann, W., Lewis, S. L., Hagen, S., Petrova, S., White, L., Silman, M., and Morel, A.: Benchmark map of forest carbon stocks in tropical regions across three continents, P. Natl. Acad. Sci., 108, 9899–9904, 2011.

Sarmiento, J. L. and Le Queìreì, C.: Oceanic carbon dioxide uptake in a model of century-scale global warming, Science, 274, 1346–1350, 1996.

Sarmiento, J. L., Hughes, T. M. C., Stouffer, R. J., and Manabe, S.: Simulated response of the ocean carbon cycle to anthropogenic climate warming, Nature, 393, 245–249, 1998.

Schimel, D. S., Braswell, B. H., Holland, E. A., McKeown, R., Ojima, D. S., Painter, T. H., Parton, W. J., and Townsend, A. R.: Climatic, edaphic and biotic controls over carbon and turnover of carbon in soils, Global Biogeochem. Cy., 8, 279–293, 1994.

Schwinger, J., Tjiputra, J. F., Heinze, C., Bopp, L., Christian, J. R., Gehlen, M., Ilyina, T., Jones, C. D., Salas-Mélia, D., Segschneider, J., Séférian, R., and Totterdell, I. J.: Nonlinearity of Ocean Carbon Cycle Feedbacks in CMIP5 Earth System Models, J. Climate, 27, 3869–3888, 2014.

Séférian, R., Gehlen, M., Bopp, L., Resplandy, L., Orr, J. C., Marti, O., Dunne, J. P., Christian, J. R., Doney, S. C., Ilyina, T., Lindsay, K., Halloran, P. R., Heinze, C., Segschneider, J., Tjiputra, J., Aumont, O., and Romanou, A.: Inconsistent strategies to spin up models in CMIP5: implications for ocean biogeochemical model performance assessment, Geosci. Model Dev., 9, 1827–1851, doi:10.5194/gmd-9-1827-2016, 2016.

Sentman, L. T., Shevliakova, E., Stouffer, R. J., and Malyshev, S.: Time scales of terrestrial carbon response related to land-use application: Implications for initializing an Earth System Model, Earth Interactions, 15, 1–16, 2011.

Sitch, S., Friedlingstein, P., Gruber, N., Jones, S. D., Murray-Tortarolo, G., Ahlström, A., Doney, S. C., Graven, H., Heinze, C., Huntingford, C., Levis, S., Levy, P. E., Lomas, M., Poulter, B., Viovy, N., Zaehle, S., Zeng, N., Arneth, A., Bonan, G., Bopp, L., Canadell, J. G., Chevallier, F., Ciais, P., Ellis, R., Gloor, M., Peylin, P., Piao, S. L., Le Quéré, C., Smith, B., Zhu, Z., and Myneni, R.: Recent trends and drivers of regional sources and sinks of carbon dioxide, Biogeosciences, 12, 653–679, doi:10.5194/bg-12-653-2015, 2015.

Sweeney, C., Gloor, E., Jacobson, A. R., Key, R. M., McKinley, G., Sarmiento, J. L., and Wanninkhof, R.: Constraining global air-sea gas exchange for CO_2 with recent bomb ^{14}C measurements, Global Biogeochem. Cy., 21, GB2015, doi:10.1029/2006GB002784, 2007.

Strassmann, K. M., Joos, F., and Fischer, G.: Simulating effects of land use changes on carbon fluxes: Past contributions to atmospheric CO_2 increases and future commitments due to losses of terrestrial sink capacity, Tellus B, 60, 583–603, 2008.

Tagliabue, A., Mtshali, T., Aumont, O., Bowie, A. R., Klunder, M. B., Roychoudhury, A. N., and Swart, S.: A global compilation of dissolved iron measurements: focus on distributions and processes in the Southern Ocean, Biogeosciences, 9, 2333–2349, doi:10.5194/bg-9-2333-2012, 2012.

Takahashi, T., Sutherland, S. C., Wanninkhof, R., Sweeney, C., Feely, R. A., Chipman, D. W., Hales, B., Friederich, G., Chavez, F., Sabine, C., Watson, A., Bakker, D. C. E., Schuster, U., Metzl, N., Yoshikawa-Inoue, H., Ishii, M., Midorikawa, T., Nojiri, Y., Kortzinger, A., Steinhoff, T., Hoppema, M., Olafsson, J., Arnarson, T. S., Tilbrook, B., Johannessen, T., Olsen, A., Bellerby, R., Wong, C. S., Delille, B., Bates, N. R., and de Baar, H. J. W.: Climatological mean and decadal change in surface ocean pCO_2, and net sea–air CO_2 flux over the global oceans, Deep Sea Res. II, 56, 554–577, 2009.

Taylor, K. E., Stouffer, R. J., and Meehl, G. A.: An overview of CMIP5 and the experiment design, B. Am. Meteorol. Soc., 93, 485–498, 2012.

Thompson, S. L., Govindasamy, B., Mirin, A., Caldeira, K., Delire, C., Milovich, J., Wickett, M., and Erickson, D.: Quantifying the effects of CO_2-fertilized vegetation on future global climate, Geophys. Res. Lett., 31, L23211, doi:10.1029/2004GL021239, 2004.

Thornton, P. E., Doney, S. C., Lindsay, K., Moore, J. K., Mahowald, N., Randerson, J. T., Fung, I., Lamarque, J.-F., Feddema, J. J., and Lee, Y.-H.: Carbon-nitrogen interactions regulate climate-carbon cycle feedbacks: results from an atmosphere-

ocean general circulation model, Biogeosciences, 6, 2099–2120, doi:10.5194/bg-6-2099-2009, 2009.

Tjiputra, J. F., Roelandt, C., Bentsen, M., Lawrence, D. M., Lorentzen, T., Schwinger, J., Seland, Ø., and Heinze, C.: Evaluation of the carbon cycle components in the Norwegian Earth System Model (NorESM), Geosci. Model Dev., 6, 301–325, doi:10.5194/gmd-6-301-2013, 2013.

Tjiputra, J. F., Olsen, A., Bopp, L., Lenton, A., Pfeil, B., Roy, T., Segschneider, J., Totterdell, I., and Heinze, C.: Long-term surface pCO_2 trends from observations and models, Tellus B, 66, 23083, doi:10.3402/tellusb.v66.23083, 2014.

Todd-Brown, K. E. O., Randerson, J. T., Hopkins, F., Arora, V., Hajima, T., Jones, C., Shevliakova, E., Tjiputra, J., Volodin, E., Wu, T., Zhang, Q., and Allison, S. D.: Changes in soil organic carbon storage predicted by Earth system models during the 21st century, Biogeosciences, 11, 2341–2356, doi:10.5194/bg-11-2341-2014, 2014.

Trumbore, S.: Age of soil organic matter and soil respiration: radiocarbon constraints on belowground C dynamics, Ecol. Appl., 10, 399–411, 2000

van den Hurk, B., Kim, H., Krinner, G., Seneviratne, S. I., Derksen, C., Oki, T., Douville, H., Colin, J., Ducharne, A., Cheruy, F., Viovy, N., Puma, M., Wada, Y., Li, W., Jia, B., Alessandri, A., Lawrence, D., Weedon, G. P., Ellis, R., Hagemann, S., Mao, J., Flanner, M. G., Zampieri, M., Law, R., and Sheffield, J.: The Land Surface, Snow and Soil moisture Model Intercomparison Program (LS3MIP): aims, set-up and expected outcome, Geosci. Model Dev. Discuss., doi:10.5194/gmd-2016-72, in review, 2016.

Wenzel, S., Cox, P. M., Eyring, V., and Friedlingstein, P.: Emergent constraints on climate-carbon cycle feedbacks in the CMIP5 Earth system models, J. Geophys. Res.-Biogeosci., 119, 794–807, doi:10.1002/2013JG002591, 2014.

Wieder, W. R., Cleveland, C. C., Smith, W. K., and Todd-Brown, K.: Future productivity and carbon storage limited by terrestrial nutrient availability, Nature Geosci., 8, 441–444, doi:10.1038/ngeo2413, 2015.

Xia, J. Y., Luo, Y. Q., Wang, Y.-P., Weng, E. S., and Hararuk, O.: A semi-analytical solution to accelerate spin-up of a coupled carbon and nitrogen land model to steady state, Geosci. Model Dev., 5, 1259–1271, doi:10.5194/gmd-5-1259-2012, 2012.

Xia, J., Luo, Y., Wang, Y.-P., and Hararuk, O.. Traceable components of terrestrial carbon storage capacity in biogeochemical models, Glob. Change Biol., 19, 2104–2116, doi:10.1111/gcb.12172, 2013.

Zaehle, S. and Dalmonech, D.: Carbon–nitrogen interactions on land at global scales: Current understanding in modelling climate biosphere feedbacks, Curr. Opin. Environ. Sustainability, 3, 311–320, doi:10.1016/j.cosust.2011.08.008, 2011.

Zaehle, S., Medlyn, B. E., De Kauwe, M. G., Walker, A. P., Dietze, M. C., Hickler, T., Luo, Y., Wang, Y.-P., El-Masri, B., Thornton, P., Jain, A., Wang, S., Warlind, D., Weng, E., Parton, W., Iversen, C. M., Gallet-Budynek, A., McCarthy, H., Finzi, A., Hanson, P. J., Prentice, I. C., Oren, R., and Norby, R. J.: Evaluation of 11 terrestrial carbon–nitrogen cycle models against observations from two temperate free-air CO_2 enrichment studies, New Phytol., 202, 803–822, doi:10.1111/nph.12697, 2014.

Zaehle, S., Jones, C. D., Houlton, B., Lamarque, J.-F., and Robertson, E.: Nitrogen Availability Reduces CMIP5 Projections of Twenty-First-Century Land Carbon Uptake, J. Climate, 28, 2494–2511, 2015.

3. Feedback analysis and carbon cycle projections

3.1. A linearised carbon cycle feedback framework and its application

At a very broad level, the global carbon cycle can be characterised by two strong and opposing responses: how it responds to rising atmospheric CO_2 and how it responds to a changing climate (Prentice et al., 2001). Firstly, as CO_2 increases, natural carbon sinks act to take up carbon from the atmosphere – on land primarily due to CO_2 fertilisation and improved water use efficiency of plants (Lloyd and Farquhar, 1996), and in the ocean due to chemical dissolution in sea water because atmospheric CO_2 concentration exceeds the surface ocean pCO_2 (Broecker et al., 1979). Secondly, increasing CO_2 – a greenhouse gas - causes a warming of the climate and this climate change also affects natural carbon sinks. Regional responses to climate change can vary, but at a global level enhanced decomposition of dead organic matter and increased ecosystem respiration on land, and stratification and reduced solubility of CO_2 in the ocean act to reduce natural sinks.

In order to derive a feedback framework for the carbon cycle, we also need to consider how sensitive the climate system is to increasing CO_2, and so to characterise the system we have three sensitivities: i) how CO_2 itself directly drives carbon sinks; ii) how CO_2 affects climate; and iii) how climate change modifies carbon sinks. A simple linearised framework can thus be derived with three parameters to measure the strength of each of these sensitivities:

Alpha, α = how CO_2 affects the climate. Defined in terms of global mean temperature as the warming per ppm of CO_2 increase.

$$\Delta T = \alpha \, \Delta CO_2 \qquad (1)$$

Beta, β = how CO_2 affects carbon sinks. Defined as the carbon sink per ppm of CO_2 increase when only CO_2 increases but not temperature.

$$\Delta C = \beta \, \Delta CO_2 \qquad (2)$$

Gamma, γ = how climate affects carbon sinks. Defined as the carbon sink per degree of global temperature increase when only climate changes and not CO_2.

$$\Delta C = \gamma \Delta T \quad (3)$$

When CO_2 and climate change together these are assumed to be additive. The limitation of this assumption is discussed later.

$$\Delta C = \beta \Delta CO_2 + \gamma \Delta T \quad (4)$$

I performed the simulations with the Hadley Centre model, HadCM3LC, which contributed to the first C4MIP intercomparison (**Friedlingstein et al., 2006**) to try to understand why different models projected different future CO_2 concentration. The feedback metrics cannot all be measured by a single simulation because land and ocean carbon stores respond to both CO_2 and climate so a single simulation cannot distinguish β and γ. Therefore, as well as a fully coupled ("COU") simulation, a second simulation, called "uncoupled" ("UNC" - see Glossary) was performed in which the rising CO_2 concentration did not exert a radiative forcing on climate so that ΔT was zero and only the sensitivity to CO_2 (β) acted on the carbon stores (eqn 5). The assumption was made that β was invariant across simulations and therefore could be subtracted from the fully coupled run to diagnose γ (eqn 6).

$$\beta = \frac{\Delta C^{UNC}}{\Delta CO_2^{UNC}} \quad (5)$$

$$\gamma = \frac{\Delta C^{COU} - \beta \Delta CO_2^{UNC}}{\Delta T^{COU}} \quad (6)$$

According to feedback theory (e.g. Hansen et al., 1984; Bates, 2007), a feedback gain can be used to calculate the feedback factor, or total amplification of an initial perturbation. If the gain, g, is the amplification of the signal for one loop of the feedback circuit, then the full amplification factor, G, can be found by Taylor expansion as the sum of the infinite series $1+g+g^2+g^3+\ldots$, giving simply:

$$G = \frac{\Delta {CO_2}^{COU}}{\Delta {CO_2}^{UNC}} = \frac{1}{1-g} \quad (7)$$

where $\Delta {CO_2}^{UNC}$ represents the change in atmospheric CO_2 without climate feedback and $\Delta {CO_2}^{COU}$ with the feedback. Therefore, for positive g in the range 0-1, $\Delta C^{COU} > \Delta C^{UNC}$: i.e. a positive feedback from climate amplifies the level of CO_2 in the atmosphere. If $g >= 1$ then the system would be unstable and lead to a runaway positive feedback. The analysis by **Friedlingstein et al. (2006)** showed how the α, β, γ metrics could be combined to calculate this system gain, *g*:

$$g = \frac{-\alpha\gamma}{1+\beta} \quad (8)$$

A stronger climate response, α, or stronger (more negative) carbon cycle response to climate, γ, lead to stronger (more positive) gain, *g*, whilst stronger carbon cycle response to CO_2, β, reduces the gain, *g*.

As noted above, climate typically reduces carbon uptake and so the value of γ as simulated by models are negative, which in turn implies a positive climate-carbon cycle feedback. This linear framework was defined by Friedlingstein et al. (2003) and became widespread after it was used to measure the multi-model response of the first C4MIP simulations (**Friedlingstein et al., 2006**).

The derivation of this feedback framework and its application to a pair of simulations with and without climate change was based on feedback theory applied to physical climate modelling (Hansen et al., 1984; Bony et al., 2006). However, it masked some important differences between climate and carbon cycle feedbacks and maybe led to over-emphasis of research and analysis on the climate effects, γ, at the expense of the response to CO_2, β.

There are some clear similarities between feedbacks in the physical climate system and the carbon cycle system that helped the community derive the carbon cycle feedback framework. If something acts to modify the top-of-atmosphere energy balance of the planet (such as reduced outgoing radiation due to the greenhouse effect) then this causes more energy to flow into the atmosphere. The planet warms in response which in turn increases the amount of outgoing energy. The emissivity of the planet scales with the fourth power of its temperature (σT^4; Boltzmann's Law) and so this represents a very strong negative (stabilising) response, known as the black-body response, or "Planck response". It is based on very well established fundamental laws of physics and is known to high precision.

On top of this stabilising response there are many feedbacks within the climate system caused by physical components responding to the change in global temperature. The response of clouds is commonly acknowledged to be the largest

and most uncertain but others include ice and snow-albedo feedbacks, water vapour or atmospheric lapse rate (Bony et al., 2006, Soden et al., 2008).

All these feedbacks act to modify the basic response and determine the overall climate response to the energy perturbation – resulting in the system's "climate sensitivity". From models, we believe the sum total of these feedbacks is positive (i.e. they amplify the climate sensitivity). However, there is a large spread between models, including in some regions the sign of feedback, resulting in substantial uncertainty in global equilibrium climate sensitivity (ECS, see Glossary). IPCC AR5 assess a likely range of 1.5-4.5^{o}C per doubling of CO_2 (Collins et al., 2013) but this range has not changed or narrowed substantially over many years (see Box 12.2 of Collins et al., 2013).

In a similar way, if additional CO_2 is introduced to the atmosphere (e.g. by anthropogenic burning of fossil fuels or deforestation) then the carbon cycle system responds by removing some of this by natural carbon sinks on land and in the oceans. This is what we measure as β in the feedback framework: the carbon cycle response to CO_2. It is a strong negative (stabilising) response and is analogous to the Planck response in the physical climate system.

As with the climate system a multitude of feedbacks operate to modify this response. Plant growth, organic matter decomposition, ocean circulation and CO_2 solubility all respond to climate change. Models tend to agree that on a global scale these feedback terms are positive (amplifying) feedbacks. In other words, there is a model consensus that γ_L and γ_O are negative. At smaller scales, however, the sign as well as the magnitude can be uncertain. It should be noted here that the definition of γ (for land and for ocean) is in terms of global mean temperature, but implicitly includes therefore changes in other climate quantities such as precipitation, radiation or ocean circulation. These can also vary regionally and affect the sign of feedbacks at small scales.

This similarity between carbon cycle and climate feedbacks led early analyses to focus on the positive feedbacks in the system. These were analogous to the climate feedbacks and were the primary drivers of uncertainty in the climate carbon cycle

gain, *g*. However, this masked a very significant difference between the two systems. In the climate system, the stabilising negative Planck feedback is very well known and almost all the uncertainty in climate sensitivity derives from the atmospheric feedbacks. However, in the carbon cycle case, the stabilising negative response is not quantitatively well known but largely neglected in early studies. I co-developed the analysis (**Gregory et al. 2009**) which showed that in fact it is both *stronger* and *more uncertain* than the carbon cycle response to climate (Figure 5). We concluded that carbon cycle feedbacks should be explicitly separated and discussed as "climate-carbon" (how climate affects carbon sinks: γ) and "concentration-carbon" (how CO_2 affects carbon sinks: β) terms. Both of these terms exhibit substantial spread across models, on land and in the oceans, and require research to reduce the uncertainties.

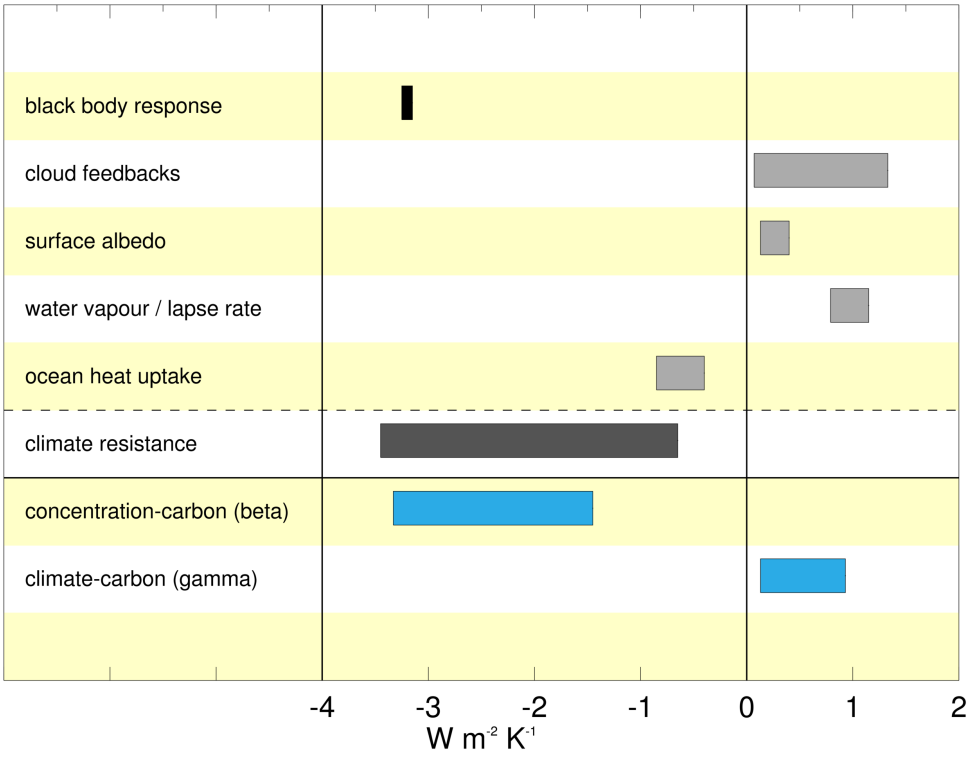

Figure 5. Comparison of response and feedback terms in the physical climate system (top portion) and the carbon cycle (bottom portion). Redrawn from **Gregory et al. (2009; figure 2)** who construct an analysis framework that allows all these terms, both physical and biogeochemical to be expressed in common units of $Wm^{-2}K^{-1}$, and so for the first time they could be quantitatively compared side-by-side. The black-body, or Planck response (black bar), combines with physical climate feedbacks (pale grey) to form the "climate resistance" (dark grey),

which is related to the climate feedback parameter but includes the effect of ocean heat uptake. The concentration-carbon and climate-carbon feedbacks (blue bars) refer to the carbon cycle response to CO_2 concentration and climate (β and γ) respectively, but also expressed in the same common units of $Wm^{-2}K^{-1}$.

This framework can be expanded to other biogeochemical feedbacks. At my suggestion as a reviewer, Arneth et al., (2009) adopted the same approach to present a synthesis of a range of biogeochemical feedbacks in common units. In IPCC AR5 I expanded on this further to develop figure 6.20 (in AR5 chapter 6; which is reproduced and explained further in section 3.2, Figure 6).

Limitations of the feedback framework

These metrics have become widely adopted for coupled carbon cycle models, although their application has not always been consistent. The original C4MIP analysis of **Friedlingstein et al. (2006)** was based on emissions-driven simulations (see Glossary). This meant that all models simulated different CO_2 concentration levels from each other, but also CO_2 differed between the coupled and uncoupled simulations from each model. The assumption that β would be constant between runs was therefore not strictly true. I performed simulations where CO_2 increased at different rates (0.5% per year, 1% per year and 2% per year), and in **Gregory et al. (2009)** we showed that scenario-dependence of metrics, especially β, was not negligible. Since **Gregory et al. (2009)** it has therefore been recommended that experiments to diagnose feedback metrics use concentration driven simulations to ensure the same CO_2 is seen across runs and across models.

Secondly, **Friedlingstein et al. (2006)** assumed linearity of β and γ so that γ could be diagnosed by subtracting the β effect from fully coupled runs. As a result of our analysis in **Gregory et al. (2009)** I proposed that for CMIP5 (Taylor et al., 2012) an extra uncoupled simulation was performed so that β and γ could both be isolated and not need to be reconstructed. Following our recommendation from **Gregory et al. (2009)** these were named according to which process was *coupled*, rather that which process was *uncoupled*. Accordingly, “biogeochemical coupled” simulations

(BGC) measure the β term and "radiatively coupled" (RAD) simulations measure the γ term (see Glossary). **Arora et al. (2013)** used these simulations to diagnose β and γ from CMIP5 simulations.

However, in **Schwinger et al. (2014)** we demonstrated that due to non-linearities in the system, especially strong in the ocean, these approaches give different results for γ. For the ocean, the effect of climate on its own (with the carbon cycle experiencing constant pre-industrial CO_2) is to reduce ocean carbon storage and outgas CO_2, but this is a fairly slow process as the warming has to penetrate to deep ocean levels. However, when climate changes in parallel to CO_2 rise, the effect of climate is to inhibit the uptake of new carbon. This inhibition acts more quickly via surface ocean temperature and circulation and hence the climate change has a much bigger effect. In other words, it is easier to reduce uptake of new carbon than to cause the ocean to release existing carbon. Therefore, γ measured as the difference between BGC and fully coupled simulations is significantly bigger than γ measured from a single RAD simulation.

Hence neither the β nor γ values derived from CMIP5 models by **Arora et al. (2013)** are directly comparable to that from **Friedlingstein et al. (2006)**. The β values are not comparable because β is particularly sensitive to the rate of change of CO_2 in the scenario and CMIP5 used a (faster) 1% CO_2 rise compared to the SRES-A2 scenario used by **Friedlingstein et al. (2006)**. The γ values are not comparable because they use different methods and therefore diagnose different quantities (RAD vs COU-BGC respectively). This effect plays a role in the fact that CMIP5 diagnosed β and γ values were systematically smaller than seen in C4MIP. As an IPCC lead author, I wrote the section of AR5 carbon cycle chapter (**Ciais et al., 2013**) which assessed the implications of these results (see section 3.2). Randerson et al. (2015) show the importance of timescales, and how these interact with ocean inertia, concluding that over multiple centuries the ocean plays an increasingly important contribution to the global carbon cycle response.

In light of this, I recognised that the latter definition (defining γ from COU-BGC simulations) is more appropriate as it measures the impact of climate in a situation where CO_2 is rising – this is the sensitivity which we want to know. In the real world,

CO_2 is rising and causing an ocean sink of carbon and we want to know what impact climate change may have on this sink. Hence for the next generation of C4MIP (**Jones et al., 2016a**; and chapter 2.3 of this thesis) I recommend going back to the original definition of γ as being diagnosed between COU – BGC simulations.

3.2. My contribution to the IPCC Fifth Assessment Report

From 2011 to 2013 I was a lead author for the writing of the carbon cycle chapter of the IPCC 5th Assessment Report (AR5). The carbon cycle chapter (**chapter 6 of Working Group 1; Ciais et al., 2013**) comprised several sections, and my role was to lead the assessment of section 6.4 on "Projections of future carbon and other biogeochemical cycles". I performed much of the analysis and writing in that section and designed and produced many of the figures. Here I present how my analysis of coupled climate carbon cycle models contributed to the IPCC AR5 Carbon cycle chapter. Figure and table numbers cited here refer to those from the AR5 WG1 (**Chapter 6; Ciais et al., 2013**). Fellow lead author Laurent Bopp contributed most of the expertise on ocean carbon cycle results, so here I focus mainly on the terrestrial carbon cycle assessment which I led. Some quotes are also taken from the chapter executive summary which highlight the contributions made by carbon cycle modelling to the key IPCC conclusions.

For the first time the IPCC WG1 carbon cycle chapter had a section devoted to the feedbacks and future projections from coupled carbon cycle ESMs. The section begins with an overview of biogeochemical feedbacks assessed from across the literature. To create Figure 6.20 (reproduced here in Figure 6), I compiled a synthesis of these and showed the carbon cycle response to climate and CO_2 were the largest and most uncertain components. I then compiled results to compare carbon cycle feedbacks between C4MIP generations and this revealed some interesting features (figure 6.21, reproduced here in Figure 7): notably the mean response of both land and ocean to both CO_2 and climate were all smaller in CMIP5 than from **Friedlingstein et al. (2006)**.

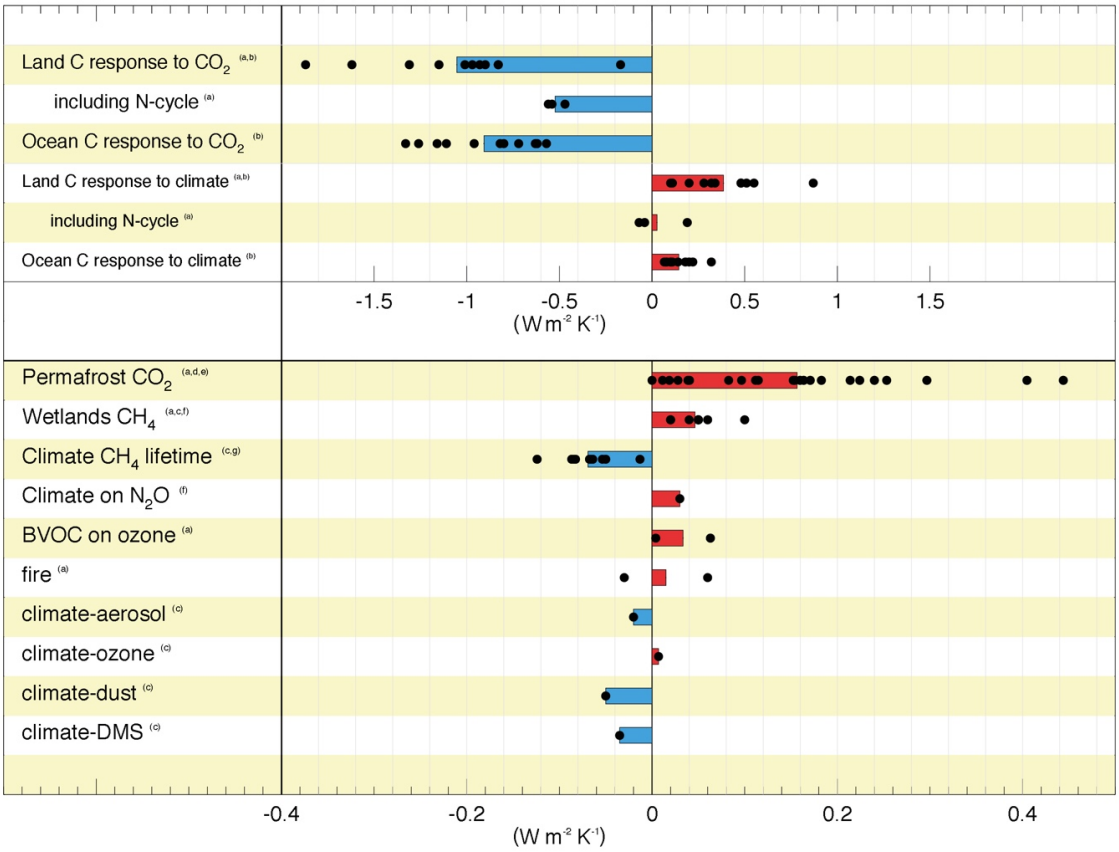

Figure 6. A synthesis of biogeochemical feedbacks with climate. Based on the quantification techniques derived in **Gregory et al. (2009)** applied to CMIP5 models and also drawing on the review by Arneth et al. (2009). Reproduced from IPCC AR5 figure 6.20.

Differences in experimental design and the rate of change of forcing in the scenario used make inferences from this result inconclusive (see discussion in section 3.1). Additionally, the small but differing sample of models also makes reliable comparison difficult between different generations of C4MIP simulations – with the exception of two outliers (UMD and HadCM3LC) in C4MIP and the models with terrestrial nitrogen cycle in CMIP5, the land response was not substantially different (Figure 7). This underlines the need for systematic diagnosis of feedback metrics in a common experimental framework.

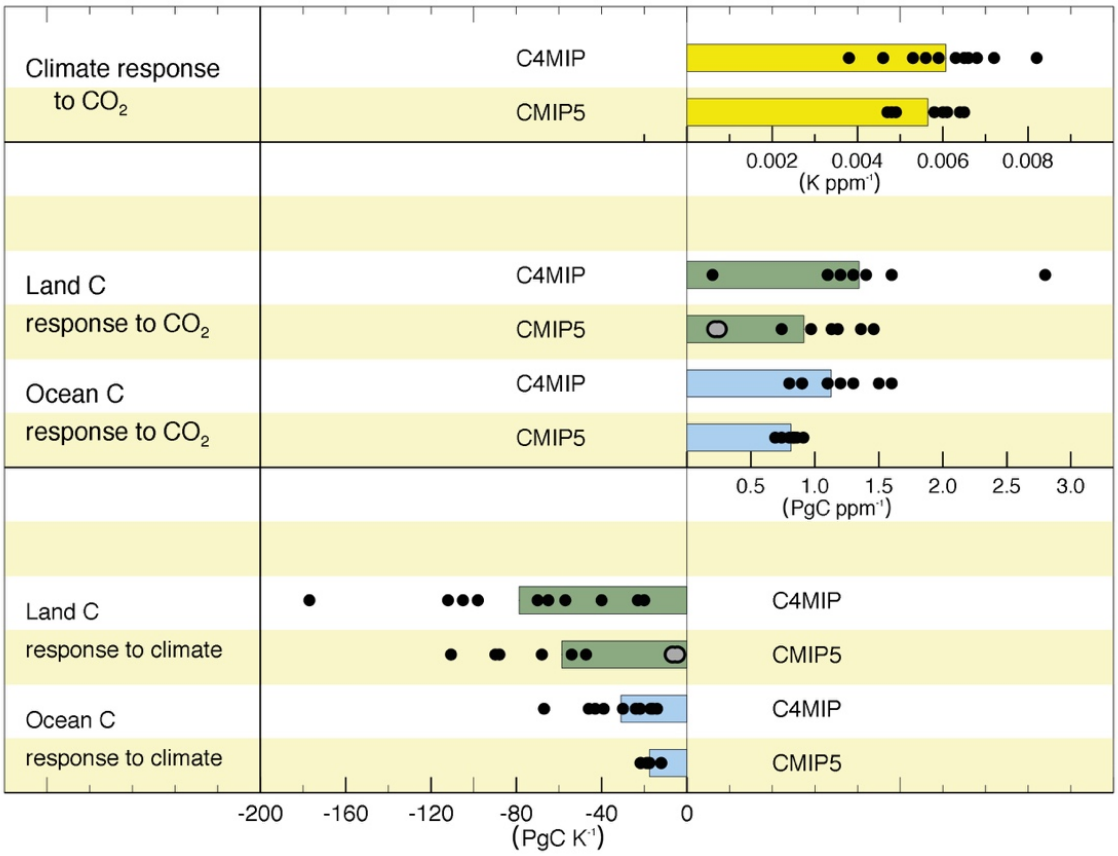

Figure 7. Summary of carbon cycle feedback metrics from C4MIP (**Friedlingstein et al., 2006**) and CMIP5 models. Reproduced from IPCC AR5 figure 6.21.

Building on the analysis of Roy et al. (2011) I helped create spatial maps of land and ocean sensitivities (figure 6.22, reproduced here in Figure 8) showing general consensus of positive β values everywhere, but changes in the sign of γ_{Land} towards high latitudes. All models simulate global aggregate γ_{Land} and γ_{Ocean} to be negative (i.e. reduced carbon storage in response to warmer climate). However, most terrestrial models simulated positive γ_{Land} (i.e. increased carbon storage in a warmer climate) at high latitudes as enhanced growth in temperature limited ecosystems outpaced enhanced turnover of soil organic carbon. The inclusion of nitrogen cycling and permafrost however may change these results in future.

> "There is *high confidence* that climate change will partially offset increases in global land and ocean carbon sinks caused by rising atmospheric CO_2." [Ch.6, Executive Summary]

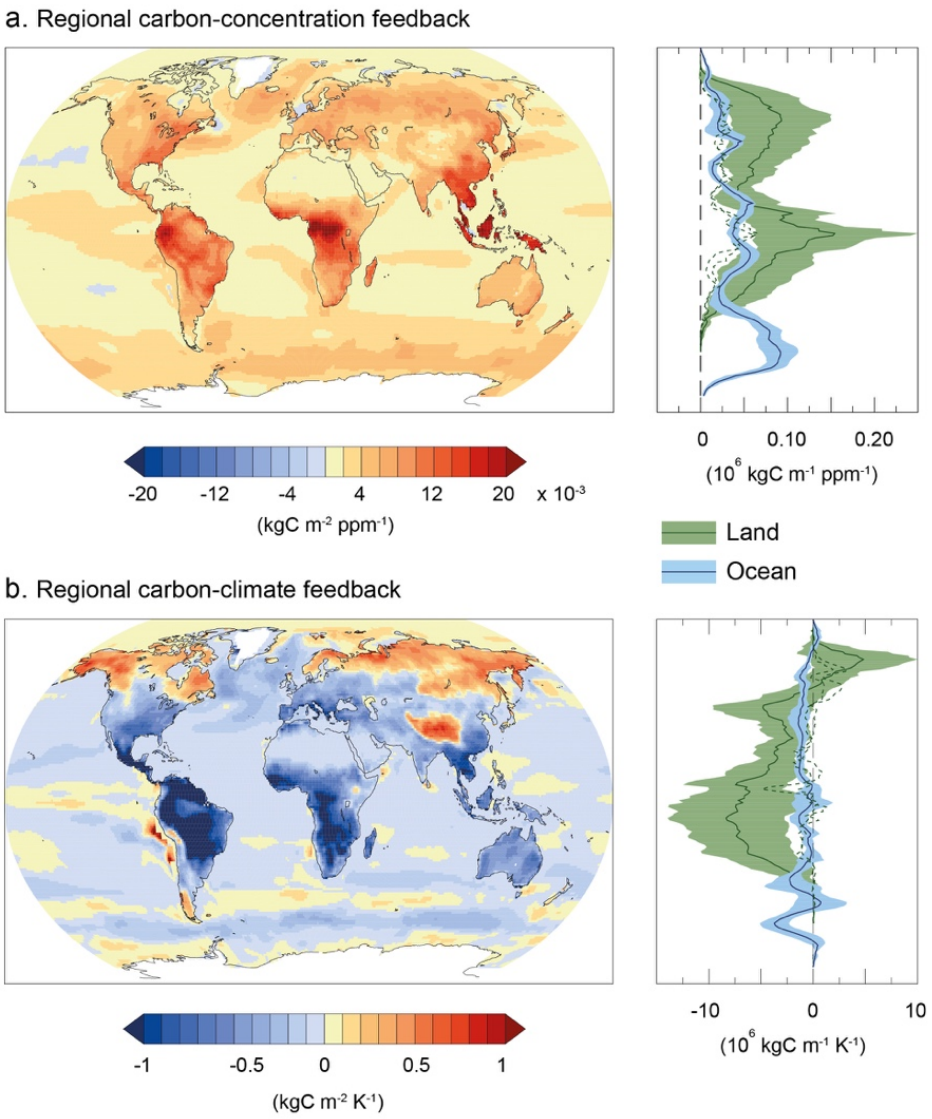

Figure 8. Global maps of CMIP5-simulated sensitivity to CO_2 (β: top panel) and to climate (γ: bottom panel). Because β and γ can be treated as additive in the linear feedback framework, results can be analysed at the level of individual gridboxes. Reproduced from IPCC AR5 figure 6.22.

I processed and compiled CMIP5 historical land and ocean simulations which showed considerable spread (figure 6.24, reproduced here in Figure 9). CMIP5 multi-model mean carbon uptake since pre-industrial was projected as 10 PgC for land and 140 PgC for ocean which agrees well with 5±40 PgC and 140±25 PgC respectively from historical estimates (IPCC AR5 table 6.12). Projections into the future showed reasonable levels of consensus for ocean carbon uptake across models and scenarios, but a much wider uncertainty for land, with model-spread comparable in magnitude to scenario-spread.

> "With *very high confidence*, ocean carbon uptake of anthropogenic CO_2 emissions will continue under all four Representative Concentration Pathways (RCPs) through to 2100, with higher uptake corresponding to higher concentration pathways. The future evolution of the land carbon uptake is much more uncertain ..." [Ch.6, Executive Summary]

As a result of this I set up a secondment at the Met Office to perform an ANOVA analysis ("**an**alysis **o**f **va**riance") of the sources of inter-model spread (**Hewitt et al., 2016**). This analysis showed that especially on land, the uncertainty is dominated by model differences whereas in the ocean it is dominated by the spread across different scenarios.

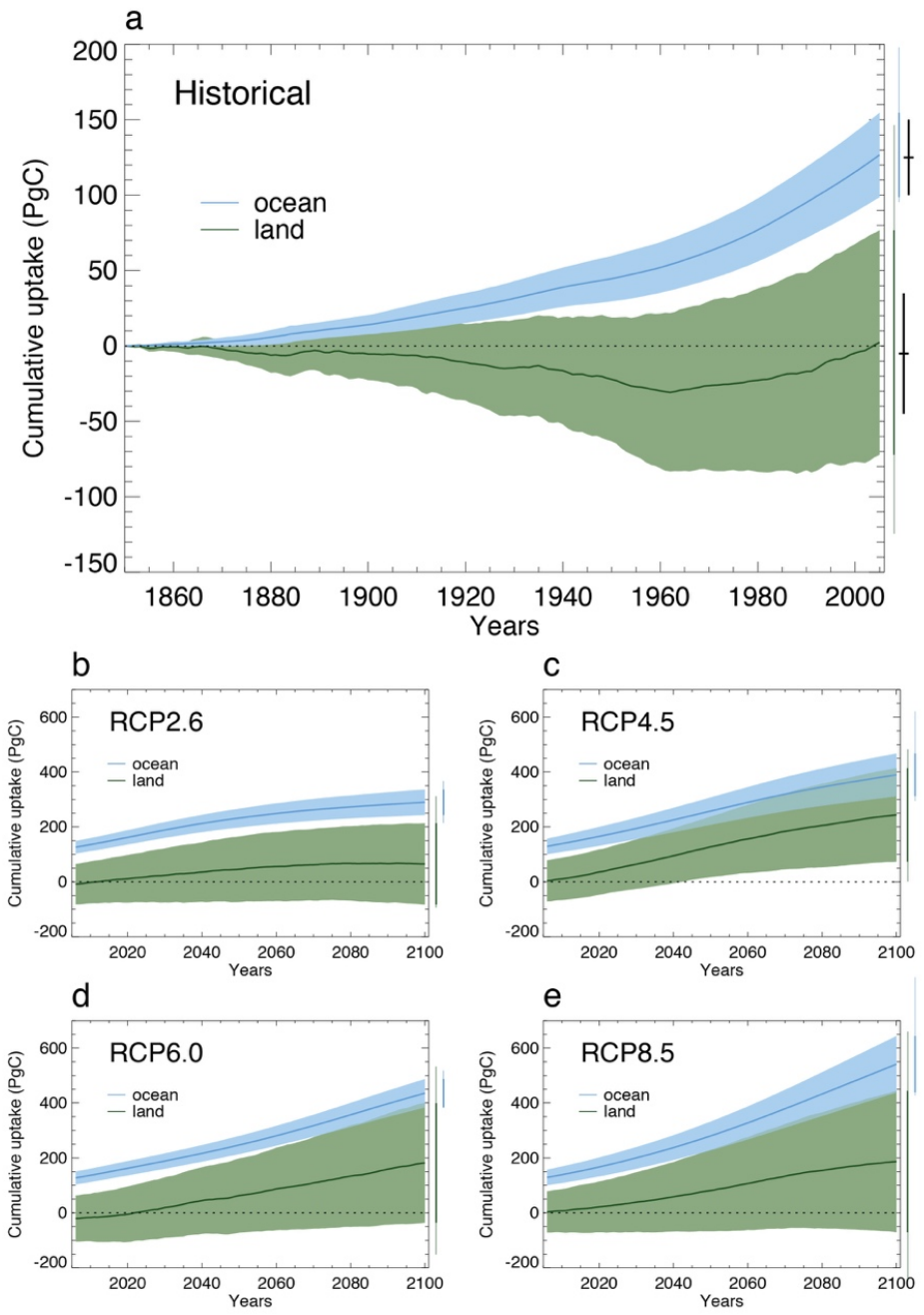

Figure 9. CMIP5 multi-model mean projections of cumulative carbon uptake by land (green) and ocean (blue). The top panel shows simulated results since pre-industrial (defined here as 1850). Panels b-e show results up to 2100 from the four RCP scenarios (see Glossary). Standard deviation of model results and full model range are shown in green and blue bars on the right-hand side of each panel. Black bars on panel (a) denote the estimated equivalent real-world uptake up to 2005. Reproduced from IPCC AR5 figure 6.24.

The most important aspect of the projections was to infer the fossil fuel emissions required to achieve certain prescribed CO_2 trajectories – so called “compatible

emissions" (**Jones et al., 2013**). In 2006 I first established the concept of "compatible" or "permissible emissions" - see section 4.2 of this thesis for a complete description of this technique. For IPCC AR5, I repeated this analysis for CMIP5 models for the four Representative Concentration Pathways (RCPs – see Glossary) in order to quantify emissions reductions to meet climate targets.

> "Taking climate and carbon cycle feedbacks into account, we can quantify the fossil fuel emissions compatible with the RCPs. .... For RCP2.6, an average 50% (range 14 to 96%) emission reduction is required by 2050 relative to 1990 levels." [Ch.6, Executive Summary]

Uncertainties and missing processes

My contribution to the IPCC AR5 carbon cycle chapter then went on to consider some processes which are not commonly represented in CMIP5 ESMs.

Nitrogen cycle. Nutrient availability, especially of nitrogen, plays an important role in moderating the amount of carbon which can be stored in biomass and soils. Future changes in climate and deposition of reactive nitrogen from human activity will both alter the amount of available nitrogen for plant growth but this was not represented in most ESMs participating in CMIP5. The two models which do incorporate treatment of this process (CESM1-BGC and NorESM-ME which both do so by using the CLM4 land surface model) show clearly much smaller sensitivity to both climate and CO_2 (grey dots in Figure 7). N-limitation reduces the ability of plants to benefit from elevated CO_2 (reduced β), but climate enhances N mineralization and may stimulate plant growth in N-limited systems (reducing the magnitude of γ, and of the positive climate-carbon cycle feedback) (Denman et al., 2007). I suggested and co-designed the analysis at a gridpoint level (**Zaehle et al., 2015**) which quantified the reduction in possible land carbon storage calculated as a result (figure 6.35, reproduced here in Figure 10). A similar analysis by Weider et al. (2015) came to similar conclusions. Across all scenarios, when accounting for inferred N-limitation, the CMIP5 mean land carbon uptake was reduced by 100-200 PgC.

"It is very likely, based on new experimental results {6.4.6.3} and modelling, that nutrient shortage will limit the effect of rising atmospheric CO_2 on future land carbon sinks" [Ch.6, Executive Summary]

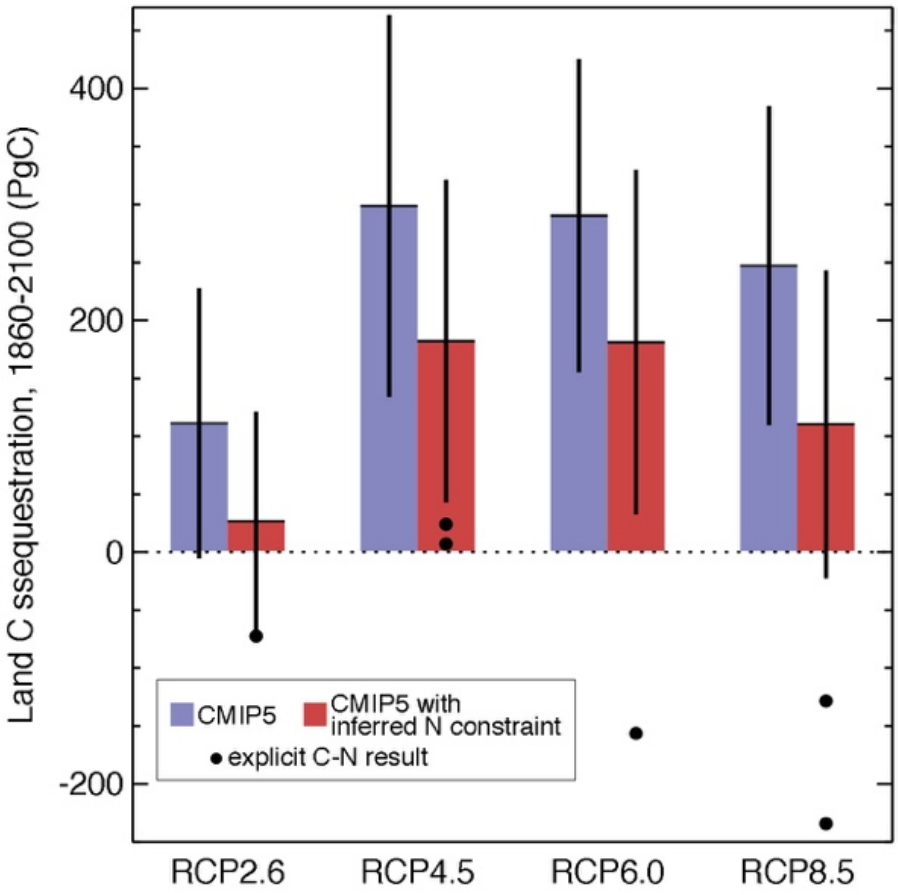

Figure 10. Land carbon sink up to 2100 simulated by CMIP5 models for each of the four RCP scenarios. Blue bars denote the land carbon uptake simulated directly by the models, while the red bars denote the uptake that can occur once the requirement for additional nitrogen has been accounted for. Reproduced from IPCC AR5 figure 6.35.

Permafrost. Northern permafrost-affected soils contain 1100-1700 PgC (**Ciais et al., 2013**; Hugelius et al. 2014), which is stabilized by being frozen and is thus vulnerable to decomposition with warming. None of the models in either C4MIP or CMIP5 considered the dynamics of carbon in permafrost layers, and thus may systematically underestimate the potential carbon loss. The timing and magnitude of eventual carbon losses, and whether the carbon is lost as CO_2 or CH_4, are highly uncertain and depend on the decomposition rate of thawed carbon, whether thawing

soils become wetter or drier upon thawing and nitrogen dynamics of permafrost soils (**Burke et al., 2013;** Koven et al., 2015; Schuur et al., 2015).

> "There is *high confidence* that reductions in permafrost extent due to warming will cause thawing of some currently frozen carbon. However, there is *low confidence* on the magnitude of carbon losses through CO_2 and CH_4 emissions to the atmosphere" [Ch.6, Executive Summary]

Vegetation dynamics and committed changes. Although anthropogenic land use change is commonly accepted as a primary driver of terrestrial carbon cycle changes, natural vegetation dynamics are not often represented in ESMs. Only two GCMs in the original C4MIP (**Friedlingstein et al., 2006**) and three in CMIP5 simulated the time evolution of the fractional coverage of vegetation types. I designed the analysis which we published in **Davies-Barnard et al. (2015)** that showed, however, the effect on carbon storage is comparable between land cover change induced by climate-change and that due to land-use-change. A specific issue is that of timescales – ecosystems may respond quickly in terms of carbon fluxes but only very slowly in terms of their species composition (Smith and Shugart, 1993). The model I helped develop in the late 1990s, HadCM3LC, did include vegetation dynamics and in **Jones et al. (2009)** I first introduced the concept of "committed ecosystem changes" showing how ecosystems may continue to respond for many decades after climate stabilisation (see section 4.1 for more details). My analysis for IPCC AR5 showed that CMIP5 models exhibited substantial post-2100 changes, especially in high-latitude ecosystems.

> "Long-term changes in vegetation structure and induced carbon storage potentially show larger changes beyond 2100 than during the 21st century as the long time scale response of tree growth and ecosystem migrations means that by 2100 only a part of the eventual committed change will be realized" [Ch.6, section 6.4.9, figure 6.38]

Vegetation dynamics are crucial also for simulating biophysical as well as biogeochemical (carbon storage) effects, as these direct changes to the land surface properties can be as important for local climate as the carbon stored or released (de Noblet et al. 2012; **Davies-Barnard et al., 2014**; **Brovkin et al., 2013**).

4. Model applications to inform mitigation policy

4.1. Committed impacts on ecosystems

Components of the Earth System affected by climate change will respond on timescales from seconds or minutes (such as clouds or plant stomata response to changes in light, vapour pressure deficit or temperature) to centuries or millennia (such as ice sheets or thermal expansion of the deep ocean). For some components, these timescales are slower than the current rate of climate change and hence the system response lags behind the degree of global warming. Thus, when the climate is stabilised these systems are not yet in equilibrium and continue to respond into the future. The long-term committed changes of physical components such as sea level rise and ice sheet melt, which have timescales of many decades or centuries, have been studied (Wigley, 1995; Gregory et al., 2006). Ecosystems have been less studied in this respect but it is likely that they also exhibit slow timescales and therefore long-term commitments.

In my paper in 2009 (**Jones et al., 2009**) which forms the rest of this section, I used a coupled climate–vegetation model to show that the global terrestrial biosphere continues to change for decades after climate stabilisation and may even be committed to long-term change before any response is observable. The paper focusses on a case-study of the Amazon forest and finds that the risk of significant loss of forest cover in Amazonia rises rapidly for a global mean temperature rise above 2^{o}C.

Ecosystem commitments do not just include dieback. A warmer future climate may enable northward expansion of the Boreal forest into present tundra regions (Scholze et al., 2006; **Sitch et al., 2008**) as it has done in past, warmer climates (Foley et al., 1994; Macdonald et al., 2008). My paper also showed significant committed increases in high-latitude tree cover following climate stabilisation at 2^{o}C. In this case, although the eventual changes are large, the *realised* changes at the time of first reaching 2^{o}C are small because the timescale of forest response is many centuries.

In a News and Views review of the paper, published in Nature Geoscience, Plattner (2009) said, “Jones and colleagues have demonstrated that committed ecosystem changes can be large and will need to be taken into account, for example, when projecting regional climate change, assessing dangerous levels of climate change or discussing future mitigation policies.”

Given that large-scale changes in ecosystem extent inevitably have a long timescale to fully adjust to a changed climate, the concept of ecosystem commitments is robust although the magnitude and even sign of commitment will vary regionally and between models. This has significant implications for both ecosystem services and terrestrial carbon storage. The conclusion is that such committed ecosystem changes must be considered in the definition of dangerous climate change, and subsequent policy development to avoid it.

nature geoscience

LETTERS

PUBLISHED ONLINE: 28 JUNE 2009 | DOI: 10.1038/NGEO555

Committed terrestrial ecosystem changes due to climate change

Chris Jones*, Jason Lowe, Spencer Liddicoat and Richard Betts

Targets for stabilizing climate change are often based on considerations of the impacts of different levels of global warming, usually assessing the time of reaching a particular level of warming. However, some aspects of the Earth system, such as global mean temperatures[1] and sea level rise due to thermal expansion[2] or the melting of large ice sheets[3], continue to respond long after the stabilization of radiative forcing. Here we use a coupled climate–vegetation model to show that in turn the terrestrial biosphere shows significant inertia in its response to climate change. We demonstrate that the global terrestrial biosphere can continue to change for decades after climate stabilization. We suggest that ecosystems can be committed to long-term change long before any response is observable: for example, we find that the risk of significant loss of forest cover in Amazonia rises rapidly for a global mean temperature rise above 2 °C. We conclude that such committed ecosystem changes must be considered in the definition of dangerous climate change, and subsequent policy development to avoid it.

Future climate change and the carbon cycle are tightly coupled[4]. Many studies (such as refs 5, 6) have now shown positive feedbacks that amplify climate change, reduce the natural uptake of carbon and influence global emissions pathways to stabilization[7,8]. On the timescale of 1 or 2 centuries, the contribution to this feedback is likely to be greater from the terrestrial biosphere than from the ocean carbon cycle[6]. Rising temperature enhances soil decomposition and together with reductions in rainfall, may also reduce plant productivity in large regions. Changes in climate may also alter the important biomes—especially tropical and boreal forests[9]. Climate impacts are often summarized for policy makers as a table of impact magnitude against global mean warming (for example, the Stern Review[10]). However, a significant limitation is that some of the impacts are taken from model simulations at the instant the temperature is reached, and fail to account for subsequent impacts as slowly responding parts of the system fully respond to the given change.

The increase in global mean temperature due to increasing greenhouse gas concentrations lags behind the radiative forcing that causes it because of the thermal inertia of the system[1]. For present-day climate, this committed rise has been predicted to be between 0.25 and 0.5 °C (ref. 11). Other components of the climate system also show committed change. Sea level rise from thermal expansion seems likely to increase for several centuries to millennia following stabilization of radiative forcing[2,11], and the contribution to sea level rise from melting of the Greenland ice sheet is also likely to continue long after radiative forcing is stabilized[3,12]. Terrestrial ecosystems might also show committed change behaviour following stabilization of forcing because changes in both vegetation cover and carbon storage are likely to lag behind that of temperature and rainfall. Hence, we introduce the new concept of committed ecosystem change and examine the extent to which biomes may be committed to significant changes in response to climate forcing before they can be observed.

The Intergovernmental Panel on Climate Change Second Assessment Report noted that climate change is expected at a rapid rate compared with forest ecosystem timescales[13] but neither subsequent IPCC Assessment reports nor the published literature have discussed the implications of this statement in terms of committed changes to important ecosystems. We present examples from the Amazon and boreal forests to show how important such committed changes may be.

The Met Office Hadley Centre climate carbon cycle model, HadCM3LC, is one of only a few coupled general circulation model (GCM)–dynamic vegetation models. Previous analysis[14,15] has examined the large-scale loss of Amazon forest simulated by this model in response to transient scenarios of climate change. Other studies that examined tropical ecosystem response under climate change simulations from a range of climate models[16,17] and using a range of vegetation models (some with a greater degree of species diversity)[9] also showed reductions in tropical forest cover, especially in Amazonia. Observational studies have also shown the vulnerability of the Amazon forest to drought[18]. Although HadCM3LC produces greater regional climate change and die-back than some offline model studies, other models do project changes that, although less extreme, are qualitatively similar[9] (see Supplementary Information). All of these studies, however, have focused on the period of changing forcing rather than behaviour subsequent to stabilization. We study here the long-term committed changes (see the Methods section and Supplementary Information).

Figure 1 shows a comparison of the realized and committed vegetation cover in a region of the Amazon forest (we consider the region of land within the area defined by 40° W–70° W and 15° S–5° N, as shown in Fig. 2). Figure 1a shows fractional forest cover in this region as it changes in time. Figure 1b shows the same data but shown as degree of die-back plotted against global mean temperature above pre-industrial. It is clear that the forest cover in the equilibrium simulations (dashed line) is significantly lower than the dynamic state. This indicates that at any time the forest is showing only a portion of the level of die-back it will eventually reach. For example, by 2050 when die-back begins to be observed in the transient simulation, the forest is already committed to eventually losing 50% of its area even without further increases in forcing (Fig. 2). This is roughly the same loss as seen in the transient simulations, with increasing forcing, by 2100 (Fig. 1). By 2100, even though only a third of tree cover has gone, the forest is committed to almost complete loss in this region. The solid line can be considered as the impact when a particular level of warming is first reached. The dashed line is the eventual impact after warming is sustained at the stabilization temperature for a long period of time.

Met Office Hadley Centre, Exeter EX1 3PB, UK. *e-mail: chris.d.jones@metoffice.gov.uk.

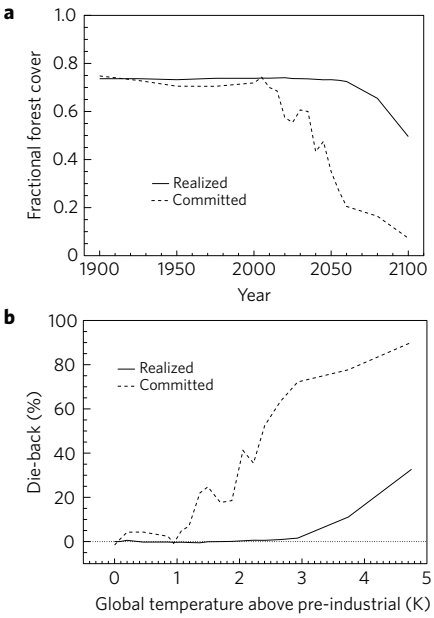

Figure 1 | Dynamic and equilibrium Amazon forest extent throughout the simulations. a, Fractional tree cover (represented as fractional coverage of broadleaf trees in the region 40°–70° W, 15° S–5° N) as it evolves dynamically through the SRES A2 simulation and the committed state corresponding to each year. **b**, The same information plotted as the percentage of complete die-back as a function of global mean temperature rise above pre-industrial (defined as 0 for the original, pre-industrial forest cover, and 100 for complete loss of tree cover in this region).

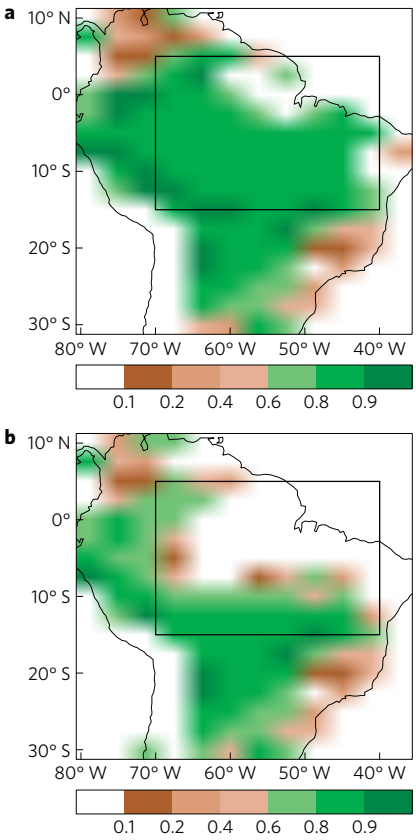

Figure 2 | Geographical distribution of Amazon forest tree cover at 2050. **a**,**b**, Realized (**a**) and committed (**b**) states represented as fractional coverage of broadleaf trees simulated by the model. The black rectangle shows the region used for calculating mean forest cover.

There seems to be a temperature below which the equilibrium state of the forest is approximately constant, but above which the equilibrium forest cover declines steadily with changing climate. This point could be seen as a threshold beyond which some degree of loss of Amazon forest is inevitable. Beyond this point there is no sudden transition from 'forest' to 'no forest', rather a gradual increase in the level of future committed die-back: the impacts are more progressive than sudden.

Our results also show that the forest may be committed to some degree of die-back before any is observed. For example, if climate forcing was stabilized at 2050, when tree cover fraction is virtually unchanged from the present day, a significant die-back would still occur subsequently over the next 100–200 years (see Supplementary Fig. S3). This has serious implications for any definition of dangerous climate change, as it means that stabilization of climate does not necessarily mean stabilization of climate impacts. It may not become apparent for some time when a threshold of committed change has been passed.

A further aspect of such committed changes is to consider the potential of the system to recover. Experiments to assess recovery of ecosystems under a return to pre-industrial global climate showed that forests did indeed have the potential for recovery but only on very long (multi-century) timescales (see Supplementary Information). This has implications for temperature-overshoot scenarios. First, from an impacts perspective, once the full change in forest cover has been achieved, the length of time that society has to exist without the forest may be so long that the change is, for practical purposes, irreversible. Second, as the amount of forest cover feeds back on to global atmospheric CO_2 concentration, the long recovery implies that the slow regrowth will make it more difficult to lower CO_2 concentrations and make it more difficult to approach a safe level of CO_2 and warming from above[19].

The concept of committed ecosystem changes applies equally to other biomes and to forest expansion as well as die-back although the response/lag times and impact on carbon storage might be different[20,21]. Figure 3 shows equivalent results for the boreal forest. Using tree cover between 45° and 80° N as a simple measure of northern latitude forest expanse, the dynamic solution shows a steady, but slow, increase in coverage up to the year 2100. Much of this is an intensification of tree cover in existing areas of forest, which occurs more rapidly than an expansion of the treeline. By 2100 we also see a northward expansion of forest cover. The committed state shows much greater expansion, by more than a factor of 3, by 2100. The large difference between realized and committed expansion is due to the slow timescales of areal changes.

The boreal forest region is expected to experience greater than average warming over the twenty-first century[22] and is a region where tree growth is generally more limited by temperature than precipitation. As most GCMs agree qualitatively on warming across high-latitude land areas, it may be expected that results here are more robust across different models (see further discussion in Supplementary Information). Boreal forest expansion has also been seen in other vegetation models[9] and in response to other climate models[16]. Pollen records and tree mortality observations indicate that previous warm periods in the mid-Holocene and medieval warm period did experience greater northward extent of boreal forest[23].

Considering long-timescale changes in ecosystems also has implications for multi-gas mitigation policies owing to the direct physiological effect of CO_2 on vegetation[24]. As ecosystems are also responding to changes in CO_2 concentration, future ecosystem commitments will probably depend not only on the stabilization of radiative forcing, but also the relative contribution of CO_2 and non-CO_2 greenhouse gas mitigation measures. For a given radiative

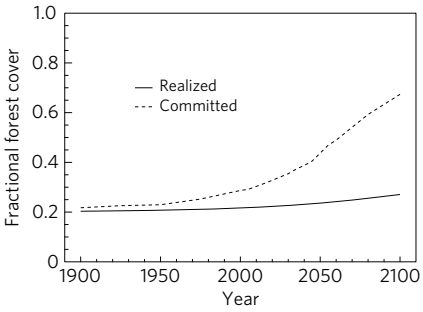

Figure 3 | Dynamic and equilibrium boreal forest extent throughout the simulations. The solid line shows the fractional tree cover (represented as fractional land coverage of both broadleaf and needleleaf trees in the region 45°–80° N) as it evolves dynamically through the SRES A2 simulation and the dashed line shows the committed state corresponding to each year.

forcing, CO_2 and non-CO_2 gases can lead to very different impacts on ecosystems[24]. Elevated CO_2 levels may aid forest resilience (for example, through improved water use efficiency[25]), implying that non-CO_2 reductions may be more effective at reducing committed ecosystem damage. However, quantifying this effect requires much more research. There are also implications for forestry practices, as degraded forest further compounds the risk of committed loss owing to increased vulnerability to fires following disturbance[26].

We have introduced the implications of the hitherto unconsidered application of the concept of committed changes to the terrestrial ecosystem. Although these results are from a single model and hence subject to quantitative uncertainty, we believe the concept of committed changes in the terrestrial biosphere is likely to be robust. The terrestrial biosphere can respond slowly to large, regional-scale forcing, but may not always be in equilibrium with that forcing at any point in time, leading to subsequent commitments to significant future change for decades or centuries following stabilization of forcing. There is a threshold beyond which some die-back is committed and this commitment rises markedly for greater global temperature rise. In our model this threshold is below 2 °C, a threshold often used by policy makers in their definition of dangerous climate change[27], although the quantitative nature of our results carries significant uncertainty. Any subsequent recovery is on such a long timescale as to make the die-back effectively irreversible on human timescales of the next 1–2 centuries.

There has been little or no discussion within the climate or ecosystem research communities on the concept of commitments to ecosystem change due to climate change. Our intention is to draw attention to committed ecosystem changes as an issue requiring serious consideration, and one that requires study with more than a single model. With increasing policy focus on climate mitigation and stabilization of climate change, quantifying such committed changes will make valuable contributions to our understanding of dangerous climate change, and to aiding development of mitigation policies. We argue that committed ecosystem changes, in addition to realized changes, should be considered in any definition of dangerous climate change. Weighing the cost of emissions reductions against the cost of climate damage may lead to very different conclusions for terrestrial ecosystems if committed ecosystem changes are considered in preference to the usual transient response.

Methods

HadCM3LC is a coupled climate/carbon cycle GCM including a dynamic vegetation model. It is able to reproduce many aspects of observed change such as the twentieth-century temperature and CO_2 record[28], observed sensitivity of CO_2 to El Nino and large volcanic eruptions[29]. We base our experiments here on the coupled HadCM3LC transient CO_2-only simulation of C4MIP (ref. 6). This experiment enables us to assess the transient response of ecosystems to the business-as-usual SRES A2 emissions scenario[30]. The changes throughout this experiment give us a projection of the state of the biosphere at any given time during the simulation. We will refer to such a state as the 'dynamic' or 'realized' state—that is, the state that occurs at a point in time as the system evolves but is not necessarily in steady state or in equilibrium with ambient climate or CO_2 levels. Owing to long timescales of response of vegetation, we use an accelerated equilibration technique (see Supplementary Methods) to determine the eventual biosphere state if the forcing was held constant at a given point in time. We will refer to this as the 'equilibrium' or 'committed' state. The difference between the two is therefore a measure of the un-realized but committed change.

Received 16 January 2009; accepted 26 May 2009; published online 28 June 2009

References

1. Hare, B. & Meinshausen, M. How much warming are we committed to and how much can be avoided? *Clim. Change* **75**, 111–149 (2006).
2. Wigley, T. M. L. Global mean-temperature and sea level consequences of greenhouse gas concentration stabilisation. *Geophys. Res. Lett.* **22**, 45–48 (1995).
3. Gregory, J. M. & Huybrechts, P. Ice-sheet contributions to future sea-level change. *Phil. Trans. R. Soc. Lond.* **364**, 1709–1731 (2006).
4. Cox, P. M. & Jones, C. D. Illuminating the modern dance of climate and CO_2. *Science* **321**, 1642–1644 (2008).
5. Cox, P. M., Betts, R. A., Jones, C. D., Spall, S. A. & Totterdell, I. J. Acceleration of global warming due to carbon-cycle feedbacks in a coupled climate model. *Nature* **408**, 184–187 (2000).
6. Friedlingstein, P. *et al.* Climate-carbon cycle feedback analysis, results from the C4MIP model intercomparison. *J. Clim.* **19**, 3337–3353 (2006).
7. Jones, C. D., Cox, P. M. & Huntingford, C. in *Avoiding Dangerous Climate Change* (eds Schellnhuber, H. J., Cramer, W., Nakicenovic, N., Wigley, T. & Yohe, G.) (Cambridge Univ. Press, 2006).
8. Matthews, H. D. Decrease of emissions required to stabilize atmospheric CO_2 due to positive carbon cycle-climate feedbacks. *Geophys. Res. Lett.* **32**, L21707 (2005).
9. Sitch, S. *et al.* Evaluation of the terrestrial carbon cycle, future plant geography and climate-carbon cycle feedbacks using 5 Dynamic Global Vegetation Models (DGVMs). *Glob. Change Biol.* **14**, 2015–2039 (2008).
10. Stern, N. *Stern Review on the Economics of Climate Change* (Cambridge Univ. Press, 2006).
11. Wigley, T. M. L. The climate change commitment. *Science* **307**, 1766–1769 (2005).
12. Ridley, J. K., Huybrechts, P., Gregory, J. M. & Lowe, J. A. Elimination of the Greenland ice sheet in a high CO_2 climate. *J. Clim.* **18**, 3409–3427 (2005).
13. IPCC. *Contribution of Working Group II to the Second Assessment of the Intergovernmental Panel on Climate Change* (eds Watson, R. T., Zinyowera, M. C. & Moss R. H.) (Cambridge Univ. Press, 1996).
14. Cox, P. M. *et al.* Amazonian forest dieback under climate-carbon cycle projections for the 21st century. *Theor. Appl. Climatol.* **78**, 137–156 (2004).
15. Betts, R. A. *et al.* The role of ecosystem-atmosphere interactions in simulated Amazonian precipitation decrease and forest dieback under global climate warming. *Theor. Appl. Climatol.* **78**, 157–175 (2004).
16. Scholze, M., Knorr, W., Arnell, N. W. & Prentice, I. C. A climate-change risk analysis for world ecosystems. *Proc. Natl Acad. Sci. USA* **103**, 13116–13120 (2006).
17. Salazar, L. F., Nobre, C. A. & Oyama, M. D. Climate change consequences on the biome distribution in tropical South America. *Geophys. Res. Lett.* **34**, L09708 (2007).
18. Phillips, O. L. *et al.* Drought sensitivity of the Amazon rainforest. *Science* **323**, 1344–1347 (2009).
19. Lowe, J. A. *et al.* How difficult is it to recover from dangerous levels of global warming? *Environ. Res. Lett.* **4**, 014012 (2009).
20. Kohlmaier, G. H., Hager, C., Nadler, A., Wurth, G. & Ludeke, M. K. B. Global carbon dynamics of higher latitude forests during an anticipated climate change: Ecophysiological versus biome-migration view. *Wat. Air Soil Pollut.* **82**, 455–464 (1995).
21. Joos, F. *et al.* Global warming feedbacks on terrestrial carbon uptake under the Intergovernmental Panel on Climate Change (IPCC) emissions scenarios. *Glob. Biogeochem. Cycles* **15**, 891–907 (2001).
22. Ruckstuhl, K. E., Johnson, E. A. & Miyanishi, K. Introduction. The boreal forest and global change. *Phil. Trans. R. Soc. B* **363**, 2243–2247 (2008).
23. Macdonald, G. M., Kremenetski, K. V. & Beilman, D. W. Climate change and the northern Russian treeline zone. *Phil. Trans. R. Soc. B* **363**, 2283–2299 (2008).
24. Betts, R. A. *et al.* Future runoff changes due to climate and plant responses to increasing carbon dioxide. *Nature* **448**, 1037–1041 (2007).
25. Harrison, S. P. & Prentice, I. C. Climate and CO_2 controls on global vegetation distribution at the Last Glacial Maximum: Analysis based on palaeovegetation data, biome modelling and palaeoclimate simulations. *Glob. Change Biol.* **9**, 983–1004 (2003).

26. Golding, N. & Betts, R. A. Fire risk in Amazonia due to climate change in the HadCM3 climate model: Potential interactions with deforestation. *Glob. Biogeochem. Cycles* **22**, GB4007 (2008).
27. European Council. *Limiting Global Climate Change to* 2 °C—*The Way Ahead for 2020 and Beyond Communication from the Commission to the Council, the European Parliament, the European Economic and Social Committee and the Committee of the Regions* (2007).
28. Jones, C. D. *et al.* Strong carbon cycle feedbacks in a climate model with interactive CO_2 and sulphate aerosols. *Geophys. Res. Lett.* **30**, 1479 (2003).
29. Jones, C. D. & Cox, P. M. Constraints on the temperature sensitivity of global soil respiration from the observed interannual variability in atmospheric CO_2. *Atmos. Sci. Lett.* **2**, 166–172 (2001).
30. Nakićenović, N. *et al. Special Report on Emissions Scenarios* (Cambridge Univ. Press, 2000).

Acknowledgements

This work was supported by the Joint DECC, Defra and MoD Integrated Climate Programme—DECC/Defra (GA01101), MoD (CBC/2B/0417_Annex C5).

Author contributions

C.J. experiment design, analysis, C.J. and J.L. analysis and text, S.L. carried out model simulations, R.B. advice on design, analysis and text.

Additional information

Supplementary information accompanies this paper on www.nature.com/naturegeoscience. Reprints and permissions information is available online at http://npg.nature.com/reprintsandpermissions. Correspondence and requests for materials should be addressed to C.J.

nature geoscience
SUPPLEMENTARY INFORMATION
DOI: 10.1038/NGEO555

Supplementary Information

1. Methods

HadCM3LC experiments to assess the transient nature of climate change and feedbacks with the carbon cycle already exist, such as those contributed to the C4MIP intercomparison[1]. These give us a projection of the state of the biosphere at any given point in time during these simulations. We will refer to such a state as the "dynamic" or "realised" state – i.e. the state that occurs at a point in time. But of course, we do not know if the biosphere is in equilibrium with climate or CO_2 levels as these simulations evolve. Due to long timescales of response of vegetation, it is likely that a substantial lag exists and the biosphere is not in equilibrium with the climate. We want to be able to also diagnose what such an equilibrium would be at each point – i.e. what would the eventual biosphere state look like if the forcing was held constant at any stage. We will refer to this as the "equilibrium" or "committed" state.

The C4MIP 1860-2100 SRES A2 transient climate change simulation was taken as a baseline and then at 19 stages, as shown in figure S1, experiments were branched off with fixed CO_2 concentrations at each point to predict the equilibrium state of the terrestrial biosphere for that climate/CO_2 state. Using an efficient numerical spin-up technique[2], these experiments were able to reach this equilibrium after just 25 years of simulation each. At 2050 a dynamic simulation was also branched off for 200 years in order to both analyse the timescale of realising committed change and to test that it gave the same results as the accelerated equilibrium technique from the same point.

DOI: 10.1038/NGEO555

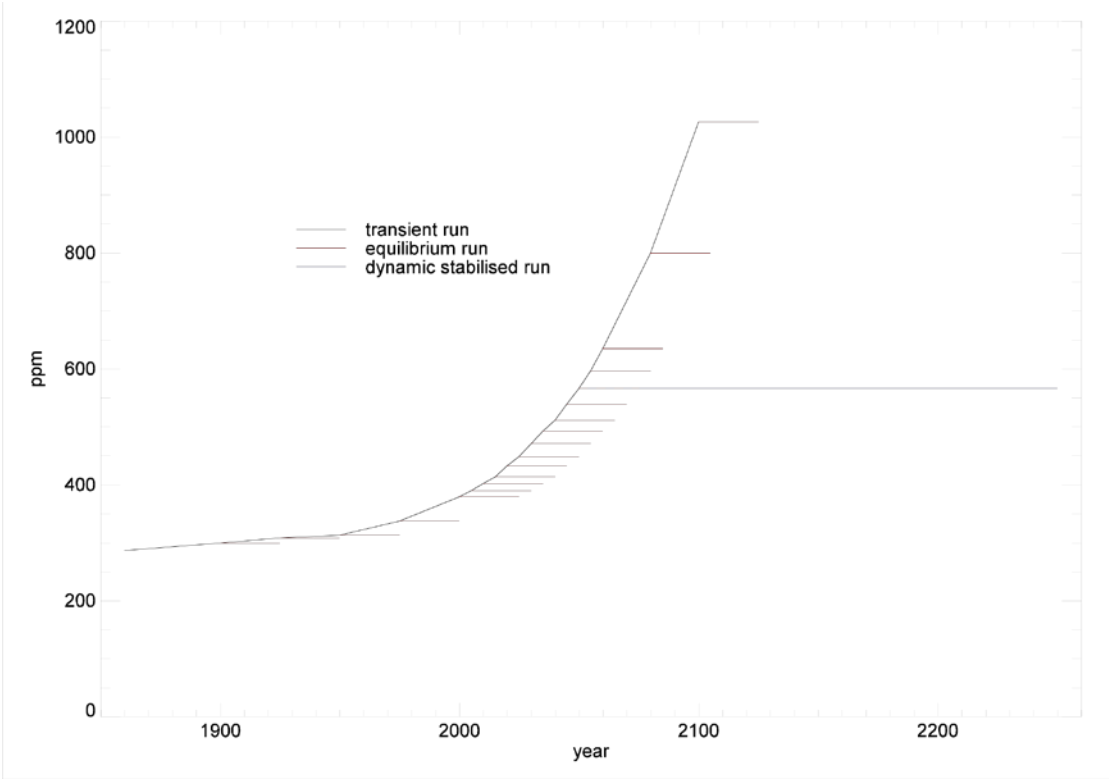

Figure S1. Schematic representation of experimental design. The black line represents the transient SRES A2 scenario from the C4MIP experiment, and the red lines denote short equilibrium simulations branched off from this at certain intervals. The blue line denotes a long, dynamic simulation at fixed CO_2 levels branched from the baseline simulation at 2050 in parallel to the equilibrium simulation from that point. The vertical axis represents atmospheric CO_2 concentration (ppm).

During each equilibrium simulation the atmosphere-ocean component of the GCM evolves in exactly the same way as for dynamic vegetation, but now the vegetation cover and terrestrial carbon pools are asynchronously coupled to the climate model so that they use accumulated fluxes over each 5-year climate period and then an implicit timestep allows a Newton-Raphson type of approach to equilibrium with that simulated climate[2]. Figure S2 shows this technique successfully reaches steady state in simulated vegetation cover and temperature. This approach damps the impact of inter-annual climate variability, but it cannot be completely removed. Figure S2(b) shows the Amazonian surface air temperature in the equilibrium simulations smoothed for display with a 5 year running mean. Simulations later in the 21st century are progressively warmer than earlier simulations but variability causes some degree

of overlap and this results in simulated vegetation cover not changing completely monotonically in time as shown in figure 3.

During the 25 year equilibrium simulations the local climate will respond to any changes in the vegetation cover, and thus the eventual state will not be just the equilibrium vegetation cover for the climate condition at the branched point, but will also include the vegetation response to any subsequent changes in local climate due to local biophysical feedbacks on albedo and the hydrological cycle[3].

DOI: 10.1038/NGEO555

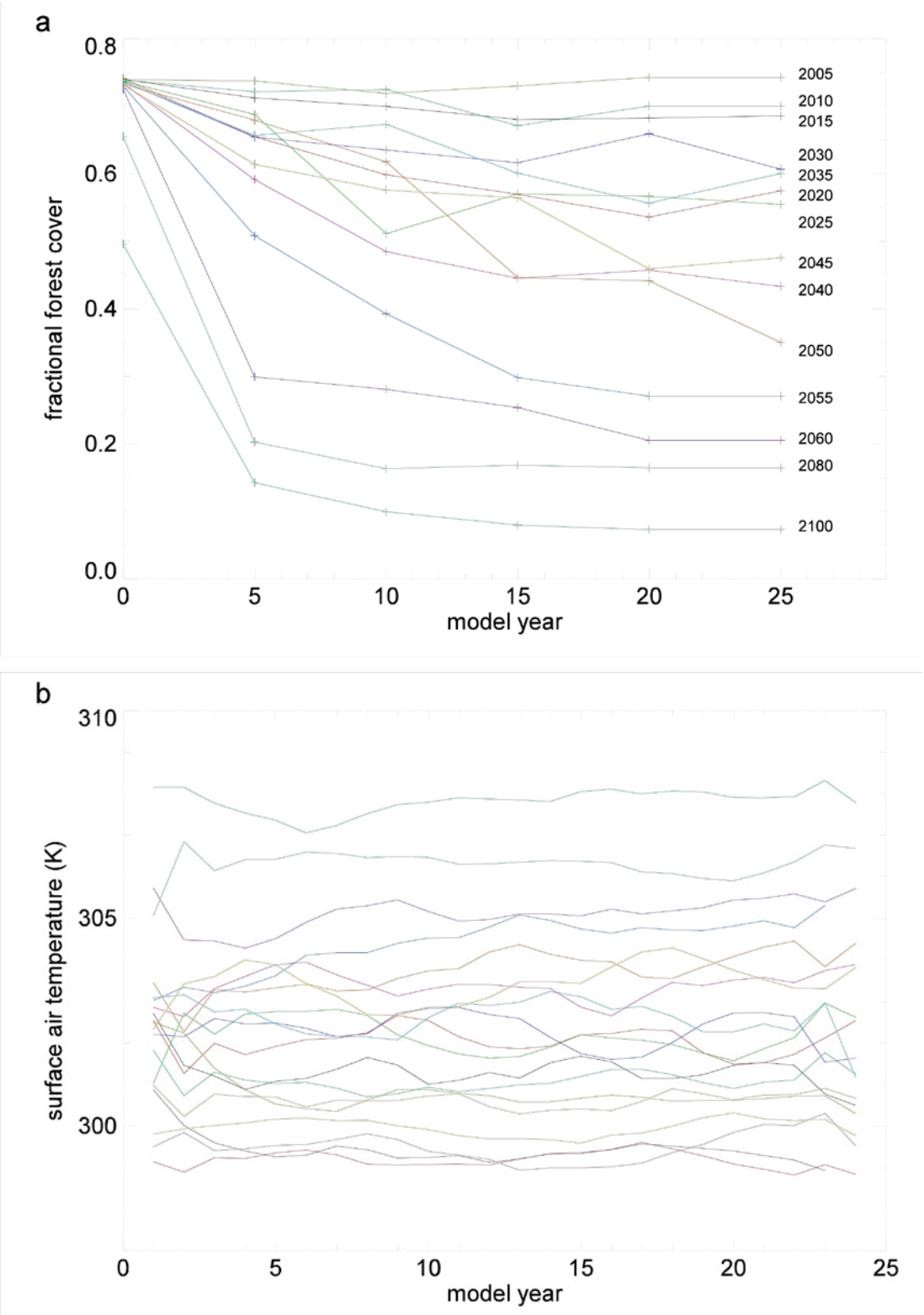

Figure S2. Evolution of model simulated quantities during each of the 25-year equilibrium simulations to determine the committed ecosystem state. (a) Amazonian forest cover, (b) surface air temperature. Both panels show results from the region 40-70^{o}W, 15^{o}S-5^{o}N. Data in panel (b) have been smoothed for display purposes with a 5-yr running mean due to interannual variability.

It may be expected that for each simulation branched off from a transient SRES A2 scenario there may be subsequent local changes in climate due to the biophysical feedbacks from changes in forest cover, and also a further global temperature rise due to the committed warming of the climate system to the stabilised radiative forcing. During the 25 year equilibrium simulations some, but not all, of this committed global warming will be realised. During the 25 year equilibrium run from 2050 global temperature increased by 0.38K, whereas during the 200 year dynamic run from the same point it increased by 0.72K (both with CO_2 concentration held fixed at 560ppm). Locally, within our Amazonian region, land temperature and precipitation changed by +1.33K and -31% in the 25 year equilibrium run and by +2.03K and -46% in the 200 year dynamic run. We conclude that the 25 year equilibrium run only realises about half of the global mean temperature commitment from stabilising CO_2 at 2050 and about two thirds of the subsequent change in Amazonian temperature and precipitation. The simulated Amazon forest fractions after 25 years of equilibrium run (35%) and after 200 years of dynamic run (21%) are similar in distribution (not shown), although the magnitude of dieback is greater in the dynamic run due to further committed climate change not realised at 2050. This demonstrates that the equilibrium runs successfully produce a reliable simulation of equilibrium vegetation cover but without including all of the effects of the further committed climate change which is only realised by running dynamically for much longer and which we would not want to consider as part of the ecosystem commitment itself.

For each of these 19 points we know both the "dynamic" ecosystem state that is realised as the full model evolves, and also the equilibrium "committed" state that it would reach in time. The difference between the two is therefore a measure of the un-realised but committed change.

2. Mechanisms of ecosystem change

2.1 Amazon dieback

Given the potentially important nature of projected possible dieback of large areas of the Amazon forest, it is important to understand the processes which cause this in the models and how model uncertainties determine the possible likelihood and extent of dieback.

DOI: 10.1038/NGEO555

Published assessments of the future of the Amazon forest show that both warming and drying in the region may contribute to reduced vegetation productivity. Whilst decreases in precipitation lead to reduced soil moisture, warmer temperatures also reduce soil moisture and have a direct impact on vegetation productivity (D. Galbraith et al., "Quantifying the contributions of different environmental factors to predictions of Amazonian rainforest dieback in three dynamic global vegetation models (DGVMs)", submitted manuscript). In particular the response of plant respiration to warming is an important determinant of the vegetation carbon balance, but this is highly uncertain[4].

Climate projections from a range of GCMs for the IPCC's 4th Assessment Report show consistent warming across the Amazonian region[5]. Changes in precipitation are more varied but with a consistent decrease in dry season rainfall in the South and East of the region. The HadCM3 model predicts a drying sufficient to cause widespread loss of forest and Malhi *et al*.[6] note that this may be more reliable than other models given HadCM3's better than average simulation of present day climate. Warming in addition to the drying would further decrease soil moisture and increase moisture stress on the vegetation. Stomatal closure under elevated CO_2 and eventual dieback of the forest both further reduce precipitation[3].

Dry season changes in precipitation are thought to be the most significant for the forest[5], and are determined by changes in tropical Atlantic sea-surface temperatures which cause a shift in the ITCZ[7]. Biophysical feedbacks from loss of forest may be particularly important in the dry season when a higher percentage of precipitation is from recycled water[5]. HadCM3 captures changes in 20th Century July-October rainfall[8], and simulates a realistic present day Amazonian climate although it has a tendency to be slightly too dry during the dry season[9].

Also, Pacific SST anomalies may cause a reduction in wet season rainfall enough to inhibit recharge of the enhanced dry-season soil moisture deficit[10]. Amazon forest net productivity therefore is reduced by temperature and precipitation driven drying of the soil and by the direct effect of temperature on productivity. Increases in water use efficiency due to elevated CO_2 levels are insufficient to offset this[6].

A recent study[11] presents simulations of future vegetation cover from 4 dynamic vegetation models and show a consensus that all 4 produce some loss of Amazon forest when driven by the HadCM3LC patterns of climate change. Two independent vegetation model studies with LPJ[12] and CPTEC-PVM[13] driven by climate output from a range of climate models conclude a significant risk of future loss of forest in the Amazonian region. The LPJ model investigations[11,12] in particular are interesting as LPJ includes greater species diversity than HadCM3LC. Different degrees of drying in Amazonia could lead to changes in forest structure away from rainforest towards seasonal forest[6] – a phenomena not able to be represented in HadCM3LC with just one broadleaf tree functional type. However LPJ (which represents tropical broadleaf evergreen and raingreen trees, and temperate broadleaf evergreen and summergreen trees) does also simulate loss of forest under the HadCM3LC future climate projection[11].

2.2 Boreal expansion

Boreal forests are projected to experience future warming greater than the global average[14]. In these ecosystems, vegetation productivity is generally more limited by temperature than by precipitation and so a warming climate may be expected to increase productivity[15,16], although increased productivity may not necessarily increase NEP or carbon storage due to parallel increases in respiration[15] and fire or pest disturbance[16]. However, increased productivity may lead to an increase in tree growth and eventual expansion of the Boreal forest treeline[17,18].

There is palaeo evidence of Boreal forest expansion in previous warm periods[17]. Pollen records for the Holocene thermal maximum (10,000-3,000 years ago) and analysis of dead trees from the medieval warm period (AD 800-1300) both indicate further northward extent of forest than at present.

Simulated increases in tree cover are due to both increased concentration of trees in already forested regions and areal expansion of the forest itself. The former can occur rapidly as is observed at present[17]. The latter takes longer and is the reason for the significant difference between realised and committed expansion. During the Holocene changes in treeline lagged the changes in climate by centuries, but not

DOI: 10.1038/NGEO555

millennia[17]. 21st century climate is projected to change much more rapidly than occurred during the Holocene.

High-latitude tree growth is largely controlled by growing season temperatures and is much less sensitive to winter temperature[19]. In our dynamic simulation, summer (June-August) temperatures between 45 and 80°N rose by 5.5K between the 1990s and 2090s.

This is a region where agreement between models is high. The IPCC 4th Assessment Report shows a consensus of marked warming in this latitude zone across climate models[20]. Studies have shown increases in northern forest extent for several vegetation models[11] and several climate models[12]. Biophysical feedbacks mean that Boreal forest expansion will also affect the local climate, in this case through decreases in albedo. As forested surfaces are darker than the tundra they would replace, especially during periods of snow cover[21], expansion produces additional warming and hence a positive feedback on climate change[22].

3. Timescale of dieback and recovery

Following stabilisation of greenhouse gas concentrations at 2050, forest cover in our Amazonia region declines steadily before stabilising at about 20% tree cover (figure S3), exceeding slightly the committed dieback level shown in figure 1 due to further committed warming as described above. This rate of dieback equates to approximately 2×10^6 ha yr^{-1} for the region shown in figure 2, which is almost half of the present day rate of deforestation across the whole of South America of about 4.3×10^6 ha yr^{-1} (ref. 23). Even following stabilisation of CO_2 at 2050 subsequent dieback is comparable in rate to current deforestation activity.

A further aspect of such committed changes is to consider the potential of the system to recover. We have shown that stabilisation of climate forcing is not sufficient to allow the forest to recover – in fact further dieback occurs, but are ecosystem changes reversible if climate and CO_2 could be returned to pre-industrial conditions?
Using techniques similar to those used to study the reversibility of the Greenland ice sheet deglaciation[24] the equilibrium vegetation state from 2050 and 2100 was transplanted into a pre-industrial control run of the model and allowed to evolve for

100 years. The results show that recovery is possible but very slow (figure S3b). The solid lines show the timescale for the forests to begin to recover. The dashed line shows the pre-industrial level of forest cover. After 100 years of dynamic simulation the forest only recovers by a relatively small amount, so two further simulations were performed to simulate the equilibrium vegetation cover under pre-industrial conditions starting from the 2050 and 2100 committed forest state.

Even though in both cases (even for almost complete lack of initial tree cover) the simulated forest recovers to its pre-industrial level of around 70-75% in this region (40-70^{o}W, 15^{o}S-5^{o}N), the striking feature of the dynamic simulations is the slowness of the rate of recovery in contrast to the rate of forest loss after stabilisation at 2050. Starting from the 2050 (2100) committed state the forest in this region has recovered only about 20% (4%) of the lost tree cover in 100 years. This phenomenon has been analysed before[25,26]. The local biophysical feedbacks between forest cover and climate reduce precipitation with respect to undisturbed pre-industrial climate and thus slow recovery of the forest. Here, imposing the 2050 surface land-cover state on 1860 climate increases annual mean temperature in this region by 0.3K and reduces precipitation by 11%. For the 2100 vegetation state the region is initially 0.9K warmer and 23% drier. This vegetation impact on local climate slows forest recovery significantly below the simple timescale for regrowing trees in a fixed climate. Forest and climate have to recover hand-in-hand to the pre-perturbation conditions. Despite possible non-linearities in the rate of forest recovery it is clear that such recovery is on multi-century timescales.

DOI: 10.1038/NGEO555

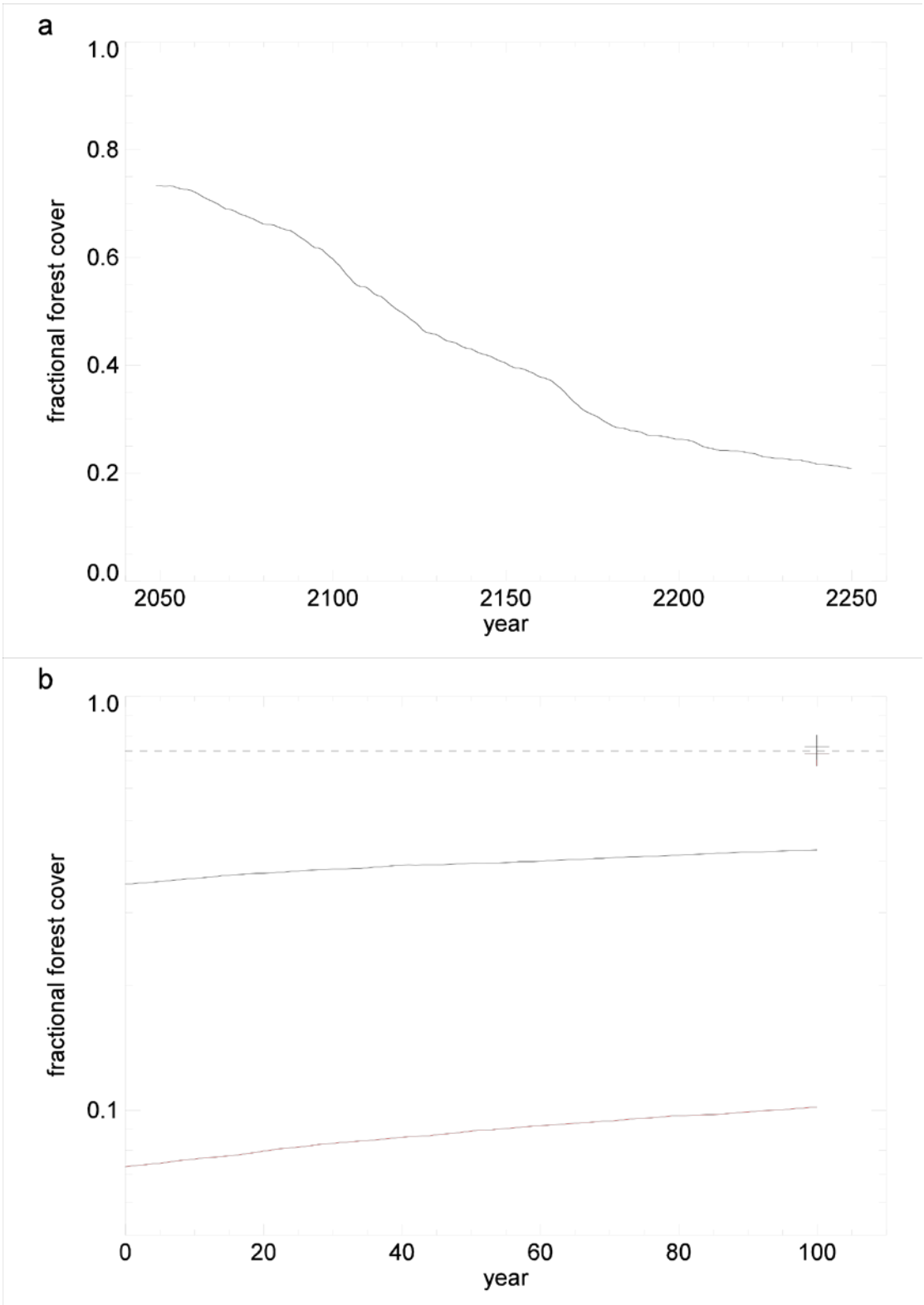

Figure S3. Timescale of dynamic Amazon dieback compared with recovery. (a) Evolution of Amazonian forest cover from the 2050 dynamic state when the model is run forwards dynamically for 200 years with fixed atmospheric composition at 2050 levels. (b) Forest recovery when climate is returned to pre-industrial conditions. The vegetation state from the committed

experiments at 2050 (black) and 2100 (red) was re-introduced into an 1860 climate state experiment and run dynamically for 100 years. The dashed line shows the pre-industrial level of forest cover. The crosses show eventual equilibrium forest cover from two further simulations using the rapid equilibration technique.

DOI: 10.1038/NGEO555

References

1. Friedlingstein P., et al. Climate-carbon cycle feedback analysis, results from the C4MIP model intercomparison. *J. Climate* **19** 3337-3353 (2006)

2. Cox, P. M., Description of the TRIFFID dynamic global vegetation model. Technical Note 24., Hadley Centre, Met Office (2001).

3. Betts R. A., et al. The role of ecosystem-atmosphere interactions in simulated Amazonian precipitation decrease and forest dieback under global climate warming. *Theor. Appl. Climatol*. **78** 157-175. (2004)

4. Lewis, S.L. Tropical forests and the changing earth system. *Phil. Trans. R. Soc. B*, **361**, 195-210. (2006)

5. Malhi, Y., et al. Climate Change, Deforestation and the Fate of the Amazon. *Science*, **319**, 169-172. (2008)

6. Malhi, Y. et al. Exploring the likelihood and mechanism of a climate-change-induced dieback of the Amazon rainforest. *Proc. Natl. Acad. Sci. USA*, doi: 10.1073/pnas.0804619106. (2009).

7. Good, P., Lowe, J.A., Collins, M., Moufouma-Okia, W. An objective tropical Atlantic sea surface temperature gradient index for studies of south Amazon dry-season climate variability and change. *Phil. Trans. R. Soc. B*, **363**, 1761-1766. (2008)

8. Cox, P.M. Increasing risk of amazonian drought due to decreasing aerosol pollution. *Nature,* **453,** 212-215 (2008)

9. Li, W.H., Fu, R., Dickinson, R.E. Rainfall and its seasonality over the Amazon in the 21st Century as assessed by the coupled models for the IPCC AR4. *J. Geophys. Res.*, **111**, D02111, doi:10.1029/2005JD006355. (2006)

10. Harris, P.P., Huntingford, C. Cox, P. Amazon basin climate under global warming: the role of the sea surface temperature. *Phil. Trans. R. Soc. B*, **363**, 1753-1759. (2008)

11. Sitch S., et al. Evaluation of the terrestrial carbon cycle, future plant geography and climate-carbon cycle feedbacks using 5 Dynamic Global Vegetation Models (DGVMs). *Glob. Change Biol.*, **14**, 2015-2039, doi 10.1111/j.1365-2486.2008.01626.x, (2008)

12. Scholze M., Knorr W., Arnell N. W., Prentice I. C., A climate-change risk analysis for world ecosystems. *Proc. Nat. Academy Sci, USA*. **103** 13116-13120 (2006)

13. Salazar, L.F., Nobre, C.A., Oyama, M.D. Climate change consequences on the biome distribution in tropical South America. *Geophys. Res. Lett.*, **34**, L09708, doi:10.1029/2007GL029695. (2007)

14. Ruckstuhl, K.E., Johnson, E.A., Miyanishi, K. Introduction. The boreal forest and global change. *Phil. Trans. R. Soc. B*, **363**, 2243-2247. (2008)

15. Luyssaert, S. et al. CO2 balance of boreal, temperate and tropical forests derived from a global database. *Glob. Change Biol.*, **13**, 2509-2537. (2007)

16. Kurz, W.A., Stinson, G., Rapmley, G. Could increased boreal forest ecosystem productivity offset carbon losses from increased disturbances? *Phil. Trans. R. Soc. B*, **363**, 2259-2268. (2008)

17. Macdonald, G.M., Kremenetski, K.V., Beilman, D.W. Climate change and the northern Russioan treeline zone. *Phil. Trans. R. Soc. B*, **363**, 2283-2299. (2008)

18. Kellomaki, S., Peltola, H., Nuutinen, T., Korhonen, K.T., Strandman, H. Sensitivity of managed boreal forests in Finland to climate change, with implications for adaptive management. *Phil. Trans. R. Soc. B*, **363**, 2339-2349. (2008)

19. Briffa, K. et al. Trends in recent temperature and radial tree growth spanning 2000 years across northwest Eurasia. *Phil. Trans. R. Soc. B*, **363**, 2269-2282. (2008)

20. Meehl, G.A. Global climate projections Climate Change 2007: The Physical Science Basis. Contribution of Working Group I to the Fourth Assessment Report of the Intergovernmental Panel on Climate Change. Eds: S. Solomon, D. Qin, M. Manning, Z. Chen, M. Marquis, K. B. Averyt, M. Tignor and H. L. Miller. Cambridge University Press (2007)

21. Betts, R.A. Offset of the potential carbon sink from boreal forestation by decreases in surface albedo. *Nature*, **408**, 187-190 (2000)

22. Foley, J.A., Kutzbach, J.E., Coe, M.T., Levis, S. Feedbacks between climate and boreal forests during the Holocene epoch. *Nature*, **371**, 52 – 54 (1994)

23. Nabuurs, G. J. et al., Forestry. In Climate Change 2007: Mitigation. Contribution of Working Group III to the Fourth Assessment Report of the Intergovernmental Panel on Climate Change, B. Metz, O.R. Davidson, P.R. Bosch, R. Dave & L.A. Meyer (Eds). Cambridge University Press, Cambridge, UK and New York, USA (2007).

DOI: 10.1038/NGEO555

24. Ridley J., Huybrechts P., Lowe J., Gregory J., 2006. Is the deglaciation of the Greenland ice sheet reversible? Hadley Centre for Climate Prediction Contract Deliverable reference number: 01.07.05.

25. Hughes, J.K. The Dynamic Response of the Global Atmosphere-Vegetation coupled system. PhD Thesis, University of Reading, Department of Meteorology. (2003)

26. Hughes, J.K., Valdes, P.J. Betts, R.A. Dynamics of a global-scale vegetation model. *Ecological Modelling*. doi:10.1016/j.ecol.model.2006.05.020. (2006)

4.2. Compatible emissions and carbon budgets

Perhaps the most common question required for mitigation policy is “by how much do we need to reduce our carbon emissions?”. It is well accepted that deep and rapid emissions cuts are required in order to stand any chance of achieving the UNFCCC’s goal of avoiding dangerous interference with the climate system, but in order to develop quantitative and measurable policy targets we must quantify the emissions compatible with any climate goal.

Early carbon cycle simulations quantified the effect of climate on natural carbon sinks and directly answered the question “how much climate change do we get for given emissions?” (**Friedlingstein et al., 2006**). In 2005, as part of a conference on Avoiding Dangerous Climate Change, I presented work which turned the question around: “how much emissions reductions are required to lead to a given climate change?”. This re-framing of the question allowed basically the same results to be presented in a much more useful way (**Jones et al., 2006a**). The concept is illustrated in Figure 11: if we know an emissions scenario then we can provide this as an input to the models, which then simulate natural land and ocean carbon sinks in response to the CO_2 and climate change allowing us to calculate the projected CO_2 rise (panel a). Conversely if we know a CO_2 pathway that we wish to follow we can prescribe that as an input to the models. They again simulate the behaviour of the natural carbon sinks and this time that allows us, by mass balance, to calculate the compatible anthropogenic emissions (panel b).

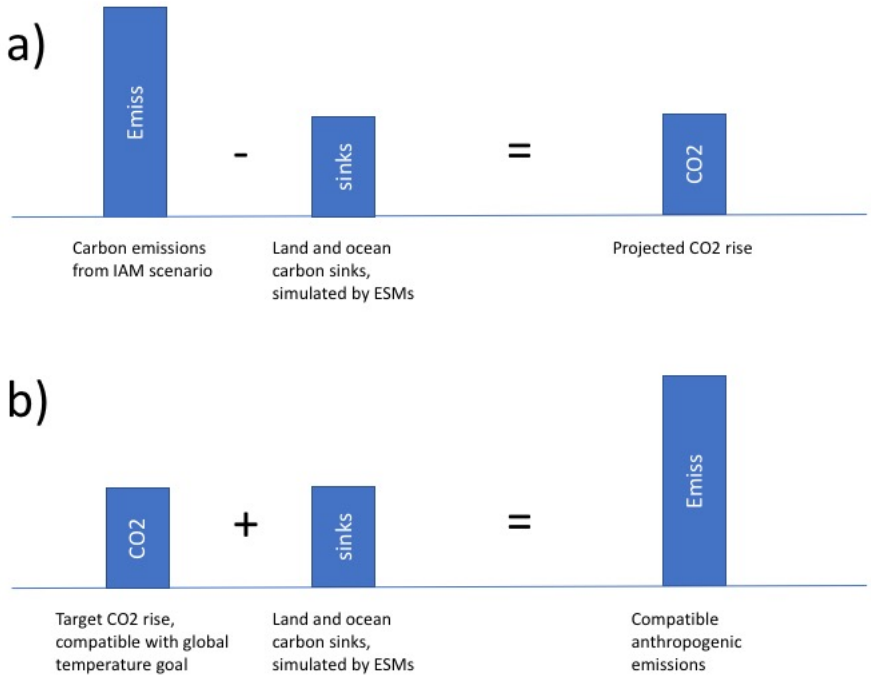

Figure 11. Schematic representation of (a) emissions-driven and (b) concentration-driven experiments (see Glossary).

The technique itself was not new – for example IPCC Third Assessment Report (Prentice et al., 2001) showed results from the Bern and ISAM models that simulated terrestrial and ocean sinks in response to prescribed CO_2 pathways and deduced the "implied emissions" to stabilise CO_2 at different levels. But my work was the first time this had been done in a coupled carbon cycle GCM with fully interactive climate and carbon cycle feedbacks. **Jones et al. (2006a)** and subsequent work and discussion with the UK government played a role in informing the UK Committee on Climate Change and their stated goal to reduce UK carbon emissions by 80% by 2050.

This approach allowed direct quantification of the anthropogenic emissions which would lead to the chosen CO_2 concentration pathway (**Jones et al., 2006a; Jones et al., 2006b;** Matthews, 2006). I performed the application of this diagnosis to the CMIP5 models, and this formed one of the significant outcomes of the IPCC AR5 carbon cycle chapter (see section 3.2 of this thesis). In my paper (**Jones et al., 2013**), which forms the remainder of this section, we show how this analysis was performed for the CMIP5 ensemble for the four RCP scenarios. Although the technique can be (and is) applied to any scenario, it is for the low scenarios (here

RCP2.6 and RCP4.5) which the results are of most policy relevance. The analysis was featured in the Met Office Hadley Centre science brochure presented in Paris at COP21 (21st Conference of the Parties to the UNFCCC) in 2015 and informed the negotiations that led to the Paris Agreement (http://www.metoffice.gov.uk/climate-guide/science/uk/cop/cop21).

Jones et al. (2013) examined the compatible emissions to follow RCP2.6 in particular and addressed the question of how much emissions reductions would be required (leading to the IPCC statement "For RCP2.6, an average 50% (range 14 to 96%) emission reduction is required by 2050 relative to 1990 levels"), and also that there was a good chance that emissions must be globally negative before the end of the century (six out of ten models studied required global emissions to be negative on average from 2080 to 2100). The concept of, and implications of, the need for negative emissions is discussed in more detail in the next section, 4.3, of this thesis.

Twenty-First-Century Compatible CO_2 Emissions and Airborne Fraction Simulated by CMIP5 Earth System Models under Four Representative Concentration Pathways

CHRIS JONES,[a] EDDY ROBERTSON,[a] VIVEK ARORA,[b] PIERRE FRIEDLINGSTEIN,[c] ELENA SHEVLIAKOVA,[d] LAURENT BOPP,[e] VICTOR BROVKIN,[f] TOMOHIRO HAJIMA,[g] ETSUSHI KATO,[h] MICHIO KAWAMIYA,[g] SPENCER LIDDICOAT,[a] KEITH LINDSAY,[i] CHRISTIAN H. REICK,[f] CAROLINE ROELANDT,[j] JOACHIM SEGSCHNEIDER,[f] AND JERRY TJIPUTRA[j]

[a] *Met Office Hadley Centre, Exeter, United Kingdom*
[b] *Canadian Centre for Climate Modelling and Analysis, Environment Canada, University of Victoria, Victoria, British Columbia, Canada*
[c] *College of Engineering, Mathematics and Physical Sciences, University of Exeter, Exeter, EX4 4QF, United Kingdom*
[d] *Department of Ecology and Evolutionary Biology, Princeton University, Princeton, New Jersey*
[e] *LSCE, IPSL, CEA, UVSQ, CNRS, Gif-sur-Yvette, France*
[f] *Max Planck Institute for Meteorology, Hamburg, Germany*
[g] *Research Institute for Global Change, Japan Agency for Marine-Earth Science and Technology, Yokohama, Japan*
[h] *Center for Global Environmental Research, National Institute for Environmental Studies, Tsukuba, Japan*
[i] *Climate and Global Dynamics Division, National Center for Atmospheric Research,[k] Boulder, Colorado*
[j] *Geophysical Institute, University of Bergen, Bergen, Norway*

(Manuscript received 31 July 2012, in final form 3 January 2013)

ABSTRACT

The carbon cycle is a crucial Earth system component affecting climate and atmospheric composition. The response of natural carbon uptake to CO_2 and climate change will determine anthropogenic emissions compatible with a target CO_2 pathway. For phase 5 of the Coupled Model Intercomparison Project (CMIP5), four future representative concentration pathways (RCPs) have been generated by integrated assessment models (IAMs) and used as scenarios by state-of-the-art climate models, enabling quantification of compatible carbon emissions for the four scenarios by complex, process-based models. Here, the authors present results from 15 such Earth system GCMs for future changes in land and ocean carbon storage and the implications for anthropogenic emissions. The results are consistent with the underlying scenarios but show substantial model spread. Uncertainty in land carbon uptake due to differences among models is comparable with the spread across scenarios. Model estimates of historical fossil-fuel emissions agree well with reconstructions, and future projections for representative concentration pathway 2.6 (RCP2.6) and RCP4.5 are consistent with the IAMs. For high-end scenarios (RCP6.0 and RCP8.5), GCMs simulate smaller compatible emissions than the IAMs, indicating a larger climate–carbon cycle feedback in the GCMs in these scenarios. For the RCP2.6 mitigation scenario, an average reduction of 50% in emissions by 2050 from 1990 levels is required but with very large model spread (14%–96%). The models also disagree on both the requirement for sustained negative emissions to achieve the RCP2.6 CO_2 concentration and the success of this scenario to restrict global warming below 2°C. All models agree that the future airborne fraction depends strongly on the emissions profile with higher airborne fraction for higher emissions scenarios.

1. Introduction

The global carbon cycle has long been known to be a crucial component of future climate change, closely linking anthropogenic CO_2 emissions with future changes in atmospheric CO_2 concentration and hence climate (e.g., Prentice et al. 2001). Including the carbon cycle as

[k] The National Center for Atmospheric Research is sponsored by the National Science Foundation.

Corresponding author address: Chris Jones, Met Office Hadley Centre, FitzRoy Road, Exeter EX1 3PB, United Kingdom.
E-mail: chris.d.jones@metoffice.gov.uk

DOI: 10.1175/JCLI-D-12-00554.1

an interactive component in comprehensive climate models has become common, and the Coupled Carbon Cycle Climate Model Intercomparison Project (C^4MIP; Friedlingstein et al. 2006) presented results of 11 such models. All models participating in the C^4MIP study showed an increase in future atmospheric CO_2 concentration for the same anthropogenic emissions because of positive feedbacks of climate on natural carbon sinks (albeit neglecting nitrogen cycle processes). However, this comparison of models also showed large quantitative uncertainty in the magnitude of this effect. This large range in future carbon uptake seen between models also exists because of parameter uncertainty within single models (Booth et al. 2012).

Such coupled climate–carbon cycle models simulate the natural exchange of carbon by the land and ocean with the atmosphere and thus provide a predictive link between emissions and atmospheric concentrations of CO_2. In emissions-driven simulations such as in C^4MIP, these models calculate changes in atmospheric CO_2 concentration given a scenario of emissions. They can also be used to compute the emissions required to follow a prescribed concentration pathway (Jones et al. 2006; Matthews 2006; Plattner et al. 2008). This method has become widespread and was recommended by Hibbard et al. (2007) as the experimental design for phase 5 of the Coupled Model Intercomparison Project (CMIP5; http://cmip-pcmdi.llnl.gov/cmip5/index.html) and has subsequently been used to present compatible emissions from individual models for the CMIP5 scenarios (Arora et al. 2011). Johns et al. (2011) also used this approach to quantify the uncertainty in compatible emissions across an ensemble of models that had performed simulations under the same CO_2 pathway.

The latest generation of state-of-the-art Earth system general circulation models (ES-GCMs) has recently been used to carry out simulations of a new set of scenarios for CMIP5 (Taylor et al. 2012; Moss et al. 2010). The CMIP5 simulations include four future socioeconomic scenarios referred to as representative concentration pathways (RCPs; Moss et al. 2010; van Vuuren et al. 2011): RCP2.6, RCP4.5, RCP6.0, and RCP8.5. These future scenarios include a CO_2 concentration pathway computed to be consistent with anthropogenic carbon emissions as generated by four integrated assessment models (IAMs). The RCPs are labeled according to the approximate global radiative-forcing level at 2100 with CO_2 concentrations reaching 421, 538, 670, and 936 ppm, respectively (Fig. 1a). The RCP2.6 CO_2 pathway peaks at a concentration of 443 ppm at 2050 before declining in the latter half of the century and is alternatively known as RCP3 peak and decline (RCP3PD).

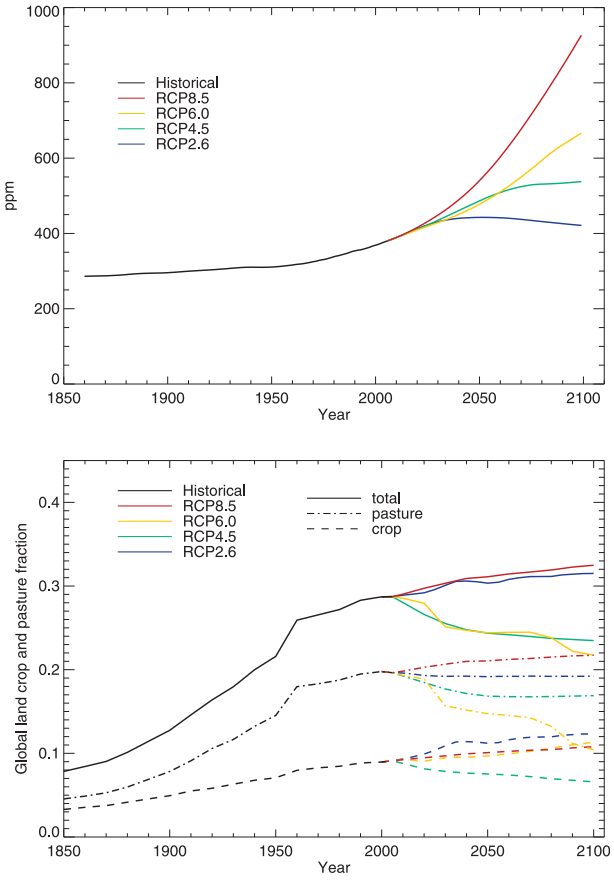

FIG. 1. RCP scenarios of (a) atmospheric CO_2 concentration and (b) anthropogenic land-use change for the historical period and future RCP scenarios. Plotted for the land-use scenarios are the fractions of global land area occupied by crops (dashed lines), pasture (dotted–dashed lines), and their total (solid lines).

Within the socioeconomic scenarios that drive the RCPs, representation of climate policy has been included to enable the scenario to achieve the target radiative forcing by 2100. A simple climate–carbon cycle model was then used to calculate atmospheric CO_2 concentration from the scenario emissions (Meinshausen et al. 2011). IAMs' estimates of future economic activities, including land-use changes, are driven by simplified, often regional models of future climate and carbon cycle, which are substantially different from those in ES-GCMs. The complexity and high degree of uncertainty in resolving biosphere–climate interactions (Friedlingstein et al. 2006; Johns et al. 2011) makes it important to establish consistency between the two modeling frameworks. A key step in establishing consistency between the frameworks is the comparison of compatible emissions diagnosed from the CMIP5 CO_2 concentration–driven ES-GCM experiments, to the emissions generated by the IAMs.

Especially of interest for very low mitigation scenarios, such as RCP2.6, are quantification of short-term emissions reductions required and the question of whether the scenario is achievable without the requirement of long-term globally negative emissions, which might only be possible with the use of large-scale deliberate carbon dioxide removal and storage. Use of the CMIP5 range of ES-GCMs also enables us to estimate the uncertainty in the compatible emissions to follow a given radiative-forcing pathway. The process of scenario development is intended to be iterative (Moss et al. 2010), so these results will inform subsequent development and calibration of IAMs.

Land-use change has a profound influence on both biophysical features of the land and also its carbon storage, adding 156 PgC to the atmosphere from 1850 to 2005. Past land-use changes have been influential in emitting CO_2 to the atmosphere (Houghton 2008; Denman et al. 2007) and future changes in land use will continue to strongly perturb the terrestrial carbon cycle and may also be used deliberately to try to mitigate climate change through reduced emissions (e.g., REDD; Gullison et al. 2007). Land-use trajectories in the four RCP scenarios show very distinct trends and cover a wide range of projections (see Fig. 1b). The area of cropland and pasture increases in RCP8.5, mostly driven by an increasing global population, but cropland area also increases in the RCP2.6, despite a smaller population increase, as a result of increased bioenergy production used for climate mitigation. RCP6.0 shows an increasing use of cropland but a decline in pasture land. RCP4.5 is the only scenario to show a decrease in global cropland. There is not a monotonic progression from ''low'' to ''high'' land use through the scenarios in the same way that there is for radiative forcing and the impact of this will be shown to be important for future changes in the fraction of emissions taken up by land. Land-use emissions of CO_2 are fundamentally different from fossil-fuel emissions, which add a new supply of CO_2 to the atmosphere–land–ocean system, whereas land-use emissions merely relocate carbon from one component to another within this system. We describe in the methods section (section 2) that, when diagnosing permissible emissions from ES-GCMs, fossil-fuel emissions can be easily diagnosed as changes in the total carbon held in the simulated atmosphere–land–ocean system. Land-use emissions, however, are harder to diagnose within the ES-GCMs.

Section 2 describes the models and methods used in the analysis and section 3 presents results of future changes in land and ocean carbon uptake and the diagnosed compatible fossil-fuel emissions and their airborne fraction. Discussion and conclusions follow in section 4.

2. Experiments and methods

a. CMIP5 experimental design

The CMIP5 experimental design is described in Taylor et al. (2012) and was discussed in Hibbard et al. (2007). The simulations presented here are the future (twenty-first century) RCP simulations (CMIP5 experiments 4.1–4.4), which are ''concentration driven'' rather than ''emissions driven.'' In these simulations, the time evolution of atmospheric CO_2 is specified and the simulated exchange of carbon between the atmosphere and the underlying land and ocean allows us to diagnose anthropogenic emissions that are compatible with the prescribed concentration pathway. This approach has been used before for simplified models (e.g., Prentice et al. 2001), but CMIP5 is the first time it has been used for a coordinated set of experiments for multiple ES-GCMs.

The CMIP5 models are run using prescribed inputs of atmospheric CO_2 (Fig. 1a), other greenhouse gases, aerosols, and natural forcings such as solar and volcanic aerosol emissions. Scenarios of land-use change are also available (Fig. 1b), but their implementation differs considerably between models or, in two cases considered here, is not represented at all.

b. Compatible emissions diagnosis

Studies that have used this approach in the past to estimate compatible emissions have only discussed the resulting emissions in the context of total anthropogenic emission and not a breakdown into fossil or land-use emissions (Jones et al. 2006; Matthews 2006; Plattner et al. 2008). The models used in those studies did not include any direct effect of land use or human disturbance on land carbon storage or land-cover characteristics, and so diagnosis of total emissions was all that could be achieved. For the CMIP5 simulations, many models now include representation of the effect of land-use disturbance on the terrestrial carbon cycle making, in principle, diagnosis of emissions possible from both fossil-fuel use and land-use change. However, because of a multitude of different land-use processes being included or excluded from different models and the number of different possible definitions of ''land-use emission,'' it is very difficult to clearly present land-use emissions from these simulations. Arora and Boer (2010) discuss some of the issues and challenges of defining and quantifying uncertainty in land-use emissions. In the appendix, we show that, regardless of difficulties in diagnosing the land-use emission component, the simulations can be used to diagnose the fossil-fuel component of the compatible emissions and compare with IAM/RCP values.

For the combined atmosphere–land–ocean system, the rate of change of carbon may be written as

$$\frac{dC_{\mathrm{Tot}}}{dt} = \frac{dC_A}{dt} + \frac{dC_L}{dt} + \frac{dC_O}{dt} = E_F, \quad (1)$$

where $C_{\mathrm{Tot}} = C_A + C_L + C_O$ is the sum of carbon in the atmosphere, land, and ocean components (the latter including seafloor sediments) and E_F is an external addition of carbon into the atmosphere such as from anthropogenic fossil-fuel burning. The equations for the atmosphere, land, and ocean are

$$\begin{aligned}
\frac{dC_L}{dt} &= F_L = F_{L,\mathrm{NAT}} - E_{\mathrm{LUC}} \\
\frac{dC_O}{dt} &= F_O \\
\frac{dC_A}{dt} &= F_A + E_F \\
&= -F_L - F_O + E_F \\
&= -F_{L,\mathrm{NAT}} - F_O + (E_F + E_{\mathrm{LUC}}) \quad (2)
\end{aligned}$$

where $(F_L + F_O) = -F_A$ are the fluxes between the atmosphere and the underlying land and ocean, taken to be positive into the components. The atmosphere–land CO_2 flux is made up of natural atmosphere–land CO_2 flux $F_{L,\mathrm{NAT}}$ and anthropogenic land-use change E_{LUC} components and total emissions E_T are thus given by $E_T = E_F + E_{\mathrm{LUC}}$.

Integrating Eqs. (1) and (2) from initial time to t gives

$$\Delta C_{\mathrm{Tot}} = \Delta C_A + \Delta C_L + \Delta C_O = \int_0^t E_F \, dt = \tilde{E}_F, \quad (3)$$

where $\tilde{E}_F$ is the cumulative fossil-fuel input to the system. Division by $\tilde{E}_F$ yields all terms in fractional form

$$f_A + f_L + f_O = 1, \quad (4)$$

where f_A is the airborne fraction of cumulative fossil-fuel emissions and f_L and f_O are fractional cumulative fossil-fuel emissions taken up by the land and ocean.

The land-use scenario and how it is implemented in ES-GCMs affects the land carbon pools and thus the diagnosed E_F, but land-use emissions themselves cannot be measured from these simulations alone. To diagnose E_{LUC} it would be necessary to repeat the simulations without land-use disturbance and compare the different evolution of C_L with and without land use (see, e.g., Arora and Boer 2010). This definition of E_{LUC} would be different from the direct deforestation emissions that some models can diagnose and also differs in definition from historical reconstructions such as by Houghton (2008), who uses a constant (non-time-varying assumption of T and CO_2) baseline condition against which to measure emissions. Not all the ES-GCMs use the full range of information available from the land-use change scenarios such as wood harvest projections, subgrid-scale shifting cultivation, or representation of primary and secondary forests; these processes can have a bigger impact than the choice of RCP land-use scenario (Hurtt et al. 2011).

To diagnose carbon emissions from land-use additional ES-GCM experiments will be necessary. These experiments therefore are a research priority and are the focus of the Land-Use and Climate, Identification of Robust Impacts (LUCID)–CMIP5 experiment (Brovkin et al. 2013). From here on, this paper deals only with the diagnosed fossil-fuel emissions. It remains an important research gap to be able to quantify land-use carbon emissions from these ES-GCMs in a reliable, consistent, and well-defined way.

c. Model output data

Land surface models typically partition carbon into various pools such as different types of living tissue or ages of soil carbon or harvested/stored wood products. To facilitate intercomparison, the CMIP5 data request was for models to aggregate their own component pools into four common outputs, whose short network Common Data Form (NetCDF) output names are as follows:

- cVeg, carbon stored in living biomass (both above and below ground);
- cSoil, carbon stored as dead organic matter in mineral soils;
- cLitter, freshly dropped dead organic carbon before it is incorporated into the soil carbon; and
- cProduct, carbon stored in wood products (including anything from paper to furniture).

In our analysis we make use of standard CMIP5 output from the Program for Climate Model Diagnosis and Intercomparison (http://pcmdi3.llnl.gov/esgcet/home.htm) as provided by the models listed in Table 1. Not all models have performed all the RCP simulations, so we use data available at the time of writing as listed in Table 1. Not all models include all of these pools, but for each model the total terrestrial carbon C_L is calculated as the sum of all available land pools.

All but two of these models (INM-CM4.0 and BCC-CSM1.1) include representation of anthropogenic land-use change in these simulations. While data are available for these two models, which would allow calculation of compatible emissions, the influence of land-use on terrestrial carbon stores as described above means this would not allow a like-for-like comparison. Hence, we have shown results from these models for comparison as dashed lines in figures showing land and ocean carbon changes, but we omit them from the comparison of compatible emissions.

TABLE 1. List of models and institutes contributing to CMIP5 whose data have been used for this analysis. Not all models have performed all scenarios. The table lists the data available at the time of preparation of this analysis. Here, [y] denotes that model data were available but that the model did not include representation of land-use change.

Modeling center	Model name	Model expansion	Historical	RCP2.6	RCP4.5	RCP6.0	RCP8.5
Beijing Climate Center (BCC)	BCC-CSM1.1	BCC Climate System Model 1.1	[y]	[y]	[y]	[y]	[y]
Canadian Centre for Climate Modelling and Analysis (CCCma)	CanESM2	Second Generation Canadian Earth System Model	y	y	y		y
National Science Foundation (NSF)–U.S. Department of Energy (DOE)–National Center for Atmospheric Research (NCAR)	CESM1-BGC	Community Earth System Model 1	y		y		y
National Oceanic and Atmospheric Administration (NOAA) GFDL	GFDL-ESM2G	GFDL Earth System Model 2G	y	y	y	y	y
NOAA GFDL	GFDL-ESM2M	GFDL Earth System Model 2M	y	y	y	y	y
Met Office Hadley Centre (MOHC)	HadGEM2-ES	Hadley Centre Global Environmental Model version 2 Earth System configuration	y	y	y	y	y
MOHC	HadGEM2-CC	Hadley Centre Global Environmental Model version 2 Carbon Cycle configuration	y		y		y
Institute of Numerical Mathematics (INM)	INM-CM4.0	INM Coupled Model version 4.0	[y]		[y]		[y]
L'Institut Pierre-Simon Laplace (IPSL)	IPSL-CM5A-LR	IPSL Coupled Model version 5A, low resolution	y	y	y	y	y
IPSL	IPSL-CM5A-MR	IPSL Coupled Model version 5A, medium resolution	y	y	y		y
IPSL	IPSL-CM5B-LR	IPSL Coupled Model version 5B, low resolution	y		y		y
Japan Agency for Marine-Earth Science and Technology, Atmosphere and Ocean Research Institute (The University of Tokyo), and National Institute for Environmental Studies, Center for Climate System Research (CCSR)	MIROC-ESM	Model for Interdisciplinary Research on Climate Earth System Model	y	y	y	y	y
CCSR	MIROC-ESM-CHEM	Model for Interdisciplinary Research on Climate Earth System Model, atmospheric chemistry coupled version	y	y	y	y	y
Max Planck Institute for Meteorology (MPI)	MPI-ESM-LR	MPI Earth System Model, low resolution	y	y	y		y
Norwegian Climate Centre (NCC)	NorESM1-ME	Norwegian Earth System Model 1	y	y	y	y	y

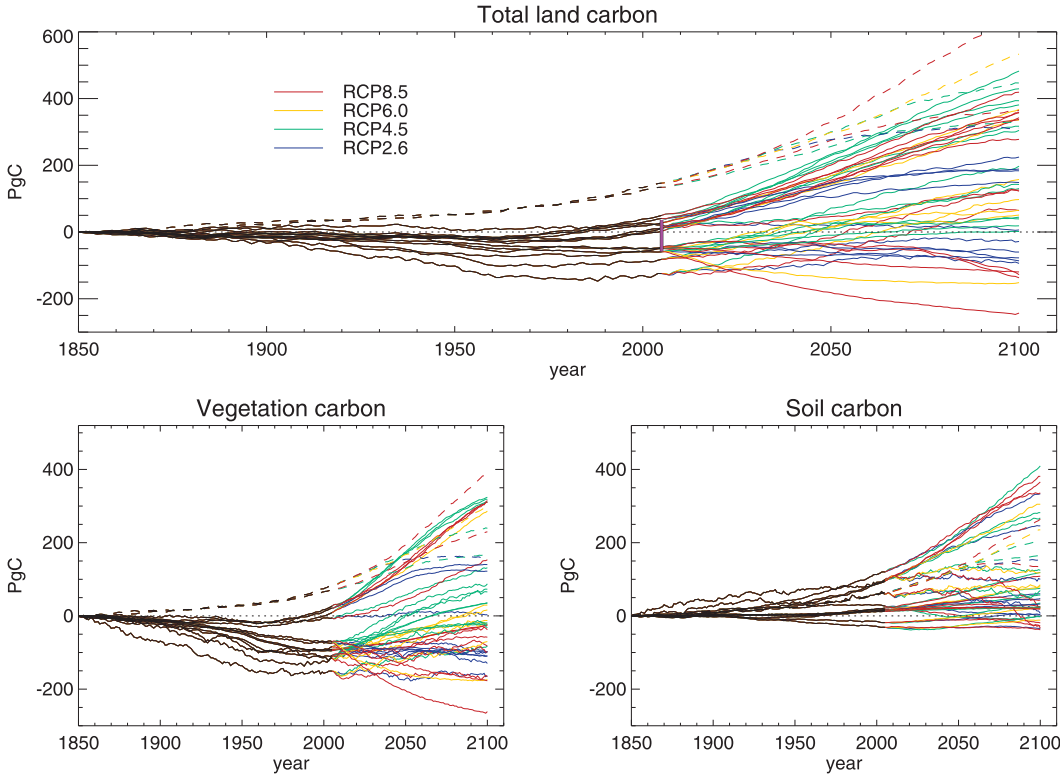

FIG. 2. Changes in (top) total land carbon store, (bottom left) vegetation carbon, and (bottom right) soil carbon (defined as cSoil + cLitter) for the CMIP5 models. An observationally derived estimate of net changes (Arora et al. 2011) is shown by the vertical pink bar in (top). Dashed lines represent output from ES-GCMs without representation of land-use change (INM-CM4.0 and BCC-CSM1.1).

The initial size of these pools is poorly constrained by observations and varies substantially across models, with preindustrial vegetation and soil carbon ranging from 410 to 890 PgC and from 500 to 2930 PgC, respectively, across models. Todd-Brown et al. (2013) have evaluated soil carbon simulations from CMIP5 models and find a wide range of model abilities to recreate observed distributions of soil carbon. In our analysis, it is changes in storage that are important for diagnosing compatible emissions. It is not yet known to what extent errors in the initial state have an influence on future projections.

For ocean carbon storage, we use the CMIP5 reported values of air-to-sea flux fgco2 and integrate this over time to give a change in ocean storage. For atmospheric CO_2, we use the globally uniform concentration (ppm) provided by the RCP scenarios and multiply it by 2.12 PgC ppm^{-1} to obtain the atmospheric carbon burden C_A (PgC).

3. Results

a. Changes in land carbon uptake and storage

Figure 2 shows changes in the total land carbon storage (Fig. 2a) and individual changes in vegetation and soil (Figs. 2b,c), where we have combined here cSoil and cLitter. Carbon stored in wood products is generally small (less than 10 PgC) and so contributes little to the total storage or its changes for most models. The exceptions are the Geophysical Fluid Dynamics Laboratory (GFDL) models, which include more detailed treatment of land-use transitions and also consideration of land-use changes from 1700 to 1850, leading to greater cProduct values. There is a large spread in model response for both historical and future periods. Most models show a decline since preindustrial due to increasing areas of deforestation, followed by a recovery in the final decades of the twentieth century, attributed mainly to CO_2 fertilization. This is in qualitative agreement with observational estimates (Trudinger et al. 2002), although there is much uncertainty over the magnitude. All models that include land-use changes show some decline in vegetation carbon at least in the early part of the simulation, but those which exclude land-use change (INM-CM4.0 and BCC-CSM1.1) simulate a steady increase in land carbon during the twentieth century. Spread of changes in land carbon storage across the models, which represent land-use change, ranges from −124 to +50 PgC by 2005, consisting of

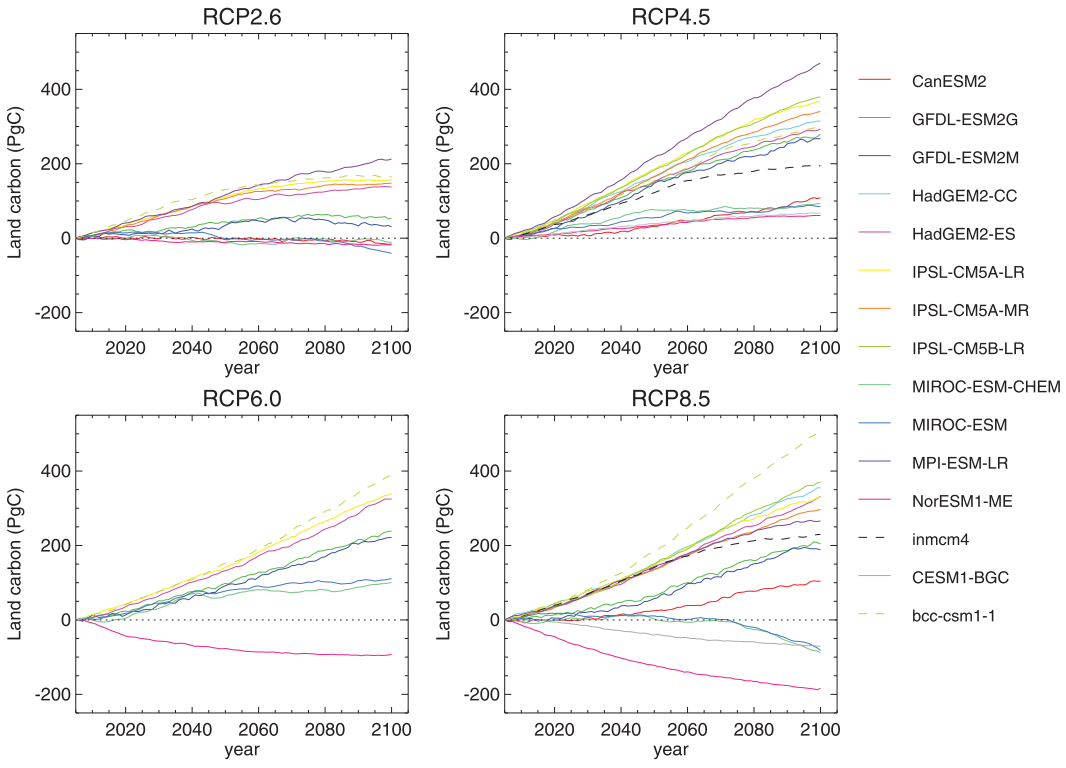

FIG. 3. As in Fig. 2a, but from 2005, shown separately for each RCP scenario. Individual models are denoted in separate colors for comparison across scenarios. Dashed lines represent output from ES-GCMs without representation of land-use change (INM-CM4.0 and BCC-CSM1.1).

from −151 to +27 PgC from vegetation and from −31 to +120 PgC from soil (including litter) carbon.

Arora et al. (2011) estimate the observation-based cumulative historical (1850–2005) land carbon uptake, which is difficult to observe directly, as −11 ± 47 PgC (i.e., a source to the atmosphere) as the residual of the observed change in atmospheric carbon burden and cumulative fossil-fuel emissions based on the CMIP5 dataset and observation-based estimates of cumulative ocean carbon uptake based on Sabine and Feely (2007) up to 1999 and extended to 2005 using values from Denman et al. (2007). The wide range in historical land carbon uptake among models is the result of intermodel uncertainty in both the strength of the CO_2 fertilization effect (Arora et al. 2013) as well as differences in the manner they implement land-use change. This estimate of net land carbon change is very close to the multimodel mean of −19 PgC, and the range encompasses 9 out of 13 models (Fig. 2), although this cannot be partitioned into changes in vegetation and soil carbon separately. Only one model falls outside twice this observational uncertainty: GFDL-ESM2M simulates a loss of 124 PgC.

Cumulative land carbon uptake for the future duration shows similar large intermodel spread, which overwhelms the interscenario spread. Figure 3 shows each scenario separately, anomalized relative to 2005 to better show the future changes in each scenario clearly. For RCPs 2.6 and 8.5, which both include increasing areas of land use in their scenario, four models project decreases in future land carbon storage, although most models project an increase. For RCPs 4.5 and 6.0, whose scenarios include decreasing areas of land use, all models agree on future increases in land carbon storage, although with large spread, with RCP4.5 showing the largest values of land carbon accumulation.

At present, it is not easy to quantify the impact of land use on the terrestrial carbon cycle within a single model without carrying out multiple simulations. These simulations are being carried out by some groups as part of the LUCID–CMIP5 activity but are not part of the standard CMIP5 protocol (Brovkin et al. 2013).

b. Changes in ocean carbon uptake and storage

Whether expressed as annual fluxes (Fig. 4, top) or cumulative changes in inventory (Fig. 4, bottom), ocean carbon storage shows a consistent picture for each RCP across most ES-GCMs. Oceanic uptake is driven primarily by ΔpCO_2 (the gradient of CO_2 concentration between atmosphere and ocean), so for higher CO_2

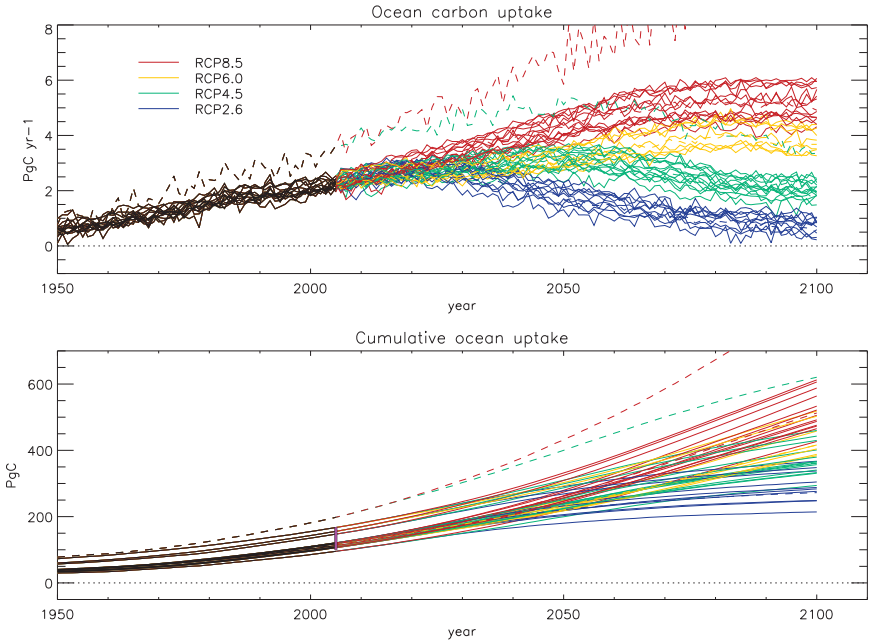

FIG. 4. Changes in annual (top) oceanic carbon uptake and (bottom) cumulative uptake since 1850 from the CMIP5 models. An observationally derived estimate of net changes (Arora et al. 2011; C. Le Quéré 2012, personal communication) is shown by the vertical pink bar in (bottom). For consistency with Figs. 2 and 3, dashed lines represent output from ES-GCMs without representation of land-use change (INM-CM4.0 and BCC-CSM1.1). For better visibility of the near past and the twenty-first century, the *x* axis begins here at 1950.

concentration pathways all models simulate greater ocean carbon uptake. Observationally constrained estimates for cumulative oceanic uptake from 1850 to 2005 are 125 ± 25 PgC [based on the Ocean Carbon-Cycle Model Intercomparison Project (OCMIP) process-based global ocean biogeochemical models forced by observed meteorological fields; C. Le Quéré 2012, personal communication] and 141 ± 27 PgC (Arora et al. 2011). These estimates of net oceanic uptake are very close to the multimodel mean of 127 PgC and the combined range (100–168 PgC) encompasses 13 out of 15 models (Fig. 4). CanESM2 falls just below this range with 95.3-PgC uptake, and INM-CM4.0 falls outside twice this observational uncertainty with 198-PgC uptake. INM-CM4.0 also falls outside the envelope of behavior of the other models and has significantly large interannual variability (see Fig. 4). Analysis of the reasons for this is beyond the scope of this study, but we note that INM-CM4.0 is excluded from our compatible emissions comparison as described above owing to it not representing land-use change.

Under increasing rates of CO_2 rise in the RCP8.5 scenario, models simulate continuing increases in oceanic carbon for most of the century before beginning to level out by 2100, whereas for the peak-and-decline RCP2.6 scenario uptake reduces to close to zero. In the RCP4.5 scenario, atmospheric CO_2 initially exceeds that in the RCP6.0 and hence so do ocean carbon fluxes, although by 2100 uptake under RCP6.0 has increased to exceed that in RCP4.5.

Unlike for cumulative land uptake, intermodel spread within a scenario is typically smaller than the interscenario spread of the model means and so the clusters of simulations for each scenario tend not to overlap much. This is in agreement with feedback analysis of the idealized 1% yr^{-1} CO_2 simulations by Arora et al. (2013). They show that the differences in the modeled responses of the carbon budget to changes in CO_2 and climate are 3–4 times larger for the land components than the ocean components and that the CMIP5 generation of ES-GCMs appear to show closer consensus in their future oceanic uptake than did the C^4MIP carbon cycle models, although the experimental design differs slightly.

c. *Compatible fossil-fuel emissions*

Figure 5 and Table 2 present the diagnosed compatible fossil-fuel emissions based on Eqs. (1) and (2) for the historical and the twenty-first century from the CMIP5 ES-GCMs. For both the twentieth and twenty-first centuries, the multimodel mean fossil-fuel emissions from the ES-GCMs compare well with the observation-based

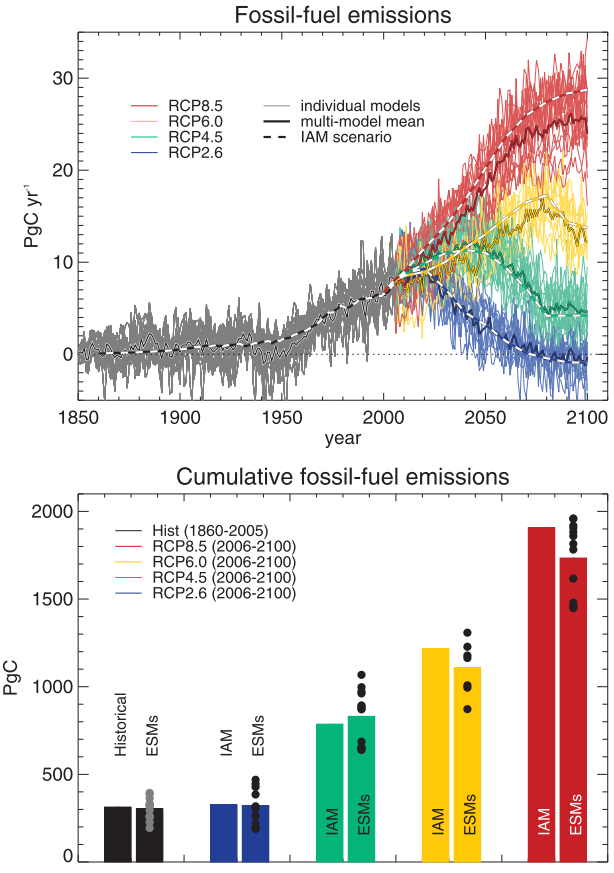

FIG. 5. Compatible fossil-fuel emissions from CMIP5 models for the historical period (black) and the four RCP scenarios for the twenty-first century (colors). (top) Time series of annual emissions: the thick solid lines denote the multimodel mean and the thick dashed lines the historical and RCP scenarios. Individual model estimates are shown in the thin lines. (bottom) Cumulative emissions for historical (1850–2005) and twenty-first century (2006–2100). The left-hand bars in each pair show the cumulative emissions from the historical reconstruction or from the RCP scenario as generated by IAM models, and the right-hand bars the CMIP5 multimodel mean. Black/gray circles show individual model values.

TABLE 2. Compatible fossil-fuel emissions for the historical period and future scenarios as provided by IAMs and as simulated by CMIP5 models. Values (PgC) are rounded to the nearest whole number, and are for the following periods: 1850–2005 (historical) and 2006–2100 (RCPs). The standard deviation across models as well as the full minimum–maximum model range is also given.

			CMIP5 models		
		Obs/IAM	Mean	$\pm 1\sigma$	Min–max range
Historical		313	303	61	194–394
RCP, 2006–2100	2.6	325	322	106	189–469
	4.5	786	831	155	640–1068
	6.0	1217	1107	153	872–1308
	8.5	1907	1734	209	1448–1959

estimates for the historical period and with the emissions the four IAMs generated for each scenario. In the high-end scenarios, RCP8.5 and to a lesser extent RCP6.0, the CMIP5 models on average project lower compatible emissions than the IAMs. This indicates that the sensitivity to climate warming, which leads to reduced natural carbon uptake (Friedlingstein et al. 2006; Arora et al. 2013), is stronger in ES-GCMs than in the IAMs under higher levels of climate change.

The RCP pathways of CO_2 concentration were generated using the Model for the Assessment of Greenhouse-Gas-Induced Climate Change (MAGICC6) calibrated to represent the median of CMIP3 climate models and C^4MIP carbon cycle responses (Meinshausen et al. 2011). Friedlingstein et al. (2012, manuscript submitted to *J. Climate*) show a similar systematic difference between the RCP CO_2 concentrations and the CMIP5 models in the emissions-driven RCP8.5 simulation and attribute this to greater ocean uptake in the MAGICC6 calibration, caused by one or two models in the C^4MIP ensemble having excessive ocean carbon uptake. The CMIP5 models show greater consensus in ocean uptake and this may explain the difference between CMIP5 compatible emissions and the RCP CO_2 pathways.

The RCP2.6 scenario represents an aggressive mitigation scenario aimed at limiting global radiative forcing to be as low as possible by 2100. Here, we assess results from the 10 ES-GCMs that performed this scenario in the context of the achievability of the scenario in terms of the emissions reduction required to follow the CO_2 concentration pathway. We look at implied at mid-century emissions reductions targets and the longer-term implications for the eventual level of emission reductions required by the end of the century. Table 3 shows the compatible fossil-fuel emissions as simulated by the models for decades centered on 1990 and 2050 for RCP2.6, along with the percentage reduction in emissions required by 2050 from 1990 levels to achieve the RCP2.6 peak-and-decline pathway. There is a very large spread in the required percentage reductions by 2050, with values ranging from 14% to 96% for the available models. The average 2050 emissions from these models show a requirement for 50% reductions from the average 1990 emissions.

A key question is whether or not global net negative emissions are required to achieve the target CO_2 pathway in this scenario. Because of interannual variability (largely in the land uptake), many models simulate occasional negative fossil-fuel emissions in some years by 2100, but a more relevant measure is the requirement for long-term average negative emissions. The 10 CMIP5 models analyzed here disagree on this (Fig. 6a).

TABLE 3. Compatible fossil-fuel emissions for the two decades centered on 1990 (1985–95) and 2050 (2045–55) for the 10 models that have supplied enough data to calculate compatible emissions for the RCP2.6. The final column shows the percentage reduction from 1990 levels required by 2050 to achieve the RCP2.6 CO_2 concentration pathway.

Model	1990s emissions	2050s emissions	% reduction
CanESM2	5.15	1.66	68
GFDL-ESM2G	5.16	3.11	40
GFDL-ESM2M	6.16	3.71	40
HadGEM2-ES	5.67	3.05	46
IPSL-CM5A-LR	6.52	4.76	27
IPSL-CM5A-MR	7.15	4.55	36
MIROC-ESM-CHEM	5.75	0.54	91
MIROC-ESM	4.69	0.17	96
MPI-ESM-LR	6.23	5.38	14
BCC-CSM1.1	5.12	2.30	55
Model mean	5.76 ± 0.8	2.92 ± 1.8	50
Historical	6.4 ± 0.5		

To follow the prescribed decrease in atmospheric CO_2 from 443 to 421 ppm, 6 out of 10 models (CanESM2, GFDL-ESM2G, GFDL-ESM2M, MIROC-ESM-CHEM, MIROC-ESM, and BCC-CSM1.1) simulate the need for negative emissions on average from 2080 to 2100 while the other 4 (HadGEM2-ES, IPSL-CM5A-LR, IPSL-CM5A-MR, and MPI-ESM-LR) achieve the scenario without the need for sustained negative emissions. Model CanESM2 projects a requirement for sustained negative emissions from as early as 2060. The six models projecting negative emissions (paler blue in Fig. 6) are consistently lower and with an earlier peak than the four models that do not. They are slightly below the 1990s observed emissions, while the four models projecting sustained positive emissions are slightly above the 1990s estimate. Hence, there is no clear observational constraint on which set of models is more likely to be reliable.

Figure 6b demonstrates additionally if following the RCP2.6 concentration pathway also achieves the commonly cited climate target of restricting warming below 2°C above preindustrial levels. The vertical axis shows the peak twenty-first-century warming and the horizontal axis the average fossil-fuel emission level for the final 20 yr, 2080–2100. As described above, some models show a requirement for net negative emissions and some do not. Similarly, some models simulate global temperature increase above 2°C and some below. Two models, HadGEM2-ES and MPI-ESM-LR, predict that global temperatures can be kept below 2°C warming without the need for negative emissions. Three models, CanESM2 and the two MIROC-ESM variants, show that even with global negative emissions global temperatures may still exceed 2°C.

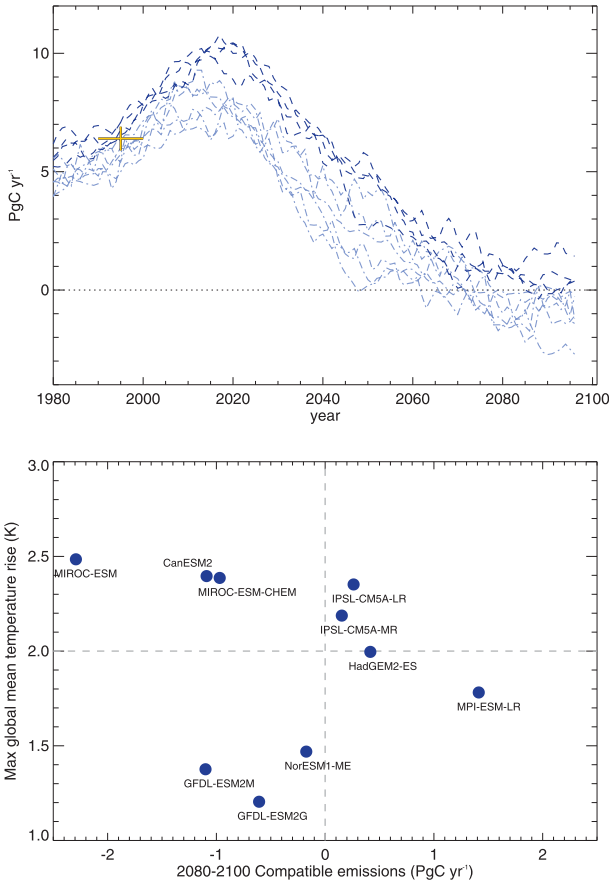

FIG. 6. Compatible fossil-fuel emissions for the peak-and-decline RCP2.6 scenario. (a) Plotted with 10-yr smoothing from CMIP5 models: CanESM2, GFDL-ESM2G, GFDL-ESM2M, MIROC-ESM-CHEM, MIROC-ESM, and NorESM1-ME require sustained negative emissions beyond 2080 and are shown in paler blue dotted–dash lines, and HadGEM2-ES, IPSL-CM5A-LR, IPSL-CM5A-MR, and MPI-ESM-LR are shown in darker blue dashed lines. Historical fossil-fuel emissions for the 1990s are shown by the black and yellow bar. (b) The 20-yr end-of-century average compatible emissions (2080–2100) (x axis) against peak twenty-first-century warming, defined as maximum of 10-yr running mean above preindustrial (y axis).

It remains uncertain therefore, both whether or not the RCP2.6 concentration pathway will restrict global temperatures to below 2°C above preindustrial. It is also uncertain whether this concentration pathway is achievable without the need for active carbon sequestration to globally exceed residual fossil-fuel carbon emissions.

d. Future changes in the airborne fraction

The airborne fraction (AF) of anthropogenic CO_2 emissions is commonly quoted as an instantaneous quantity as the ratio of the change in atmospheric CO_2 for a year to the emissions in that year, although it can also be calculated as a cumulative fraction over a longer

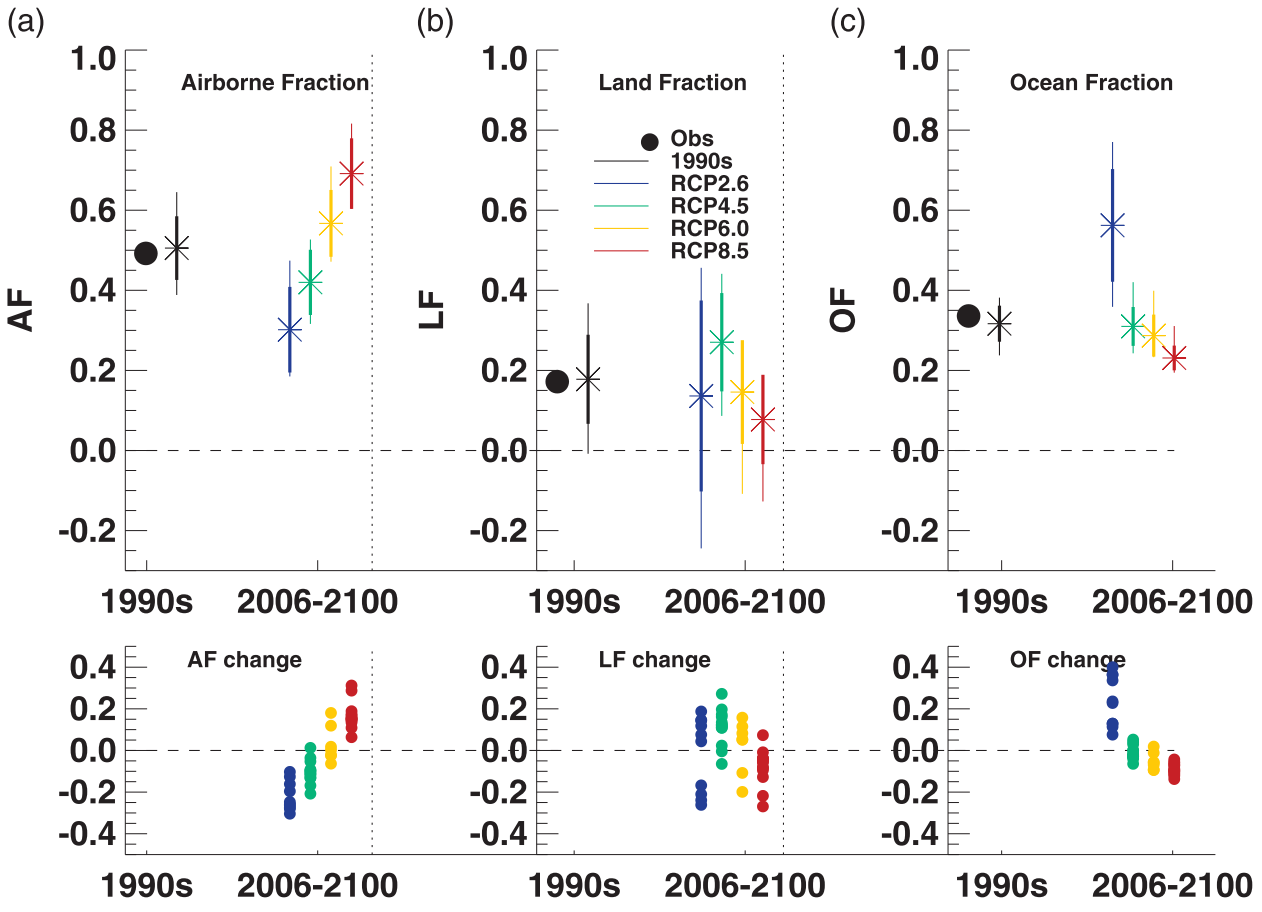

FIG. 7. (top) Changes in (a) airborne, (b) land, and (c) ocean fraction of compatible fossil-fuel emissions. Multimodel mean, ± standard deviation, and range shown by stars and thick and thin vertical lines, respectively, for 1990s (black) and four RCPs (colored). Observational estimate for 1990s is shown as black dots. RCP values are calculated as cumulative over the twenty-first century (defined for RCPs as 2006–2100). (bottom) The changes in each uptake fraction shown for individual models (each dot is a separate model).

period. The airborne fraction can be calculated relative to fossil-fuel emissions (as per Keeling et al. 1995) or more commonly relative to total anthropogenic (fossil + land use) emissions (e.g., Denman et al. 2007; Le Quéré et al. 2009). The observed AF has been relatively constant apart from interannual variability for several decades since direct CO_2 observations began in the late 1950s (Keeling et al. 1995; Denman et al. 2007). Recent studies have claimed a small but measurable upward trend is now detectable in the observations (Canadell et al. 2007; Le Quéré et al. 2009), although uncertainty in land-use emissions makes this detection difficult (Knorr 2009). AF is not simply a constant property of the climate–carbon cycle system but depends strongly on the emissions pathway. Faster increase in emissions implies higher airborne fraction since the land and ocean carbon sinks are unable to keep up with the rate of emissions. Consequently, any deviation from the historical near-exponential increase in anthropogenic emissions may be expected to lead to significant changes in AF (Raupach et al. 2008).

Because of the difficulties of diagnosing land-use emissions consistently from CMIP5 models, we present here explicitly the fossil-fuel AF f_A [see Eq. (4)] calculated from prescribed changes in atmospheric CO_2 and the compatible fossil-fuel emissions from the ES-GCMs presented in section 3c. To prevent large interannual variability affecting our results (especially the case for scenarios where emissions become very small or even zero or negative), we calculate a cumulative f_A over the period 1990–99 and also over 2006–2100 for the four RCPs.

The 1990s value can be compared with observational estimates, which we calculate as 0.49 (average CO_2 increase of 3.15 PgC yr^{-1} and fossil-fuel emissions of 6.4 PgC yr^{-1} for the 1990s). The CMIP5 multimodel mean is 0.52 ± 0.07 (range of 0.45–0.65), with 9 of 13 models falling between 0.45 and 0.55 (Fig. 7).

Figure 7 shows the change of f_A from the 1990s to the twenty-first century from the CMIP5 models for the four RCPs. The figure also shows land and oceanic uptake fractions of fossil fuel f_L and f_O, which are defined

similarly as the fractional uptake of the compatible emissions by land or ocean [Eq. (4)].

A notable feature of the simulations is that during the course of each simulation f_A can vary markedly over the twenty-first century relative to the 1990s. It evolves very differently for different scenarios and even simulated by the same model may increase or decrease, depending on the scenario. From a present-day average value of 0.52 (cf. 0.49 estimated from observations), the models simulate values ranging from 0.18 to 0.82 over the twenty-first century. As may be expected from the theoretical grounds discussed above, in the CMIP5 simulations the lower RCP pathways give rise to lower AF and higher CO_2 concentrations lead to higher AF. All models simulate a decrease in AF for RCP2.6 and all but one simulate a decrease for RCP4.5. All models simulate an increase for RCP8.5. RCP6.0 has on average very small change with four models simulating an increase in AF and three simulating a decrease. Model mean values for the twenty-first-century airborne fraction for each scenario are as follows: 0.30 for RCP2.6; 0.42 for RCP4.5; 0.57 for RCP6.0; and 0.69 for RCP8.5. The emissions pathway is the leading order cause of changes in AF having a greater effect than the climate effect on the carbon cycle. Although there is much model spread in magnitude and change of AF, every model agrees on the order of f_A across scenarios: RCP8.5 $>$ RCP6.0 $>$ RCP4.5 $>$ RCP2.6.

Figure 7b shows future changes in the land fraction of emissions. There is much model spread in this quantity, in part related to the treatment of land-use in these models and in part to how vegetation and soil carbon dynamics are represented in them. Out of 13 models, 11 simulate an increase in f_L for RCP4.5 by on average 0.11 because of a decrease in both crop fraction and pasture fraction and the associated increase in forest area. The RCP6.0 scenario includes a decrease in pasture area but an increase in crop fraction, which combine to give very little change in the average land uptake fraction with five models showing an increase and two showing a decrease. RCP8.5 has large-scale future increases in crop and pasture leading to suppression of the land sink and a small decrease in f_L. A total of 12 out of 13 models agree on a decrease in f_L for RCP8.5. This demonstrates the importance of land use for the future terrestrial carbon store and that this may be of comparable importance to the response of terrestrial carbon to climate or increased CO_2. RCP2.6 has generally the smallest increase in land carbon (Fig. 3a) and much lower compatible emissions than the other scenarios. This combination of smaller numbers in both the numerator and denominator in the land-fraction ratio leads to a much bigger model spread for this scenario with some models showing a large increase and some a large decrease in f_L.

Figure 7c shows twenty-first-century ocean carbon uptake fraction f_O. For two scenarios, RCP6.0 and RCP8.5, there is a common signal across models of reduction in the ocean uptake fraction and small spread across models (consistent with ocean fluxes discussed in section 3b). RCP4.5 has a mixed signal with four models simulating an increase in ocean uptake fraction and nine simulating a decrease. RCP2.6 is a clear outlier in f_O behavior, showing a large increase for all models. Significant model spread can be seen in the RCP2.6 ocean fraction and is explained in this case, not by model spread in oceanic uptake, but by model spread in the compatible emissions. Remember that f_O is defined as the ratio of changes in ocean carbon to compatible emissions, which themselves are sensitive to land uptake changes. Hence, in this analysis, where compatible emissions are diagnosed from simulations with prescribed atmospheric CO_2 pathways, uncertainty in land uptake manifests itself as uncertainty in the fraction of emissions taken up by the ocean even though it does not directly affect the oceanic uptake amount.

4. Conclusions

The global carbon cycle, as well as its response to changing climate and CO_2 concentrations, determines future anthropogenic emissions permitted to follow any given CO_2 pathway and is therefore of relevance to both the scientific and policy communities. The CMIP5 modeling activity provides a coordinated protocol for climate modeling centers to perform concentration-driven simulations for the four representative concentration pathways with state-of-the-art Earth system GCMs in order to diagnose the compatible emissions. Here, we present results from 15 such models although each model may only currently have provided a subset of the required data and scenarios. Compatible fossil-fuel emissions are calculated for 13 models that represent anthropogenic land-use change in their simulations.

The concentration-driven framework for model simulations reduces spread in climate projections by preventing feedback from the carbon cycle onto atmospheric CO_2 and hence climate, but it produces spread in emissions (e.g., see Fig. 2 of Hibbard et al. 2007). The compatible emissions thus derived include uncertainty from all processes (climate, climate–carbon, and carbon concentration) but without these processes operating as fully interactive feedbacks. The emissions-driven framework for model simulations allows full end-to-end uncertainty in CO_2 and climate with fully interactive

feedbacks (Friedlingstein et al. 2012, manuscript submitted to *J. Climate*).

We have shown that there is significant model spread in the diagnosed compatible emissions, dominated by projections of land carbon changes, due in part to the diverse response of land carbon cycle models to changes in CO_2 and climate and widely different treatments of land-use change. We recommend that particular effort is required to better evaluate and improve terrestrial carbon cycle stocks in ES-GCMs. Anav et al. (2013) show a very wide range of vegetation and soil carbon stores simulated and, although there is not a one-to-one relation between present stocks and future changes, it is clearly a priority for ES-GCMs to better represent the magnitude of carbon amounts before we can have confidence in projections of future changes.

We find that land carbon storage may increase or decrease in future dependent on scenario and the treatment of future land-use change, although most models simulate an increase for most scenarios. The spread in land carbon uptake among models is as high as across the RCP scenarios. Models largely agree that ocean carbon storage will increase under all scenarios, with higher atmospheric CO_2 driving greater ocean carbon uptake. Projections of ocean carbon changes show much greater agreement than projections of land carbon changes. Overall, uncertainty in concentration scenario is the major cause of uncertainty in emissions (and airborne fraction) and not uncertainty in climate–carbon cycle processes.

CMIP5 simulated compatible fossil-fuel emissions for the historical period (303 ± 61 PgC) agree closely with historical estimates (313 PgC), as do CMIP5 model mean uptake amounts for the land and ocean individually. CMIP5 Earth system GCMs also show close agreement with the low RCPs (RCP2.6 and RCP4.5). For RCP6.0 and especially RCP8.5 they simulate systematically lower carbon uptake and therefore lower compatible emissions than the RCP scenarios generated by the MAGICC6 model calibrated to CMIP3 climate and C^4MIP carbon cycle GCMs.

Compatible emissions for the four RCPs (defined for the period 2006–2100) range from 332 to 1734 PgC for RCP2.6–RCP8.5. For the period 2000–50, model-mean cumulative emissions range from 337 PgC for RCP2.6 to 602 PgC for RCP8.5, with RCP4.5 and RCP6.0 having very similar totals over this period of 523 and 453 PgC, respectively. RCP6.0 exceeds RCP4.5 later in the century. For RCP2.6 models simulate a requirement on average for 50% emissions reductions by 2050 relative to 1990 levels but with very large model spread in this measure from 14% to 96%. The Integrated Model to Assess the Global Environment (IMAGE), which generated the RCP2.6 scenario, projected the need for globally negative emissions from 2070 to 2100 in order to achieve the peak-and-decline CO_2 pathway. We find that 6 out of 10 complex Earth system models also simulate a need for negative emissions, while 4 do not.

Future airborne fraction, averaged over the twenty-first century, is found to be strongly dependent on the anthropogenic emissions scenario as are the fractions of emissions taken up by land and ocean. All models agree that the higher the atmospheric CO_2 scenario, the higher the airborne fraction and the lower the ocean uptake fraction. The land uptake fraction is sensitive to both the CO_2 and climate scenario but also strongly depends on the land-use change assumed, which is not necessarily related to global CO_2 levels. Out of 13 models, 11 agree that the mid–low CO_2 scenario, RCP4.5, has the highest land-uptake fraction during the twenty-first century because of decreases in areas of agriculture and increases in forest extent. Increases in land-use areas in RCP2.6 and RCP8.5 lead to reduced land-uptake fractions in these scenarios.

Acknowledgments. MOHC authors were supported by the Joint DECC/Defra Met Office Hadley Centre Climate Programme (GA01101), and work to perform HadGEM2-ES and MPI-ESM CMIP5 simulations was supported by the EU-FP7 COMBINE project (Grant 226520). JS was supported by the EU-FP7 CARBOCHANGE project (Grant 284679). We acknowledge the World Climate Research Programme's Working Group on Coupled Modelling, which is responsible for CMIP, and we thank the climate modeling groups (listed in Table 1 of this paper) for producing and making available their model output. For CMIP, the U.S. Department of Energy's Program for Climate Model Diagnosis and Intercomparison provides coordinating support and led development of software infrastructure in partnership with the Global Organization for Earth System Science Portals. JT and CR were supported by the Research Council of Norway through the EarthClim (207711/E10) project.

APPENDIX

Diagnosing Emissions from Changes in Carbon Stores

Figure A1 shows schematically how the carbon pools that are represented in these models respond to fossil-fuel emissions and emissions from land-use/land-cover change. We regard the atmosphere–land–ocean system as a closed system here, as none of these models represent the longer-term fluxes due to rock weathering, volcanism, etc. Thus, without perturbation, the total system

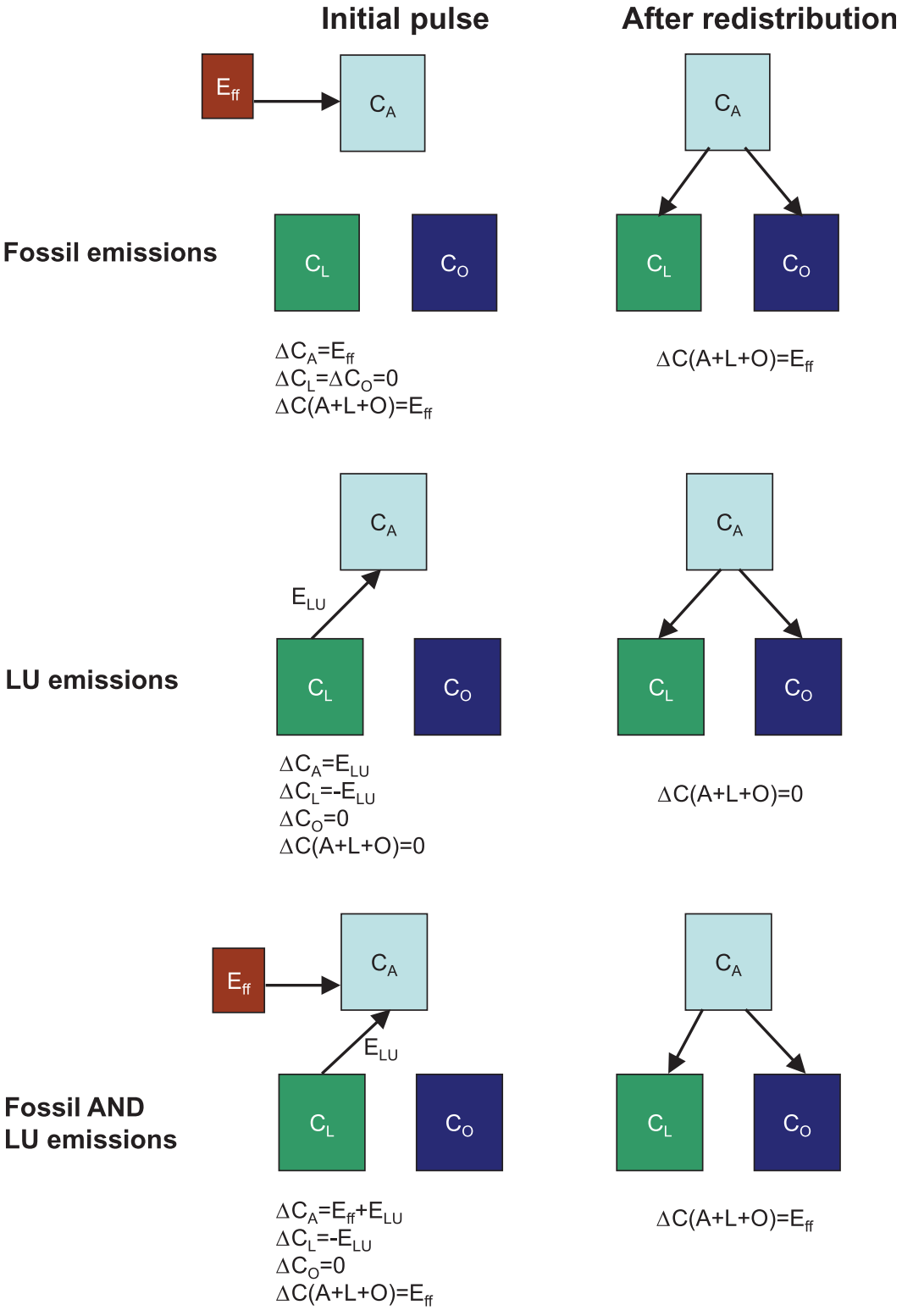

FIG. A1. Schematic demonstrating the difference between fossil and land-use CO_2 emissions in a closed atmosphere–land–ocean system. (top) Fossil-fuel emissions represent an addition of new carbon to the system, initially to the atmosphere, but after redistribution between the component reservoirs the total perturbed amount is conserved. (middle) Land-use emissions represent an initial movement of carbon from the land to atmosphere with zero net change in the system. Even after redistribution, between the components the net change remains zero. When both fossil and land-use emissions are present, they combine such that the total carbon in the system only changes by the fossil-fuel input, with land-use emissions again having no net impact on the system total.

carbon, $C_{\mathrm{Tot}} = C_A + C_L + C_O$, remains constant in time: $\Delta C_{\mathrm{Tot}} = 0$. By using ocean flux to diagnose changes in ocean storage, sedimentation, which is included in some models can be seen as an internal partitioning within a generic ''ocean carbon'' pool in this analysis.

The top panel of Fig. A1 shows the evolution of the system in response to fossil-fuel emissions: when fossil fuel is added, the total system carbon increases by E_F: all of which is initially in the atmosphere. After some finite time the system has responded (not necessarily reaching equilibrium) by repartitioning the added carbon among its reservoirs, but the total system carbon has not changed and, relative to the unperturbed state, $\Delta C_{\mathrm{Tot}} = E_F$. The same is true for a transient, continued (but time varying) emission. At any point in time, the rate of change of total carbon is given by the emission rate E_{ff} and the total change in system carbon by the cumulative emission,

$$\frac{dC_{\mathrm{Tot}}}{dt} = E_{\mathrm{ff}}$$

$$\Delta C_{\mathrm{Tot}} = \int_0^t E_{\mathrm{ff}}\, dt.$$

Conversely, the middle panel of Fig. A1 shows the system response to a land-use change. In this case, some externally forced disturbance event acts to repartition some of the land carbon initially into the atmosphere, such that $\Delta C_L = -E_{\mathrm{LUC}}$ and $\Delta C_A = E_{\mathrm{LUC}}$. Initially, ΔC_O is zero, and so the total system carbon is unchanged, $\Delta C_{\mathrm{Tot}} = 0$. After some time, the system may respond to move carbon between the reservoirs (e.g., ΔC_O may change), but overall $\Delta C_{\mathrm{Tot}} = 0$. In other words, land-use change may represent a strong perturbation to the land carbon and ultimately to all the three reservoirs individually, but as a closed system it does not change the total amount of carbon. Note that in each case the fossil or land-use emissions may be positive or negative: removal (such as through forest regrowth or deliberate carbon dioxide removal) as well as emission is treated in conceptually the same way.

The bottom panel of Fig. A1 shows the response to both fossil and land-use emissions together. Although the specific effects of the emissions (and indeed any changes in climate) on the individual carbon reservoirs may not be the simple sum of the two sources of emissions, the net effect on the system total carbon is simply that due to fossil emissions: $\Delta C_{\mathrm{Tot}} = E_F$. The land-use emissions have had no net effect on the total carbon in the system.

This schematic represents how the CMIP5 ES-GCMs behave in ''emissions driven'' simulations and how the real world behaves on time scales where other long-term sources/sinks of carbon can be neglected (typically up to a few centuries). However, for the ''concentration driven'' simulations analyzed here, the system is not balancing and conserving carbon in this way. Emissions do not exist as an input to the system, but rather the evolution of C_A is forced to follow a predefined pathway used as an input to the models. Here, C_L and C_O respond to this concentration and also to any changes in climate and in response to prescribed land-use disturbance but do not affect C_A itself. In this case the system total carbon evolves in time: $\Delta C_{\mathrm{Tot}} \neq 0$. By analogy to the schematic in Fig. A1a, we can see that the time evolution of ΔC_{Tot} is the fossil-fuel emission E_F and not the total $E_F + E_{\mathrm{LUC}}$. In other words, in order to recreate the CO_2 concentration pathway in an emissions-driven setup, one would prescribe this diagnosed emission as the fossil-fuel input to the system. In these simulations, therefore, the effect of land use will be to perturb the land carbon cycle and to affect how carbon is partitioned between the three reservoirs.

REFERENCES

Anav, A., and Coauthors, 2013: Evaluating the land and ocean components of the global carbon cycle in the CMIP5 Earth system models. *J. Climate,* in press.

Arora, V. K., and G. J. Boer, 2010: Uncertainties in the 20th century carbon budget associated with land use change. *Global Change Biol.,* **16,** 3327–3348.

——, and Coauthors, 2011: Carbon emission limits required to satisfy future representative concentration pathways of greenhouse gases. *Geophys. Res. Lett.,* **38,** L05805, doi:10.1029/2010GL046270.

——, and Coauthors, 2013: Carbon–concentration and carbon–climate feedbacks in CMIP5 Earth system models. *J. Climate,* in press.

Booth, B. B. B., and Coauthors, 2012: High sensitivity of future global warming to land carbon cycle processes. *Envon. Res. Lett.,* **7,** 024002, doi:10.1088/1748-9326/7/2/024002.

Brovkin, V., and Coauthors, 2013: Effect of anthropogenic land-use and land-cover changes on climate and land carbon storage in CMIP5 projections for the twenty-first century. *J. Climate,* in press.

Canadell, J. G., and Coauthors, 2007: Contributions to accelerating atmospheric CO_2 growth from economic activity, carbon intensity, and efficiency of natural sinks. *Proc. Nat. Acad. Sci. USA,* **104,** 18 866–18 870.

Denman, K. L., and Coauthors, 2007: Couplings between changes in the climate system and biogeochemistry. *Climate Change 2007: The Physical Science Basis,* S. Solomon et al., Eds., Cambridge University Press, 499–587.

Friedlingstein, P., and Coauthors, 2006: Climate–carbon cycle feedback analysis: Results from the C^4MIP model intercomparison. *J. Climate,* **19,** 3337–3353.

Gullison, R. E., and Coauthors, 2007: Tropical forests and climate policy. *Science,* **316,** 985–986, doi:10.1126/science.1136163.

Hibbard, K. A., G. A. Meehl, P. Cox, and P. Friedlingstein, 2007: A strategy for climate change stabilization experiments. *Eos, Trans. Amer. Geophys. Union,* **88,** 217, doi:10.1029/2007EO200002.

Houghton, R. A., cited 2008: Carbon flux to the atmosphere from land-use changes: 1850–2005. Trends: A compendium of data on global change, U.S. Department of Energy Oak Ridge National Laboratory Carbon Dioxide Information Analysis Center. [Available online at http://cdiac.ornl.gov/trends/landuse/houghton/houghton.html.]

Hurtt, G., and Coauthors, 2011: Harmonization of land-use scenarios for the period 1500–2100: 600 years of global gridded annual land-use transitions, wood harvest, and resulting secondary lands. *Climatic Change,* **109,** 117–161, doi:10.1007/s10584-011-0153-2.

Johns, T. C., and Coauthors, 2011: Climate change under aggressive mitigation: The ENSEMBLES multi-model experiment. *Climate Dyn.,* **37,** 1975–2003, doi:10.1007/s00382-011-1005-5.

Jones, C. D., P. M. Cox, and C. Huntingford, 2006: Climate-carbon cycle feedbacks under stabilization: Uncertainty and observational constraints. *Tellus,* **58B,** 603–613.

Keeling, C. D., T. Whorf, M. Whalen, and J. V. der Plicht, 1995: Interannual extremes in the rate of rise of atmospheric carbon dioxide since 1980. *Nature,* **375,** 666–670.

Knorr, W., 2009: Is the airborne fraction of anthropogenic CO_2 emissions increasing? *Geophys. Res. Lett.,* **36,** L21710, doi:10.1029/2009GL040613.

Le Quéré, C., and Coauthors, 2009: Trends in the sources and sinks of carbon dioxide. *Nat. Geosci.,* **2,** 831–836, doi:10.1038/ngeo689.

Matthews, H. D., 2006: Emissions targets for CO_2 stabilization as modified by carbon cycle feedbacks. *Tellus,* **58B,** 591–602.

Meinshausen, M., and Coauthors, 2011: The RCP greenhouse gas concentrations and their extension from 1765 to 2300. *Climatic Change,* **109,** 213–241, doi:10.1007/s10584-011-0156-z.

Moss, R., and Coauthors, 2010: The next generation of scenarios for climate change research and assessment. *Nature,* **463,** 747–756.

Plattner, G.-K., and Coauthors, 2008: Long-term climate commitments projected with climate–carbon cycle models. *J. Climate,* **21,** 2721–2751.

Prentice, I. C., and Coauthors, 2001: The carbon cycle and atmospheric carbon dioxide. *Climate Change 2001: The Scientific Basis,* J. T. Houghton et al., Eds., Cambridge University Press, 183–238.

Raupach, M. R., J. G. Canadell, and C. Le Quéré, 2008: Anthropogenic and biophysical contributions to increasing atmospheric CO_2 growth rate and airborne fraction. *Biogeosciences,* **5,** 1601–1613.

Sabine, C. L., and R. A. Feely, 2007: The oceanic sink for carbon dioxide. *Greenhouse Gas Sinks,* D. S. Reay et al., Eds., CABI, 31–49.

Taylor, K. E., R. J. Stouffer, and G. A. Meehl, 2012: An overview of CMIP5 and the experiment design. *Bull. Amer. Meteor. Soc.,* **93,** 485–498.

Todd-Brown, K. E. O., J. T. Randerson, W. M. Post, F. M. Hoffman, C. Tarnocai, E. A. G. Schuur, and S. D. Allison, 2013: Causes of variation in soil carbon simulations from CMIP5 Earth system models and comparison with observations. *Biogeosciences,* **10,** 1717–1736, doi:10.5194/bg-10-1717-2013.

Trudinger, C. M., I. G. Enting, P. J. Rayner, and R. J. Francey, 2002: Kalman filter analysis of ice core data 2. Double deconvolution of CO_2 and $\delta^{13}C$ measurements. *J. Geophys. Res.,* **107,** 4423, doi:10.1029/2001JD001112.

van Vuuren, D. P., and Coauthors, 2011: The representative concentration pathways: An overview. *Climatic Change,* **109,** 5–31, doi:10.1007/s10584-011-0148-z.

4.3. Paris agreement and low CO_2 pathways

A development from the concept of compatible emissions was the link between climate warming and total emissions of carbon. Initially there was a lot of focus on how to derive specific pathways to achieve a long-term temperature goal. Wigley et al. (1996) derived the "WRE" scenarios (so-called after the authors, Wigley, Richels and Edmonds) and these were slightly different from the "S" (stabilisation) scenarios of Enting et al. (1994). Some were idealised conceptual pathways based on smooth mathematical functions, others involved assumptions about smooth rates of decrease of fossil fuel dependence, or followed existing scenarios until a given date before diverging onto a stabilisation pathway. The result was that constraints from physical sciences (climate and carbon cycle feedbacks) became intricately mixed with constraints from technological and socio-economic communities (such as infrastructure lock-in and maximal rates of decarbonisation). In 2009 two papers presented the idea that the two could be separated by noting that the degree of global warming was much more closely linked to the total (cumulative) carbon emissions than it was to the time profile or pathway of the emissions. I was a co-author on a study by **Allen et al. (2009)** which, along with a similar study by Matthews et al. (2009), both demonstrated this and discussed how this would simplify the mitigation problem: the climate-carbon cycle system would determine the total carbon emissions compatible with a climate target, but then social sciences and available technology could determine the most cost-optimal method of achieving this. This former quantity – the total carbon emissions compatible with a target – can therefore be seen as a budget. The world has a quantifiable "carbon budget" which it can "spend". The timing of how we spend (burn) it does not strongly affect the eventual warming, and so it is a societal choice whether we spend our budget in the near term or save more for future generations.

Now that nations have adopted the Paris Agreement, which entered into force in November 2016, the requirement to quantify carbon budgets for low climate targets has grown. IPCC AR5 assessed a total carbon budget of 790 PgC to likely (66% chance) remain below 2^{o}C, of which 565 PgC has already been emitted by 2016 (Le Quéré et al., 2016). However, the uncertainty in the remaining carbon budget to

achieve 1.5 or 2°C is very large – of the order of 100s PgC. This large uncertainty hinders the potential usefulness to policy makers of quantified carbon budgets.

Earth System Modelling therefore has a clear and high priority remit to address and reduce this uncertainty. To date almost all carbon cycle modelling and feedback analysis has focussed on high, monotonic CO_2 scenarios (see Figure 12): from IS92a (**Cox et al., 2000**) to SRES-A2 (**Friedlingstein et al., 2006**) to the RCP8.5 and 1% idealised experiments of CMIP5 (**Arora et al., 2013; Friedlingstein et al., 2014**). In contrast, RCP2.6 peaks CO_2 at 443 ppm by 2050, just 40ppm above 2016 levels. Although we know that the carbon cycle may behave differently under low scenarios such as RCP2.6, very little specific feedback analysis has been conducted on low stabilisation or peak-and-decline scenarios.

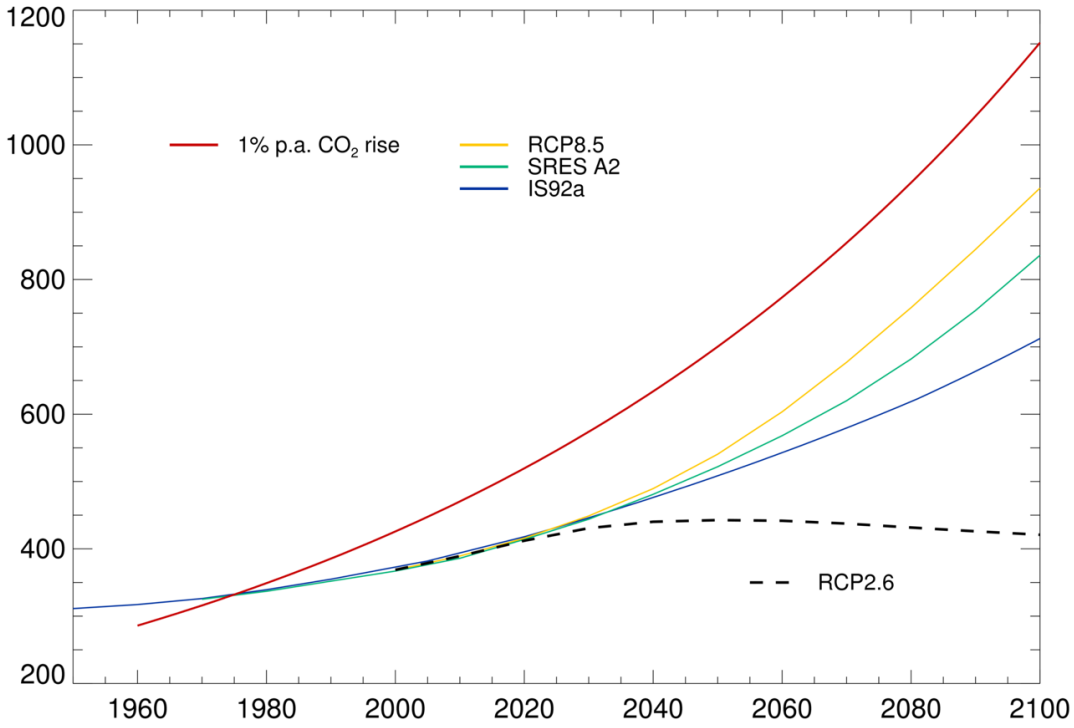

Figure 12. CO_2 concentration scenarios widely used for carbon cycle simulations – previous analysis has focused on rapid/monotonic increase. For example, **Cox et al. (2000)** used IS92a (blue line), the first C4MIP (**Friedlingstein et al., 2006**) used SRES A2 (green line) and CMIP5 simulations drew on both 1% per annum increase (red line: **Arora et al., 2013; Ciais et al., 2013**) and RCP8.5 (yellow line: **Friedlingstein et al., 2014**; Collins et al., 2013). Note 1% per annum increase nominally begins in 1850 but plotted here relative to 1960 for ease of comparison on

this schematic figure. A more relevant scenario which should be used is RCP2.6 (black dashed line).

Scenarios which achieve 2°C almost always rely on large amounts of active CO_2 removal from the atmosphere. For example, RCP2.6 which peaks at 443 ppm before declining to 420ppm by 2100 cannot be achieved by natural carbon sinks alone (**Jones et al., 2013**), and requires active removal of CO_2 from the atmosphere by human activity (van Vuuren et al., 2011). This is known as carbon dioxide removal (CDR) or negative emissions techniques (NETs) – see Glossary. It seems inevitable therefore that future emissions scenarios will deviate very strongly indeed from continued exponential increase and therefore that the future airborne fraction may depart from its historical value of approximately half. Crucial questions to address, therefore, are how the carbon cycle responds to negative emissions and whether or not climate-carbon cycle feedbacks behave in the same way as under high CO_2 scenarios.

A key requirement for low carbon pathways is to quantify the effectiveness of negative emissions technologies which will be strongly affected by carbon cycle feedbacks (see chapter 3). I led an analysis, **Jones et al. (2016b**) which forms the rest of this section in which we explore the carbon cycle response to a low overshoot scenario (RCP2.6). We found that ESMs suggest significant weakening, even potential reversal, of the ocean and land sinks under future low emission scenarios. In the same way that sinks respond to positive emissions (by absorbing more carbon from the atmosphere) they may respond to negative emissions by absorbing *less*. This behaviour is expected and has been described before in intermediate complexity models (e.g. Cao and Caldeira, 2010). In this paper, we see it consistently in CMIP5 ESM simulations of RCP2.6. For the RCP2.6 concentration pathway, models project land and ocean sinks to weaken to 0.8±0.9 and 1.1±0.3 $PgCyr^{-1}$ respectively for the second half of the 21st century and to −0.4±0.4 and 0.1±0.2 $PgCyr^{-1}$ respectively for the second half of the 23rd century.

The analysis was featured in the Met Office Hadley Centre science brochure presented at COP22 (22nd Conference of the Parties to the UNFCCC) in 2016

(http://www.metoffice.gov.uk/climate-guide/science/uk/cop/cop22). Weakening of natural carbon sinks in response to removal of CO_2 hinders the effectiveness of the negative emissions. The paper concludes that “Failure to accurately account for carbon cycle feedbacks which increase the need for such negative emissions may strongly and adversely affect the feasibility of achieving these targets.”

Environmental Research Letters

LETTER

Simulating the Earth system response to negative emissions

C D Jones[1], P Ciais[2], S J Davis[3], P Friedlingstein[4], T Gasser[2,5], G P Peters[6], J Rogelj[7,8], D P van Vuuren[9,10], J G Canadell[11], A Cowie[12], R B Jackson[13], M Jonas[14], E Kriegler[15], E Littleton[16], J A Lowe[1], J Milne[17], G Shrestha[18], P Smith[19], A Torvanger[6] and A Wiltshire[1]

[1] Met Office Hadley Centre, FitzRoy Road, Exeter, EX1 3PB, UK
[2] Laboratoire des Sciences du Climat et de l'Environnement, CEA CNRS UVSQ, Gif-sur-Yvette, France
[3] Department of Earth System Science, University of California, Irvine, USA
[4] College of Engineering, Mathematics and Physical Sciences, University of Exeter, Exeter EX4 4QE, UK
[5] Centre International de Recherche en Environnement et Développement, CNRS-PontsParisTech-EHESS-AgroParisTech-CIRAD, F-94736 Nogent-sur-Marne, France
[6] Center for International Climate and Environmental Research—Oslo (CICERO), Gaustadalléen 21, NO-0349 Oslo, Norway
[7] Energy Program, International Institute for Applied Systems Analysis, Schlossplatz 1, A-2361 Laxenburg, Austria
[8] Institute for Atmospheric and Climate Science, ETH Zurich, Universitätstrasse 16, 8092 Zurich, Switzerland
[9] PBL Netherlands Environmental Assessment Agency, The Netherlands
[10] Copernicus Institute for Sustainable Development, Utrecht University, The Netherlands
[11] Global Carbon Project, CSIRO Oceans and Atmosphere Research, GPO Box 3023, Canberra, Australian Capital Territory 2601, Australia
[12] NSW Department of Primary Industries, University of New England, Armidale NSW 2351, Australia
[13] Department of Earth System Science, Woods Institute for the Environment and Precourt Institute for Energy, Stanford University, Stanford, CA 94305, USA
[14] Advanced Systems Analysis Program, International Institute for Applied Systems Analysis, Schlossplatz 1, A-2361 Laxenburg, Austria
[15] Potsdam Institute for Climate Impact Research (PIK), PO Box 60 12 03, D-14412 Potsdam, Germany
[16] University of East Anglia, Norwich Research Park, Norwich NR4 7TJ, UK
[17] Stanford University 473 Via Ortega, Stanford, CA 94305-2205, USA
[18] US Carbon Cycle Science Program, US Global Change Research Program, Washington, DC 20006, USA
[19] Institute of Biological and Environmental Sciences, University of Aberdeen, 23 St Machar Drive, Aberdeen, AB24 3UU, UK

E-mail: chris.d.jones@metoffice.gov.uk

Keywords: climate, carbon cycle, earth system, negative emissions, carbon dioxide removal, mitigation scenarios

Supplementary material for this article is available online

OPEN ACCESS

RECEIVED
24 March 2016

REVISED
26 August 2016

ACCEPTED FOR PUBLICATION
26 August 2016

PUBLISHED
20 September 2016

Abstract

Natural carbon sinks currently absorb approximately half of the anthropogenic CO_2 emitted by fossil fuel burning, cement production and land-use change. However, this airborne fraction may change in the future depending on the emissions scenario. An important issue in developing carbon budgets to achieve climate stabilisation targets is the behaviour of natural carbon sinks, particularly under low emissions mitigation scenarios as required to meet the goals of the Paris Agreement. A key requirement for low carbon pathways is to quantify the effectiveness of negative emissions technologies which will be strongly affected by carbon cycle feedbacks. Here we find that Earth system models suggest significant weakening, even potential reversal, of the ocean and land sinks under future low emission scenarios. For the RCP2.6 concentration pathway, models project land and ocean sinks to weaken to 0.8 ± 0.9 and 1.1 ± 0.3 GtC yr^{-1} respectively for the second half of the 21st century and to -0.4 ± 0.4 and 0.1 ± 0.2 GtC yr^{-1} respectively for the second half of the 23rd century. Weakening of natural carbon sinks will hinder the effectiveness of negative emissions technologies and therefore increase their required deployment to achieve a given climate stabilisation target. We introduce a new metric, the perturbation airborne fraction, to measure and assess the effectiveness of negative emissions.

1. Introduction

In the recently adopted UN Paris Agreement on climate change, countries agreed to focus international climate policy on keeping global mean temperature increase well below 2 °C above pre-industrial levels and pursue actions to further limit warming to 1.5 °C (UNFCCC 2015). Scenarios consistent with such

targets typically require large amounts of carbon dioxide removal (Clarke *et al* 2014, Gasser *et al* 2015, Rogelj *et al* 2015), achieved by deliberate human efforts to remove CO_2 from the atmosphere. Negative emissions technologies (NETs) are therefore present in the majority of scenarios that give a more than 50% chance of limiting warming to below 2 °C (Fuss *et al* 2014) and all scenarios that give more than a 50% chance of staying below 1.5 °C (Rogelj *et al* 2015).

In low emission pathways, the presence of NETs offsets continued positive emissions from fossil fuels and land-use change to strongly reduce the anthropogenic input into the atmosphere. In some cases it even reverses the sign so that the effect of human activity is a net flow out of the atmosphere ('net negative emissions'). Gasser *et al* (2015) stress the need to separately quantify the magnitude of continued positive emissions and the amount of carbon removed by negative emission technologies.

Fuss *et al* (2014) called for renewed efforts to develop a consistent and comprehensive narrative around NETs and the need to develop a framework for examining implications of NETs in a wider context. Smith *et al* (2016) reviewed costs and biophysical limits associated with different NET technologies. Research into NETs needs to address both demand-side (how much NETs are required?) and supply-side (how much NETs are possible?) questions. This paper specifically explores the Earth system responses to different amounts of negative emissions. Understanding of the behaviour of natural carbon sinks is crucial to quantify the demand for NETs to achieve climate targets.

Although the natural carbon cycle is now commonly represented in Earth system models (ESMs), there has been little specific analysis of the behavior of different components of the carbon cycle when forced by net negative emissions. Previous analysis of CMIP5 ESMs has shown that approximately half of the models require globally net negative emissions for CO_2 to follow the RCP2.6 pathway (Jones *et al* 2013). Tokarska and Zickfeld (2015) used an ESM of intermediate complexity to simulate the response to a range of future NET scenarios. It is known that redistribution across natural carbon stocks weakens the effect of negative emissions on atmospheric CO_2 (see e.g. Cao and Caldeira 2010, Matthews 2010, Ciais *et al* 2013, MacDougall 2013). Reducing the amount of CO_2 in the atmosphere reduces the natural carbon sinks due to the fact that vegetation productivity will decrease when CO_2 decreases and that ocean CO_2 uptake will also decrease with decreasing CO_2.

In this paper, we assess the impact on the global carbon cycle across different time horizons and consider different balances of emissions and fluxes, and how the natural carbon cycle responds. For this, we use, for the first time, CMIP5 model simulations to quantify how the Earth system may respond to NETs, and how this response may depend on the state of the climate and the background scenario.

We stress the need to know *quantitatively* what happens to this redistribution of carbon under specific scenarios in order to both plan the requirement for NETs, and to understand their effectiveness and any implications or side effects. Despite the fact that they lack some important processes such as permafrost carbon, process-based and spatially explicit ESMs remain an essential tool for this exploration. Reducing uncertainty in projected carbon sinks behaviour, especially under low emissions scenarios, is a pressing research priority.

Section 2 of this paper draws on existing CMIP5 ESM simulations of the RCP2.6 scenario, extended to 2300 with sustained global negative emissions, and section 3 makes use of a simple climate-carbon cycle model to explore the scenario dependence of the response of carbon sinks to negative emissions.

2. Earth system response over time

The contemporary carbon cycle can be summarised at a global scale: human activity puts CO_2 into the atmosphere, natural sinks remove about half of those emissions and the remainder accumulates in the atmosphere such that atmospheric CO_2 concentrations increase (figure 1). Since pre-industrial times, human activity has always resulted in net positive emissions to the atmosphere, leading to an increase of atmospheric CO_2 concentration, from about 288 to 400 ppm over the last 150 years or so. Natural ecosystems, both land and oceans, have been persistent sinks of CO_2 (Le Quéré *et al* 2015).We will build on figure 1 throughout this paper to depict schematically how the carbon cycle responds to carbon dioxide removal.

Different types of anthropogenic activity have different effects on the Earth system and carbon pools. Figure 2 shows schematically how each pool is affected by direct anthropogenic activity and subsequent redistribution between pools. We restrict consideration here to those carbon pools which respond on timescales up to a few centuries. By this we mean the atmosphere; the land vegetation and near surface (top metre or so) soil organic matter but not deep permafrost or geologically stored carbon; and the ocean store of dissolved (organic or inorganic) carbon and biomass in various forms of plankton, but not ocean sediments.

Land-use change, mainly in the form of deforestation, was the first major human perturbation to the carbon cycle (Le Quéré *et al* 2015). Its net result was to move carbon from the land pool (L) to the atmosphere (A) (shown in figure 2(a)). Over time, natural sinks redistributed part of this additional carbon in the atmosphere between the other pools. Atmospheric CO_2 (A) increases, but the total mass of carbon (A+L +O) is not changed.

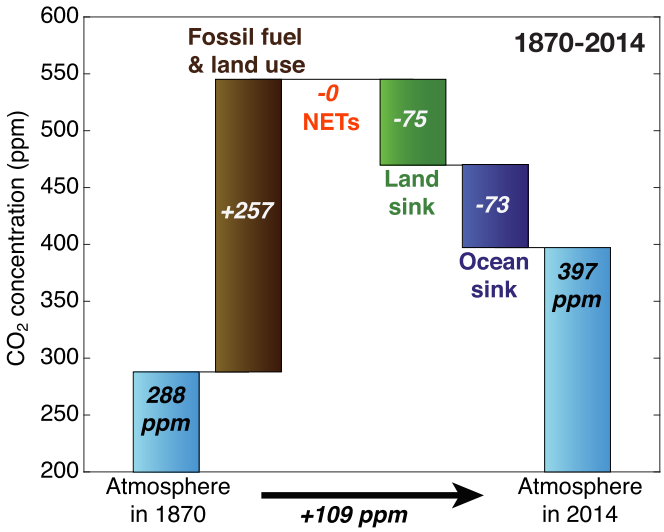

Figure 1. Summary of changes in the global carbon budget since 1870. (Redrawn based on http://folk.uio.no/roberan/img/GCP2015/PNG/s15_Waterfall_sources_and_sinks.png). Atmospheric CO_2 concentration has changed from about 288 ppm in 1870 to 397 in 2014 due to emissions from fossil fuel burning and land-use change and natural sinks on land and ocean. For consistency with later analysis we introduce a bar to this figure to represent NETs, but its magnitude over this period has been zero. For full details of the global carbon budget see Le Quéré *et al* (2015).

Since about 1950, the burning of fossil fuel represents a larger source of CO_2 to the atmosphere than land-use change and this has a different effect on the carbon cycle (figure 2(b)) because carbon originating from a separate reservoir is introduced, firstly to the atmosphere and subsequently partly redistributed between the land and ocean. A major difference from land-use emissions is that the total amount of carbon in the atmosphere-land-ocean system increases. This is depicted in figure 2 by an increased size of the pie chart in row b relative to the original size, shown by the dotted circle.

Figure 2 then shows two possible ways of obtaining carbon-neutral energy. The first is through use of bioenergy (figure 2(c)) whereby carbon is first drawn down from the atmosphere by vegetation growth and stored in biomass (arrow '1' in figure 2(c)) before this biomass is burned to release energy, releasing the stored carbon back to the atmosphere (arrow '2' in figure 2(c)). We note that the drawdown of carbon into vegetation may have occurred many years prior to the burning of the fuel, and so the concept of bioenergy being carbon neutral is not necessarily true on short timescales (Cherubini *et al* 2011). The fourth row in figure 2 then shows how fossil fuel can be burned, but can be brought to being approximately carbon neutral by using carbon capture and storage technology (CCS). In reality not all the carbon will be captured (IPCC 2005, Benson *et al* 2012), and some may escape during the capture, transport and ultimate storage processes, but conceptually the figure captures the intention of CCS to enable low-carbon fossil fuel use.

Now we consider the role of NETs. If CO_2 is removed from the atmosphere and stored in land vegetation and soils (e.g. by afforestation) then the total amount of carbon (A+L+O) does not change and in the context of this figure, this is just a form of land-use change. However, if the NET employed stores the carbon in a geological formation (or deep ocean or inert soil pool), as depicted in figure 2(e), then the size of the active carbon cycle is reduced (smaller pie chart in row e). The figure shows two specific activities: bioenergy with carbon capture and storage (BECCS) removes carbon from the atmosphere via the land (arrows 1 and 2) whereas direct air capture removes it directly from the atmosphere. Other NETs could also be depicted in a similar way but we show just two here for clarity. In the same way that additions to the atmosphere lead to redistributions of carbon to land and ocean, removal from the atmosphere also leads to redistribution between the three pools (Cao and Caldeira 2010).

2.1. Research questions

All these anthropogenic activities have substantially different effects on the Earth system, but one common theme (except for CCS in an idealised case) is the redistribution of carbon between reservoirs, which continues for some time after the initial activity. For all actions depicted in figure 2, the long-term response (in the right hand columns) differs from the immediate effect shown in the left-hand column. In order to understand the impact of any action we need to quantitatively understand how this redistribution will operate at the process level. The natural carbon sinks that drive this redistribution are affected by the prevailing climate and CO_2 concentration and also historical changes in their environmental conditions.

In scenarios where CO_2 growth slows and CO_2 concentration either stabilizes, or even peaks and

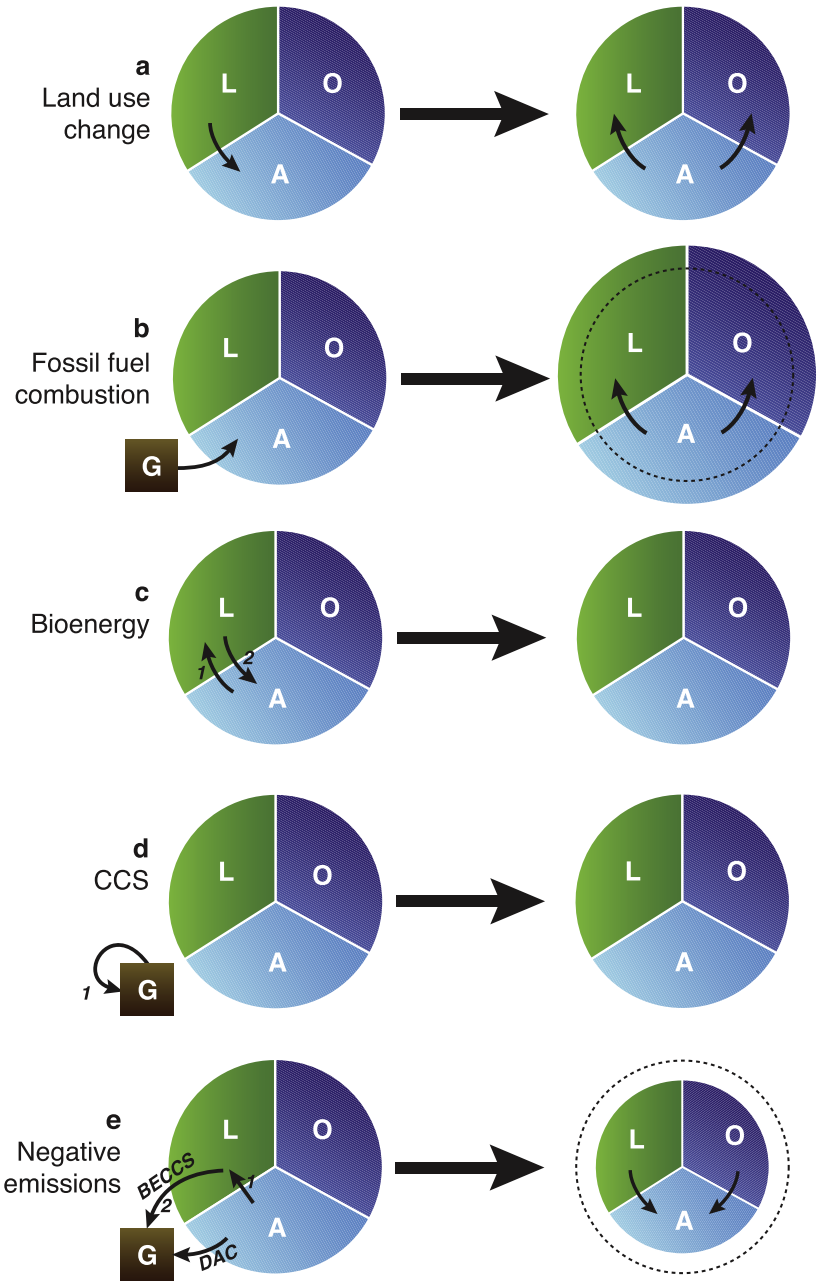

Figure 2. Schematic representation of how the carbon cycle system responds to anthropogenic activity. Each row depicts the initial action and the subsequent response of the system in terms of distribution of carbon between three pools: atmosphere (A), land (L) and ocean (O). As explained in the text, we do not include pools that only respond on very long timescales such as geological carbon or ocean sediments. The sizes of the three pools are not to scale (for example the ocean carbon pool is much bigger than the other two). The five rows depict different anthropogenic activities in an approximate chronological sequence as discussed in the text: (a) land use change; (b) fossil fuel burning; (c) bioenergy (without carbon capture); (d) carbon capture and storage (CCS) applied to fossil fuel burning; (e) negative emission technologies (NETs) with BECCS and DAC shown as examples and described in the text. In rows (b) and (e) the dotted circle on the right-hand pie chart denotes the original size of the pie chart from the left hand side.

declines, then natural sinks may behave rather differently than currently where concentration is always on the rise. The airborne fraction of emissions (AF) has been approximately constant for many decades now but this is not a fundamental behaviour of the Earth system, but largely a result of near-exponential growth in carbon emissions (Raupach 2013, Raupach *et al* 2014). AF may change markedly in the next century dependent on the scenario of anthropogenic emissions. Jones *et al* (2013) showed strong changes in the land and ocean uptake fraction for the 21st century compared with the 20th century. Beyond 2100, we may expect further changes and qualitatively different behaviour of the land and ocean sinks.

Long simulations using ESMs provide a quantitative understanding of the multiple trade offs and competing factors within the Earth system. Here we explore a case study of RCP2.6 (van Vuuren *et al* 2011) using simulations from CMIP5 ESMs. This scenario is the only high mitigation scenario that has been

Table 1. List of models and modelling centres contributing to CMIP5 whose data has been used for this analysis. In terms of their climate and carbon cycle response under RCP2.6, these models represent a reasonable span of model spread from the CMIP5 ensemble (see the supplementary information or for example figure 6(b) of Jones *et al* 2013).

Modelling centre	Model name
Canadian Centre for Climate modelling and analysis (CCCma)	CanESM2
Met Office Hadley Centre (MOHC)	HadGEM2-ES
Institut Pierre-Simon Laplace (IPSL)	IPSL-CM5A-LR
Max Planck Institute for Meteorology (MPI-M)	MPI-ESM-LR

simulated by multiple ESMs—it shows emissions peaking at just over 10 GtC yr^{-1} in 2020, then declining, becoming net negative during the 2080s. The reduction in global emissions is driven partly by reduced fossil fuel use and partly by the introduction of BECCS as early as 2020. The total NETs deployed during the 21st century is much bigger than the amount of global net negative emissions after 2080. An extension to the scenario exists which assumes constant emissions (of −0.42 GtC yr^{-1}) from 2100 until 2300 (Meinshausen *et al* 2011).

Here we look at the available CMIP5 models (table 1) which extended their simulations up to 2300. A fifth model, BCC-CSM1.1, also performed this simulation, but without land-use change as a forcing of the land carbon cycle meaning that its land carbon response is therefore very different from the other models (see figure 2(a) of Jones *et al* 2013) and so we do not include it here.

2.2. Results

In this section we present the results following a narrative beginning with anthropogenic emissions and leading through to the simulated land and ocean sinks and their resulting effect on atmospheric CO_2. The methods section of the supplementary information explains how we derive these results from the CMIP5 concentration-driven simulations and how we construct the figures shown here. We start by showing the RCP2.6 CO_2 pathway and the simulated land and ocean carbon fluxes by the 4 ESMs as well as the IMAGE integrated assessment model which generated the RCP2.6 scenario (figure 3).

The emissions, CO_2 concentration and simulated response of land and ocean sinks are detailed in table S1. The behaviour of the simulated carbon sinks is as expected from figure 1; as anthropogenic emissions increase (not shown), natural sinks increase to absorb approximately half of this, and therefore atmospheric CO_2 increases. For comparison, the MAGICC calculations (Meinshausen *et al* 2011) have been added in figure 3(b), showing consistent results. This provides confidence that IAM calculations (using MAGICC) are able to simulate similar dynamics over time to the current state-of-the-art descriptions of the carbon cycle in ESMs.

During the 21st century, anthropogenic NETs along with other mitigation activities come into play in the scenario and gradually reduce and eventually reverse anthropogenic total input from strong positive emissions to weak positive and then a global negative emission. The land and ocean sinks do not respond to the instantaneous emission rate but to the history of the land and ocean carbon reservoirs and level of atmospheric CO_2 and climate change above pre-industrial levels. To illustrate this clearly we analyze the simulations in 50 year sections and calculate the multi-model mean response. Figure 4 shows quantitatively the balance between the various components as they evolve in time:

- 2000–2050. The application of NETs begins but anthropogenic activity remains dominated by positive emissions (figure 4(a)). Land and ocean sinks persist. The AF remains close to half of emissions and CO_2 concentration continues to rise.
- 2050–2100. Fossil fuel emissions decline and NETs grow further in this scenario. The anthropogenic total is still positive but much smaller (figure 4(b)). Natural sinks persist—a little reduced but still absorbing carbon due to past history and therefore CO_2 begins to decrease, despite the anthropogenic total still being positive.
- 2100–2150. NETs exceed fossil inputs and human activity removes more CO_2 than it emits at a global scale (figure 4(c)). During this first 50 years of anthropogenic net carbon removal, the natural sinks weaken significantly due to the rapid decrease in atmospheric CO_2. Hence there is an atmospheric CO_2 reduction due to the combination of net negative anthropogenic emissions and land and ocean still absorbing carbon, however not as strong as might have been expected if strong natural sinks had persisted.
- 2150–2200 and on to 2250. Behaviour is qualitatively similar to figure 4(c), but now natural sinks have weakened further and CO_2 decrease is slowed. Towards 2250 natural sinks are all but gone. In fact 3 out of 4 ESMs simulate a reversal of the land carbon sink to become a source.
- 2250–2300. In the final stage the land and ocean system has become a net source of CO_2. Most ESMs still simulate the ocean as a sink, but the overall (land plus ocean) flux is positive (figure 4(d)). The atmospheric CO_2 decrease is weakened as the natural carbon cycle is releasing carbon to the atmosphere, working in the opposite direction to the anthropogenic removal via NETs.

In summary, these results show a clear succession of events: from 2000 to 2050 the emergence of NETs has a slowing effect on anthropogenic emission but the

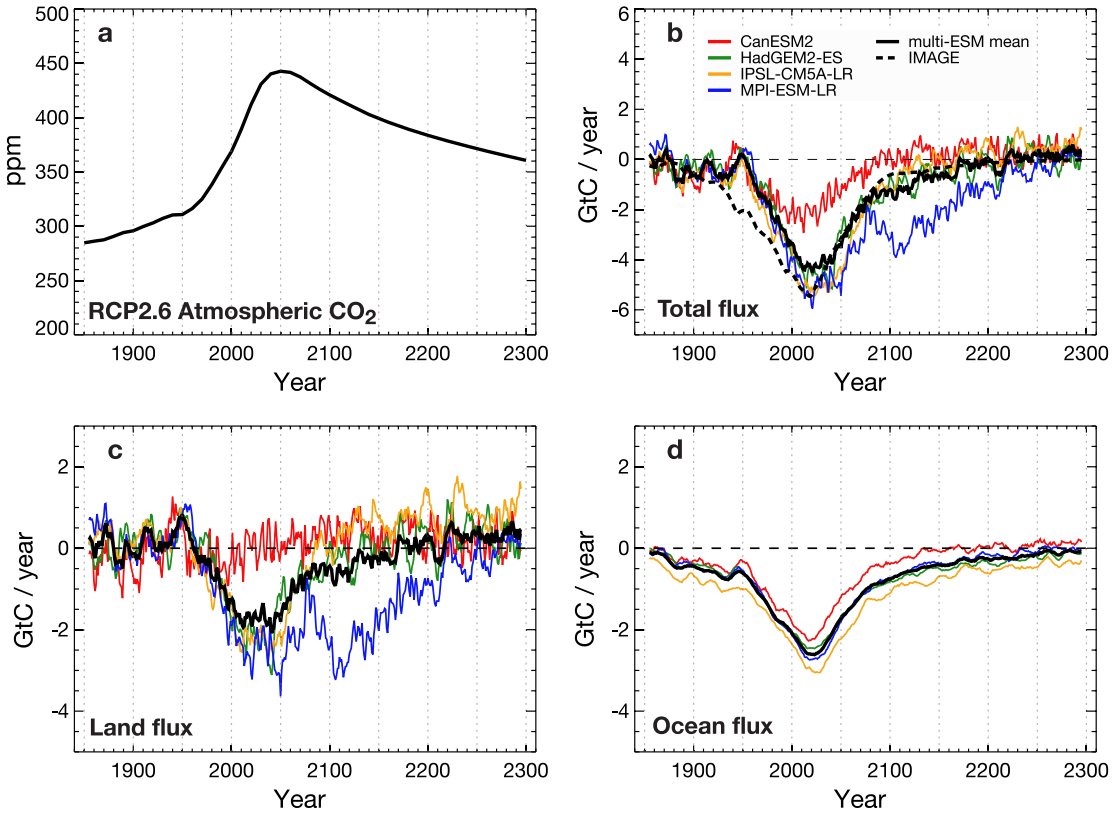

Figure 3. RCP2.6 scenario and CMIP5 simulated carbon fluxes. (a) RCP2.6 CO_2 concentration pathway; (b) total (land plus ocean) carbon flux from CMIP5 ESMs; (c) and (d) land and ocean fluxes separately. Four CMIP5 ESMs were used (listed in table 1) and results are shown as 10 year smoothed fluxes. The black line shows the multi-ESM mean and the dashed black line in (b) shows the MAGICC results for the RCP2.6 scenario (used by the IMAGE IAM in creating RCP2.6). The sign convention is to plot the land and ocean as positive for a flux to the atmosphere and negative to represent a sink. Vertical dotted lines show 50 year time periods used to aggregate results discussed in the text.

general balance is not changed from the historical period; from 2050 to 2100 natural sinks outweigh (still positive) anthropogenic emissions and CO_2 begins to fall; from 2100 to 2250 NETs exceed fossil emissions and human activity is a global negative emission; finally, from 2250 to 2300 natural sinks saturate and reverse and oppose any further removal.

3. State and scenario dependence of the Earth system response

We know that natural carbon sinks and the AF of emissions are sensitive to climate change and behave differently under different future scenarios. It is therefore important to understand how the effectiveness of NETs may also differ depending on the scenario against which they are applied. In this section we look at the range of Earth system responses to different levels of negative emissions when applied under different climate and CO_2 scenarios.

To this end we perform new simulations as perturbations to the RCP set of projections. Using the Hadley Centre Simple Climate-Carbon Model widely used in previous studies (Jones *et al* 2003, 2006, House *et al* 2008, Huntingford *et al* 2009—see SI for more details) we quantify the effect of the level of past emissions and climate change on the effectiveness of different levels of NETs.

We take each of the four RCP emissions scenarios as a baseline and apply on top of them four idealised scenarios of additional negative emissions (figure 5(a)). The negative emissions scenarios we impose all begin in 2020 and comprise:

(a) Constant removal of 1 GtC yr^{-1}.

(b) Constant removal of 4 GtC yr^{-1}.

(c) A linear increase in removal from 1 GtC yr^{-1} in 2020 up to 4 GtC yr^{-1} in 2080 followed by sustained 4 GtC yr^{-1} removal until 2100.

(d) The same as (c) but reversed in time to remove 4 GtC yr^{-1} from 2020 to 2040 and then gradually reduce the removal rate to 1 GtC yr^{-1} by 2100.

The total CO_2 removal for the 2020–2100 period under these idealised scenarios is 80 and 320 GtC under the first two and 230 GtC for the last two. The idealised NET profiles are added to the four RCP emissions scenarios (figure 5(b)). The simple model is run in emissions-driven configuration taking these emissions as input and simulating the response of natural

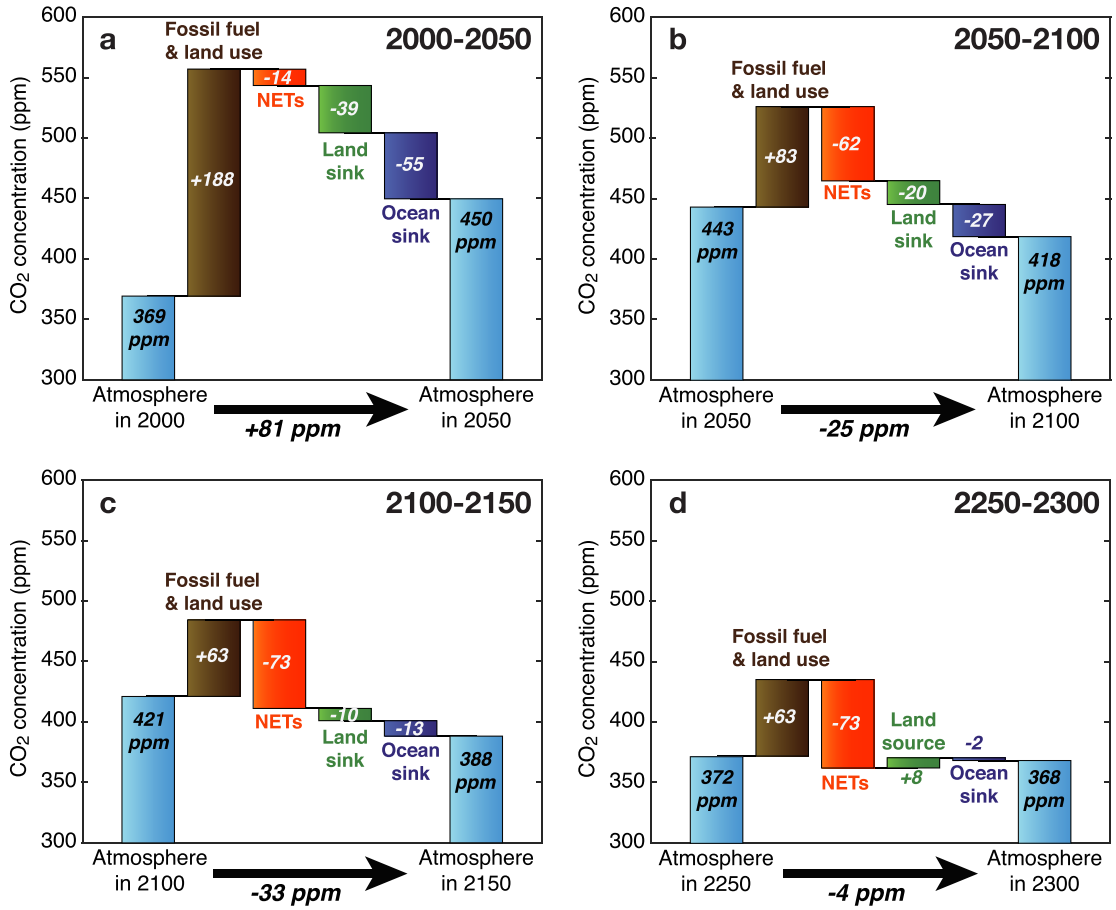

Figure 4. The four stages of succession of the differing balance between flux components. As for figure 1 the bars show changes in atmospheric CO_2 (ppm) due to that emission or flux. Each panel shows a selected 50 year period from the RCP2.6 simulations to analyze the changing balance of the flux components. Due to small differences between the compatible emissions diagnosed from the four ESMs and the emissions in the scenario each 50 year period does not balance precisely (see SI for details).

sinks and atmospheric CO_2 concentration (figure 5(c)). Here we explore the effect of the applied negative emission and to what extent the Earth-system response depends on the magnitude or time profile of the NET or the state or scenario of background climate and CO_2.

Figure 5(c) shows the obvious result that with additional NETs applied to each scenario, the simulated CO_2 is reduced. But the degree of reduction varies significantly between scenarios. For example, the same 320 GtC removal results in reduced atmospheric CO_2 by 178, 211, 237 and 274 GtC for RCP2.6 to RCP8.5 respectively. It is clear that the effectiveness of negative emissions varies depending on the scenario and the state of the Earth system. It is therefore desirable to define a new metric that can measure this dependence.

The AF is a commonly used metric and we adopt it here to allow a first analysis of the results. It can be defined as an instantaneous value as the ratio of a single year rise in CO_2 divided by that year's emissions, or a long-term cumulative quantity defined as the change over many years of CO_2 divided by the cumulative emissions over that period. When considering either emissions close to zero or CO_2 changes that can change sign, then the former definition is not always well behaved or well defined, and so we adopt the latter definition (hereafter named the cumulative airborne fraction, CAF).

Table 2 shows the cumulative emissions and their impact on atmospheric CO_2 for the scenarios with and without added negative emissions over the 80 year period from 2020–2099. The table shows the CAF for the un-modified RCP scenarios, and then also for each modified scenario. A detailed derivation of the terms shown in table 2 is given in the supplementary information.

The CAF of the original RCP scenarios varies markedly across RCPs, with RCP2.6 having a small fraction of cumulative emissions remaining in the atmosphere for the 2020–2099 period (only 15%) while the other RCPs have a higher fraction of cumulative emissions remaining in the atmosphere, ranging from 48% for RCP4.5 to 72% for RCP8.5 (column 7 in table 2, and see SI text and figure S3). This is consistent with previous studies (Ciais *et al* 2013, Jones *et al* 2013). When we look at the CAF under the modified scenarios (column 8) we find two things. For

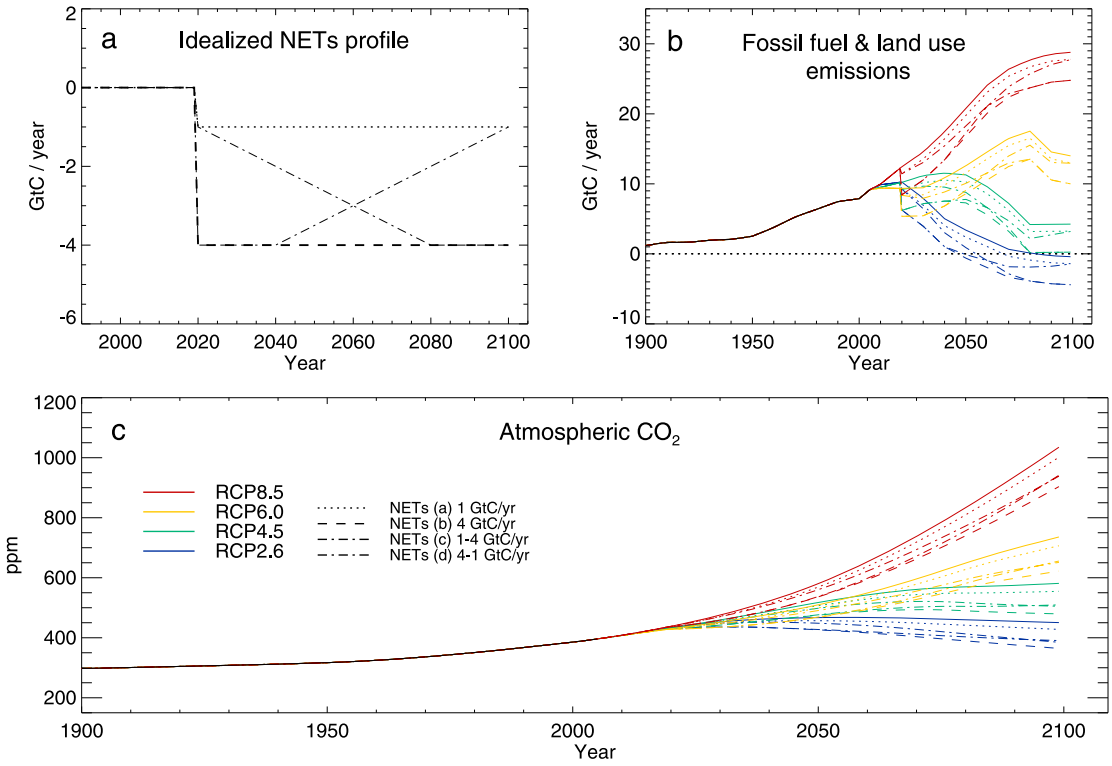

Figure 5. Simulated CO_2 concentration under four RCP emissions scenarios with added idealised profiles of CO_2 removal from NETs. The top panels show the inputs to the model: (a) the idealised NET profiles and (b) the total anthropogenic emissions when these NETs are added to the RCP emissions scenarios. RCP emissions (solid lines) with the idealised NETs added (dashed lines). The bottom panel (c) shows the resulting atmospheric CO_2 simulated by the simple carbon cycle model.

RCP2.6 the values vary hugely between the three additional NET scenarios (figure S3e). This is because either or both the cumulative emissions or the change in atmospheric CO_2 are negative and this leads to changes in sign of CAF and values greater than one because the denominator in the definition is small. For RCP6 and RCP8.5 (and to some extent for RCP4.5) we find an opposite result—the CAF is rather insensitive to the CO_2 removal and stays close to the value from the un-modified scenario. In either case this metric therefore is not very useful as a measure of either the effect of the negative emission on the Earth system or of the Earth system on the negative emission.

We also calculate the fraction of the CO_2 removal which has remained out of the atmosphere—i.e. the AF of the negative emission (final column of table 2; figure S3 panels m–p). For each RCP this metric is rather insensitive to the amount of removal and is different from (and generally bigger than) the CAF of the RCP itself for the same period. This means that the effect of NETs on atmospheric CO_2 in the long term is more closely controlled by the background scenario and level of climate change than by the amount of NETs themselves. Comparing the ramped removals with different time profiles of the same cumulative amount we see that the response is not strongly affected by the removal pathway. Tokarska and Zickfeld (2015) also calculated a CAF of their carbon removal and found it to be less dependent on the amount of removal than a CAF based on total emissions. Here we have shown that this property applies across the full range of RCP scenarios. We argue that this perturbation AF (PAF) is therefore a more suitable metric to assess the efficiency of NET than the CAF of the emissions from a single simulation.

This result has several significant implications. Firstly, that it is meaningful to define an AF of a perturbed emission on top of a background scenario in order to measure the effect on atmospheric CO_2 of the additional emission or removal. Secondly, this PAF is not the same as the AF of the background scenario itself. Hence, if it is desired to calculate the effect of adding or removing an amount of carbon on top of an existing scenario, then knowing the AF of the scenario does not help—one must calculate the AF of the extra carbon removed instead, i.e. the PAF. Thirdly, though, the PAF from a given scenario is rather insensitive to the magnitude and timing of additional emission. This may be expected when the additional emission is a small fraction of the total emitted carbon for the scenario, but it appears to hold here too even for RCP2.6 when the total carbon removal is bigger than the cumulative emission in the underlying scenario. This means that once a PAF has been calculated relative to a scenario it can be approximately applied to other perturbations about that scenario to estimate their eventual impact.

Table 2. Cumulative emissions and changes in atmospheric CO_2 for the simple model simulations of the original and modified RCPs with additional NET scenarios added. The cumulative airborne fraction (CAF) is calculated for the scenarios and also just for the NET components as described in the text.* The definition and calculation of these metrics is explained in more detail in the SI.

RCP scenario	Idealised NET profile/GtC yr^{-1}	RCP cumulative emission (2020–2099)/GtC	Cumulative additional NE/GtC	Cumulative total emission (2020–2099)/GtC	Change in atmospheric CO_2/GtC	CAF of back-ground RCP* (2020–2099)	CAF of modified RCP * with NET (2020–2099)	Perturbation-AF of the additional negative emission *
RCP2.6		**243**			**37**	**0.15**		
	−1		−80	163	−10		−0.06	0.6
	−4		−320	−77	−141		1.83	0.57
	−1 to −4		−230	13	−101		−7.8	0.6
	−4 to −1		−230	13	−86		−6.6	0.55
RCP 4.5		**663**			**316**	**0.48**		
	−1		−80	583	261		0.45	0.7
	−4		−320	343	105		0.3	0.67
	−1 to −4		−230	433	155		0.35	0.7
	−4 to −1		−230	433	169		0.39	0.66
RCP 6.0		**1060**			**649**	**0.61**		
	−1		−80	980	588		0.6	0.78
	−4		−320	740	412		0.55	0.75
	−1 to −4		−230	830	470		0.56	0.78
	−4 to −1		−230	830	483		0.58	0.74
RCP 8.5		**1764**			**1265**	**0.72**		
	−1		−80	1684	1195		0.71	0.89
	−4		−320	1444	991		0.68	0.87
	−1 to −4		−230	1534	1061		0.69	0.89
	−4 to −1		−230	1534	1071		0.70	0.86

4. Conclusions

Other studies have outlined various socio-economic costs, biophysical limits and implications of different NETs (Fuss *et al* 2014, Smith *et al* 2016, Williamson 2016). Here we have shown how NETs interact with the physical climate-carbon cycle system. Our analysis of the Earth system response to negative emissions has provided new insights and identified future research priorities.

Our results contribute to the need to quantify the interactions between the climate, carbon cycle and anthropogenic NETs in determining future redistribution of carbon between atmosphere, land and ocean reservoirs. By viewing the scenarios and the evolution of carbon sinks and sources in a sequence of phases we have revealed qualitatively different behaviour of the Earth system at different points in time. The combined effect of anthropogenic and natural sources and sinks can change over time, sometimes resulting in positive and sometimes negative changes in atmospheric CO_2 concentration. The behavior of atmospheric CO_2 is not predictable from the instantaneous anthropogenic emission alone, but requires knowledge of past emissions and Earth system state. For example, CMIP5 simulations following the RCP2.6 pathway to 2300 exhibited periods where atmospheric CO_2 decreased despite ongoing net positive emissions from anthropogenic activity. Conversely, later in the scenarios, natural sinks weakened and even reversed, especially on land, and offset the effects of globally negative anthropogenic emissions.

We found significant state-dependence of the Earth system behaviour in response to NETs. Our results showed that the effect of NETs on atmospheric CO_2 is more closely controlled by the background scenario and level of climate change than by the amount or timing of NETs themselves. We propose a new metric, the PAF, defined as the ratio of CO_2 reduction to the amount of NETs applied. This metric can be used to transfer model results that quantify the effect of NETs under a given scenario to estimate the effect of different levels of NETs against the same scenario.

Simplified climate-carbon cycle models, calibrated against complex ESMs and often used in IAMs for scenario generation are capable of reproducing this behaviour at a global scale. This means that existing IAMs are not systematically wrong in their estimates of NETs required within scenarios. However, large uncertainty remains, due primarily to model spread in the simulation of future carbon sinks and this hinders robust determination of carbon budgets to meet climate targets.

ESMs still lack some important processes such as the role of nutrient cycles that may limit future land carbon storage (Zaehle *et al* 2015), burning of old land carbon stocks (e.g. peat fires in Indonesia, Lestari *et al* 2014) or release of carbon from thawing permafrost (Schuur *et al* 2015). The latter in particular has potentially significant impacts on the requirement for negative emissions, as once released from thawed permafrost it would take centuries to millennia for the same carbon to re-accumulate, making it effectively irreversible on human timescales (MacDougal *et al* 2015). Uncertainty also exists on the strength and persistence of concentration-dependent carbon uptake, especially on land (so-called 'CO_2 fertilisation'). IPCC 5th Assessment Report assessed '*low confidence* on the magnitude of future land carbon changes' (Ciais *et al* 2013). It is increasingly important to bring observational constraints to bear to reduce this uncertainty especially focusing on low emissions scenarios.

It is increasingly clear that negative emissions could be very important in achieving ambitious climate targets, and in fact many scenarios rely on them to do so. Failure to accurately account for carbon cycle feedbacks which increase the need for such negative emissions may strongly and adversely affect the feasibility of achieving these targets. We lack important understanding about the costs and implications of negative emissions, and also knowledge related to the Earth-system dynamics. It is vital to address these knowledge gaps in order to quantify the requirement for, and implications of negative emissions.

Acknowledgments

The work of CDJ, JAL and AW was supported by the Joint UK BEIS/Defra Met Office Hadley Centre Climate Programme (GA01101). CDJ, JAL, AW, PF, EK and DvV are supported by the European Union's Horizon 2020 research and innovation programme under grant agreement No 641816 (CRESCENDO). GPP was supported by the Norwegian Research Council (project 209701). PC acknowledges support from the European Research Council Synergy grant ERC-2013-SyG-610028 IMBALANCE-P. We acknowledge the World Climate Research Programme's Working Group on Coupled Modelling, which is responsible for CMIP, and we thank the climate modeling groups (listed in table 1 of this paper) for producing and making available their model output. For CMIP the US Department of Energy's Program for Climate Model Diagnosis and Intercomparison provides coordinating support and led development of software infrastructure in partnership with the Global Organisation for Earth system Science Portals.

References

Benson S M *et al* 2012 *Global Energy Assessment Toward a Sustainable Future* (Cambridge: Cambridge University Press) ch 13

Cao L and Caldeira K 2010 Atmospheric carbon dioxide removal: long-term consequences and commitment *Environ. Res. Lett.* **5** 024011

Cherubini F, Peters G P, Bernsten T, Stromman A H and Hertwich E 2011 CO_2 emissions from biomass combustion for bioenergy: atmospheric decay and contribution to global warming *GCB Bioenergy* **3** 413–26

Ciais P *et al* 2013 Carbon and other biogeochemical cycles *Climate Change 2013: The Physical Science Basis. Contribution of Working Group I to the Fifth Assessment Report of the Intergovernmental Panel on Climate Change* ed T F Stocker *et al* (Cambridge: Cambridge University Press)

Clarke L *et al* 2014 Assessing transformation pathways *Climate Change 2014: Mitigation of Climate Change. Contribution of Working Group III to the Fifth Assessment Report of the Intergovernmental Panel on Climate Change* ed O Edenhofer *et al* (Cambridge: Cambridge University Press)

Fuss S *et al* 2014 Betting on negative emissions *Nat. Clim. Change* **4** 850–3

Gasser T, Guivarch C, Tachiiri K, Jones C D and Ciais P 2015 Negative emissions physically needed to keep global warming below 2 °C *Nat. Commun.* **6** 7958

House J, Huntingford C, Knorr W, Cornell S E, Cox P M, Harris G R, Jones C D, Lowe J A and Prentice C I 2008 What do recent advances in quantifying climate and carbon cycle uncertainties mean for climate policy? *Environ. Res. Lett.* **3** 044002

Huntingford C, Lowe J A, Booth B B B, Jones C D, Harris G R, Gohar L K and Meir P 2009 Contributions of carbon cycle uncertainty to future climate projection spread *Tellus* **61B** 355–60

IPCC 2005 *IPCC Special Report on Carbon Dioxide Capture and Storage. Working Group III of the Intergovernmental Panel on Climate Change* ed B Metz *et al* (Cambridge: IPCC) pp 1–431

Jones C D *et al* 2013 Twenty-first-century compatible CO_2 emissions and airborne fraction simulated by CMIP5 Earth system models under four representative concentration pathways *J. Clim.* **26** 4398–413

Jones C D, Cox P M and Huntingford C 2003 Uncertainty in climate-carbon cycle projections associated with the sensitivity of soil respiration to temperature *Tellus* **55B** 642–8

Jones C D, Cox P M and Huntingford C 2006 Climate-carbon cycle feedbacks under stabilization: uncertainty and observational constraints *Tellus* **58B** 603–13

Lestari R K, Watanabe M, Imada Y, Shiogama H, Field R D, Takemura T and Kimoto M 2014 Increasing potential of biomass burning over Sumatra, Indonesia induced by anthropogenic tropical warming *Environ. Res. Lett.* **9** 104010

Le Quéré C *et al* 2015 Global carbon budget 2015 *Earth Syst. Sci. Data* **7** 349–96

MacDougal A H 2013 Reversing climate warming by artificial atmospheric carbon-dioxide removal: can a Holocene-like climate be restored? *Geophys. Res. Lett.* **40** 5480–5

MacDougal A H, Zickfeld K, Knutti R and Matthews H D 2015 Sensitivity of carbon budgets to permafrost carbon feedbacks and non-CO_2 forcings *Environ. Res. Lett.* **10** 125003

Matthews H D 2010 Can carbon cycle geoengineering be a useful complement to ambitious climate mitigation? *Carbon Manage.* **1** 135–44

Meinshausen M *et al* 2011 The RCP greenhouse gas concentrations and their extension from 1765 to 2300 *Clim. Change* **109** 213–41

Raupach M R 2013 The exponential eigenmodes of the carbon-climate system, and their implications for ratios of responses to forcings *Earth Syst. Dynam.* **4** 31–49

Raupach M R, Gloor M, Sarmiento J L, Canadell J G, Frölicher T L, Gasser T, Houghton R A, Le Quéré C and Trudinger C M 2014 The declining uptake rate of atmospheric CO_2 by land and ocean sinks *Biogeosciences* **11** 3453–75

Rogelj J, Luderer G, Pietzcker R C, Kriegler E, Schaeffer M, Krey V and Riahi K 2015 Energy system transformations for limiting end-of-century warming to below 1.5 °C *Nature Clim. Change* **5** 519–27

Schuur E A G *et al* 2015 Climate change and the permafrost carbon feedback *Nature* **520** 171–9

Smith P *et al* 2016 Biophysical and economic limits to negative CO_2 emissions *Nat. Clim. Change* **6** 42–50

Tokarska K B and Zickfeld K 2015 The effectiveness of net negative carbon dioxide emissions in reversing anthropogenic climate change *Environ. Res. Lett.* **10** 094013

UNFCCC 2015 FCCC/CP/2015/L.9/Rev.1: Adoption of the Paris Agreement. Paris, France, UNFCCC: 1-32

van Vuuren D P *et al* 2011 The representative concentration pathways: an overview *Clim. Change* **109** 5–31

Williamson P 2016 Scrutinize CO_2 removal methods *Nature* **530** 153–5

Zaehle S, Jones C D, Houlton B, Lamarque J-F and Robertson E 2015 Nitrogen availability reduces CMIP5 projections of twenty-first-century land carbon uptake *J. Clim.* **28** 2494–511

Supplementary Information for ‘Simulating the Earth system response to negative emissions.’

C D Jones[1], P Ciais[2], S J Davis[3], P Friedlingstein[4], T Gasser[5,2], G P Peters[6], J Rogelj[7,8], D P van Vuuren[9,10], J G Canadell[11], A Cowie[12], R B Jackson[13], M Jonas[14], E Kriegler[15], E Littleton[16], J A Lowe[1], J Milne[17], G Shrestha[18], P Smith[19], A Torvanger[20] and A Wiltshire[1]

Methods: use of CMIP5 ESMs and processing of concentration-driven scenario simulations.

Section 2 of the main text analyses results from CMIP5 Earth system model simulations. Although we can only draw on 4 models here they span a reasonable spread in the bigger multi-model ensemble which is available up to 2100. The models span global temperature rise at 2100 from 1.8 to 2.4 K above pre-industrial and 2080-2100 global emissions from -1.1 to +1.4 GtC yr^{-1}.

Table S1 shows the observed and RC2.6 scenario values for anthropogenic emissions broken down into gross positive (fossil fuel and land-use change emissions) and gross negative (NETs) terms, and changes in atmospheric CO_2 expressed in units of ppm as commonly reported and also converted into GtC for direct comparison with other rows in the table. Also shown are the model results from the four CMIP5 ESMs and from the MAGICC model, which is the simple climate model used to convert IAM emissions into atmospheric CO_2 concentrations (Meinshausen et al., 2011).

CMIP5 experimental design includes coupled climate-carbon cycle simulations which are both concentration-driven and emissions-driven (see e.g. Box 6.4 of Ciais et al., 2013). However, only concentration-driven simulations were extended past 2100 with multiple ESMs, and so our analysis draws on those results. In these numerical experiments the CO_2 concentration pathway is prescribed as a boundary condition for the models which then simulate the land and ocean carbon fluxes. From these we diagnose the compatible anthropogenic emissions as the emission that would have been required to drive the changes in CO_2 given the simulated land and ocean fluxes. This allows us to compare simulations for the same CO_2 concentration pathway across multiple models and infer how the Earth system responds over time to changes in the rates of emissions and sinks.

Figure 3(a) in the main text shows the prescribed atmospheric CO_2 concentration from the RCP2.6 scenario which is used as input to all the ESMs. Panels (b)-(d) then show the land and ocean fluxes which are simulated by the models in response to this prescribed concentration scenario.

Figure 4 in the main text uses the waterfall format of figure 1 to depict the changes in time of the different components of the global carbon budget under the RCP2.6 extension to 2300. To construct this figure, we took data from different sources as follows. In each panel:

- The first bar in each panel shows the atmospheric CO_2 concentration at the start of the 50-year period. In the case of panel (a) this is the observed concentration for the year 2000, and for the other panels it is taken from the RCP2.6 scenario.
- To this we add the anthropogenic emissions from the scenario averaged over the 50-year period. These are shown by the second and third bar in each panel and represent the split between positive emissions due to fossil fuel and land-use change, and negative emissions due to NETs.
- The next two bars show the simulated land and ocean carbon uptake averaged over the 50-year period and averaged across all four ESMs. In the figure we just show the model mean, but the full model range can be seen in figure 3, panels (c) and (d). Table S1 lists the mean and standard deviation across models for each 50-year period.
- The final bar shows the atmospheric CO_2 concentration that would result from this balance of fluxes at the end of the 50-year period. Because we have mixed the emissions from the IMAGE integrated assessment model with the sinks from the CMIP5 ESMs the calculated change in CO_2 does not match precisely the CO_2 pathway prescribed from the scenario. For example, panel (a) shows a CO_2 concentration for 2050 of 450ppm, whereas panel (b) shows the scenario value for 2050 of 443 ppm. This difference is because the CO_2 in the scenario was derived using the MAGICC model. Figure 3(b) shows that the land and ocean combined sink simulated by MAGICC is close to, but not identical to, the ESM mean.

Table S1. CO_2 concentration and simulated response of land and ocean sinks for the RCP2.6 and the 4 CMIP5 ESMs. All values are averages over each 50 year period, expressed as mean fluxes or rates of change in GtC per year (except the penultimate row which is ppm per year). First 3 rows, labeled as "Anthropogenic" are from the RCP2.6 scenario. The CMIP5 entries are the mean and standard deviation over the 4 models listed in table 1of the main text. The MAGICC natural flux is inferred as the difference between the RCP2.6 scenario emissions and CO_2 concentration.

		Historical period			RCP2.6					
Source		1850-1900	1900-1950	1950-2000	2000-2050	2050-2100	2100-2150	2150-2200	2200-2250	2250-2300
Observed / scenario	Anthropogenic fossil and land-use emission / GtC yr^{-1}	0.88	1.88	5.67	7.98	3.53	2.69	2.69	2.69	2.69
	Anthropogenic NET / GtC yr^{-1}	0	0	0	-0.58	-2.61	-3.11	-3.11	-3.11	-3.11
	Anthropogenic total / GtC yr^{-1}	0.88	1.88	5.67	7.4	0.92	-0.42	-0.42	-0.42	-0.42
Observed / scenario	Change in atmospheric CO_2 / ppm yr^{-1}	0.24	0.30	1.16	1.48	-0.44	-0.43	-0.31	-0.24	-0.22
	Change in atmospheric CO_2 / GtC yr^{-1}	0.51	0.64	2.46	3.14	-0.93	-0.91	-0.66	-0.51	-0.47
CMIP5 ESMs	Land flux / GtC yr^{-1}	0.08 ± 0.21	0.18 ± 0.14	-0.38 ± 0.16	-1.66 ± 1.22	-0.83 ± 0.91	-0.43 ± 1.41	-0.06 ± 0.80	0.22 ± 0.56	0.36 ± 0.39
	ocean flux / GtC yr^{-1}	-0.31 ± 0.15	-0.60 ± 0.21	-1.37 ± 0.22	-2.32 ± 0.35	-1.13 ± 0.34	-0.54 ± 0.30	-0.32 ± 0.24	-0.23 ± 0.22	-0.10 ± 0.20
	natural (land plus ocean) total flux / GtC yr^{-1}	-0.23 ± 0.20	-0.42 ± 0.12	-1.75 ± 0.30	-3.97 ± 1.52	-1.96 ± 1.10	-0.98 ± 1.40	-0.38 ± 0.76	-0.01 ± 0.45	0.27 ± 0.27
MAGICC	MAGICC natural (land plus ocean) total flux / GtC yr^{-1}	-0.32	-1.21	-3.20	-4.60	-1.69	-0.50	-0.24	-0.10	-0.04

Documenting the simple climate-carbon cycle model

To explore the scenario dependence of the cumulative airborne fraction (CAF) of negative emissions we use a simple climate-carbon cycle model that has been documented and used elsewhere (e.g. Jones et al., 2003; 2006; House et al., 2008; Huntingford et al., 2009).

Jones et al. (2003) and Jones et al. (2006) describe the model in detail. Briefly, it comprises a global box model of climate and the carbon cycle. For the land carbon cycle GPP is simulated as a Michaelis-Menton function of CO_2 and a quadratic function of temperature. GPP leads to an increase in vegetation carbon which turnover to form soil carbon which itself respires to the atmosphere. The ocean carbon cycle is represented by an impulse response function after Joos et al., (1996).

Simple model parameters used for this study are very close to those used in Jones et al. (2003), and close to the most likely of the frequency distributions shown in figure 4 of Jones et al. (2006). We adopt here: q10 =2 for both soil and plant respiration, CI_half=350 which corresponds to CA_half of 437.50 ppm (based on a ratio of internal to atmospheric CO_2 of CI:CA=0.8). d2GPP/dT2 = -0.006 K^{-2} and dGPP/dT=0 which leads to a T_{opt}=0. In this configuration it closely mimics the HadCM3LC model.

The model was first tested for the four RCP scenarios in concentration driven mode using CO_2 forcing data used in CMIP5. From these simulations we can infer the compatible emissions that would be required to follow the prescribed CO_2 pathway. Figure S1 shows the emissions diagnosed from these simulations compared with the emissions from the RCPs. Agreement is very close.

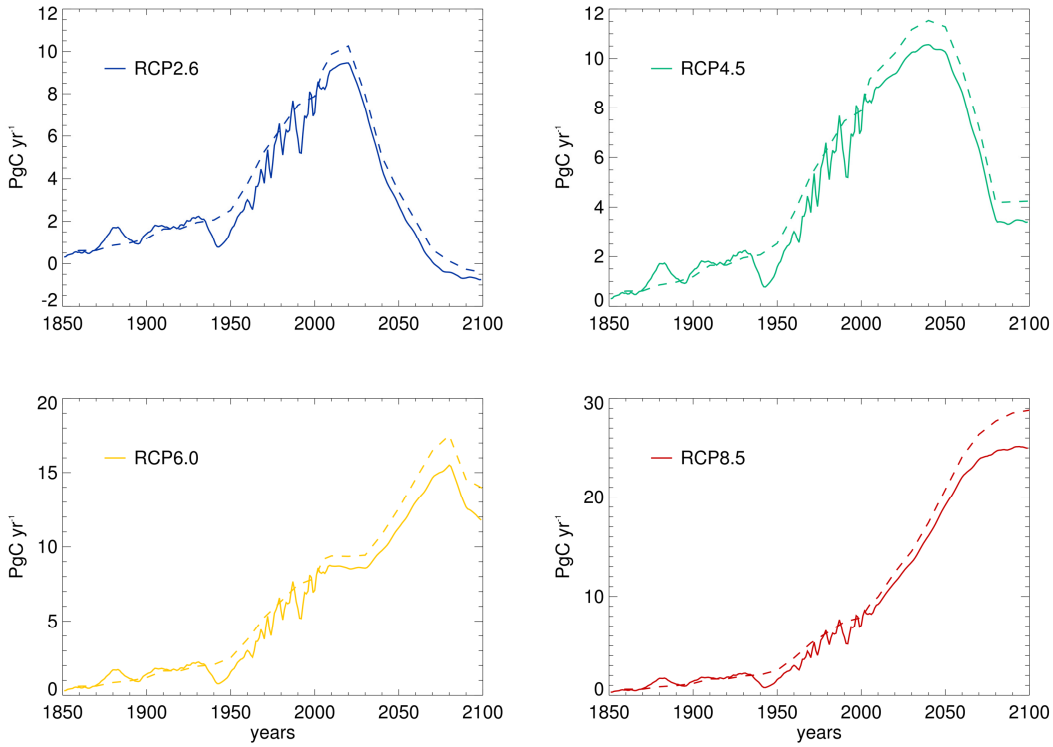

Figure S1. Compatible CO_2 emissions diagnosed from concentration-driven simple model simulations (solid lines) compared with those from the RCPs (dashed lines). RCP2.6 (top left), RCP4.5 (top right), RCP6.0 (lower left), RCP8.5 (lower right).

A second test is to perform these simulations in emissions-driven mode, forcing the model with the RCP CO_2 emissions and simulating the atmospheric concentration. Figure S2 shows close agreement, although the simple model projects slightly too high CO_2 compared with the RCP pathway for all four scenarios.

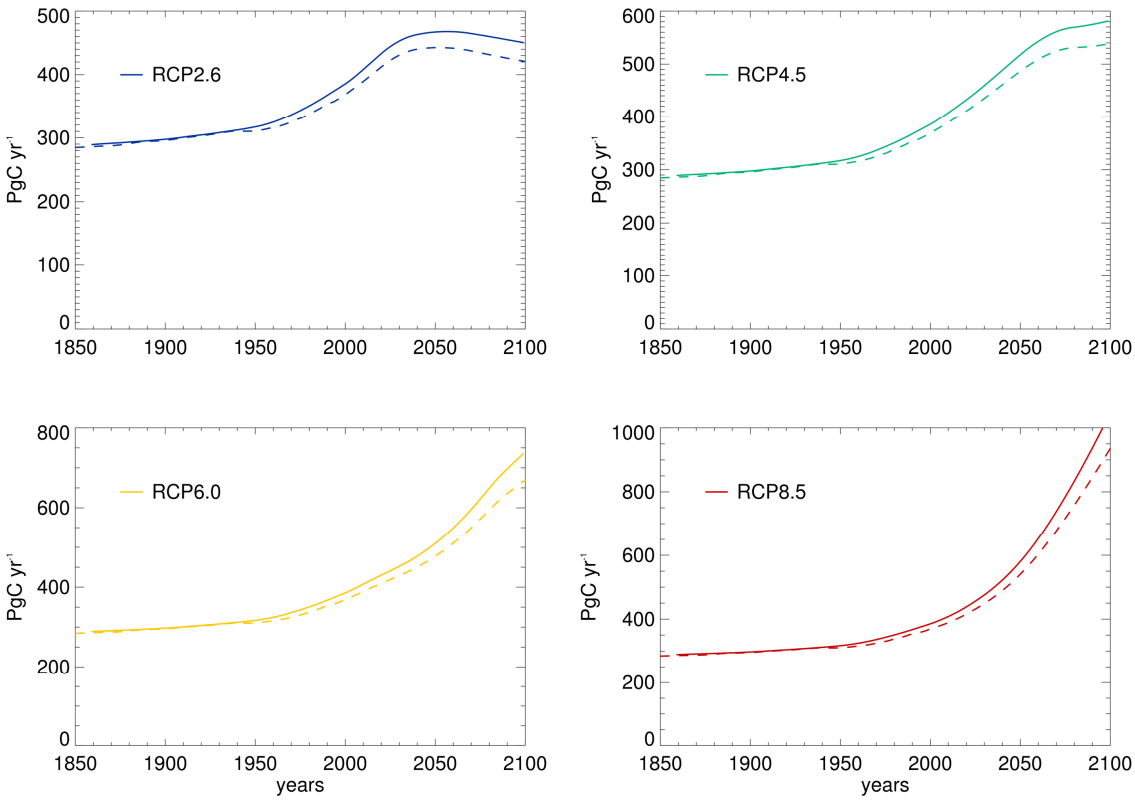

Figure S2. Atmospheric CO_2 concentration simulated in emission-driven simple model simulations (solid lines) compared with those from the RCPs (dashed lines). RCP2.6 (top left), RCP4.5 (top right), RCP6.0 (lower left), RCP8.5 (lower right).

Deriving cumulative airborne fraction metrics

Section 3 of the main text describes results from some cumulative airborne fraction metrics used to quantify the impact on the Earth system of the additional NETs applied to the RCP scenarios. Figure S3 shows the scenario of emissions applied and the derivation of the cumulative airborne fraction metrics. Each row of the figure shows the same quantity, but arranged from left to right for each scenario: RCP2.6 (blue lines); RCP4.5 (green); RCP6.0 (yellow); RCP8.5 (red).

The top row (panels a-d) shows the cumulative emissions from 2020 with the un-modified RCP scenario in solid lines, and the scenarios with additional NETs in dashed lines. The values by 2100 are shown in table 2 of the main text, in columns 3 and 5.

The second row (panels e-h) shows the cumulative airborne fraction (CAF) of the simulations. This is defined as the change in atmospheric CO_2 since 2020 in each simulation divided by the cumulative emission since 2020. Un-modified RCP scenarios are shown by solid lines, and the scenarios with additional NETs in dashed lines. The values by 2100 are shown in table 2 of the main text, in columns 7 and 8. As described in the main text it is particularly the case for RCP2.6 that this measure varies markedly and can change rapidly in both magnitude and sign especially if the cumulative emissions change sign. In this case the simulation with a constant 4 GtC yr^{-1} of NETs achieves negative cumulative emission at 2080 and this drives a singularity in the cumulative airborne fraction defined here.

The third row (panels i-l) shows the reduction in atmospheric CO_2 between the 4 modified (additional NETs) simulations and the un-modified RCP simulation. Although the form of these results appears similar for all RCPs, the magnitude differs.

The fourth row (panels m-p) shows the cumulative airborne fraction *of* the NETs. This is defined as the difference in CO_2 between the two simulations (with and without the additional NETs) divided by the cumulative emissions to that year. This is referred to in the main text as the "perturbation airborne fraction" (PAF) and the values by 2100 are shown in table 2 of the main text, in column 9. This quantity differs from that of the second row because it is calculated from the change in CO_2 concentration for the same year between simulations rather than the change in CO_2 between years in a single simulation.

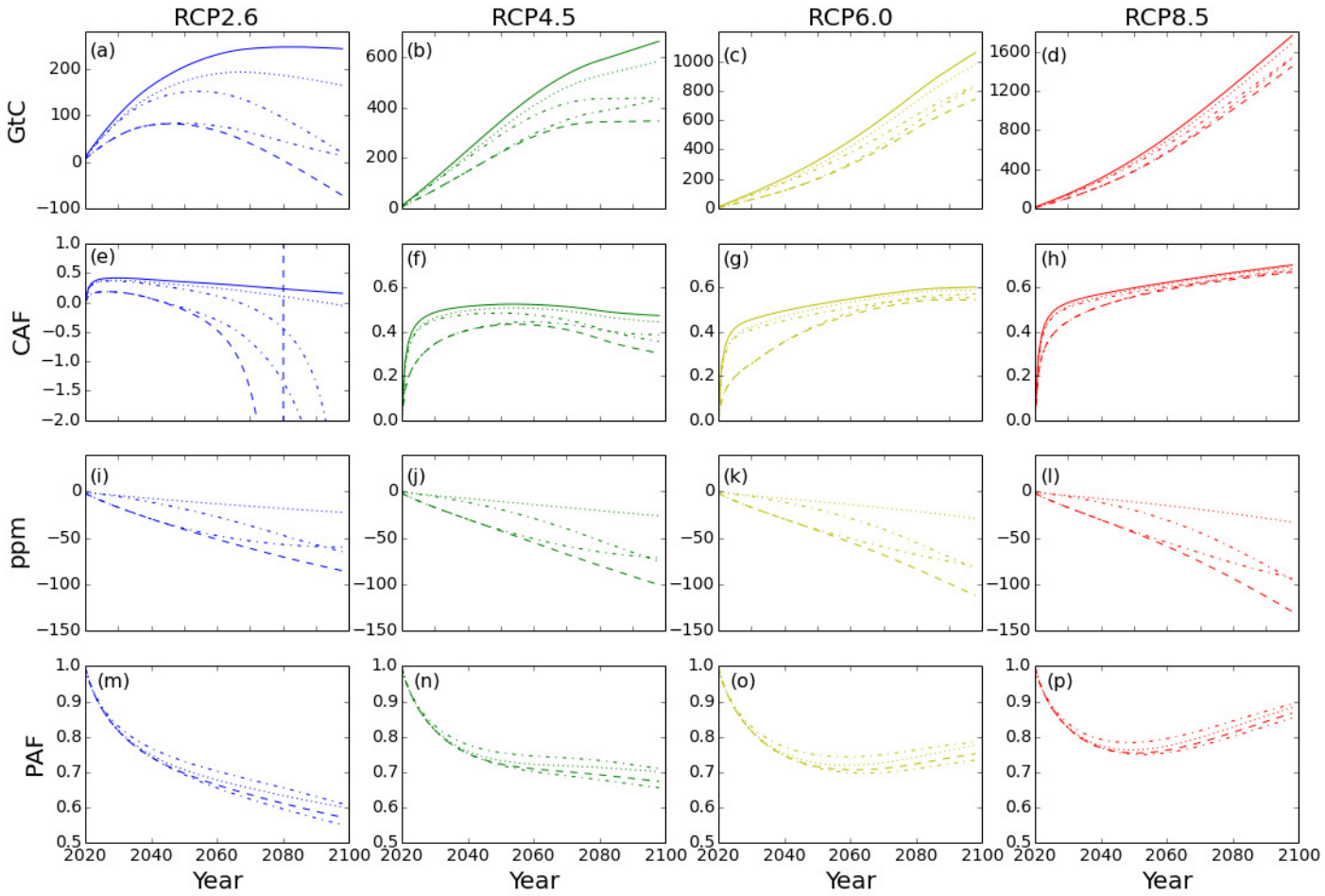

Figure S3.Cumulative emissions and airborne fraction metrics from RCP simulations with additional NETs. (a-d) cumulative emissions since 2020; (e-h) cumulative airborne fraction; (i-l) resulting change in atmospheric CO_2 concentration; (m-p) perturbation airborne fraction. See SI text for full details.

References

Ciais, P, et al. 2013 Carbon and Other Biogeochemical Cycles. In: Climate Change 2013: The Physical Science Basis. Contribution of Working Group I to the Fifth Assessment Report of the Intergovernmental Panel on Climate Change [Stocker, T.F., D. Qin, G.-K. Plattner, M. Tignor, S.K. Allen, J. Boschung, A. Nauels, Y. Xia, V. Bex and P.M. Midgley (eds.)]. Cambridge University Press, Cambridge, United Kingdom and New York, NY, USA.

House J, Huntingford C, Knorr W, Cornell S E, Cox P M, Harris G R, Jones C D, Lowe J A and Prentice C I 2008 What do recent advances in quantifying climate and carbon cycle uncertainties mean for climate policy? *Environ. Res. Lett*. 3044002

Huntingford, C, Lowe, J A, Booth, B B B, Jones, C D, Harris, G R, Gohar L K and Meir P 2009 Contributions of carbon cycle uncertainty to future climate projection spread. *Tellus*, **61B**, 355-360

Jones, C D, Cox, P M and Huntingford, C 2003 Uncertainty in climate-carbon cycle projections associated with the sensitivity of soil respiration to temperature. *Tellus* **55B**, 642–648.

Jones, C D, Cox, P M and Huntingford, C 2006 Climate-carbon cycle feedbacks under stabilization: uncertainty and observational constraints. *Tellus*, **58B**, 603-613

Joos, F, Bruno, M, Fink, R, Siegenthaler, U, Stocker, T, Le Quéré, C and Sarmiento, J 1996 An efficient and accurate representation of complex oceanic and biospheric models of anthropogenic carbon uptake. *Tellus,* **48B**, 397–417

Meinshausen, M, et al. 2011 The RCP Greenhouse Gas Concentrations and their Extension from 1765 to 2300, *Clim. Change*, Special RCP Issue.

5. Concluding comments

In the wake of the Paris Agreement it is clearer than ever that climate science has a central role to play in helping the world achieve its ambitious goals of avoiding dangerous climate change and limiting global warming well below 2^{o}C. But the science advice required has changed and focusses now on how to shape our socio-economic and technological development in a way that decouples economic growth from intensive fossil fuel use and CO_2 emissions.

Quantifying carbon budgets is a vital part of this because international negotiations and agreements need to know the emissions reductions compatible with climate goals and the consequences if these budgets are exceeded. Increasing focus is also placed on the need for cross-disciplinary co-operation and research to avoid unintended consequences and trade-offs of policy actions and to exploit co-benefits. For example, policies that aim to reduce CH_4 and black-carbon aerosol emissions have immediate benefits on local air quality as well as longer term benefits for climate. Conversely reliance in scenarios on widespread adoption of bioenergy (either with or without carbon capture and storage), without considering the impacts on agricultural land and crop production, risks major unintended disruption to global food security. The UN's Sustainable Development Goals (SDGs – see Glossary) provide a framework for ensuring future sustainable development within which addressing climate change is just one strand alongside others such as eradicating poverty and ensuring adequate food, water and energy supplies for all.

The discussion around negative emissions technologies (NETs) is therefore an important and truly cross-disciplinary one, and one where carbon cycle research is central. Field and Mach (2017) recently made a call to "rightsize" carbon dioxide removal: whilst achieving the goals of the Paris Agreement without negative emissions may appear almost impossible to achieve, relying on massive deployment of currently untested technology also appears hugely risky. This is firstly because it may not be successful on the required scale, and secondly because it may diminish efforts to reduce emissions thereby locking us into a pathway of higher CO_2 or committed to the unintended trade-offs of NETs. In a scientific area with a rapidly expanding and diverse literature it will be increasingly important to distinguish

between what can be termed “demand side” and “supply side” aspects of the negative emissions debate. This is something that many published studies do not explicitly discuss. For example, quantifying carbon budgets compatible with climate targets is essential to quantify the *demand* for negative emissions (“how much NET is required?”). Conversely, numerical modelling of the land-surface and ecosystems, and their response to CO_2, climate and human management, is needed to quantify the capacity of technologies such as BECCS to *supply* NETs (“how much negative emission is possible?”). Carbon cycle and Earth System science contributes to both sides of this debate (Figure 13), and must also engage with socio-economic and technology research to understand the possible co-benefits or unintended side-effects of NETs. By more careful framing of our research outputs we can attempt to answer the question “can supply [of NETs] meet demand?” and hence we can begin to know how to “rightsize” the negative emissions in policy relevant scenarios. This PhD has contributed strongly to defining the appropriate level of *demand* needed for different stabilisation targets (Chapter 4; **Jones et al., 2013; Jones et al., 2016b**).

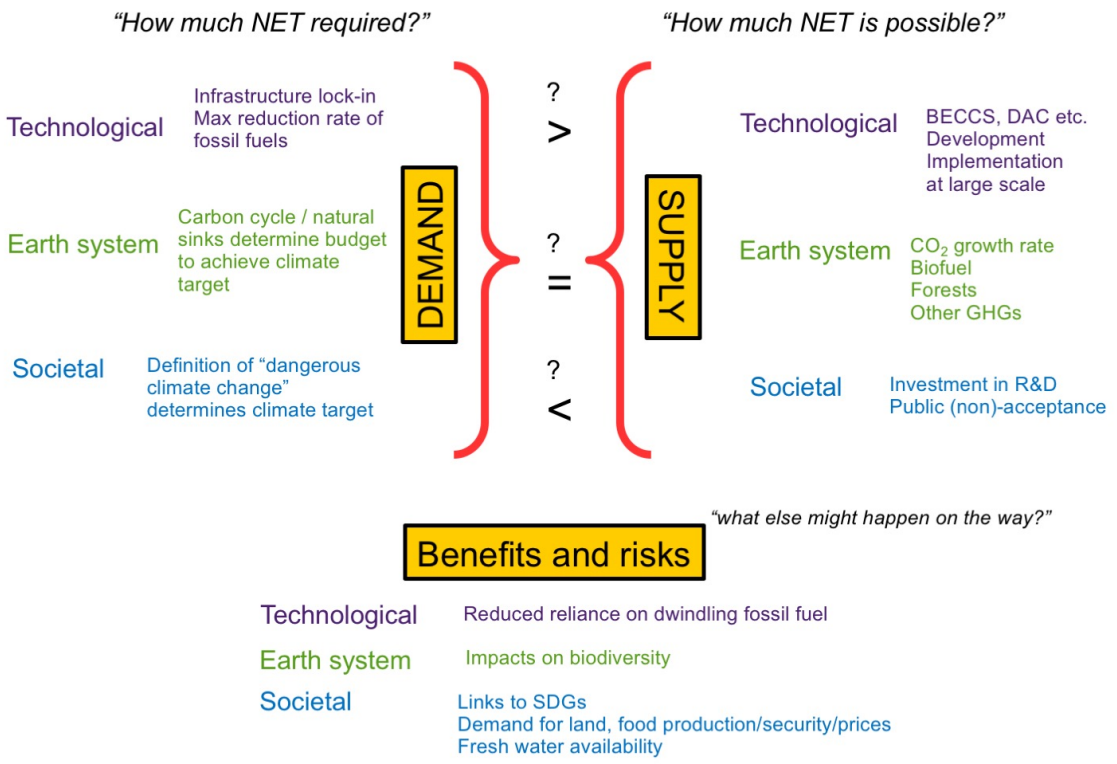

Figure 13. Schematic representation of the need to consider both "demand" and "supply" of NETs. It illustrates how cross-disciplinary research is required to know if the supply can meet the demand required to achieve climate targets.

However, while quantification of carbon budgets (and potential *demand* for negative emissions) to achieve global climate targets has been a major component of this PhD, and is a vital aim of our research, the persistent uncertainty in results is a major hindrance in informing climate policy. The near-linear relationship between global warming and cumulative emissions was one of the new and innovative outcomes of the IPCC AR5 WG1 report. The high-profile figure SPM.10 (reproduced here, Figure 14) showed this relationship – known as TCRE: the Transient Climate Response to cumulative carbon Emissions (see Glossary).

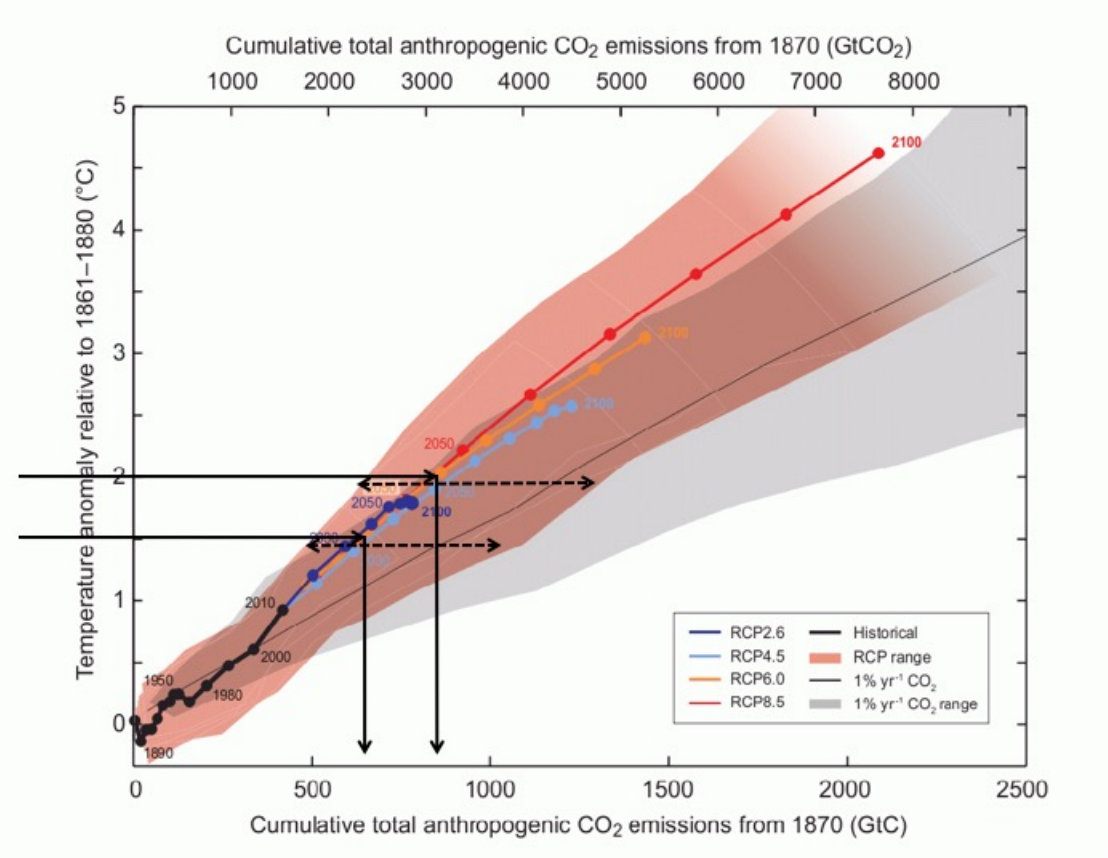

Figure 14. TCRE: the transient climate response to cumulative carbon emissions. Black solid arrows show how to read off from a climate target (global mean temperature on the y-axis) to see the compatible carbon budget (on the x-axis). Black dashed arrows show the uncertainty in this quantity, seen here as the width of the orange plume which originates from the spread of results from CMIP5 model simulations.

The spread of model results means that the uncertainty in carbon budgets is large – possibly as large as the budget itself. The IPCC Synthesis report (IPCC, 2014) summarises this in their table 2.2, showing the budgets to achieve different global targets at different levels of probability. The huge (100s PgC) difference between the carbon budgets associated with different confidence levels for the same target introduces a confusion and disagreement which international negotiators must overcome. This is an additional dimension of uncertainty that needs to be described, in parallel with that of uncertainties in the climate response to given atmospheric greenhouse gas concentration pathways.

The priority is clear therefore: reduce this uncertainty. Carbon cycle science must be central to this. As described throughout this thesis, my contribution to coupled

climate-carbon cycle modelling has been instrumental in getting this far. I played a major role in building the first coupled carbon cycle GCM and in analysis of its first results. These studies gave new insights into the coupled system and guided subsequent development of models and more importantly the international co-operation and coordination of carbon cycle modelling. I have led development and application of the Met Office Hadley Centre Earth System Model, HadGEM2-ES to the major CMIP5 modelling activity and led the subsequent analysis of results for IPCC AR5. I have developed ways of framing the research outcomes to be more relevant and highlighted the long-term risks of committed climate changes on ecosystems.

Looking forward, these priorities will inform the direction of research, including the Carbon Feedbacks Grand Challenge of the World Climate Research Programme (WCRP: https://www.wcrp-climate.org/grand-challenges/gc-carbon-feedbacks – see Glossary). A recent review by the WCRP (Marotzke et al., 2017) identified three key summary questions for climate science. The first one, and most relevant to this PhD, being “where does the carbon go?”, highlighting the high priority of carbon cycle research, especially into carbon sinks. The other two questions are: “How does weather change with climate?” and, “How does climate influence the habitability of the Earth and its regions?”, highlighting the crucial role for physical climate processes and the need to see our research through the lens of impacts on people and therefore sustainability.

Specific research activities underway at the moment gives cause for optimism that we can make tangible progress in reducing uncertainty in the coming years. Firstly, there is growing recognition of the need for more thorough evaluation of biogeochemical processes in ESMs. Foley et al. (2013) clearly distinguish between “top-down”, or system-level evaluation, and “bottom-up” or process-level evaluation. The former is required to ensure models get the right answer and the latter to ensure that they do so for the right reasons. A particular problem with carbon cycle feedbacks is the fine balance between the large and opposing effects of climate and CO_2. Whilst it is vital to continually refine our modelling of the underlying processes, the top-down view is also required to help judge if the resulting balance between them is also robust. We also know that there are some leading order terms not yet

included in CMIP ESMs – for example the role of nutrient cycles in moderating terrestrial carbon storage (Zaehle et al., 2015; Weider et al., 2015) and the potential for large amounts of organic carbon being released from thawed permafrost (Burke et al., 2013; Chadburn et al., 2017). As we progress towards increasing complexity in ESMs we must ensure the careful evaluation of these new processes keeps pace with that development. As a Research Theme leader in the ongoing CRESCENDO project (https://www.crescendoproject.eu) I am leading the work of three workpackages that focus on process evaluation of land and marine biogeochemical cycles and atmospheric trace gases and aerosols. Through closer collaboration with the remote sensing community and in-situ process observations experts, we can make significant progress in our ability to evaluate our ESMs.

Secondly, there is exciting progress in the field of "emergent constraints". Emergent constraints harness the potential of observations of present day behaviour to constrain future projections by using quantitative relationships between short-term and long-term responses across a range of models. For example, the seminal work of Hall and Qu (2006) found a constrainable relationship between the seasonal cycle of snow cover and its long-term climate-albedo feedback. More recently some carbon cycle emergent constraints have been developed using the interannual variability and changes in seasonal cycle of atmospheric CO_2 to constrain tropical land carbon response to climate (Cox et al., 2013) and extra-tropical land carbon response to CO_2 (Wenzel et al., 2016) respectively. Two outstanding aspects relating to the use of emergent constraints are (i) that we need to find a way to combine multiple constraints, and (ii) that the constraint be applied to quantities of importance. For example, simply constraining tropical land carbon "gamma" is of limited use *per se* unless we can translate this constraint into, say, reduced uncertainty in TCRE or compatible carbon budgets. I am working at the forefront of efforts to develop an analytical framework to bring together multiple partial constraints across the Earth System to apply to TCRE.

These advances, taking forward research presented in this PhD, and in tandem with my leadership of C4MIP ahead of the next IPCC report, will enable more careful evaluation of the coupled carbon cycle models, process understanding of the feedbacks and sensitivities, and more relevant choice of scenarios for future

projections. In this way, quantitative carbon cycle modelling will continue to be of direct relevance in informing climate mitigation policy.

Appendix. Full publication list for Christopher Jones

As of May 2017, I have 113 published peer-reviewed papers, 19 as lead author, with an H-index of 46 according to Thomson Reuters ISI Web of Science. I have been listed on the ISI highly cited author list in Geosciences for both 2015 and 2016. My papers are listed below, ordered by year of publication.

2017

Booth, BBB, GR. Harris, JM. Murphy, JI. House, **CD. Jones**, D. Sexton, and SA. Sitch. 2017. “Narrowing the range of future climate projections using historical observations of atmospheric CO2”, *J. Clim.*, DOI:http://dx.doi.org/10.1175/JCLI-D-16-0178.1

Erb, K-H, S. Luyssaert, P. Meyfroidt, J. Pongratz, A. Don, S. Kloster, T. Kuemmerle, T. Fetzel, R. Fuchs, M. Herold, H. Haber, **CD. Jones**, E. Marin-Spiotta, I. Mccallum, E.Robertson, V.Seufert, S.Fritz, A. Valade, A.Wiltshire and AJ. Dolman. 2017. “Land management: data availability and process understanding for global change studies”, *Global Change Biology*, doi: 10.1111/gcb.13443

2016

Jones, CD, V Arora, P Friedlingstein, L Bopp, V Brovkin, J Dunne, H Graven, F Hoffman, T Ilyina, JG John, M Jung, M Kawamiya, C Koven, J Pongratz, T Raddatz, JT Randerson, and S Zaehle. 2016a. "C4MIP-The Coupled Climate-Carbon Cycle Model Intercomparison Project: experimental protocol for CMIP6." *Geoscientific Model Development* 9 (8):2853-2880. doi: 10.5194/gmd-9-2853-2016.

Jones, CD, P Ciais, SJ Davis, P Friedlingstein, T Gasser, GP Peters, J Rogelj, DP van Vuuren, JG Canadell, A Cowie, RB Jackson, M Jonas, E Kriegler, E Littleton, JA Lowe, J Milne, G Shrestha, P Smith, A Torvanger, and A Wiltshire. 2016b. "Simulating the Earth system response to negative emissions." *Environmental Research Letters* 11 (9). doi: 10.1088/1748-

9326/11/9/095012.

Andrews, T, R.A. Betts, BBB. Booth, **CD. Jones**, GS. Jones. 2016. “Effective radiative forcing from historical land use change.” *Clim. Dyn*., DOI 10.1007/s00382-016-3280-7

Betts, RA, **CD Jones**, JR Knight, RF Keeling, and JJ Kennedy. 2016. "El Nino and a record CO2 rise." *Nature Climate Change* 6 (9):806-810.

Fuss, S, **CD Jones**, F Kraxner, GP Peters, P Smith, M Tavoni, DP van Vuuren, JG Canadell, RB Jackson, J Milne, JR Moreira, N Nakicenovic, A Sharifi, and Y Yamagata. 2016. "Research priorities for negative emissions." *Environmental Research Letters* 11 (11). doi: 10.1088/1748-9326/11/11/115007.

Harper, AB, PM Cox, P Friedlingstein, AJ Wiltshire, **CD Jones**, S Sitch, LM Mercado, M Groenendijk, E Robertson, J Kattge, G Bonisch, OK Atkin, M Bahn, J Cornelissen, U Niinemets, V Onipchenko, J Penuelas, L Poorter, PB Reich, NA Soudzilovskaia, and P van Bodegom. 2016. "Improved representation of plant functional types and physiology in the Joint UK Land Environment Simulator (JULES v4.2) using plant trait information." *Geoscientific Model Development* 9 (7):2415-2440. doi: 10.5194/gmd-9-2415-2016.

Harrington, LJ, DJ Frame, EM Fischer, E Hawkins, M Joshi, and **CD Jones**. 2016. "Poorest countries experience earlier anthropogenic emergence of daily temperature extremes." *Environmental Research Letters* 11 (5). doi: 10.1088/1748-9326/11/5/055007.

Hewitt, AJ, BBB Booth, **CD Jones**, ES Robertson, AJ Wiltshire, PG Sansom, DB Stephenson, and S Yip. 2016. "Sources of Uncertainty in Future Projections of the Carbon Cycle." *Journal of Climate* 29 (20):7203-7213. doi: 10.1175/JCLI-D-16-0161.1.

Lawrence, DM, GC Hurtt, A Arneth, V Brovkin, KV Calvin, AD Jones, **CD Jones**, PJ Lawrence, N de Noblet-Ducoudre, J Pongratz, SI Seneviratne, and E Shevliakova. 2016. "The Land Use Model Intercomparison Project (LUMIP) contribution to CMIP6: rationale and experimental design." *Geoscientific Model Development* 9 (9):2973-2998. doi: 10.5194/gmd-9-2973-2016.

Luo, YQ, A Ahlstrom, SD Allison, NH Batjes, V Brovkin, N Carvalhais, A Chappell, P Ciais, EA Davidson, AC Finzi, K Georgiou, B Guenet, O Hararuk, JW Harden, YJ He, F Hopkins, LF Jiang, C Koven, RB Jackson, **CD Jones**, MJ Lara, JY Liang, AD McGuire, W Parton, CH Peng, JT Randerson, A Salazar, CA Sierra,

MJ Smith, HQ Tian, KEO Todd-Brown, M Torn, KJ van Groenigen, YP Wang, TO West, YX Wei, WR Wieder, JY Xia, X Xu, XF Xu, and T Zhou. 2016. "Toward more realistic projections of soil carbon dynamics by Earth system models." *Global Biogeochemical Cycles* 30 (1):40-56. doi: 10.1002/2015GB005239.

Smith, P, SJ Davis, F Creutzig, S Fuss, J Minx, B Gabrielle, E Kato, RB Jackson, A Cowie, E Kriegler, DP van Vuuren, J Rogelj, P Ciais, J Milne, JG Canadell, D McCollum, G Peters, R Andrew, V Krey, G Shrestha, P Friedlingstein, T Gasser, A Grubler, WK Heidug, M Jonas, **CD Jones**, F Kraxner, E Littleton, J Lowe, JR Moreira, N Nakicenovic, M Obersteiner, A Patwardhan, M Rogner, E Rubin, A Sharifi, A Torvanger, Y Yamagata, J Edmonds, and Y Cho. 2016. "Biophysical and economic limits to negative CO2 emissions." *Nature Climate Change* 6:42-50. doi: 10.1038/NCLIMATE2870.

2015

Anav, A, P Friedlingstein, C Beer, P Ciais, A Harper, **C Jones**, G Murray-Tortarolo, D Papale, NC Parazoo, P Peylin, SL Piao, S Sitch, N Viovy, A Wiltshire, and MS Zhao. 2015. "Spatiotemporal patterns of terrestrial gross primary production: A review." *Reviews of Geophysics* 53 (3):785-818. doi: 10.1002/2015RG000483.

Davies-Barnard, T, PJ Valdes, JS Singarayer, AJ Wiltshire, and **CD Jones**. 2015. "Quantifying the relative importance of land cover change from climate and land use in the representative concentration pathways." *Global Biogeochemical Cycles* 29 (6):842-853. doi: 10.1002/2014GB004949.

Gasser, T, C Guivarch, K Tachiiri, **CD Jones**, and P Ciais. 2015. "Negative emissions physically needed to keep global warming below 2 degrees C." *Nature Communications* 6. doi: 10.1038/ncomms8958.

Halloran, PR, BBB Booth, **CD Jones**, FH Lambert, DJ McNeall, IJ Totterdell, and C Volker. 2015. "The mechanisms of North Atlantic CO2 uptake in a large Earth System Model ensemble." *Biogeosciences* 12 (14):4497-4508. doi: 10.5194/bg-12-4497-2015.

Koven, CD, JQ Chambers, K Georgiou, R Knox, R Negron-Juarez, WJ Riley, VK Arora, V Brovkin, P Friedlingstein, and **CD Jones**. 2015. "Controls on

terrestrial carbon feedbacks by productivity versus turnover in the CMIP5 Earth System Models." *Biogeosciences* 12 (17):5211-5228. doi: 10.5194/bg-12-5211-2015.

Zaehle, S, **CD Jones**, B Houlton, JF Lamarque, and E Robertson. 2015. "Nitrogen Availability Reduces CMIP5 Projections of Twenty-First-Century Land Carbon Uptake." *Journal of Climate* 28 (6):2494-2511. doi: 10.1175/JCLI-D-13-00776.1.

2014

Davies-Barnard, T, PJ Valdes, **CD Jones**, and JS Singarayer. 2014. "Sensitivity of a coupled climate model to canopy interception capacity." *Climate Dynamics* 42 (7-8):1715-1732. doi: 10.1007/s00382-014-2100-1.

Davies-Barnard, T, PJ Valdes, JS Singarayer, and **CD Jones**. 2014. "Climatic Impacts of Land-Use Change due to Crop Yield Increases and a Universal Carbon Tax from a Scenario Model." *Journal of Climate* 27 (4):1413-1424. doi: 10.1175/JCLI-D-13-00154.1.

Davies-Barnard, T, PJ Valdes, JS Singarayer, FM Pacifico, and **CD Jones**. 2014. "Full effects of land use change in the representative concentration pathways." *Environmental Research Letters* 9 (11). doi: 10.1088/1748-9326/9/11/114014.

Friedlingstein, P, M Meinshausen, VK Arora, **CD Jones**, A Anav, SK Liddicoat, and R Knutti. 2014. "Uncertainties in CMIP5 Climate Projections due to Carbon Cycle Feedbacks." *Journal of Climate* 27 (2):511-526. doi: 10.1175/JCLI-D-12-00579.1.

Fuss, S, JG Canadell, GP Peters, M Tavoni, RM Andrew, P Ciais, RB Jackson, **CD Jones**, F Kraxner, N Nakicenovic, C Le Quéré, MR Raupach, A Sharifi, P Smith, and Y Yamagata. 2014. "COMMENTARY: Betting on negative emissions." *Nature Climate Change* 4 (10):850-853.

Hoffman, F. M., J. T. Randerson, V. K. Arora, Q. Bao, P. Cadule, D. Ji, **C. D. Jones**, M. Kawamiya, S. Khatiwala, K. Lindsay, A. Obata, E. Shevliakova, K. D. Six, J. F. Tjiputra, E. M. Volodin, and T. Wu. 2014. "Causes and implications of persistent atmospheric carbon dioxide biases in Earth System Models." *Journal of Geophysical Research-Biogeosciences* 119 (2):141-162. doi:

10.1002/2013JG002381.

Schwinger, J, JF Tjiputra, C Heinze, L Bopp, JR Christian, M Gehlen, T Ilyina, **CD Jones**, D Salas-Melia, J Segschneider, R Seferian, and I Totterdell. 2014. "Nonlinearity of Ocean Carbon Cycle Feedbacks in CMIP5 Earth System Models." *Journal of Climate* 27 (11):3869-3888. doi: 10.1175/JCLI-D-13-00452.1.

Todd-Brown, K. E. O., J. T. Randerson, F. Hopkins, V. Arora, T. Hajima, **C. Jones**, E. Shevliakova, J. Tjiputra, E. Volodin, T. Wu, Q. Zhang, and S. D. Allison. 2014. "Changes in soil organic carbon storage predicted by Earth system models during the 21st century." *Biogeosciences* 11 (8):2341-2356. doi: 10.5194/bg-11-2341-2014.

2013

Jones, CD, E Robertson, V Arora, P Friedlingstein, E Shevliakova, L Bopp, V Brovkin, T Hajima, E Kato, M Kawamiya, S Liddicoat, K Lindsay, CH Reick, C Roelandt, J Segschneider, and J Tjiputra. 2013. "Twenty-First-Century Compatible CO2 Emissions and Airborne Fraction Simulated by CMIP5 Earth System Models under Four Representative Concentration Pathways." *Journal of Climate* 26 (13):4398-4413. doi: 10.1175/JCLI-D-12-00554.1.

IPCC AR5 WG1:

Ciais, P., C. Sabine, G. Bala, L. Bopp, V. Brovkin, J. Canadell, A. Chhabra, R. DeFries, J. Galloway, M. Heimann, **C. Jones**, C. Le Quéré, R.B. Myneni, S. Piao and P. Thornton, 2013: Carbon and Other Biogeochemical Cycles. In: Cli- mate Change 2013: The Physical Science Basis. Contribution of Working Group I to the Fifth Assessment Report of the Intergovernmental Panel on Climate Change [Stocker, T.F., D. Qin, G.-K. Plattner, M. Tignor, S.K. Allen, J. Boschung, A. Nauels, Y. Xia, V. Bex and P.M. Midgley (eds.)]. Cambridge University Press, Cambridge, United Kingdom and New York, NY, USA.

IPCC, 2013: Annex II: Climate System Scenario Tables [Prather, M., G. Flato, P. Friedlingstein, **C. Jones**, J.-F. Lamarque, H. Liao and P. Rasch (eds.)]. In: Climate Change 2013: The Physical Science Basis. Contribution of Working Group I to the Fifth Assessment Report of the Intergovernmental Panel on

Climate Change [Stocker, T.F., D. Qin, G.-K. Plattner, M. Tignor, S.K. Allen, J. Boschung, A. Nauels, Y. Xia, V. Bex and P.M. Midgley (eds.)]. Cambridge University Press, Cambridge, United Kingdom and New York, NY, USA.

Anav, A, P Friedlingstein, M Kidston, L Bopp, P Ciais, P Cox, **CD Jones**, M Jung, R Myneni, and Z Zhu. 2013. "Evaluating the Land and Ocean Components of the Global Carbon Cycle in the CMIP5 Earth System Models." *Journal of Climate* 26 (18):6801-6843. doi: 10.1175/JCLI-D-12-00417.1.

Arora, VK, GJ Boer, P Friedlingstein, M Eby, **CD Jones**, JR Christian, G Bonan, L Bopp, V Brovkin, P Cadule, T Hajima, T Ilyina, K Lindsay, JF Tjiputra, and T Wu. 2013. "Carbon-Concentration and Carbon-Climate Feedbacks in CMIP5 Earth System Models." *Journal of Climate* 26 (15):5289-5314. doi: 10.1175/JCLI-D-12-00494.1.

Brovkin, V., L. Boysen, V. K. Arora, J. P. Boisier, P. Cadule, L. Chini, M. Claussen, P. Friedlingstein, V. Gayler, B. J. J. M. van den Hurk, G. C. Hurtt, **C. D. Jones**, E. Kato, N. de Noblet-Ducoudre, F. Pacifico, J. Pongratz, and M. Weiss. 2013. "Effect of Anthropogenic Land-Use and Land-Cover Changes on Climate and Land Carbon Storage in CMIP5 Projections for the Twenty-First Century." *Journal of Climate* 26 (18):6859-6881. doi: 10.1175/JCLI-D-12-00623.1.

Burke, EJ, R Dankers, **CD Jones**, and AJ Wiltshire. 2013. "A retrospective analysis of pan Arctic permafrost using the JULES land surface model." *Climate Dynamics* 41 (3-4):1025-1038. doi: 10.1007/s00382-012-1648-x.

Burke, EJ, **CD Jones**, and CD Koven. 2013. "Estimating the Permafrost-Carbon Climate Response in the CMIP5 Climate Models Using a Simplified Approach." *Journal of Climate* 26 (14):4897-4909. doi: 10.1175/JCLI-D-12-00550.1.

Cox, PM, D Pearson, BB Booth, P Friedlingstein, C Huntingford, **CD Jones**, and CM Luke. 2013. "Sensitivity of tropical carbon to climate change constrained by carbon dioxide variability." *Nature* 494 (7437):341-344. doi: 10.1038/nature11882.

Foley, AM, D Dalmonech, AD Friend, F Aires, AT Archibald, P Bartlein, L Bopp, J Chappellaz, P Cox, NR Edwards, G Feulner, P Friedlingstein, SP Harrison, PO Hopcroft, **CD Jones**, J Kolassa, JG Levine, IC Prentice, J Pyle, NV Riveiros, EW Wolff, and S Zaehle. 2013. "Evaluation of biospheric

components in Earth system models using modern and palaeo-observations: the state-of-the-art." *Biogeosciences* 10 (12):8305-8328. doi: 10.5194/bg-10-8305-2013.

Good, P, **C Jones**, J Lowe, R Betts, and N Gedney. 2013. "Comparing Tropical Forest Projections from Two Generations of Hadley Centre Earth System Models, HadGEM2-ES and HadCM3LC." *Journal of Climate* 26 (2):495-511. doi: 10.1175/JCLI-D-11-00366.1.

Huntingford, C, P Zelazowski, D Galbraith, LM Mercado, S Sitch, R Fisher, M Lomas, AP Walker**, CD Jones**, BBB Booth, Y Malhi, D Hemming, G Kay, P Good, SL Lewis, OL Phillips, OK Atkin, J Lloyd, E Gloor, J Zaragoza-Castells, P Meir, R Betts, PP Harris, C Nobre, J Marengo, and PM Cox. 2013. "Simulated resilience of tropical rainforests to CO2-induced climate change." *Nature Geoscience* 6 (4):268-273. doi: 10.1038/NGEO1741.

Joos, F, R Roth, JS Fuglestvedt, GP Peters, IG Enting, W von Bloh, V Brovkin, EJ Burke, M Eby, NR Edwards, T Friedrich, TL Frolicher, PR Halloran, PB Holden, **C Jones**, T Kleinen, FT Mackenzie, K Matsumoto, M Meinshausen, GK Plattner, A Reisinger, J Segschneider, G Shaffer, M Steinacher, K Strassmann, K Tanaka, A Timmermann, and AJ Weaver. 2013. "Carbon dioxide and climate impulse response functions for the computation of greenhouse gas metrics: a multi-model analysis." *Atmospheric Chemistry and Physics* 13 (5):2793-2825. doi: 10.5194/acp-13-2793-2013.

Liddicoat, S, **C Jones**, and E Robertson. 2013. "CO2 Emissions Determined by HadGEM2-ES to be Compatible with the Representative Concentration Pathway Scenarios and Their Extensions." *Journal of Climate* 26 (13):4381-4397. doi: 10.1175/JCLI-D-12-00569.1.

2012

Booth, BBB, **CD Jones**, M Collins, IJ Totterdell, PM Cox, S Sitch, C Huntingford, RA Betts, GR Harris, and J Lloyd. 2012. "High sensitivity of future global warming to land carbon cycle processes." *Environmental Research Letters* 7 (2). doi: 10.1088/1748-9326/7/2/024002.

Boucher, O, PR Halloran, EJ Burke, M Doutriaux-Boucher, **CD Jones**, J Lowe, MA Ringer, E Robertson, and P Wu. 2012. "Reversibility in an Earth System

model in response to CO2 concentration changes." *Environmental Research Letters* 7 (2). doi: 10.1088/1748-9326/7/2/024013.

Burke, EJ, IP Hartley, and **CD Jones**. 2012. "Uncertainties in the global temperature change caused by carbon release from permafrost thawing." *Cryosphere* 6 (5):1063-1076. doi: 10.5194/tc-6-1063-2012.

Falloon, P. D., R. Dankers, R. A. Betts, **C. D. Jones**, B. B. B. Booth, and F. H. Lambert. 2012. "Role of vegetation change in future climate under the A1B scenario and a climate stabilisation scenario, using the HadCM3C Earth system model." *Biogeosciences* 9 (11):4739-4756. doi: 10.5194/bg-9-4739-2012.

Gottschalk, P., J. U. Smith, M. Wattenbach, J. Bellarby, E. Stehfest, N. Arnell, T. J. Osborn, **C. Jones**, and P. Smith. 2012. "How will organic carbon stocks in mineral soils evolve under future climate? Global projections using RothC for a range of climate change scenarios." *Biogeosciences* 9 (8):3151-3171. doi: 10.5194/bg-9-3151-2012.

Luo, YQ, JT Randerson, G Abramowitz, C Bacour, E Blyth, N Carvalhais, P Ciais, D Dalmonech, JB Fisher, R Fisher, P Friedlingstein, K Hibbard, F Hoffman, D Huntzinger, **CD Jones**, C Koven, D Lawrence, DJ Li, M Mahecha, SL Niu, R Norby, SL Piao, X Qi, P Peylin, IC Prentice, W Riley, M Reichstein, C Schwalm, YP Wang, JY Xia, S Zaehle, and XH Zhou. 2012. "A framework for benchmarking land models." *Biogeosciences* 9 (10):3857-3874. doi: 10.5194/bg-9-3857-2012.

Pacifico, F, GA Folberth, **CD Jones**, SP Harrison, and WJ Collins. 2012. "Sensitivity of biogenic isoprene emissions to past, present, and future environmental conditions and implications for atmospheric chemistry." *Journal of Geophysical Research-Atmospheres* 117. doi: 10.1029/2012JD018276.

2011

Jones, CD, JK Hughes, N Bellouin, SC Hardiman, GS Jones, J Knight, S Liddicoat, FM O'Connor, RJ Andres, C Bell, KO Boo, A Bozzo, N Butchart, P Cadule, KD Corbin, M Doutriaux-Boucher, P Friedlingstein, J Gornall, L Gray, PR Halloran, G Hurtt, WJ Ingram, JF Lamarque, RM Law, M Meinshausen, S Osprey, EJ Palin, LP Chini, T Raddatz, MG Sanderson, AA Sellar, A Schurer,

P Valdes, N Wood, S Woodward, M Yoshioka, and M Zerroukat. 2011. "The HadGEM2-ES implementation of CMIP5 centennial simulations." *Geoscientific Model Development* 4 (3):543-570. doi: 10.5194/gmd-4-543-2011.

Betts, RA, M Collins, DL Hemming, **CD Jones**, JA Lowe, and MG Sanderson. 2011. "When could global warming reach 4 degrees C?" *Philosophical Transactions of the Royal Society a-Mathematical Physical and Engineering Sciences* 369 (1934):67-84. doi: 10.1098/rsta.2010.0292.

Clark, D. B., L. M. Mercado, S. Sitch, **C. D. Jones**, N. Gedney, M. J. Best, M. Pryor, G. G. Rooney, R. L. H. Essery, E. Blyth, O. Boucher, R. J. Harding, C. Huntingford, and P. M. Cox. 2011. "The Joint UK Land Environment Simulator (JULES), model description - Part 2: Carbon fluxes and vegetation dynamics." *Geoscientific Model Development* 4 (3):701-722. doi: 10.5194/gmd-4-701-2011.

Collins, WJ, N Bellouin, M Doutriaux-Boucher, N Gedney, P Halloran, T Hinton, J Hughes, **CD Jones**, M Joshi, S Liddicoat, G Martin, F O'Connor, J Rae, C Senior, S Sitch, I Totterdell, A Wiltshire, and S Woodward. 2011. "Development and evaluation of an Earth-System model-HadGEM2." *Geoscientific Model Development* 4 (4):1051-1075. doi: 10.5194/gmd-4-1051-2011.

Falloon, P, **CD Jones**, M Ades, and K Paul. 2011. "Direct soil moisture controls of future global soil carbon changes: An important source of uncertainty." *Global Biogeochemical Cycles* 25. doi: 10.1029/2010GB003938.

Good, P, J Caesar, D Bernie, JA Lowe, P van der Linden, SN Gosling, R Warren, NW Arnell, S Smith, J Bamber, T Payne, S Laxon, M Srokosz, S Sitch, N Gedney, G Harris, H Hewitt, L Jackson, **CD Jones**, F O'Connor, J Ridley, M Vellinga, P Halloran, and D McNeall. 2011. "A review of recent developments in climate change science. Part I: Understanding of future change in the large-scale climate system." *Progress in Physical Geography* 35 (3):281-296. doi: 10.1177/0309133311407651.

Good, P, **C Jones**, J Lowe, R Betts, B Booth, and C Huntingford. 2011. "Quantifying Environmental Drivers of Future Tropical Forest Extent." *Journal of Climate* 24 (5):1337-1349. doi: 10.1175/2010JCLI3865.1.

Hurtt, GC, LP Chini, S Frolking, RA Betts, J Feddema, G Fischer, JP Fisk, K Hibbard,

RA Houghton, A Janetos, **CD Jones**, G Kindermann, T Kinoshita, KK Goldewijk, K Riahi, E Shevliakova, S Smith, E Stehfest, A Thomson, P Thornton, DP van Vuuren, and YP Wang. 2011. "Harmonization of land-use scenarios for the period 1500-2100: 600 years of global gridded annual land-use transitions, wood harvest, and resulting secondary lands." *Climatic Change* 109 (1-2):117-161. doi: 10.1007/s10584-011-0153-2.

Mahowald, N., K. Lindsay, D. Rothenberg, S. C. Doney, J. K. Moore, P. Thornton, J. T. Randerson, and **C. D. Jones**. 2011. "Desert dust and anthropogenic aerosol interactions in the Community Climate System Model coupled-carbon-climate model." *Biogeosciences* 8 (2):387-414. doi: 10.5194/bg-8-387-2011.

Martin, G. M., N. Bellouin, W. J. Collins, I. D. Culverwell, P. R. Halloran, S. C. Hardiman, T. J. Hinton, **C. D. Jones**, R. E. McDonald, A. J. McLaren, F. M. O'Connor, M. J. Roberts, J. M. Rodriguez, S. Woodward, M. J. Best, M. E. Brooks, A. R. Brown, N. Butchart, C. Dearden, S. H. Derbyshire, I. Dharssi, M. Doutriaux-Boucher, J. M. Edwards, P. D. Falloon, N. Gedney, L. J. Gray, H. T. Hewitt, M. Hobson, M. R. Huddleston, J. Hughes, S. Ineson, W. J. Ingram, P. M. James, T. C. Johns, C. E. Johnson, A. Jones, C. P. Jones, M. M. Joshi, A. B. Keen, S. Liddicoat, A. P. Lock, A. V. Maidens, J. C. Manners, S. F. Milton, J. G. L. Rae, J. K. Ridley, A. Sellar, C. A. Senior, I. J. Totterdell, A. Verhoef, P. L. Vidale, A. Wiltshire, and HadGEM2 Dev Team. 2011. "The HadGEM2 family of Met Office Unified Model climate configurations." *Geoscientific Model Development* 4 (3):723-757. doi: 10.5194/gmd-4-723-2011.

Pacifico, F, SP Harrison, **CD Jones**, A Arneth, S Sitch, GP Weedon, MP Barkley, PI Palmer, D Serca, M Potosnak, TM Fu, A Goldstein, J Bai, and G Schurgers. 2011. "Evaluation of a photosynthesis-based biogenic isoprene emission scheme in JULES and simulation of isoprene emissions under present-day climate conditions." *Atmospheric Chemistry and Physics* 11 (9):4371-4389. doi: 10.5194/acp-11-4371-2011.

2010

Jones, C, S Liddicoat, and J Lowe. 2010. "Role of terrestrial ecosystems in determining CO2 stabilization and recovery behaviour." *Tellus Series B-Chemical and Physical Meteorology* 62 (5):682-699. doi: 10.1111/j.1600-

0889.2010.00490.x.

Cadule, P., P. Friedlingstein, L. Bopp, S. Sitch, **C. D. Jones**, P. Ciais, S. L. Piao, and P. Peylin. 2010. "Benchmarking coupled climate-carbon models against long-term atmospheric CO2 measurements." *Global Biogeochemical Cycles* 24. doi: 10.1029/2009GB003556.

Churkina, G, S Zaehle, J Hughes, N Viovy, Y Chen, M Jung, BW Heumann, N Ramankutty, M Heimann, and **C Jones**. 2010. "Interactions between nitrogen deposition, land cover conversion, and climate change determine the contemporary carbon balance of Europe." *Biogeosciences* 7 (9):2749-2764. doi: 10.5194/bg-7-2749-2010.

Huntingford, C, BBB Booth, S Sitch, N Gedney, JA Lowe, SK Liddicoat, LM Mercado, MJ Best, GP Weedon, RA Fisher, MR Lomas, P Good, P Zelazowski, AC Everitt, AC Spessa, and **CD Jones**. 2010. "IMOGEN: an intermediate complexity model to evaluate terrestrial impacts of a changing climate." *Geoscientific Model Development* 3 (2):679-687. doi: 10.5194/gmd-3-679-2010.

O'Connor, FM, O Boucher, N Gedney, **CD Jones**, GA Folberth, R Coppell, P Friedlingstein, WJ Collins, J Chappellaz, J Ridley, and CE Johnson. 2010. "Possible role of wetlands, permafrost and methane hydrates in the methane cycle under future climate change: A review". *Reviews of Geophysics* 48. doi: 10.1029/2010RG000326.

Peters, W, MC Krol, GR van der Werf, S Houweling, **CD Jones**, J Hughes, K Schaefer, KA Masarie, AR Jacobson, JB Miller, CH Cho, M Ramonet, M Schmidt, L Ciattaglia, F Apadula, D Helta, F Meinhardt, AG di Sarra, S Piacentino, D Sferlazzo, T Aalto, J Hatakka, J Strom, L Haszpra, HAJ Meijer, S van der Laan, REM Neubert, A Jordan, X Rodo, JA Morgui, AT Vermeulen, E Popa, K Rozanski, M Zimnoch, AC Manning, M Leuenberger, C Uglietti, AJ Dolman, P Ciais, M Heimann, and PP Tans. 2010. "Seven years of recent European net terrestrial carbon dioxide exchange constrained by atmospheric observations." *Global Change Biology* 16 (4):1317-1337. doi: 10.1111/j.1365-2486.2009.02078.x.

2009

Jones, CD, J Lowe, S Liddicoat, and R Betts. 2009. "Committed terrestrial ecosystem changes due to climate change." *Nature Geoscience* 2 (7):484-487. doi: 10.1038/ngeo555.

Jones, CD and P Falloon. 2009. "Sources of uncertainty in global modelling of future soil organic carbon storage." *Uncertainties in Environmental Modelling and Consequences For Policy Making*:283-315. doi: 10.1007/978-90-481-2636-1_13.

Allen, MR, DJ Frame, C Huntingford, **CD Jones**, JA Lowe, M Meinshausen, and N Meinshausen. 2009. "Warming caused by cumulative carbon emissions towards the trillionth tonne." *Nature* 458 (7242):1163-1166. doi: 10.1038/nature08019.

Boucher, O, JA Lowe, and **CD Jones.** 2009. "Implications of delayed actions in addressing carbon dioxide emission reduction in the context of geo-engineering." *Climatic Change* 92 (3-4):261-273. doi: 10.1007/s10584-008-9489-7.

Cowling, SA, **CD Jones**, and PM Cox. 2009. "Greening the terrestrial biosphere: simulated feedbacks on atmospheric heat and energy circulation." *Climate Dynamics* 32 (2-3):287-299. doi: 10.1007/s00382-008-0481-8.

Falloon, P., P.Smith, R.Betts, **CD. Jones**, J. Smith, D.Hemming and A.Challinor. 2009. “Carbon Sequestration and Greenhouse Gas Fluxes from Cropland Soils – Climate Opportunities and Threats”, in: S.N. Singh (ed.), Climate Change and Crops, Environmental Science and Engineering, DOI 10.1007/978-3-540-88246-6 5, Springer-Verlag Berlin Heidelberg

Galvin, J. F. P., and **C. D. Jones**. 2009. "The weather and climate of the tropics: Part 10-Tropical agriculture." *Weather* 64 (6):156-161. doi: 10.1002/wea.369.

Gregory, JM, **CD Jones**, P Cadule, and P Friedlingstein. 2009. "Quantifying Carbon Cycle Feedbacks." *Journal of Climate* 22 (19):5232-5250. doi: 10.1175/2009JCLI2949.1.

Huntingford, C, JA Lowe, BBB Booth, **CD Jones**, GR Harris, LK Gohar, and P Meir. 2009. "Contributions of carbon cycle uncertainty to future climate projection spread." *Tellus Series B-Chemical and Physical Meteorology* 61 (2):355-360. doi: 10.1111/j.1600-0889.2009.00414.x.

Lowe, J. A., C. Huntingford, S. C. B. Raper, **C. D. Jones**, S. K. Liddicoat, and L. K. Gohar. 2009. "How difficult is it to recover from dangerous levels of global

warming?" *Environmental Research Letters* 4 (1). doi: 10.1088/1748-9326/4/1/014012.

Pacifico, F, SP Harrison, **CD Jones**, and S Sitch. 2009. "Isoprene emissions and climate." *Atmospheric Environment* 43 (39):6121-6135. doi: 10.1016/j.atmosenv.2009.09.002.

Pinto, E., Y. Shin, S. A. Cowling, and **C. D. Jones**. 2009. "Past, present and future vegetation-cloud feedbacks in the Amazon Basin." *Climate Dynamics* 32 (6):741-751. doi: 10.1007/s00382-009-0536-5.

2008

Cowling, SA, PM Cox, **CD Jones**, MA Maslin, M Peros, and SA Spall. 2008. "Simulated glacial and interglacial vegetation across Africa: implications for species phylogenies and trans-African migration of plants and animals." *Global Change Biology* 14 (4):827-840. doi: 10.1111/j.1365-2486.2007.01524.x.

Cowling, SA, Y Shin, E Pinto, and **CD Jones**. 2008. "Water recycling by Amazonian vegetation: coupled versus uncoupled vegetation-climate interactions." *Philosophical Transactions of the Royal Society B-Biological Sciences* 363 (1498):1865-1871. doi: 10.1098/rstb.2007.0035.

Cox, P, and **C Jones**. 2008. "Climate change - Illuminating the modern dance of climate and CO2." *Science* 321 (5896):1642-1644. doi: 10.1126/science.1158907.

Cox, PM, PP Harris, C Huntingford, RA Betts, M Collins, **CD Jones**, TE Jupp, JA Marengo, and CA Nobre. 2008. "Increasing risk of Amazonian drought due to decreasing aerosol pollution." *Nature* 453 (7192):212-U7. doi: 10.1038/nature06960.

Harrison, R. G., **C. D. Jones**, and J. K. Hughes. 2008. "Competing roles of rising CO2 and climate change in the contemporary European carbon balance." *Biogeosciences* 5 (1):1-10.

House, JI, C Huntingford, W Knorr, SE Cornell, PM Cox, GR Harris, **CD Jones**, JA Lowe, and IC Prentice. 2008. "What do recent advances in quantifying climate and carbon cycle uncertainties mean for climate policy?" *Environmental Research Letters* 3 (4). doi: 10.1088/1748-9326/3/4/044002.

Huntingford, C, RA Fisher, L Mercado, BBB Booth, S Sitch, PP Harris, PM Cox, **CD Jones**, RA Betts, Y Malhi, GR Harris, M Collins, and P Moorcroft. 2008. "Towards quantifying uncertainty in predictions of Amazon 'dieback'." *Philosophical Transactions of the Royal Society B-Biological Sciences* 363 (1498):1857-1864. doi: 10.1098/rstb.2007.0028.

Plattner, GK, R Knutti, F Joos, TF Stocker, W von Bloh, V Brovkin, D Cameron, E Driesschaert, S Dutkiewicz, M Eby, NR Edwards, T Fichefet, JC Hargreaves, **CD Jones**, MF Loutre, HD Matthews, A Mouchet, SA Muller, S Nawrath, A Price, A Sokolov, KM Strassmann, and AJ Weaver. 2008. "Long-term climate commitments projected with climate-carbon cycle models." *Journal of Climate* 21 (12):2721-2751. doi: 10.1175/2007JCLI1905.1.

Sitch, S., C. Huntingford, N. Gedney, P. E. Levy, M. Lomas, S. L. Piao, R. Betts, P. Ciais, P. Cox, P. Friedlingstein, **C. D. Jones**, I. C. Prentice, and F. I. Woodward. 2008. "Evaluation of the terrestrial carbon cycle, future plant geography and climate-carbon cycle feedbacks using five Dynamic Global Vegetation Models (DGVMs)." *Global Change Biology* 14 (9):2015-2039. doi: 10.1111/j.1365-2486.2008.01626.x.

Stott, PA, C Huntingford, **CD Jones**, and JA Kettleborough. 2008. "Observed climate change constrains the likelihood of extreme future global warming." *Tellus Series B-Chemical and Physical Meteorology* 60 (1):76-81. doi: 10.1111/j.1600-0889.2007.00329.x.

Vetter, M., G. Churkina, M. Jung, M. Reichstein, S. Zaehle, A. Bondeau, Y. Chen, P. Ciais, F. Feser, A. Freibauer, R. Geyer, **C. Jones**, D. Papale, J. Tenhunen, E. Tomelleri, K. Trusilova, N. Viovy, and M. Heimann. 2008. "Analyzing the causes and spatial pattern of the European 2003 carbon flux anomaly using seven models." *Biogeosciences* 5 (2):561-583.

2007

Betts, RA, O Boucher, M Collins, PM Cox, PD Falloon, N Gedney, DL Hemming, C Huntingford, **CD Jones**, DMH Sexton, and MJ Webb. 2007. "Projected increase in continental runoff due to plant responses to increasing carbon dioxide." *Nature* 448 (7157):1037-U5. doi: 10.1038/nature06045.

Cowling, SA**, CD Jones**, and PM Cox. 2007. "Consequences of the evolution of C-4

photosynthesis for surface energy and water exchange." *Journal of Geophysical Research-Biogeosciences* 112 (G1). doi: 10.1029/2005JG000095.

Falloon, P, **CD Jones**, CE Cerri, R Al-Adamat, P Kamoni, T Bhattacharyya, M Easter, K Paustian, K Killian, K Coleman, and E Milne. 2007. "Climate change and its impact on soil and vegetation carbon storage in Kenya, Jordan, India and Brazil." *Agriculture Ecosystems & Environment* 122 (1):114-124. doi: 10.1016/j.agee.2007.01.013.

Gullison, RE, PC Frumhoff, JG Canadell, CB Field, DC Nepstad, K Hayhoe, R Avissar, LM Curran, P Friedlingstein, **CD Jones**, and C Nobre. 2007. "Tropical forests and climate policy." *Science* 316 (5827):985-986. doi: 10.1126/science.1136163.

Pope, V., S. Brown, R. Clark, M. Collins, W. Collins, C. Dearden, J. Gunson, G. Harris, **C. Jones**, A. Keen, J. Lowe, M. Ringer, C. Senior, S. Sitch, M. Webb, and S. Woodward. 2007. "The Met Office Hadley Centre climate modelling capability: the competing requirements for improved resolution, complexity and dealing with uncertainty." *Philosophical Transactions of the Royal Society a-Mathematical Physical and Engineering Sciences* 365 (1860):2635-2657. doi: 10.1098/rsta.2007.2087.

2006

Jones, CD., PM. Cox and C Huntingford. 2006a. “Impact of Climate-Carbon Cycle Feedbacks on Emissions Scenarios to Achieve Stabilisation”, in: Avoiding Dangerous Climate Change, Eds: HJ. Schellnhuber, W. Cramer, N. Nakicenovic, T. Wigley, G. Yohe, Cambridge University Press

Jones, CD, PM Cox, and C Huntingford. 2006b. "Climate-carbon cycle feedbacks under stabilization: uncertainty and observational constraints." *Tellus Series B-Chemical and Physical Meteorology* 58 (5):603-613. doi: 10.1111/j.1600-0889.2006.00215.x.

Cox, PM., C. Huntingford and **CD. Jones**. 2006. “Conditions for Sink-to-Source Transitions and Runaway Feedbacks from the Land Carbon Cycle.” in: Avoiding Dangerous Climate Change, Eds: HJ. Schellnhuber, W. Cramer, N. Nakicenovic, T. Wigley, G. Yohe, Cambridge University Press

Friedlingstein, P, P Cox, R Betts, L Bopp, W Von Bloh, V Brovkin, P Cadule, S Doney, M Eby, I Fung, G Bala, J John, **C Jones**, F Joos, T Kato, M Kawamiya, W Knorr, K Lindsay, HD Matthews, T Raddatz, P Rayner, C Reick, E Roeckner, KG Schnitzler, R Schnur, K Strassmann, AJ Weaver, C Yoshikawa, and N Zeng. 2006. "Climate-carbon cycle feedback analysis: Results from the (CMIP)-M-4 model intercomparison." *Journal of Climate* 19 (14):3337-3353. doi: 10.1175/JCLI3800.1.

2005

Jones, CD, and PM Cox. 2005. "On the significance of atmospheric CO2 growth rate anomalies in 2002-2003." *Geophysical Research Letters* 32 (14). doi: 10.1029/2005GL023027.

Jones, CD, J Gregory, R Thorpe, P Cox, J Murphy, D Sexton, and P Valdes. 2005. "Systematic optimisation and climate simulation of FAMOUS, a fast version of HadCM3." *Climate Dynamics* 25 (2-3):189-204. doi: 10.1007/s00382-005-0027-2.

Jones, CD, C McConnell, K Coleman, P Cox, P Falloon, D Jenkinson, and D Powlson. 2005. "Global climate change and soil carbon stocks; predictions from two contrasting models for the turnover of organic carbon in soil." *Global Change Biology* 11 (1):154-166. doi: 10.1111/j.1365-2486.2004.00885.x.

Andreae, MO, **CD Jones**, and PM Cox. 2005. "Strong present-day aerosol cooling implies a hot future." *Nature* 435 (7046):1187-1190. doi: 10.1038/nature03671.

2004

Betts, RA, PM Cox, M Collins, PP Harris, C Huntingford, and **CD Jones**. 2004. "The role of ecosystem-atmosphere interactions in simulated Amazonian precipitation decrease and forest dieback under global climate warming." *Theoretical and Applied Climatology* 78 (1-3):157-175. doi: 10.1007/s00704-004-0050-y.

Cowling, SA, RA Betts, PM Cox, VJ Ettwein, **CD Jones**, MA Maslin, and SA Spall. 2004. "Contrasting simulated past and future responses of the Amazonian

forest to atmospheric change." *Philosophical Transactions of the Royal Society B-Biological Sciences* 359 (1443):539-547. doi: 10.1098/rstb.2003.1427.

Cox, PM, RA Betts, M Collins, PP Harris, C Huntingford, and **CD Jones**. 2004. "Amazonian forest dieback under climate-carbon cycle projections for the 21st century." *Theoretical and Applied Climatology* 78 (1-3):137-156. doi: 10.1007/s00704-004-0049-4.

2003

Jones, CD. 2003. "A fast ocean GCM without flux adjustments." *Journal of Atmospheric and Oceanic Technology* 20 (12):1857-1868. doi: 10.1175/1520-0426(2003)020<1857:AFOGWF>2.0.CO;2.

Jones, CD, P Cox, and C Huntingford. 2003. "Uncertainty in climate-carbon-cycle projections associated with the sensitivity of soil respiration to temperature." *Tellus Series B-Chemical and Physical Meteorology* 55 (2):642-648. doi: 10.1034/j.1600-0889.2003.01440.x.

Jones, CD, PM Cox, RLH Essery, DL Roberts, and MJ Woodage. 2003. "Strong carbon cycle feedbacks in a climate model with interactive CO2 and sulphate aerosols." *Geophysical Research Letters* 30 (9). doi: 10.1029/2003GL016867.

Sanderson, MG, **CD Jones**, WJ Collins, CE Johnson, and RG Derwent. 2003. "Effect of climate change on isoprene emissions and surface ozone levels." *Geophysical Research Letters* 30 (18). doi: 10.1029/2003GL017642.

2001

Jones, CD, and PM Cox. 2001a. "Modeling the volcanic signal in the atmospheric CO2 record." *Global Biogeochemical Cycles* 15 (2):453-465. doi: 10.1029/2000GB001281.

Jones, CD, and PM Cox. 2001b. "Constraints on the temperature sensitivity of global soil respiration from the observed interannual variability in atmospheric CO(2)." *Atmospheric Science Letters* 2 (1-4):166-172. doi: 10.1006/asle.2001.0041.

Jones, CD, M Collins, PM Cox, and SA Spall. 2001. "The carbon cycle response to

ENSO: A coupled climate-carbon cycle model study." *Journal of Climate* 14 (21):4113-4129. doi: 10.1175/1520-0442(2001)014<4113:TCCRTE>2.0.CO;2.

2000

Cox, PM, RA Betts, **CD Jones**, SA Spall, and IJ Totterdell. 2000. "Acceleration of global warming due to carbon-cycle feedbacks in a coupled climate model." *Nature* 408 (6809):184-187. doi: 10.1038/35041539.

1997

Jones, CD. and B. Macpherson. 1997. “A latent heat nudging scheme for the assimilation of precipitation data into an operational mesoscale model.”, *Meteorol. Appl*. **4**, 269-277

Glossary

Assessment Report (AR) (of the ***IPCC***). Approximately every 5-7 years the IPCC publishes an Assessment Report summarizing the key knowledge in the areas of climate change. The report spans three working groups: WG1 on the physical science basis, WG2 on impacts and vulnerability, and WG3 on mitigation of climate change. The first AR (***FAR***) was published in 1990, the second (***SAR***) in 1996, the third (***TAR***) in 2001, fourth (***AR4***) in 2006 and the fifth (***AR5***) in 2013. The sixth Assessment Report (***AR6***) is scheduled to be published in 2021.

Biogeochemically coupled (BGC). A technical term when used in the context of climate-carbon cycle feedback diagnosis. See "***carbon cycle coupling***" for full description.

Carbon cycle coupling. In order to measure the effect of a single change on the climate or carbon cycle, ESMs can be configured to disable some of the processes within them so that individual responses can be isolated. In "fully coupled" ("COU") climate-carbon cycle simulations both climate and CO_2 will affect land and ocean carbon sinks. To separate these terms, the models can be changed so that only the biogeochemistry experiences the effects of CO_2 (termed "biogeochemically coupled" (BGC) by **Gregory et al. (2009**) and originally termed "uncoupled" ("UNC") by **Friedlingstein et al. (2006))**; the models can also be configured so that only the radiation component of the model experiences changes in CO_2 (termed "radiatively coupled" (RAD) by **Gregory et al., 2009**).

Carbon dioxide removal (CDR). See Negative emissions.

C4MIP. Coupled climate-carbon cycle model intercomparison project (see also ***MIP***). A comparison of coordinated simulations by carbon cycle GCMs. See www.c4mip.net.

Coupled Model Intercomparison Project (CMIP). See also ***MIP***. The use of coordinated multi-model intercompariosns has become widespread and in particular

the use of coupled (here meaning atmosphere-ocean) GCMs intercomparison projects. CMIP is an activity established under the **World Climate Research Programme (WCRP)** to coordinate coupled modelling across climate research centres around the world (Meehl et al. 2005). Results are usually made freely available for download by researchers anywhere around the world. The activity is independent from IPCC but is usually coordinated so that a major intercomparison is scheduled and completed ahead of each Assessment Report (see AR). After CMIP3 delivered results for assessment by AR4, the labels of CMIP generations were changed to synchronise with IPCC reports, so that CMIP5 was the modelling activity which fed into AR5. The next generation of CMIP will be CMIP6 (Eyring et al., 2016), and it is planned that these simulations will be available for assessment in AR6.

Concentration-driven. A configuration of a carbon cycle model experiment in which the atmospheric concentration of CO_2 is prescribed as an external forcing or boundary condition to the model. See Box 6.4 of **Ciais et al. (2013)** for fuller details.

Dynamic global vegetation model (DGVM). A class of numerical model which simulates the exchange and storage of carbon and water between land and atmosphere by representing the behaviour of vegetation. Commonly vegetation is split into discrete Plant Functional Types (PFTs) such as broadleaf or needleleaf trees.

Emissions-driven. (see also “Concentration-driven”). A configuration of a carbon cycle model experiment in which the atmospheric concentration of CO_2 is simulated by the model as a prognostic variable which can evolve in response to external forcing of anthropogenic emissions of CO_2. See Box 6.4 of **Ciais et al. (2013)** for fuller details.

Equilibrium climate sensitivity (ECS). The change in global average surface temperature, due to a doubling of atmospheric CO_2 simulated by a climate model when it has been run for a sufficiently long period for all the components to reach a new steady state, and the resulting increase in outgoing long-wave radiation of a warmer planet balances the reduced outgoing radiation absorbed by the CO_2.

Earth System Model (ESM). For the purposes of this thesis, a class of numerical model which has a GCM at its core but also represents an interactive carbon cycle both on land and in the ocean.

General circulation model (GCM). A class of numerical model which is formed around a 3D representation of the world and simulates the evolution of the atmosphere or ocean by numerically solving discretized equations of fluid dynamics.

HadCM3LC. Hadley Centre Coupled Model, version 3, low-resolution, carbon cycle. A configuration of the Met Office Unified Model developed in the late 1990s. It was based on the HadCM3 climate model (Gordon et al., 2000), but with an interactive carbon cycle. In order to accommodate the added complexity of an ocean carbon cycle its horizontal resolution was reduced from 1.25x1.25 degrees to 2.5x3.75 degrees. It was the first coupled climate-carbon cycle GCM, and was used for the simulations published by **Cox et al. (2000)** and many subsequent publications including **Jones et al. (2009).**

HadGEM2-ES. Hadley Centre Global Environment Model, version 2, Earth System configuration. A configuration of the Met Office Unified Model developed in 2010. It was based on the HadGEM2 climate model (**Martin et al., 2011**), but with an interactive carbon cycle and atmospheric chemistry (**Collins et al., 2011**). It was configured and used to perform the CMIP5 simulations as described by **Jones et al. (2011)**.

Intergovernmental Panel on Climate Change (IPCC). A United Nations body, founded in 1988, which evaluates climate change science. It assesses research on climate change and synthesises it into major **Assessment Reports (*AR*)** every 5–7 years

Model Intercomparison Project (MIP). A coordinated set of numerical simulations performed by multiple models following a common protocol. By ensuring that all models perform the same experiments with the same input data, the results can be more rigorously interpreted as they depend much less on individual modelling centre's choices.

Negative emissions techniques (NETs). Also known as ***CDR***. Deliberate and direct removal of CO_2 from the atmosphere by human activity. Such techniques include direct capture of CO_2 from air by chemical means, sequestration in soil through biochar, enhanced weathering of rocks, the use of bioenergy with carbon capture and storage or enhanced uptake in the ocean.

Radiatively coupled (RAD). A technical term when used in the context of climate-carbon cycle feedback diagnosis. See "***carbon cycle coupling***" for full description.

Representative Concentration Pathways (RCPs). A set of four scenarios of greenhouse gas concentrations adopted by the **IPCC** for its Fifth Assessment Report. They are taken from the Integrated Assessment literature and aim to span approximately 10^{th} to 90^{th} percentiles of levels of radiative forcing at 2100. The RCPs are labelled by this radiative forcing: e.g. RCP2.6 achieves 2.6 Wm^{-2} of global radiative forcing by 2100. The others are RCP4.5, RCP6.0 and RCP8.5.

Sustainable Development Goals (SDGs). The UN has adopted 17 goals that together form a framework to guide future development and to try to ensure single goals are not achieved at the expense of others. The goals include an end to poverty and hunger and improving access to health and education for all. The full set are listed and described here: http://www.un.org/sustainabledevelopment/sustainable-development-goals/

Transient climate response to cumulative carbon emissions (TCRE). The change in global average temperature that results from the emission of a given mass of CO_2 into the atmosphere. This quantity accounts for the response of the carbon cycle as well as the response of the climate to CO_2 and as such is a more generalized form of climate sensitivity.

Uncoupled. A technical term when used in the context of climate-carbon cycle feedback diagnosis. See "***carbon cycle coupling***" for full description.

United Nations Environment Programme (***UNEP).*** An agency of United Nations and coordinates its environmental activities.

United Nations Framework Convention on Climate Change (UNFCCC). An international treaty established in 1992 to "stabilise greenhouse gas concentrations in the atmosphere at a level that would prevent dangerous anthropogenic interference with the climate system". Amongst other agreements, it established the Kyoto Protocol in 1997 and the Paris Agreement in 2015.

World Climate Research Programme (WCRP). Established in 1980 by the **WMO** to coordinate international research to further the fundamental understanding of the climate system.

WCRP Grand Challenges. Recently established areas of emphasis for climate research regarded as top priorities for the coming decade. They include a Grand Challenge on "carbon feedbacks in the climate system".

World Meteorological Organisation (WMO). As a specialized agency of the United Nations, WMO is dedicated to international cooperation and coordination on the state and behaviour of the Earth's atmosphere, its interaction with the land and oceans, the weather and climate it produces, and the resulting distribution of water resources (source: https://public.wmo.int/en/our-mandate/what-we-do).

Bibliography

Allen, MR, DJ Frame, C Huntingford, CD Jones, JA Lowe, M Meinshausen, and N Meinshausen. 2009. "Warming caused by cumulative carbon emissions towards the trillionth tonne." *Nature* 458 (7242):1163-1166. doi: 10.1038/nature08019.

Arneth, A, SP Harrison, S Zaehle, K Tsigaridis, S Menon, PJ Bartlein, J Feichter, A Korhola, M Kulmala, D O'Donnell, G Schurgers, S Sorvari, and T Vesala. 2010. "Terrestrial biogeochemical feedbacks in the climate system." *Nature Geoscience* 3 (8):525-532. doi: DOI 10.1038/ngeo905.

Arora, VK, GJ Boer, P Friedlingstein, M Eby, CD Jones, JR Christian, G Bonan, L Bopp, V Brovkin, P Cadule, T Hajima, T Ilyina, K Lindsay, JF Tjiputra, and T Wu. 2013. "Carbon-Concentration and Carbon-Climate Feedbacks in CMIP5 Earth System Models." *Journal of Climate* 26 (15):5289-5314. doi: 10.1175/JCLI-D-12-00494.1.

Arrhenius, S. 1896: On the influence of carbonic acid in the air upon the temperature of the ground. Philosophical Magazine 41, 237-76.

Bacastow, R.B., 1993. “The effect of temperature change of the warm surface waters of the oceans on atmospheric CO2.” Global Biogeochemical Cycles, 10, 319-333.

Bates, JR. 2007. "Some considerations of the concept of climate feedback." *Quarterly Journal of the Royal Meteorological Society* 133 (624):545-560. doi: 10.1002/qj.62.

Battin, TJ, S Luyssaert, LA Kaplan, AK Aufdenkampe, A Richter, and LJ Tranvik. 2009. "The boundless carbon cycle." *Nature Geoscience* 2 (9):598-600. doi: 10.1038/ngeo618.

Bony, S, R Colman, VM Kattsov, RP Allan, CS Bretherton, JL Dufresne, A Hall, S Hallegatte, MM Holland, W Ingram, DA Randall, BJ Soden, G Tselioudis, and MJ Webb. 2006. "How well do we understand and evaluate climate change feedback processes?" *Journal of Climate* 19 (15):3445-3482. doi: 10.1175/JCLI3819.1.

Broecker, W.S., T. Takahashi, H. J. Simpson, T.-H. Peng. 1979. “Fate of fossil fuel carbon dioxide and global carbon budget.” Science 206, 409.

Brovkin, V, L Boysen, VK Arora, JP Boisier, P Cadule, L Chini, M Claussen, P Friedlingstein, V Gayler, BJJM van den Hurk, GC Hurtt, CD Jones, E Kato, N de Noblet-Ducoudre, F Pacifico, J Pongratz, and M Weiss. 2013. "Effect of Anthropogenic Land-Use and Land-Cover Changes on Climate and Land Carbon Storage in CMIP5 Projections for the Twenty-First Century." *Journal of Climate* 26 (18):6859-6881. doi: 10.1175/JCLI-D-12-00623.1.

Burke, EJ, CD Jones, and CD Koven. 2013. "Estimating the Permafrost-Carbon Climate Response in the CMIP5 Climate Models Using a Simplified Approach." *Journal of Climate* 26 (14):4897-4909. doi: 10.1175/JCLI-D-12-00550.1.

Cao, L, and K Caldeira. 2010. "Atmospheric carbon dioxide removal: long-term consequences and commitment." *Environmental Research Letters* 5 (2). doi: 10.1088/1748-9326/5/2/024011.

Chadburn, SE, EJ Burke, PM Cox, P Friedlingstein, G Hugelius, and S Westermann. 2017. "An observation-based constraint on permafrost loss as a function of global warming." *Nature Climate Change* 7 (5): doi: 10.1038/NCLIMATE3262.

Ciais, P., C. Sabine, G. Bala, L. Bopp, V. Brovkin, J. Canadell, A. Chhabra, R. DeFries, J. Galloway, M. Heimann, C. Jones, C. Le Quéré, R.B. Myneni, S. Piao and P. Thornton, 2013: Carbon and Other Biogeochemical Cycles. In: Climate Change 2013: The Physical Science Basis. Contribution of Working Group I to the Fifth Assessment Report of the Intergovernmental Panel on Climate Change [Stocker, T.F., D. Qin, G.-K. Plattner, M. Tignor, S.K. Allen, J. Boschung, A. Nauels, Y. Xia, V. Bex and P.M. Midgley (eds.)]. Cambridge University Press, Cambridge, United Kingdom and New York, NY, USA.

Collins, M., R. Knutti, J. Arblaster, J.-L. Dufresne, T. Fichefet, P. Friedlingstein, X. Gao, W.J. Gutowski, T. Johns, G. Krinner, M. Shongwe, C. Tebaldi, A.J. Weaver and M. Wehner, 2013: Long-term Climate Change: Projections, Commitments and Irreversibility. In: Climate Change 2013: The Physical Science Basis. Contribution of Working Group I to the Fifth Assessment Report of the Intergovernmental Panel on Climate Change [Stocker, T.F., D. Qin, G.-K. Plattner, M. Tignor, S.K. Allen, J. Boschung, A. Nauels, Y. Xia, V. Bex and P.M. Midgley (eds.)]. Cambridge University Press, Cambridge, United Kingdom and New York, NY, USA.

Collins, WJ, N Bellouin, M Doutriaux-Boucher, N Gedney, P Halloran, T Hinton, J Hughes, CD Jones, M Joshi, S Liddicoat, G Martin, F O'Connor, J Rae, C Senior, S Sitch, I Totterdell, A Wiltshire, and S Woodward. 2011. "Development and evaluation of an Earth-System model-HadGEM2." *Geoscientific Model Development* 4 (4):1051-1075. doi: 10.5194/gmd-4-1051-2011.

Cox, PM, RA Betts, CD Jones, SA Spall, and IJ Totterdell. 2000. "Acceleration of global warming due to carbon-cycle feedbacks in a coupled climate model." *Nature* 408 (6809):184-187. doi: 10.1038/35041539.

Cox, PM, D Pearson, BB Booth, P Friedlingstein, C Huntingford, CD Jones, and CM Luke. 2013. "Sensitivity of tropical carbon to climate change constrained by carbon dioxide variability." *Nature* 494 (7437):341-344. doi: 10.1038/nature11882.

Cramer, W., A. Bondeau, F. I. Woodward, I. C. Prentice, R. A. Betts, V. Brovkin, P. M. Cox, V. Fisher, J. A. Foley, A. D. Friend, C. Kucharik, M. R. Lomas, N. Ramankutty, S. Sitch, B. Smith, A. White, and C. Young-Molling. 2001. "Global response of terrestrial ecosystem structure and function to CO2 and climate change: results from six dynamic global vegetation models." *Global Change Biology* 7 (4):357-373.

Cubasch, U., D. Wuebbles, D. Chen, M.C. Facchini, D. Frame, N. Mahowald, and J.-G. Winther, 2013: Introduction. In: Climate Change 2013: The Physical Science Basis. Contribution of Working Group I to the Fifth Assessment Report of the Intergovernmental Panel on Climate Change [Stocker, T.F., D. Qin, G.-K. Plattner, M. Tignor, S.K. Allen, J. Boschung, A. Nauels, Y. Xia, V. Bex and P.M. Midgley (eds.)]. Cambridge University Press, Cambridge, United Kingdom and New York, NY, USA.

Davies-Barnard, T, PJ Valdes, JS Singarayer, FM Pacifico, and CD Jones. 2014. "Full effects of land use change in the representative concentration pathways." *Environmental Research Letters* 9 (11). doi: 10.1088/1748-9326/9/11/114014.

Davies-Barnard, T, PJ Valdes, JS Singarayer, AJ Wiltshire, and CD Jones. 2015. "Quantifying the relative importance of land cover change from climate and land use in the representative concentration pathways." *Global Biogeochemical Cycles* 29 (6):842-853. doi: 10.1002/2014GB004949.

de Noblet-Ducoudre, N, JP Boisier, A Pitman, GB Bonan, V Brovkin, F Cruz, C Delire, V Gayler, BJJM van den Hurk, PJ Lawrence, MK van der Molen, C Muller, CH Reick, BJ Strengers, and A Voldoire. 2012. "Determining Robust Impacts of Land-Use-Induced Land Cover Changes on Surface Climate over North America and Eurasia: Results from the First Set of LUCID Experiments." *Journal of Climate* 25 (9):3261-3281. doi: 10.1175/JCLI-D-11-00338.1.

Denman, K. L., G. Brasseur, C. Heinze, E. Holland, D. Jacob, U. Lohmann, S. Ramachandran, P. L. da Silva Dias, S. C. Wofsy, and X. Zhang. 2007. Couplings Between Changes in the Climate System and Biogeochemistry. In *In: Climate Change 2007: The Physical Science Basis. Contribution of Working Group I to the Fourth Assessment Report of the Intergovernmental Panel on Climate Change [Solomon, S., D. Qin, M. Manning, Z. Chen, M. Marquis, K.B. Averyt, M.Tignor and H.L. Miller (eds.)].* Cambridge University Press, Cambridge, United Kingdom and New York, NY, USA.

Enting, I.G., T.M.L. Wigley and M. Heimann. 1994. “Future emissions and concentrations of carbon dioxide: Key Ocean/Atmosphere/Land analyses”. *CSIRO Division of Atmospheric Physics Technical paper no. 31*, 120pp.

Eyring, V, S Bony, GA Meehl, CA Senior, B Stevens, RJ Stouffer, and KE Taylor. 2016. "Overview of the Coupled Model Intercomparison Project Phase 6 (CMIP6) experimental design and organization." *Geoscientific Model Development* 9 (5):1937-1958. doi: 10.5194/gmd-9-1937-2016.

Field, CB, MJ Behrenfeld, JT Randerson, and P Falkowski. 1998. "Primary production of the biosphere: Integrating terrestrial and oceanic components." *Science* 281 (5374):237-240. doi: 10.1126/science.281.5374.237.

Field, CB, JT Randerson, and CM Malmstrom. 1995. "Global net primary production - combining ecology and remote-sensing." *Remote Sensing of Environment* 51 (1):74-88. doi: 10.1016/0034-4257(94)00066-V.

Field, CB, and KJ Mach. 2017. "Rightsizing carbon dioxide removal." *Science* 356 (6339):706-707. doi: 10.1126/science.aam9726.

Foley, AM, D Dalmonech, AD Friend, F Aires, AT Archibald, P Bartlein, L Bopp, J Chappellaz, P Cox, NR Edwards, G Feulner, P Friedlingstein, SP Harrison, PO Hopcroft, CD Jones, J Kolassa, JG Levine, IC Prentice, J Pyle, NV Riveiros, EW Wolff, and S Zaehle. 2013. "Evaluation of biospheric

components in Earth system models using modern and palaeo-observations: the state-of-the-art." *Biogeosciences* 10 (12):8305-8328. doi: 10.5194/bg-10-8305-2013.

Foley, JA, JE Kutzbach, MT Coe, and S Levis. 1994. "Feedbacks between climate and boreal forests during the holocene epoch." *Nature* 371 (6492):52-54. doi: 10.1038/371052a0.

Friedlingstein, P., L. Bopp, P. Ciais, J. L. Dufresne, L. Fairhead, H. LeTreut, P. Monfray, and J. Orr. 2001. "Positive feedback between future climate change and the carbon cycle." *Geophysical Research Letters* 28 (8):1543-1546.

Friedlingstein, P, JL Dufresne, PM Cox, and P Rayner. 2003. "How positive is the feedback between climate change and the carbon cycle?" *Tellus Series B-Chemical and Physical Meteorology*:692-700.

Friedlingstein, P, P Cox, R Betts, L Bopp, W Von Bloh, V Brovkin, P Cadule, S Doney, M Eby, I Fung, G Bala, J John, C Jones, F Joos, T Kato, M Kawamiya, W Knorr, K Lindsay, HD Matthews, T Raddatz, P Rayner, C Reick, E Roeckner, KG Schnitzler, R Schnur, K Strassmann, AJ Weaver, C Yoshikawa, and N Zeng. 2006. "Climate-carbon cycle feedback analysis: Results from the (CMIP)-M-4 model intercomparison." *Journal of Climate* 19 (14):3337-3353. doi: 10.1175/JCLI3800.1.

Friedlingstein, P, RM Andrew, J Rogelj, GP Peters, JG Canadell, R Knutti, G Luderer, MR Raupach, M Schaeffer, DP van Vuuren, and C Le Quéré. 2014. "Persistent growth of CO2 emissions and implications for reaching climate targets." *Nature Geoscience* 7 (10):709-715. doi: 10.1038/NGEO2248.

Frolicher, TL, JL Sarmiento, DJ Paynter, JP Dunne, JP Krasting, and M Winton. 2015. "Dominance of the Southern Ocean in Anthropogenic Carbon and Heat Uptake in CMIP5 Models." *Journal of Climate* 28 (2):862-886. doi: 10.1175/JCLI-D-14-00117.1.

Gordon, C, C Cooper, CA Senior, H Banks, JM Gregory, TC Johns, JFB Mitchell, and RA Wood. 2000. "The simulation of SST, sea ice extents and ocean heat transports in a version of the Hadley Centre coupled model without flux adjustments." *Climate Dynamics* 16 (2-3):147-168. doi: 10.1007/s003820050010.

Gregory, JM, and P Huybrechts. 2006. "Ice-sheet contributions to future sea-level change." *Philosophical Transactions of the Royal Society a-Mathematical*

Physical and Engineering Sciences 364 (1844):1709-1731. doi: 10.1098/rsta.2006.1796.

Gregory, JM, CD Jones, P Cadule, and P Friedlingstein. 2009. "Quantifying Carbon Cycle Feedbacks." *Journal of Climate* 22 (19):5232-5250. doi: 10.1175/2009JCLI2949.1.

Hall, A, and X Qu. 2006. "Using the current seasonal cycle to constrain snow albedo feedback in future climate change." *Geophysical Research Letters* 33 (3). doi: 10.1029/2005GL025127.

Hansen, J., A. Lacis, D. Rind, G. Russell, P. Stone, I. Fung, R. Ruedy, and J. Lerner, 1984: Climate sensitivity: Analysis of feedback mechanisms. Climate Processes and Climate Sensitivity, Geophys. Monogr., Vol. 29, Amer. Geophys. Union, 130-163.

Hewitt, AJ, BBB Booth, CD Jones, ES Robertson, AJ Wiltshire, PG Sansom, DB Stephenson, and S Yip. 2016. "Sources of Uncertainty in Future Projections of the Carbon Cycle." *Journal of Climate* 29 (20):7203-7213. doi: 10.1175/JCLI-D-16-0161.1.

Hugelius, G, J Strauss, S Zubrzycki, JW Harden, EAG Schuur, CL Ping, L Schirrmeister, G Grosse, GJ Michaelson, CD Koven, JA O'Donnell, B Elberling, U Mishra, P Camill, Z Yu, J Palmtag, and P Kuhry. 2014. "Estimated stocks of circumpolar permafrost carbon with quantified uncertainty ranges and identified data gaps." *Biogeosciences* 11 (23):6573-6593. doi: 10.5194/bg-11-6573-2014.

IPCC, 2014: Climate Change 2014: Synthesis Report. Contribution of Working Groups I, II and III to the Fifth Assessment Report of the Intergovernmental Panel on Climate Change [Core Writing Team, R.K. Pachauri and L.A. Meyer (eds.)]. IPCC, Geneva, Switzerland, 151 pp.

Jenkinson, DS, DE Adams, and A Wild. 1991. "Model estimates of CO2 emissions from soil in response to global warming." *Nature* 351 (6324):304-306. doi: 10.1038/351304a0.

Jones, CD, and PM Cox. 2001a. "Modeling the volcanic signal in the atmospheric CO2 record." *Global Biogeochemical Cycles* 15 (2):453-465. doi: 10.1029/2000GB001281.

Jones, CD, and PM Cox. 2001b. "Constraints on the temperature sensitivity of global soil respiration from the observed interannual variability in atmospheric

CO(2)." *Atmospheric Science Letters* 2 (1-4):166-172. doi: 10.1006/asle.2001.0041.

Jones, CD, M Collins, PM Cox, and SA Spall. 2001. "The carbon cycle response to ENSO: A coupled climate-carbon cycle model study." *Journal of Climate* 14 (21):4113-4129. doi: 10.1175/1520-0442(2001)014<4113:TCCRTE>2.0.CO;2.

Jones, C. D., P. M. Cox, and C. Huntingford. 2006a. "Impact of climate carbon cycle feedbacks on emission scenarios to achieve stabilization." In *Avoiding Dangerous Climate Change*, edited by W. Cramer H. J. Schellnhuber, N. Nakicenovic, T. Wigley and G. Yohe. Cambridge University Press.

Jones, CD, PM Cox, and C Huntingford. 2006b. "Climate-carbon cycle feedbacks under stabilization: uncertainty and observational constraints." *Tellus Series B-Chemical and Physical Meteorology* 58 (5):603-613. doi: 10.1111/j.1600-0889.2006.00215.x.

Jones, C, J Lowe, S Liddicoat, and R Betts. 2009. "Committed terrestrial ecosystem changes due to climate change." *Nature Geoscience* 2 (7):484-487. doi: 10.1038/ngeo555.

Jones, CD, JK Hughes, N Bellouin, SC Hardiman, GS Jones, J Knight, S Liddicoat, FM O'Connor, RJ Andres, C Bell, KO Boo, A Bozzo, N Butchart, P Cadule, KD Corbin, M Doutriaux-Boucher, P Friedlingstein, J Gornall, L Gray, PR Halloran, G Hurtt, WJ Ingram, JF Lamarque, RM Law, M Meinshausen, S Osprey, EJ Palin, LP Chini, T Raddatz, MG Sanderson, AA Sellar, A Schurer, P Valdes, N Wood, S Woodward, M Yoshioka, and M Zerroukat. 2011. "The HadGEM2-ES implementation of CMIP5 centennial simulations." *Geoscientific Model Development* 4 (3):543-570. doi: 10.5194/gmd-4-543-2011.

Jones, C, E Robertson, V Arora, P Friedlingstein, E Shevliakova, L Bopp, V Brovkin, T Hajima, E Kato, M Kawamiya, S Liddicoat, K Lindsay, CH Reick, C Roelandt, J Segschneider, and J Tjiputra. 2013. "Twenty-First-Century Compatible CO2 Emissions and Airborne Fraction Simulated by CMIP5 Earth System Models under Four Representative Concentration Pathways." *Journal of Climate* 26 (13):4398-4413. doi: 10.1175/JCLI-D-12-00554.1.

Jones, CD, V Arora, P Friedlingstein, L Bopp, V Brovkin, J Dunne, H Graven, F Hoffman, T Ilyina, JG John, M Jung, M Kawamiya, C Koven, J Pongratz, T Raddatz, JT Randerson, and S Zaehle. 2016a. "C4MIP-The Coupled Climate-

Carbon Cycle Model Intercomparison Project: experimental protocol for CMIP6." *Geoscientific Model Development* 9 (8):2853-2880. doi: 10.5194/gmd-9-2853-2016.

Jones, CD, P Ciais, SJ Davis, P Friedlingstein, T Gasser, GP Peters, J Rogelj, DP van Vuuren, JG Canadell, A Cowie, RB Jackson, M Jonas, E Kriegler, E Littleton, JA Lowe, J Milne, G Shrestha, P Smith, A Torvanger, and A Wiltshire. 2016b. "Simulating the Earth system response to negative emissions." *Environmental Research Letters* 11 (9). doi: 10.1088/1748-9326/11/9/095012.

Joos, F, GK Plattner, TF Stocker, O Marchal, and A Schmittner. 1999. "Global warming and marine carbon cycle feedbacks an future atmospheric CO2." *Science* 284 (5413):464-467. doi: 10.1126/science.284.5413.464.

Kicklighter, DW, M Bruno, S Donges, G Esser, M Heimann, J Helfrich, F Ift, F Joos, J Kaduk, GH Kohlmaier, AD McGuire, JM Melillo, R Meyer, B Moore, A Nadler, IC Prentice, W Sauf, AL Schloss, S Sitch, U Wittenberg, and G Wurth. 1999. "A first-order analysis of the potential role of CO(2) fertilization to affect the global carbon budget: a comparison of four terrestrial biosphere models." *Tellus Series B-Chemical and Physical Meteorology* 51 (2):343-366. doi: 10.1034/j.1600-0889.1999.00017.x.

Kirschbaum, MUF. 1995. "The temperature-dependence of soil organic-matter decomposition, and the effect of global warming on soil organic-C storage." *Soil Biology & Biochemistry* 27 (6):753-760. doi: 10.1016/0038-0717(94)00242-S.

Koven, CD, EAG Schuur, C Schadel, TJ Bohn, EJ Burke, G Chen, X Chen, P Ciais, G Grosse, JW Harden, DJ Hayes, G Hugelius, EE Jafarov, G Krinner, P Kuhry, DM Lawrence, AH MacDougall, SS Marchenko, AD McGuire, SM Natali, DJ Nicolsky, D Olefeldt, S Peng, VE Romanovsky, KM Schaefer, J Strauss, CC Treat, and M Turetsky. 2015. "A simplified, data-constrained approach to estimate the permafrost carbon-climate feedback." *Philosophical Transactions of the Royal Society a-Mathematical Physical and Engineering Sciences* 373 (2054). doi: 10.1098/rsta.2014.0423.

Lawrence, DM, GC Hurtt, A Arneth, V Brovkin, KV Calvin, AD Jones, CD Jones, PJ Lawrence, N de Noblet-Ducoudre, J Pongratz, SI Seneviratne, and E Shevliakova. 2016. "The Land Use Model Intercomparison Project (LUMIP)

contribution to CMIP6: rationale and experimental design." *Geoscientific Model Development* 9 (9):2973-2998. doi: 10.5194/gmd-9-2973-2016.

Le Quéré, C., Andrew, R. M., Canadell, J. G., Sitch, S., Korsbakken, J. I., Peters, G. P., Manning, A. C., Boden, T. A., Tans, P. P., Houghton, R. A., Keeling, R. F., Alin, S., Andrews, O. D., Anthoni, P., Barbero, L., Bopp, L., Chevallier, F., Chini, L. P., Ciais, P., Currie, K., Delire, C., Doney, S. C., Friedlingstein, P., Gkritzalis, T., Harris, I., Hauck, J., Haverd, V., Hoppema, M., Klein Goldewijk, K., Jain, A. K., Kato, E., Körtzinger, A., Landschützer, P., Lefèvre, N., Lenton, A., Lienert, S., Lombardozzi, D., Melton, J. R., Metzl, N., Millero, F., Monteiro, P. M. S., Munro, D. R., Nabel, J. E. M. S., Nakaoka, S.-I., O'Brien, K., Olsen, A., Omar, A. M., Ono, T., Pierrot, D., Poulter, B., Rödenbeck, C., Salisbury, J., Schuster, U., Schwinger, J., Séférian, R., Skjelvan, I., Stocker, B. D., Sutton, A. J., Takahashi, T., Tian, H., Tilbrook, B., van der Laan-Luijkx, I. T., van der Werf, G. R., Viovy, N., Walker, A. P., Wiltshire, A. J., and Zaehle, S.: Global Carbon Budget 2016, Earth Syst. Sci. Data, 8, 605-649, doi:10.5194/essd-8-605-2016, 2016

Lloyd, J, and GD Farquhar. 1996. "The CO2 dependence of photosynthesis, plant growth responses to elevated atmospheric CO2 concentrations and their interaction with soil nutrient status .1. General principles and forest ecosystems." *Functional Ecology* 10 (1):4-32. doi: 10.2307/2390258.

MacDonald, GM, KV Kremenetski, and DW Beilman. 2008. "Climate change and the northern Russian treeline zone." *Philosophical Transactions of the Royal Society B-Biological Sciences* 363 (1501):2285-2299. doi: 10.1098/rstb.2007.2200.

Marotzke, J, C Jakob, S Bony, PA Dirmeyer, PA O'Gorman, E Hawkins, S Perkins-Kirkpatrick, C Le Quere, S Nowicki, K Paulavets, SI Seneviratne, B Stevens, and M Tuma. 2017. "Climate research must sharpen its view." *Nature Climate Change* 7 (2):89-91.

Martin, G. M., N. Bellouin, W. J. Collins, I. D. Culverwell, P. R. Halloran, S. C. Hardiman, T. J. Hinton, C. D. Jones, R. E. McDonald, A. J. McLaren, F. M. O'Connor, M. J. Roberts, J. M. Rodriguez, S. Woodward, M. J. Best, M. E. Brooks, A. R. Brown, N. Butchart, C. Dearden, S. H. Derbyshire, I. Dharssi, M. Doutriaux-Boucher, J. M. Edwards, P. D. Falloon, N. Gedney, L. J. Gray, H. T. Hewitt, M. Hobson, M. R. Huddleston, J. Hughes, S. Ineson, W. J. Ingram, P.

M. James, T. C. Johns, C. E. Johnson, A. Jones, C. P. Jones, M. M. Joshi, A. B. Keen, S. Liddicoat, A. P. Lock, A. V. Maidens, J. C. Manners, S. F. Milton, J. G. L. Rae, J. K. Ridley, A. Sellar, C. A. Senior, I. J. Totterdell, A. Verhoef, P. L. Vidale, A. Wiltshire, and HadGEM2 Dev Team. 2011. "The HadGEM2 family of Met Office Unified Model climate configurations." *Geoscientific Model Development* 4 (3):723-757. doi: 10.5194/gmd-4-723-2011.

Matthews, H.D. 2006. "Emissions targets for CO2 stabilization as modified by carbon cycle feedbacks." *Tellus* 58B:591-602.

Matthews, H. D., N. P. Gillett, P. A. Stott, and K. Zickfeld. 2009. "The proportionality of global warming to cumulative carbon emissions." *Nature* 459 (7248):829-U3. doi: 10.1038/nature08047.

McGuire, A. D., S. Sitch, J. S. Clein, R. Dargaville, G. Esser, J. Foley, M. Heimann, F. Joos, J. Kaplan, D. W. Kicklighter, R. A. Meier, J. M. Melillo, B. Moore, I. C. Prentice, N. Ramankutty, T. Reichenau, A. Schloss, H. Tian, L. J. Williams, and U. Wittenberg. 2001. "Carbon balance of the terrestrial biosphere in the twentieth century: Analyses of CO2, climate and land use effects with four process-based ecosystem models." *Global Biogeochemical Cycles* 15 (1):183-206.

Meehl, GA, C Covey, B McAvaney, M Latif, and RJ Stouffer. 2005. "Overview of the Coupled Model Intercomparison Project." *Bulletin of the American Meteorological Society* 86 (1):89-93. doi: 10.1175/BAMS-86-1-89.

Myhre, G., D. Shindell, F.-M. Bréon, W. Collins, J. Fuglestvedt, J. Huang, D. Koch, J.-F. Lamarque, D. Lee, B. Mendoza, T. Nakajima, A. Robock, G. Stephens, T. Takemura and H. Zhang, 2013: Anthropogenic and Natural Radiative Forcing. In: Climate Change 2013: The Physical Science Basis. Contribution of Working Group I to the Fifth Assessment Report of the Intergovernmental Panel on Climate Change [Stocker, T.F., D. Qin, G.-K. Plattner, M. Tignor, S.K. Allen, J. Boschung, A. Nauels, Y. Xia, V. Bex and P.M. Midgley (eds.)]. Cambridge University Press, Cambridge, United Kingdom and New York, NY, USA.

Plattner, GK. 2009. "Terrestrial ecosystem inertia." *Nature Geoscience* 2 (7):467-468. doi: 10.1038/ngeo570.

Pope, V., S. Brown, R. Clark, M. Collins, W. Collins, C. Dearden, J. Gunson, G. Harris, C. Jones, A. Keen, J. Lowe, M. Ringer, C. Senior, S. Sitch, M. Webb,

and S. Woodward. 2007. "The Met Office Hadley Centre climate modelling capability: the competing requirements for improved resolution, complexity and dealing with uncertainty." *Philosophical Transactions of the Royal Society a-Mathematical Physical and Engineering Sciences* 365 (1860):2635-2657. doi: 10.1098/rsta.2007.2087.

Prentice, I. C., G. D. Farquhar, M.J.R. Fasham, M.L. Goulden, M. Heimann, V.J. Jaramillo, H.S. Kheshgi, C. Le Quéré, R. J. Scholes, and D.W.R. Wallac. 2001. "The Carbon Cycle and Atmospheric Carbon Dioxide." In *Climate Change 2001: The Scientific Basis*, edited by J. T. Houghton, Y. Ding, D. J. Griggs, M. Noguer, P. J. van der Linden, A. Dai, K. Maskell and C. A. Johnson. New York: Cambridge University Press.

Randerson, JT, K Lindsay, E Munoz, W Fu, JK Moore, FM Hoffman, NM Mahowald, and SC Doney. 2015. "Multicentury changes in ocean and land contributions to the climate-carbon feedback." *Global Biogeochemical Cycles* 29 (6):744-759. doi: 10.1002/2014GB005079.

Roy, T, L Bopp, M Gehlen, B Schneider, P Cadule, TL Frolicher, J Segschneider, J Tjiputra, C Heinze, and F Joos. 2011. "Regional Impacts of Climate Change and Atmospheric CO2 on Future Ocean Carbon Uptake: A Multimodel Linear Feedback Analysis." *Journal of Climate* 24 (9):2300-2318. doi: DOI 10.1175/2010JCLI3787.1.

Sabine, CL, RA Feely, N Gruber, RM Key, K Lee, JL Bullister, R Wanninkhof, CS Wong, DWR Wallace, B Tilbrook, FJ Millero, TH Peng, A Kozyr, T Ono, and AF Rios. 2004. "The oceanic sink for anthropogenic CO2." *Science* 305 (5682):367-371. doi: 10.1126/science.1097403.

Sarmiento, JL, and C LeQuéré. 1996. "Oceanic carbon dioxide uptake in a model of century-scale global warming." *Science* 274 (5291):1346-1350. doi: 10.1126/science.274.5291.1346.

Sarmiento, J. L., T. M. C. Hughes, R. J. Stouffer, and S. Manabe. 1998. "Simulated response of the ocean carbon cycle to anthropogenic climate warming." *Nature* 393:245-249.

Schimel, DS, BH Braswell, EA Holland, R McKeown, DS Ojima, TH Painter, WJ Parton, and AR Townsend. 1994. "Climatic, edaphic, and biotic controls over storage and turnover of carbon in soils." *Global Biogeochemical Cycles* 8 (3):279-293. doi: 10.1029/94GB00993.

Scholze, M, W Knorr, NW Arnell, and IC Prentice. 2006. "A climate-change risk analysis for world ecosystems." *Proceedings of the National Academy of Sciences of the United States of America* 103 (35):13116-13120. doi: DOI 10.1073/pnas.0601816103.

Schuur, EAG, AD McGuire, C Schadel, G Grosse, JW Harden, DJ Hayes, G Hugelius, CD Koven, P Kuhry, DM Lawrence, SM Natali, D Olefeldt, VE Romanovsky, K Schaefer, MR Turetsky, CC Treat, and JE Vonk. 2015. "Climate change and the permafrost carbon feedback." *Nature* 520 (7546):171-179. doi: 10.1038/nature14338.

Schwinger, J, JF Tjiputra, C Heinze, L Bopp, JR Christian, M Gehlen, T Ilyina, CD Jones, D Salas-Melia, J Segschneider, R Seferian, and I Totterdell. 2014. "Nonlinearity of Ocean Carbon Cycle Feedbacks in CMIP5 Earth System Models." *Journal of Climate* 27 (11):3869-3888. doi: 10.1175/JCLI-D-13-00452.1.

Sitch, S., C. Huntingford, N. Gedney, P. E. Levy, M. Lomas, S. L. Piao, R. Betts, P. Ciais, P. Cox, P. Friedlingstein, C. D. Jones, I. C. Prentice, and F. I. Woodward. 2008. "Evaluation of the terrestrial carbon cycle, future plant geography and climate-carbon cycle feedbacks using five Dynamic Global Vegetation Models (DGVMs)." *Global Change Biology* 14 (9):2015-2039. doi: 10.1111/j.1365-2486.2008.01626.x.

Smith, TM, and HH Shugart. 1993. "The transient-response of terrestrial carbon storage to a perturbed climate." *Nature* 361 (6412):523-526. doi: 10.1038/361523a0.

Soden, BJ, IM Held, R Colman, KM Shell, JT Kiehl, and CA Shields. 2008. "Quantifying climate feedbacks using radiative kernels." *Journal of Climate* 21 (14):3504-3520. doi: 10.1175/2007JCLI2110.1.

Takahashi, T, SC Sutherland, C Sweeney, A Poisson, N Metzl, B Tilbrook, N Bates, R Wanninkhof, RA Feely, C Sabine, J Olafsson, and Y Nojiri. 2002. "Global sea-air CO2 flux based on climatological surface ocean pCO(2), and seasonal biological and temperature effects." *Deep-Sea Research Part Ii-Topical Studies in Oceanography* 49 (9-10):1601-1622. doi: 10.1016/S0967-0645(02)00003-6.

Taylor, KE, RJ Stouffer, and GA Meehl. 2012. "An overview of CMIP5 and the experiment design." *Bulletin of the American Meteorological Society* 93

(4):485-498. doi: 10.1175/BAMS-D-11-00094.1.

Thompson, S. L., B. Govindasamy, A. Mirin, K. Caldeira, C. Delire, J. Milovich, M. Wickett, and D. Erickson. 2004. "Quantifying the effects of CO2-fertilized vegetation on future global climate and carbon dynamics." *Geophysical Research Letters* 31 (23):L23211, doi:10.1029/2004GL021239.

Tyndall, John (1861). "On the Absorption and Radiation of Heat by Gases and Vapours, and on the Physical Connection of Radiation, Absorption, and Conduction" (PDF). Philosophical Magazine. 4. 22: 169-94, 273-85.

van Vuuren, DP, J Edmonds, M Kainuma, K Riahi, A Thomson, K Hibbard, GC Hurtt, T Kram, V Krey, JF Lamarque, T Masui, M Meinshausen, N Nakicenovic, SJ Smith, and SK Rose. 2011. "The representative concentration pathways: an overview." *Climatic Change* 109 (1-2):5-31. doi: 10.1007/s10584-011-0148-z.

Watson, AJ, C Robinson, JE Robinson, PJL Williams, and MJR Fasham. 1991. "Spatial variability in the sink for atmospheric carbon-dioxide in the North-Atlantic." *Nature* 350 (6313):50-53. doi: 10.1038/350050a0.

Wenzel, S, PM Cox, V Eyring, and P Friedlingstein. 2016. "Projected land photosynthesis constrained by changes in the seasonal cycle of atmospheric CO2." *Nature* 538 (7626): doi: 10.1038/nature19772.

Wieder, WR, CC Cleveland, WK Smith, and K Todd-Brown. 2015. "Future productivity and carbon storage limited by terrestrial nutrient availability." *Nature Geoscience* 8 (6):441-444. doi: 10.1038/NGEO2413.

Wigley, T. M. L. 1995. "Global mean temperature and sea-level consequences of greenhouse-gas concentration stabilization." *Geophysical Research Letters* 22 (1):45-48.

Wigley, T. M. L., R. Richels, and J. A. Edmonds. 1996. "Economic and environmental choices in the stabilization of atmospheric CO2 concentrations." *Nature* 379 (6562):240-243.

Zaehle, S, CD Jones, B Houlton, JF Lamarque, and E Robertson. 2015. "Nitrogen Availability Reduces CMIP5 Projections of Twenty-First-Century Land Carbon Uptake." *Journal of Climate* 28 (6):2494-2511. doi: 10.1175/JCLI-D-13-00776.1.